IONOSPHERIC RESPONSE TO SOLAR PHENOMENA AND THUNDERSTORMS

A THESIS

Submitted in fulfilment of the
requirements for the award of the degree
of

DOCTOR OF PHILOSOPHY

in

EARTH SCIENCES

By

DINESH KUMAR SHARMA

DEPARTMENT OF EARTH SCIENCES
INDIAN INSTITUTE OF TECHNOLOGY ROORKEE
ROORKEE–247 667 (INDIA)

DECEMBER, 2003

551.0012
SHA

INDIAN INSTITUTE OF TECHNOLOGY ROORKEE
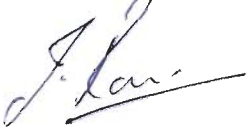
CANDIDATE'S DECLARATION

I hereby certify that the work which is being presented in the thesis entitled **"Ionospheric response to solar phenomena and thunderstorms"** in fulfilment of the requirement for the award of the degree of Doctor of Philosophy and submitted in the **Department of Earth Sciences** of the institute is an authentic record of my own work carried out during period from January 2000 to December 2003 under the supervision of **Dr. M. Israil** and **Prof. Jagdish Rai**.
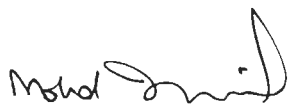
The matter presented in this thesis has not been submitted by me for the award of any other degree of this or any other institute.
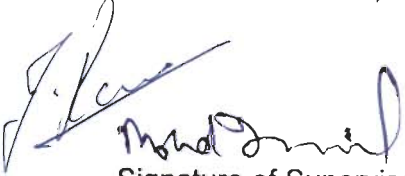
Date: December 29, 2003

(Dinesh Kumar Sharma)
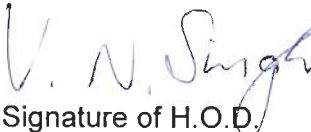
This is to certify that the above statement made by the candidate is correct to the best of our knowledge.

(Dr. Jagdish Rai)
Professor
Department of Physics,
Indian Institute of Technology,
Roorkee - 247 667, India

(Dr. M. Israil)
Assistant Professor
Department of Earth Sciences,
Indian Institute of Technology,
Roorkee - 247 667, India

The Ph. D. Viva-Voce examination of **Mr. Dinesh Kumar Sharma**, Research Scholar, has been held on 21st May 2007

Signature of Supervisor(s)   Signature of H.O.D.   Signature of External Examiner

ABSTRACT

The region lying from 65-70 km to about 1000 km altitude above the earth surface containing free electrons and ions is known as ionosphere. The equatorial ionosphere is formed primarily by the ionization of neutral gas atoms/molecules present in the upper atmosphere by exposure to solar radiation. The free thermal electrons produced by high-energy photoelectron collision with neutral atoms, form more than 90% of the flux in the ionosphere.

Many modern technological systems are affected by ionospheric phenomena. The ionospheric weather plays an important role in communication, navigation, exploration of near earth space and even exploration of deeper part of earth's interior. Natural electromagnetic fields generated by the interaction of solar wind, magnetosphere and ionosphere as well as generated by thunderstorms and lightning/sprites are affected by the ionospheric weather. The natural electromagnetic fields in the frequency range from 10^4 Hz to 10^{-4} Hz are used as a source in magnetotelluric method of geo-exploration. Understanding the role of ionosphere in generating, propagating and attenuating these fields are crucial for an effective exploration program using magnetotelluric currents. The weather disturbances like thunderstorms alter the ion-electron production rate and hence change the ionospheric temperature and density. The thunderstorms are the main source of lightning and sprites. The sprites propagating from cloud top to the ionosphere generate the radiations from ULF to VLF, which in turn propagate still

upwards and heat the local plasma. Further, the solar phenomena such as solar flares, coronal mass ejection etc. also play an important role in changing the ionospheric temperatures and ion density. Recently it has been observed that the electromagnetic flux associated with the seismic activity also affects the ionospheric phenomena.

Present work is devoted to the study of ionospheric electron and ion temperature variations in the low latitude $F2$ region (altitude ranges 425-625 km) over India during the period from 1995 to 1998 (which covers the 1995-96 solar minimum year). The average diurnal, seasonal and latitudinal behavior of electron and ion temperatures has been studied in details. The study also includes the ionospheric response to the sunrise, solar flares and active thunderstorms. The data for these studies have been obtained by Retarding Potential Analyzer (RPA) payload aboard SROSS-C2 satellite during the period from 1995 to 1998. Thunderstorm data were obtained from India Meteorological Department (IMD) and that on Solar flares from National Geophysical Data Center (NGDC), Boulder, Colorado, U. S. A. The International Reference Ionosphere (IRI) model values for the same period were used for comparison. The present thesis is a systematic presentation of the work done on the behavior of ionospheric temperatures, the diurnal, seasonal and latitudinal variations and their response to thunderstorms and solar phenomena. Some studies on tropospheric aerosols in relation to meteorological parameters have also been carried out and the same has been included as an appendix.

A brief history of ionospheric studies has been presented in **Chapter-I**. Work done on the variations in ionospheric parameters using another satellite data has been reviewed. A Japanese satellite (Hinotori) which had a near circular orbit of ~600 km provided an ideal database for the study of the temporal and spatial variation of electron temperature in the topside ionosphere. The descriptions of the solar phenomena, thunderstorms, lightning/sprites and their electromagnetic fields have also been given in this chapter.

Chapter-II deals with the details of data used and their sources. It gives a brief description of RPA payload aboard SROSS-C2 satellite used in the measurement of ionospheric temperatures. The SROSS-C2 was launched by ISRO on May 4, 1994. It was successfully operated continuously for seven years and on July 12, 2001 returned to the earth. The IRI model has also been discussed briefly.

Diurnal, seasonal and latitudinal variation of ionospheric temperatures of the topside F region ionosphere over India during the solar minimum year (1995-96) at an average altitude of ~500 km have been presented in **Chapter-III**. The measured electron and ion temperature data have been analysed for three different seasons; summer (May, June, July and August), winter (November, December, January and February) and equinoxes (March, April, September and October) during the solar minimum year to study the diurnal, seasonal and latitudinal behaviour of electron and ion temperatures. This study reveals that the electron and ion temperatures have lowest values during night hours and show

variations during daytime in all seasons. The daytime electron temperature shows atleast two peak values with different magnitudes. The peak during sunrise hours is relatively sharp and high in magnitude and the peak during sunset hours are diffused and lower in magnitude. Similar variations in the ion temperature have also been observed. However, their amplitude and sharpness are smaller in comparison with the behaviour of electron temperature. The predicted values by IRI-95 model show a good agreement with electron and ion temperatures during night hours. The daytime electron temperature variation and sunrise peak values are under estimated by IRI-95 model and unable to produce secondary peaks during sunset. The electron and ion temperatures show a positive correlation with latitude during daytime over the geographical region under study. However, no latitudinal dependence has been observed during night hours at an altitude of ~500 km.

The sunrise effect on the ionospheric electron and ion temperatures as measured by the SROSS-C2 satellite during the period from 1995 to 1998 (which cover the solar minimum year of 1995-96) for specific location of Bhopal (23.16° N, 77.36° E) and Chennai (13.04° N, 80.19° E) in India have been presented in **Chapter-IV**. It has been found that the electron and ion temperatures are minimum during the local night hours and maximum at the local sunrise time. The nighttime electron temperature (T_e) varies nearly from 800 to 1000 K and rises sharply at sunrise to 3000 K or more. The nighttime ion temperature (T_i) varies from nearly 600 to 800 K and also rises at sunrise to about 2000 K or more.

Chapter-V has been dedicated to the study of the effect of thunderstorms on ionospheric temperatures. The study reveals that there is a consistent enhancement of electron and ion temperatures recorded during active thunderstorms over the normal day temperatures. It is worth mentioning that in the present analysis the data were selected in such a way that the effect of diurnal, seasonal, latitudinal, longitudinal and altitude variations are minimized. It has been concluded that the ionospheric temperature anomalies are directly related to the thunderstorm events. The enhancements in ionospheric electron and ion temperatures have been attributed to the lightning/sprites activity and the associated phenomena such as the radiations from ULF to VLF range, which in turn, may propagate still upward and heat the local plasma in the F region ionosphere.

The effect of solar flares on ionospheric electron and ion temperatures over the topside F region has been presented in Chapter-VI. This study reveals that there is a consistent enhancement of the ionospheric electron and ion temperatures recorded during solar flares. The enhancement in case of electron temperature is slightly higher than the enhancement in ion temperature. The data selection and analysis shows that the enhancement of ionospheric temperatures can be related to the solar flares. The effect of solar flare on the nightside ionospheric temperatures has not been detected in the altitude range from 425 to 625 km.

Chapter-VII summarizes the work done in the present thesis and the conclusions have been drawn on the basis of our studies.

An **Appendix** has also been added to the thesis, which describes the work done on aerosol studies. It reviews the studies on aerosol generation, distribution and different mechanisms involved in aerosol formation and their relation to meteorological parameters. A brief description of the instrument used for aerosols study has also been given.

The study of aerosols number concentration in relation to some meteorological parameters (relative humidity, temperature, wind speed and rainfall) during the period from April to July 1999 at Roorkee for different size ranges viz. 0.3-0.5 μm, 0.5-1.0 μm, 1.0-2.0 μm and 2.0-5.0 μm has been presented.

ACKNOWLEDGEMENTS

It is my great pleasure and privilege to express my deep sense of gratitude and profound indebtedness towards **Dr. M. Israil**, Department of Earth Sciences and **Prof. Jagdish Rai**, Department of Physics, Indian Institute of Technology, Roorkee, for their incessant invaluable guidance, inspiring encouragement and kind cooperation during the progress of the work. I am very thankful to them for suggesting the problem and for having had the opportunity to work with them. The work could not have been completed without their helpful counsel and constant cooperation. The long hours of fruitful discussions and pertinent suggestions not only strengthened my skills in research methodology but also helped me a more confident personality. Right from the very beginning I have admired them for their wonderful homely behavior.

During this research, the department has had three heads; Prof. A. K. Awasthi, Prof. B. Prakesh and Prof. V. N. Singh and most fortunately all of them encouraged me by extending every sort of help as and when sought for. I wish to express my gratefulness to Prof. Ishwar Singh, the Head of Physics Department and Prof. S. Auluck, former head of Physics Department for supporting my efforts in various ways and providing the necessary facilities for my research.

I would like to make a special note of thank to Prof. P. K. Gupta, Prof. R. P. Gupta, Prof. S. K. Upadhayay and other faculty members of the Department of Earth Sciences for their co-operation. I shall equally remain indebted to Prof. Vir Singh and Prof B. D. Indu from the Department of Physics for their constant

(Dinesh Kumar Sharma)

LIST OF PUBLICATIONS

A. *In journals:*

1. D. K. Sharma, Jagdish Rai, M. Israil, P. Subrahmanyam, P. Chopra and S. C. Garg, Enhancement in ionospheric temperatures during thunderstorms, *Journal of Atmospheric & Solar Terrestrial Physics*, 66 (2004) 51-56.

2. D. K. Sharma, J. Rai, M. Israil and S. C. Garg, Lightning induced heating of the ionosphere, *Atmosfera*, 17 (2004) 31-38.

3. D. K. Sharma, Jagdish Rai, M. Israil, Shalini Priti, P. Subrahmanyam, P. Chopra and S. C. Garg, Sunrise effect on ionospheric temperature as measured by SROSS-C2 satellite, *J. Ind. Geophysical Union,* 7 (2003) 117-123.

4. D. K. Sharma, J. Rai, M. Israil and Partap Singh, Summer variation of the atmospheric aerosol number concentration over Roorkee, India, *Journal of Atmospheric & Solar Terrestrial Physics*, 65 (2003) 1007-1019.

5. D. K. Sharma, J. Rai, M. Israil, P. Subrahmanyam, P. Chopra and S. C. Garg, The effect of lightning on ionospheric temperature determined by SROSS-C2 Satellite, *Indian J. Radio & Space Phys*, 32 (2003) 93-97.

6. D. K. Sharma, M. K. Bansal, J. Rai, and M. Israil, Variation of aerosols in relation to some meteorological parameters, *Mausam*, 52 (2001) 709-716.

7. D. K. Sharma, Jagdish Rai, M. Israil, P. Subrahmanyam, P. Chopra and S. C. Garg, Effect of solar flare on electron and ion temperatures as measured by SROSS-C2 satellite, *Indian J. Radio & Space Phys*, (in press).

8. D. K. Sharma, J. Rai, M. Israil, P. Subrahmanyam, P. Chopra and S. C. Garg, Enhancement in electron and ion temperatures due to solar flares as measured by SROSS-C2 satellite, *Annals Geophysica* (revised form submitted).

9. D. K. Sharma, J. Rai, M. Israil and P. Subrahmanyam, Diurnal, seasonal and latitudinal variation of ionospheric temperatures of the topside F region over Indian region during solar minimum year 1995-96, *Journal of Atmospheric & Solar Terrestrial Physics*, (submitted).

B. *In conference proceedings (International/ National):*

1. M. Israil, T. Harinaryana, D. K. Sharma, P. K. Gupta and J. Rai, Resistivity imaging using Straight Forward Inversion of Magnetotelluric data, Proc. International Conference on Mathematical Modeling, IIT Roorkee, 2001, 574-578.
2. M. Israil, D. K. Sharma and J. Rai, Resistivity 1D Inversion of 3D Magnetotelluric data of Geothermal Exploration, Proc. National Workshop on Recent Development in Atmospheric and Space Sciences, IIT Roorkee, 2001, 51-62.

3. D. K. Sharma, J. Rai, M. Israil and S. C. Garg, Temperature and Density variation in ionospheric plasma over different locations in India, Proc. National Conference on Advances in Contemporary Physics & Energy, IIT Delhi, 2002, 265-278.

4. Jagdish Rai, Keshav Kumar, D. K. Sharma and S. Darmora, Mapping of intra-cloud lightning discharges, Proc. 2002 Lightning Detection Conference, Tucson, AZ, (USA), 2002, paper no. 14.

5. D. K. Sharma, M. K. Bansal, and J. Rai, Effect of meteorological parameters on atmospheric aerosol concentration, Abstract book International workshop on Seismo-Electromagnetic and Space Science RBS College Agra, 2000, 59.

6. J. Rai, D. K. Sharma and M. Israil, Application of Atmospherics in Ground Water Detection, Abstract book National Workshop on Recent Development in Atmospheric and Space Sciences, IIT Roorkee, 2001, 7.

7. D. K. Sharma, J. Rai, M. Israil and S. C. Garg, Enhancement in ionospheric temperatures during thunderstorms, Abstract book Radio & Atmospheric Science Symposium (in Hindi) held at NPL New Delhi, 2003, 2/5.

8. A. K. Singh, M. K. Bansal, D. K. Sharma, and J. Rai, A comparative study of aerosol distribution for two years: influence of meteorological parameters, Abstract book TROPMAT-2000, Cochin, 2000.

9. J. Rai, D. K. Sharma, Feby Jose and D. C. Singh, Effect of pre-monsoon scenario on aerosols at Roorkee, submitted for presentation, XIII National Space Science Symposium (NSSS-2004) to be held during February 17-20, 2004 at M. J. University, Kottayam, Kerala.

CONTENTS

Chapter 1

Introduction

The ionosphere is the very important part of the earth's atmosphere because our society depends on the technological systems that can be affected by the ionospheric phenomena. The understanding, monitoring and forecasting changes in the ionospheric system are of crucial importance to communications, navigation and the exploration of the near earth space. Thus the study of the ionospheric weather has become an important field of present days research.

The region lying from 60-70 km to about 1000 km altitude above the earth surface containing free electrons and ions is known as ionosphere. Without ionosphere the radio communication is not possible. It is primarily responsible for introducing effect in transionospheric radio signals and generating magnetotelluric current sources on the earth. The equatorial ionosphere is formed primarily by the ionization of neutral gas atoms/molecules present in the upper atmosphere by exposure to solar radiation. The free thermal electrons produced by high-energy photoelectron collision with neutral atoms, form more than 90% of the flux in the ionosphere. The weather disturbances like thunderstorms alter the ion-electron production rate and hence change the ionospheric temperature and density. The thunderstorms are the main source of lightning and sprites. The sprites propagating from cloud top to the ionosphere generate the radiations from ULF to VLF, which in turn propagate still upwards and heat the local plasma. Further, the solar

phenomena such as solar flares, coronal mass ejection etc. also play an important role in changing the ionospheric temperatures and ion density. Recently it has been observed that the electromagnetic flux associated with the seismic activity also affects the ionospheric phenomena.

1.1   IONOSPHERE

The ionosphere is that part of the upper atmosphere where free electrons occur in sufficient density to have an appreciable influence on the propagation of radio frequency electromagnetic waves. It can be considered to extend from about 60 to 1000 km. Ionosphere affects the propagation of electromagnetic waves over a wide frequency range from Very Low Frequency (VLF) to microwave frequencies. The effects include the guided propagation of VLF waves; reflection, refraction and absorption; Faraday rotation and scintillation.

On the basis of density variation with altitude, the ionosphere is divided into several 'regions' or 'layers'. These ionized regions collectively are known as ionosphere. These regions are designated by the letters D, E and F. The F region is further divided into two sub regions, $F1$ and $F2$. These regions are developed due to (1) the solar spectrum deposits energy at different heights depending on absorption characteristics of the atmosphere, (2) the physics of recombination depends on density, which exponentially decreases with height, and (3) the composition of the atmosphere changes with height. Figure 1.1 shows the different ionospheric regions with altitude (Mitra, 1992).

The *D* region is that region of the ionosphere, which lies from 60 to about 90 km. In this region the charged particle number density varies from 10^2 to 10^4 cm^{-3} during the daytime. This region disappears at night due to recombination process. Ions are formed by the ionization of atmospheric neutrals by solar X-ray radiation. Due to the relatively high ambient atmospheric pressure, many negative ions are produced by electron attachment to neutral atoms and molecules. Positive and negative ions of NO, O_2, and O are dominant constituents. With increasing altitude, free electrons become more important.

The region lying between 90 to 170 km above the earth surface is known as *E* region. Maximum average electron number density is about 10^5 cm^{-3} in the daytime and about 10^4 cm^{-3} at night. Ions in this region are mainly O_2^+, produced by direct absorption of solar radiation, and NO$^+$ formed by charge transfer collisions with other ions (O$^+$, O_2^+, N_2^+), ionized by solar X-rays.

The region above about 170 km is known as the *F* region. This region is often divided into *F*1 and *F*2 regions (Figure 1.2) during daytimes. The *F*1 region has a maximum electron number density about 10^5 cm^{-3} in the altitude range of 170 to 250 km. This region disappears at night due to recombination process. The electron number density of the *F*2 region varies between 10^5 and 10^6 cm^{-3}. The altitude of maximum electron density in the *F*2 region is about 300 km.

The ionization depends primarily on the sun and its activity. Ionospheric structure and peak number densities in the ionosphere vary greatly with time (sunspot cycle, seasonal, and diurnal variations), geographical location and

3

with certain solar-related phenomena like solar ionizing flux, energetic charged particles and the electric fields imposed via the interaction between the solar wind, magnetosphere and ionosphere. The major part of the ionization is produced by solar X-ray and ultraviolet radiation and by corpuscular radiation from sun. The most noticeable effect is seen with the earth rotation with respect to the sun; ionization increases in the sunlit atmosphere and decreases on the shadowed side. Sun is the largest contributor of ionization towards the earth's ionosphere.

1.1.1 Ion Production in the Lower Atmosphere

In the earth's atmosphere the ions are produced by many different agencies. Above about 65 km altitude the main source of ionization is the electromagnetic radiation, which comes from the sun. Below about 65 km, galactic cosmic rays (GCR) and solar cosmic rays (SCR) are the main sources of ionization. Below about 3 km altitude the radioactive emissions from the earth curst and airborne radioactive substances are the dominant source of ionization.

1.1.1.1 Ionization due to cosmic rays

The cosmic rays are the charged particles from space. There are cosmic rays of galactic origin known as galactic cosmic rays (GCR). Sun also emits streams of high-energy particles and these are known as solar cosmic rays (SCR). The ionization rate due to SCR shows large variations with time because of the variation in the incident cosmic rays flux due to solar activity.

4

The intensity of galactic cosmic rays is modulated over a solar cycle (Rosenberg and Lanzerotti, 1979) and is almost isotropically distributed in the vicinity of earth (Herman and Goldberg, 1978). The earth's geomagnetic field further alters the incident flux before entering in the earth's atmosphere (Ochabova, 1989) because of their high-energy range from tens of MeV to hundreds of GeV. This energy allows them to penetrate deep into the earth's atmosphere and produce secondary radiations. Neher (1971) from their balloon measurements found that the ionization rate is a function of altitude and geomagnetic latitude. The ionization due to GCR is dominant over the SCR at low latitudes (Agarwal, 1995).

1.1.1.2   Ionization due to other sources

The radiations emitted from radioactive elements also contribute to the ionization in the earth's atmosphere (Ogawa, et al., 1964). Due to radioactive inert gases released from rocks, soils and plant transpiration etc. the natural radioactivity is formed in the earth's atmosphere. The radioactive elements like Uranium and Thorium are present in the rocks and soil. These elements give rise to the nuclear radiations, which ionize a thin layer of air near ground surface. The daughter products of these elements are the radioactive gases like radon, thoron and actinon, which produce ionization in the air. The radioactive substances on or near the earth vary from place to place and the ionization also shows special variation near the earth surface.

There are other sources like seismic activity, volcanoes, thunderstorms and lightning/sprites etc., which play an important role in changing the

ionospheric temperature and ion density in the atmosphere. Their contribution to the total ionization is small, but may be important at specific locations. Similar discharges have also been observed during volcanic eruptions and dust storms (Kamra, 1969, 1972).

1.1.2 Ion Production in the Ionosphere

The primary sources of ionization in the earth's atmosphere are neutral atoms and molecules interacting with solar radiation including particle radiation and cosmic rays. When the high-energy photoelectrons/photons collide with neutrals, they produce positive ions and free electrons. These electrons and ions have energies about tens of electron volts (eV). These electrons can travel long distances in the ionosphere and produce more ionization by collision with other neutral atoms and molecules. This process continues until the electrons thermalize and attain the energy of few eV. These electrons are called thermal electrons and more than 90% flux of the ionosphere consists of these electrons.

1.1.3 Photochemical Processes

Solar ionizing radiations produce ions either directly or through some intermediate reactions. Due to the recombination or loss processes the ion pairs produced become neutral. The important reactions in the ionosphere are as follows (Krishna Murthy and Reddi, 2000).

(i)   Electron-Ion recombination:

Three body: $A^+ + e + M \rightarrow A + M$

Radiative: $A^+ + e \rightarrow A^*$

Dissociative: $AB^+ + e \rightarrow A^* + B^*$
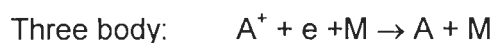
The excess energy of the excited particles is lost by radiation or collision. The three-body process is effective in D region where the neutral particle number density is quite high and is ineffective at greater heights. The radiative process is very slow and of little importance at ionospheric heights. Only in F region the chemical loss process may be faster but at such heights the transport process is dominant. However, in the E and F region dissociative recombination is the most important loss process.

(ii)   Ion-atom and charge exchange reaction:

$A^+ + BC \rightarrow AB^+ + C$ (ion-atom interchange reaction)

$A^+ + BC \rightarrow BC^+ + A$ (the charge exchange reaction)
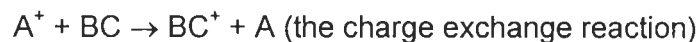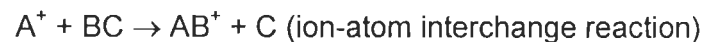
These processes are important in the E region where the atomic ions are dominant.

(iii)   Collisional detachment in the forward direction; three-body attachment in the reverse direction.

$$A^- + M \rightleftharpoons A + e + M$$
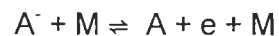
The three-body attachment is important in D region during day and night and in E region during night.

(iv)   Associative detachment in the forward direction and dissociative attachment in the reverse direction

$$A^- + B \rightleftharpoons AB + e$$

---
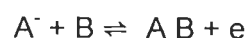
* means that the particle are left in an excited state.

These reactions are important in D and E regions especially during night and insignificant in the F region.

(v) Photo detachment in forward direction and radiative attachment in reverse direction

$$A^- + h\nu \rightleftharpoons A + e$$
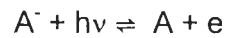
The photo detachment is important in D and E region and radiative attachment is important during nighttime in D region for the production of negative ions. The photo detachment is responsible for the absence of negative ions in the F region and radiative attachment is very week at these altitudes.

(vi) Ion-Ion recombination:

$$A^+ + B^- \rightarrow AB$$
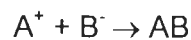
This reaction is important in D region where negative ions are appreciable in numbers. At higher altitude this process becomes less important due to drastic decrease of negative ions with height.

Here the symbols A, B and C denote neutral atoms, M a third molecule (which is required to carry away the excess energy released in the reaction) and e is an electron.

1.1.4 Ionospheric Temperatures

In the ionosphere the temperature of neutrals (T_n), ions (T_i) and electrons (T_e) are usually different. The solar Extremely Ultra Violet (EUV) radiation and X-rays etc. play an important role in heating of the ionosphere. In the process of photo-ionization the high-energy photoelectrons are produced. The collision of high-energy electron with neutral atoms/molecules increases

8

their internal energy (i.e. electronic excitation) and they radiate at longer wavelengths. Some other sources like seismic activity, volcanoes, thunderstorms and lightning/sprites also play a significant role in the local heating of the ionosphere. In early seventies it was believed that the heating efficiency of photons in the ionosphere was about 30% of total heating by all of its constituents (Chamberlin and Hunten, 1987). Later estimates brought down the efficiency to as low as 5%, with most of the energy going into space through air-glow emissions from atomic and molecular states excited through the inelastic collision process. Due to dissociation of molecular oxygen, a greater part of potential energy of ions is lost at lower latitudes. When the photoelectrons cool down to a few eV, they collide with ambient electrons (elastic collisions) and also with ions (coulomb collisions). The collisions with neutrals are more important below 200 km. Schunk and Sojka (1982) have found that generally electrons have more temperature than ions and neutrals and the ions have temperature in between the two. Figure 1.3 shows the average vertical temperature distribution in the earth's atmosphere with emphasis on the thermosphere (Banks and Kockarts, 1973).

1.1.5 Transportation of Ions

Transportation of ions also plays an important role in the observed charged particle density distribution at any geographical location and altitude. The most important transport process is the motion due to geomagnetic field and the collision of charged particles with neutrals. These produce forces, which are proportional to the difference of neutral wind and charged particle

9

velocities and the collision frequency. The daily temperature changes affect the ionization and hence it takes part in the thermal expansion and contraction.

The ionization diffuses under the action of gravity and its own pressure gradients. The electrical forces between ions and electrons tend to prevent any charge separation and thus cause electrons and ions to diffuse together, which is known as ambipolar diffusion (Krishna Murthy and Reddi, 2000). The diffusion process is rapid in the F region but slower in the lower ionosphere where collisions are more frequent.

1.2   THUNDERSTORMS AND LIGHTNING

Meteorologists classify a storm as a thundercloud or a thunderstorm, if it generates thunder. Since this acoustic disturbance has no other natural source, the presence of lightning (the electrical discharge between two opposite charge centers) is required. The lightning discharge may take place in other storms like cyclones and volcanoes. The thunderstorms are the most common source of lightning. Nuclear explosions are also known to produce lightning (Uman et al., 1972; Hill, 1973).

1.2.1 The Thundercloud

A thundercloud is generally formed when the atmosphere becomes unstable due to solar heating. When the atmospheric lapse rate exceeds the adiabatic lapse rate of the air mass, the buoyant parcel of warm air rises up and the water vapor condenses after reaching higher altitudes of the atmosphere; thus forming a convective cloud. The water drops freeze into ice particles after attending still greater heights. A typical convective cloud may

10

extend from +5° C to –50° C, where the hails, ice particles and the super cooled water drops are the major constituents.

Thunderclouds do not often produce lightning until they grow to a height of about 3 km. These are more frequent in tropics, semi-tropics and temperate zones and are rare in the polar region. In mid afternoon, when the solar heating and convection are at maximum over land, maximum formation of thunderclouds takes place. However, they can occur any time during day and night.

The main charge structure of the thundercloud is an electric dipole. The upper part of the thundercloud carriers a preponderance of positive charge, while the lower part carries a net negative charge and a small pocket of positive charge (Pathak et al., 1980). The diameter of the upper and lower charged regions of the cloud is of the order of few kms. The charges in the thundercloud can be separated through three main mechanism viz. (i) Convective mechanism (ii) Precipitation powered mechanism (iii) Electrochemical charge separation.

1.2.2 The Lightning Discharges

A lightning discharge is generally defined as a high current electric discharge, may give rise to the luminous channel having the lengths of the order of few kms. The discharge can take place between the two opposite charge centers of the cloud, or between the lower charge center of the cloud and the ground (Figure 1.4). The cloud discharges are the most frequent in nature, particularly in the tropical regions. The phenomena of ground

11

discharges are well studied and extensive literature is available on them (Wang, 1963; Markerras, 1968; Krehbiel et al., 1979; Christian et al., 1999 etc.).

Each ground discharge consists of one or more intermittent partial discharge. A total lightning with the time duration of about 1/3 sec is called a flash and each component discharge a stroke (luminous time duration of a stroke is tenths of a milliseconds). There are usually three or four strokes per flash and the successive strokes are separated by about 50 milliseconds. The total charge transferred per flash is observed to very from 3 Coulombs to as much as 90 Coulombs, the average value being 25 Coulombs.

1.2.3 Cloud to Ionosphere Lightning Discharges

In recent years a spectacular phenomena has been observed, which is known as lightning sprites or sprites or cloud to ionosphere lightning. Sprites are massive but weak luminous flashes that appear directly above an active thunderstorm system and are coincident with cloud-to-ground or intracloud lightning discharges (Bell et al., 1995; Otsuyama et al., 1999; Fishman et al., 1994; etc.). Their spatial structures range from small single or multiple vertically elongated spots, to spots with faint extrusions above and below, to bright groupings, which extend from the cloud top to altitudes up to about 95 km. Sprites are predominantly red. The brightest region lies in the altitude range from 65-75 km, above which there is often a faint red glow or wispy structure that extends to about 90 km (Bell et al., 1995; Otsuyama et al., 1999). Below the bright red region, blue tendril-like filamentary structures often extend

downward to as low as 40 km. Sprites rarely appear singly, usually occurring in clusters of two, three or more. Some of the very large events, such as shown in Figure 1.5, seem to be tightly packed clusters of many individual sprites (Wescott et al., 1995). Other events are more loosely packed and may extend across horizontal distances of 50 km or more.

Blue jets are the high altitude optical phenomenon, distinct from sprites, observed above thunderstorms using low light television systems. They are optical ejections from the top of the electrically active core regions of thunderstorms. Following their emergence from the top of the thundercloud, they typically propagate upward in narrow cones of about 15 degrees full width at vertical speeds of approximately 100 km/s, fanning out and disappearing at heights of about 40-50 km. In the fluctuation of mesospheric electric fields, conductivity of the stratosphere, mesosphere, and ionosphere and variation in the ionospheric temperature, the lightning sprites play an important role (Gupta, 1997; Inan, 1991; Pasko, 1995, 1996).

1.2.4 Electromagnetic Radiations from Lightning

The lightning discharge is a wide band transmitter of electromagnetic waves known as atmospherics. The radiations from lightning are detected in a wide frequency range from Ultra Low Frequency (ULF) to visible region and beyond. Some optical, acoustic and electrical measurements by different workers (Uman, 1969; Hill, 1979; etc.) have shown that most of the energy of lightning returns stroke (about 80-90%) is dissipated in producing thunder. Only about 0.04% is utilized in generation of electromagnetic radiations. The

13

remaining energy is used in the dissociation, ionization, excitation and kinetic energy of the particles present in the atmosphere.

An extensive work has been carried out on electromagnetic radiations from lightning in different frequency ranges viz. ELF (300 Hz – 3 kHz), VLF (3 kHz – 30 kHz) and frequency range greater than 30 kHz (Takagi and Takeuti, 1963; Taylor, 1963; Taylor and Jean, 1959; Horner and Bradley, 1964). However, most of the works pertain to the VLF emission, where the radiated power is maximum. The radiations in UHF and microwave regions are comparatively less understood. ELF and VLF frequencies are used as a source of magnetotelluric in the geophysical exploration.

The return stroke is a dominant source of atmospherics in the VLF range. K-changes and the horizontal lightning also emit the electromagnetic radiations in this frequency rage (Rao, 1967). The ELF components of atmospherics are thought to be the result of lateral corona currents flowing laterally between the leader channel and return stroke core. The atmospherics in the range of few MHz to about 100 GHz are mainly due to Bremsstrahlung from a partially ionized channel like stepped leader, K-changes and dart leader of a lightning flash (Rai et al., 1972; Rai, 1978; Cooray and Lundquist, 1982).

The electromagnetic fields of VLF radiations from lightning have been studied by many workers (Divya and Rai, 1985; Cooray, 1992; Jacobson et al., 2000; Rakov, 2002 and others). Divya and Rai (1985) were considered the ground to be perfectly conducting. Thus, only the vertical electric field component of atmospherics was studied and the horizontal electric field components were assumed to be zero. However, the ground is finitely

14

conducting. Therefore, the horizontal electric field component is also developed together with the vertical field components. The measurements of horizontal and vertical field components are used to determine the electrical conductivity of the earth (Divya and Rai, 1985).

1.2.5 Gravity Waves Propagation in the Ionosphere

Many of the motions and inhomogenities at the ionospheric heights have their origin in an organized fluctuation of the atmosphere, namely, in propagating atmospheric waves controlled by gravitational and compressional forces. Gravity waves play an important role in the dynamics and energy of the lower thermosphere (Fesen et al., 1995; Forbes and Vial, 1989; Forbes et. al., 1993; Fritts and Vincent 1987; Bristow et al., 1994). Solar UV heating as well as temporally varying momentum and energy inputs associated with magnetospheric processes can generate these waves. Rai (1974) showed that the gravity waves are generated by the thunderstorms, which propagate upward. After entering into the ionosphere, they become horizontal and cause the ionospheric disturbances. Tarantsev and Birfild (1973) had predicated that the acoustic waves are involved in the connection between seismic activity and the ionosphere. Molchanov and Hayakawa (1998) in their attempt to study the VLF signals of earthquake origin, argued that the seismogenic oscillations of the lower ionosphere boundary and related VLF signal are induced by resonant gravity waves generated during the process of earthquake preparation and relaxation. These gravity waves might be amplified at heights of 70-90 km due to a non-equilibrium situation connected with strong winds. In many theoretical

models a wind velocity of 80-100 m/s is used (Murgatroyad, 1970).

Shalimov (1992) has been studied the effect of gravity waves during seismic activity in relation to the variation of electron density in the ionosphere. He considered a few hour period gravity waves and assumed their generation by free seismic oscillations of the earth. The gravity waves with period of a few hours can only be possible when they are generated as whole process of precursory main and after shock period. In their laboratory experiment Yamada et al. (1989) observed that when rocks are fractured, they emit acoustic waves along with the electromagnetic emissions. The frequency range of electromagnetic and acoustic waves match the frequency of these waves observed during a earthquake. These acoustic waves in the atmosphere may get converted into acoustic gravity waves propagating upward with increasing amplitude, which affects the ionosphere (Rai, 1974).

1.3   SOLAR RADIATIONS

The energy from sun coming to earth is in the form of electromagnetic radiation. Most parts of this, penetrates into the earth atmosphere, is absorbed by the neutral atoms and molecule present in the upper atmosphere and only a few percent of the total flux of energy reaches the earth surface.

As one proceeds along the UV spectra of the sun towards shorter wavelengths, one finds the characteristics similar to the visible region, strong continuum with absorption lines gradually changing over the coronal type weak continuum with prominent emission lines. The change over takes place between 1600-2000 Å in the far ultraviolet region. Below 1600 Å, strong

emission lines dominate the spectrum. UV spectrum has the Lyman series of Hydrogen, ionizing Helium and other heavier atoms, while in X-rays region the emission lines due to highly stripped heavy atoms like *Fe* predominate. Study of these regions is possible only by rocket and satellite borne instruments.

1.3.1 Cosmic Rays

The cosmic rays are the charged particles from space. Those coming from galactic origin are known as galactic cosmic rays (GCR). Sun also emits streams of high-energy particles and these are known as solar cosmic rays (SCR). Due to the variation in the incident cosmic ray, the rate of ionization shows large variations with time in the SCR dominated region.

The galactic cosmic rays are almost isotropically distributed in the vicinity of the earth (Lanzerotti, 1977) and their intensity varies with time due to modulation over a solar cycle (Velinov and Mateyev, 1990). The incident flux is further altered by the earth's geomagnetic field before entering the earth's atmosphere (Ochabova, 1989). GCR penetrate deep into the earth's atmosphere because of their high range of energy from tens of MeV to hundred of GeV. Therefore, they produce secondary radiations in air, which reach to the surface of the earth. The SCR have comparatively low energies. Satellite observations indicate that intensity of the primary galactic cosmic rays in the vicinity of the earth is modulated over a solar cycle (Rosenberg and Lanzerotti. 1979). This incident flux are further altered by the earth's geomagnetic field before entering the atmosphere and their latitudinal variation depends on the particle's cut off rigidity (Goldberg, 1989). Hays and Roble (1979) suggested

17

that the galactic cosmic ray activity varies by about a factor of 2 in the lower atmosphere between the equator and pole and also the maximum ion production takes place at altitudes from 12 to 20 km depending upon the atmospheric conditions, phase of solar cycle and orography of the earth surface. Neher (1971) found from his balloon measurements that the ionization rate is a function of altitude and geomagnetic latitude. The low energy cosmic rays display greater variation over a solar cycle as compared to the high-energy cosmic rays.

1.3.2 Solar Flares

A flare is defined as a sudden, rapid and intense variation in brightness of sun. A flare occurs when magnetic energy that has built up in the solar atmosphere is suddenly released (Carrington, 1860). Radiation is emitted across virtually the entire electromagnetic spectrum, from radio waves at long wavelengths through the optical emissions and X-rays to γ-rays at short wavelengths. The amount of energy released is equivalent to millions of 100-megaton hydrogen bombs exploding at the same time. As the magnetic energy is being released, particles, including electrons, protons and heavy nuclei, are heated and accelerated (Anastasiadis, 1999; Kudryashev and Avakyan, 2000) in the solar atmosphere. During the solar flares, magnetic energy of the order of 10^{29} to 10^{33} ergs is released by means of magnetic reconnection (Anastasiadis, 1999). The energy released during solar flare is used in intense localized heating, particle acceleration and in mass flows (Priest, 1992).

1.3.3 Solar Wind

The solar wind streams off of the sun in all directions at speeds of about 400 km/s. The source of the solar wind is the sun's hot corona. The temperature of the corona is so high that the sun's gravity cannot hold on to it so that an appreciable amount of corona gas flows out of the sun's gravity. This results in a flow of steady stream of solar material and is called the 'Solar Wind'.

The solar wind is not uniform. Although it is always directed away from the sun, it changes speed and carries with it the charged particles. All the heavy and light particles move with the same velocity. The average velocity of the solar wind is about 400 km/sec. The solar wind interacts with the geomagnetic field lines and gives rise to micro-pulsations, geomagnetic storms and cause many other phenomena. The micro-pulsations on the other hand penetrate into the earth crust and generate magnetotelluric current. The measurement of electric and magnetic fields produce by this current over earth surface has formed a strong tool for electric conductivity determination with depth of the soil. This tool is known as the magnetotelluric method of Geoexploration.

1.4   A BRIEF SURVEY ON EARLIER IONOSPHERIC STUDIES

During last four decades the ionospheric weather has been studied extensively. These studies (Chestnov, 1956; Eack et. al., 2000; McCarthy and Parks; 1985; Parks et. al., 1981; Kleusberg, 1992; Kazimirovsky et al., 2003, etc.) include the experimental measurement of various ionospheric parameters

19

and the development of theoretical models and computer simulations of these parameters. Many theoretical models have been developed in order to determine the chemical composition and to determine the transport processes that affect ion composition, electron density as well as their thermal behavior in the ionosphere (Banks et. al., 1974; Brinton et. al., 1978; Knudsen, 1974; Knudsen et. al., 1977; Mahajan and Shastri, 1997; Schunk and Banks, 1975; Schunk et. al., 1976; Singh et. al., 1994; Spiro et. al., 1978; Vyas et. al., 1999; Watkins, 1978). These studies show that the ionospheric parameters are highly influenced by solar UV radiation, energetic particle precipitation, diffusion, thermospheric winds, electrodynamic drift, energy-dependent chemical reactions, solar flares, seismic activity, thunderstorms, lightning and sprites etc. In addition, the ionospheric parameters also vary with day-to-day, season, latitude, longitude, altitude and the 11-year solar cycle (Kazimirovsky et al., 2003).

The electron and ion temperature variations in the earth's ionosphere have been studied extensively through ground-based and *in situ* observations (Farley et al., 1967; Evans, 1973; Hanson et al., 1973; Oyama and Hirao, 1975; Titheridge, 1976; Brace and Theis, 1978; Oyama et al., 1985; Su et al., 1995; Watanabe et al., 1995; Bhuyan et al., 2000; Singh and Patel, 2001, etc.) and through theoretical calculations (Dalgarno et al., 1963; Geisler and Bowhill, 1965; Banks and Nagy, 1970; Mayr, 1972; Bailey et al., 1975 and others). Schunk and Raitt (1980) presented a model, which gives the information of ion composition like N^+, He^+, NO^+, O_2^+, N_2^+ and O^+. They found that the change in ionospheric composition and density due to solar cycle, seasonal and

geomagnetic activity variations has pronounced effect on the high latitude ion densities and composition. This study was limited to the daytime and performed for geographic 80° latitude.

The theoretical study of the ionospheric parameters like thermal conduction and diffusion at 73° N latitude was conduced by Schunk and Sojka (1982). They studied the ion temperature variations and density at middle and low latitudes. Figure 1.6 presents some results of ion (O^+) temperature variations for the same conditions as discussed above. In general, it was found that the ion temperature is higher in summer than winter in the solar maximum condition. At high altitudes the ion temperature profile becomes isothermal because of ion thermal conduction. The electron, ion and neutral temperature profiles with altitude have been presented in Figure 1.7 for solar maximum and solar minimum conditions for summer and low geomagnetic activity. At all altitudes ion temperature is considerably below the electron temperature.

The spatial and temporal variations of the electron temperature at equatorial anomaly latitudes has been studied by Su et al. (1996) using the Hinotori satellite at an altitude of about 600 km. Oyama et al. (1996a) have studied the morning overshoot of electron temperature (Te) by the downward plasma drift in the equatorial topside ionosphere and found that the rapid increase in electron temperature in the early morning period is consistent to the well known phenomenon called 'morning overshoot'. Oyama et al. (1996b) have also studied the seasonal, local time and longitude variations of the electron temperature at a height of about 600 km in the low latitude region. They found that an electron temperature enhancement occurs in the morning

period (between 5:00 to 8:00 LT). The peak value is highest at the magnetic equator and reaches about 5000°K for the high solar activity.

Afraimovich et al. (2001) has studied the ionospheric effects of the solar flares of September 23, 1998 and July 29, 1999 with the help of GPS network data. They found that there was no effect of the solar flares on the night side ionosphere. Thome et al. (1971) theoretically studied the effect of solar flares on electron density and found an electron density enhancement in the E and F region of the ionosphere during solar flares.

Many other agencies like thunderstorms, lightning, sprites, seismic and volcanic activities etc. may also change the ionospheric temperatures and density, whose contribution to the total ionization and heating is small but important for the local regions. An enhancement in ionospheric electron and ion temperatures has been attributed to different kind of lightning activity during a thunderstorm. Recent observations of optical phenomena such as red sprites, blue jets, blue starters, elves and associated phenomena above an active thunderstorm also play an important role in changing the ionospheric parameters (Lyons, 1994; Sentman and Wescott, 1993; Sentman et al., 1995; Wescott et al., 1996; Inan et al., 1996; Taranenko, 1993a; 1993b).

1.5 PRESENT WORK

Present work is devoted to the study of ionospheric electron and ion temperatures variation in the low latitude $F2$ region (altitude ranges 425-625 km) over India during the period from 1995 to 1998, which includes solar minimum year (1995-96). The diurnal, seasonal and latitudinal behavior of

ionospheric electron and ion temperatures over Indian region has been studied. Further, detailed studies of the effects of sunrise, solar flares and active thunderstorms on the ionospheric plasma temperatures have also been done. The data for these studies were obtained by Retarding Potential Analyzer (RPA) payload aboard SROSS-C2 satellite during the period from 1995 to 1998. Thunderstorm data were obtained from India Meteorological Department (IMD) and the Solar flares data from National Geophysical Data Center (NGDC), Boulder, Colorado, U. S. A. The International Reference Ionosphere (IRI-95) model values for the same period were also used for the present study wherever necessary for compression and data analysis. Intensive work have been conducted in the data selection, processing and statistical analysis to draw useful conclusions. The present thesis is a systematic presentation of the work done on the behavior of ionospheric plasma temperatures (annual, seasonal and diurnal variation) and its response to thunderstorms, solar flares and sunrise. Some studies on tropospheric aerosols in relation to some meteorological parameters were also carried out and the same is presented in the appendix.

The data source, selection, study region and a brief description of RPA payload aboard SROSS-C2 satellite used in the measurement of ionospheric temperatures have been presented in Chapter-II. The diurnal, seasonal and latitudinal variation of ionospheric temperatures of the topside *F* region ionosphere over India during the solar minimum year (1995-96) at an average altitude of ~500 km have been presented in Chapter-III. The sunrise effect on the ionospheric electron and ion temperatures as measured by the SROSS-C2

satellite during the period from 1995 to 1998 (which cover the solar minimum year of 1995-96) for specific location of Bhopal (23.16° N, 77.36° E) and Chennai (13.04° N, 80.19° E) in India have been presented in Chapter-IV. The effect of thunderstorms on ionospheric temperatures has been presented in Chapter-V. The effect of solar flares on ionospheric electron and ion temperatures over the topside F region has been presented in Chapter-VI. The summery of work done in the present thesis and the conclusions have been presented in Chapter-VII.

An Appendix has also been added to the thesis, which describes the work done on aerosol studies. It reviews the studies on aerosol generation, distribution and different mechanisms involved in aerosol formation and their relation to meteorological parameters. A brief description of the instrument used for aerosols study has also been given.
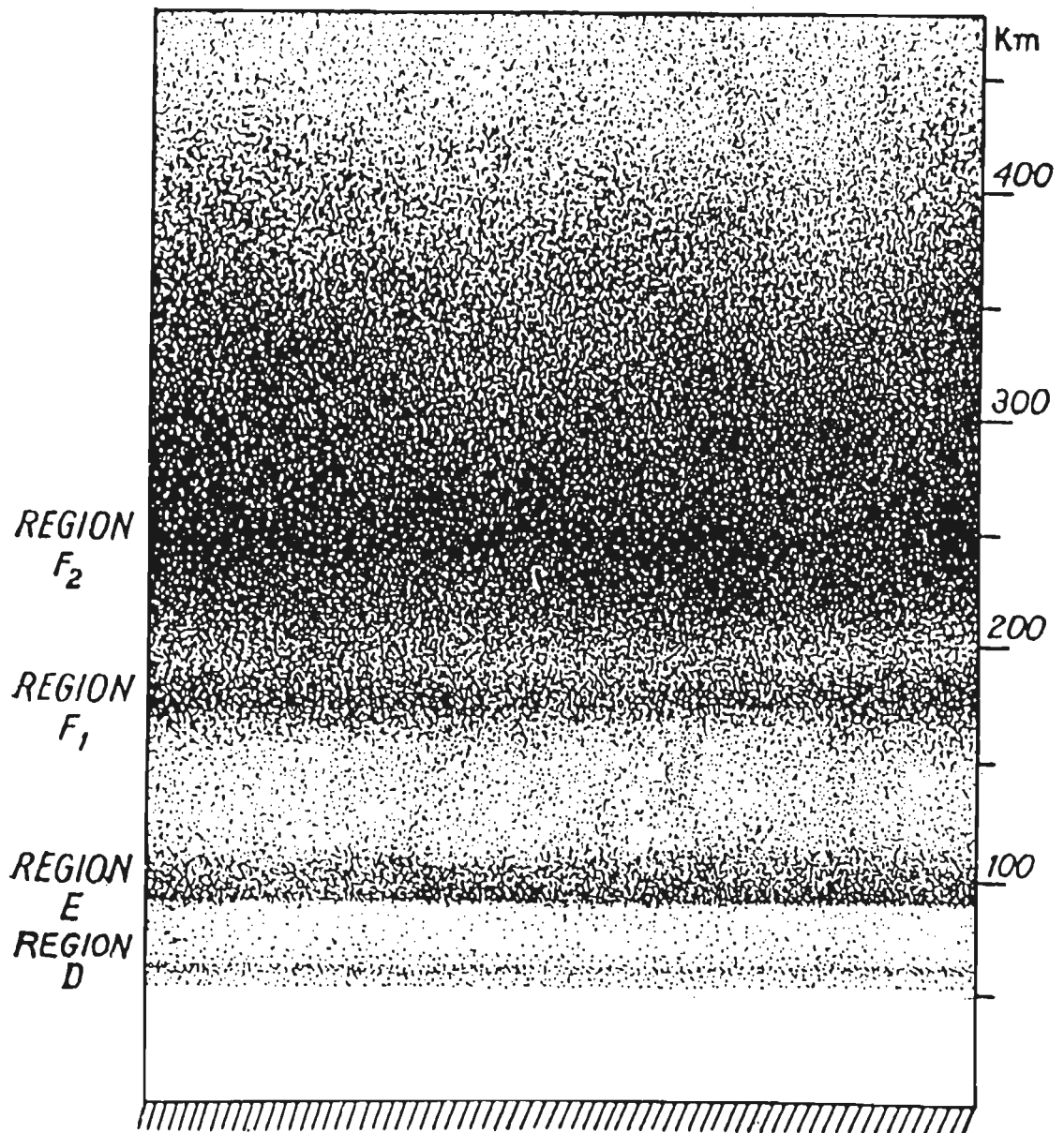
Figure 1.1   Ionized regions of the upper atmosphere. The relative density of ionization is roughly indicated by the depth of shading. Region *D* is mainly an absorbing region. At night this region disappears and also *F1* and *F2* coalesce to the form a single region *F* (Mitra, 1992).
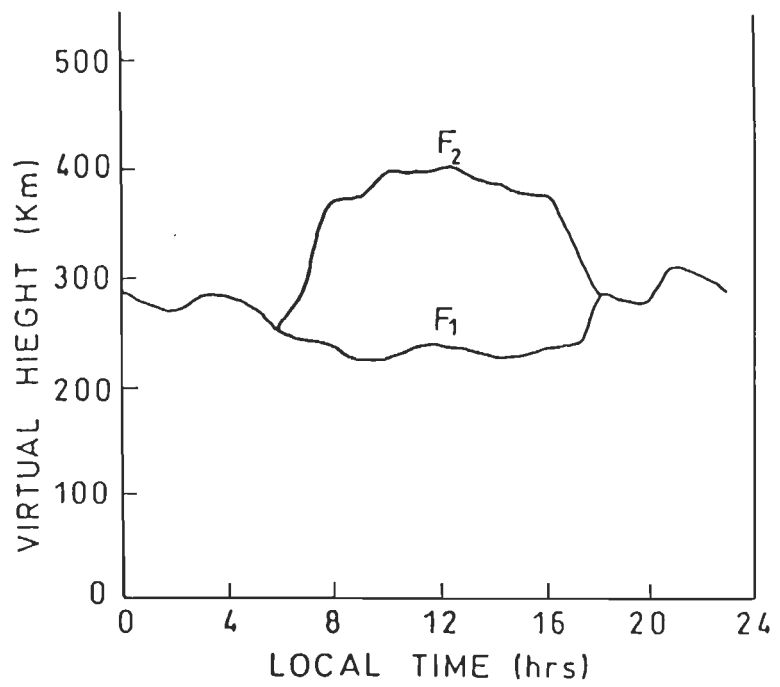
Figure 1.2   The daytime splitting of *F* region into *F1* and *F2* at Canberra (Mitra, 1992).
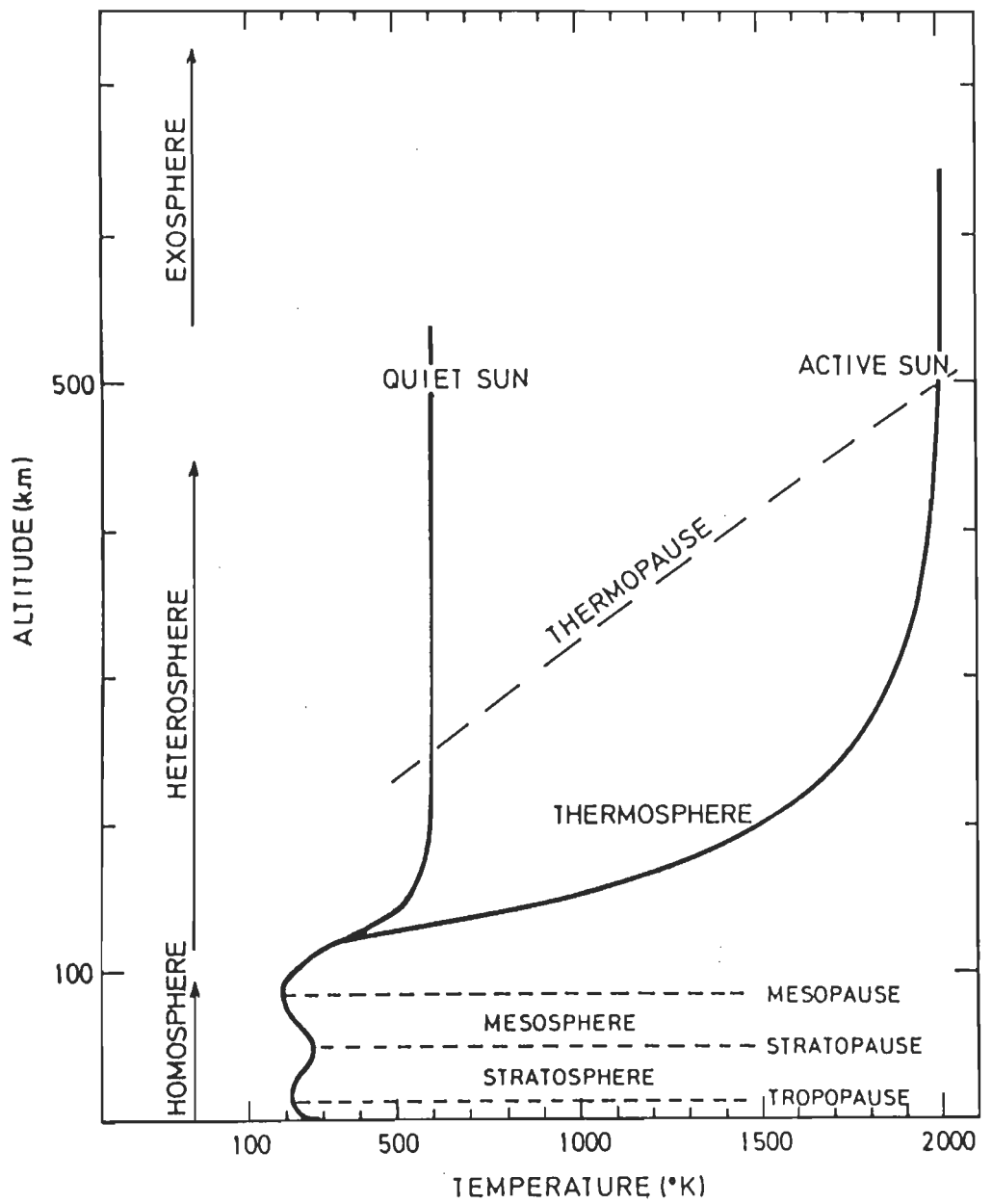
Figure 1.3 Vertical temperature distribution in the earth's atmosphere with emphasis on the thermosphere (Banks and Kockarts, 1973).

DISCHARGE WITHIN CLOUD
BETWEEN BASE AND POSTTIME
TOP IN TRA - CLOUD

INTER - CLOUD STRIKE
CLOUD TO CLOUD

DISCHARGE BETWEEN NEGATIVE AND POSITIVE CHARGE CENTERS

TYPICAL CLOUD TO GROUND
LIGHTNING BETWEEN GROUND AND
NEGATIVE CHARGE CENTERS
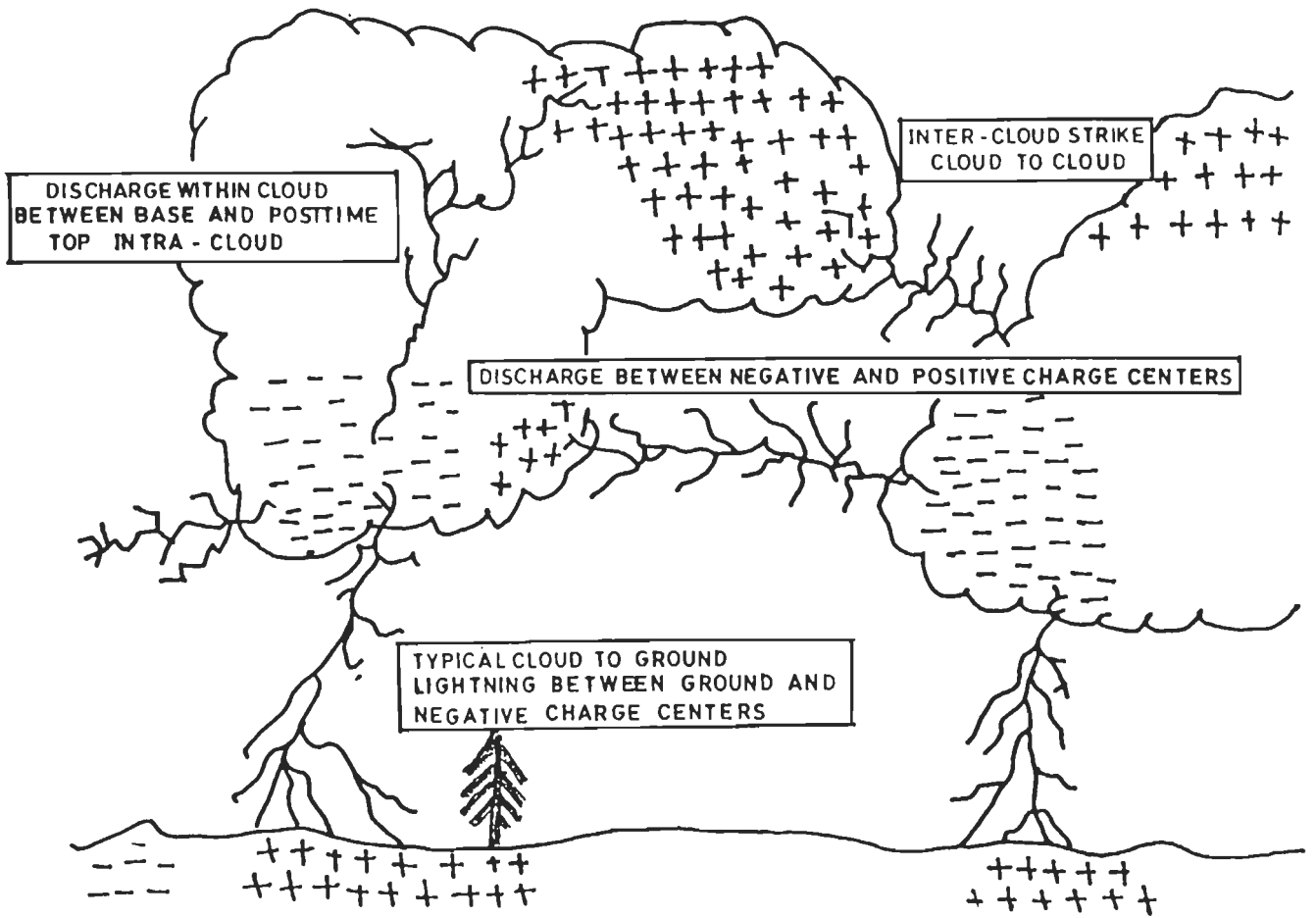
Figure 1.4   Different form of lightning discharges.
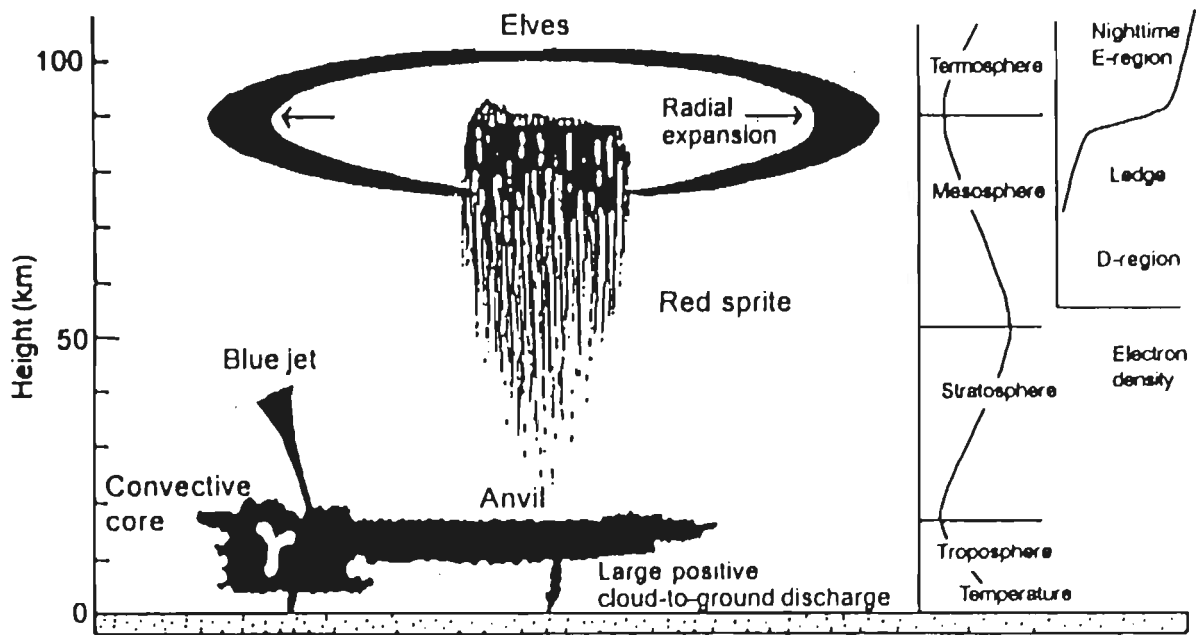
Figure 1.5   Upper atmospheric optical emissions excited by thunderstorms (Wescott et al., 1995).
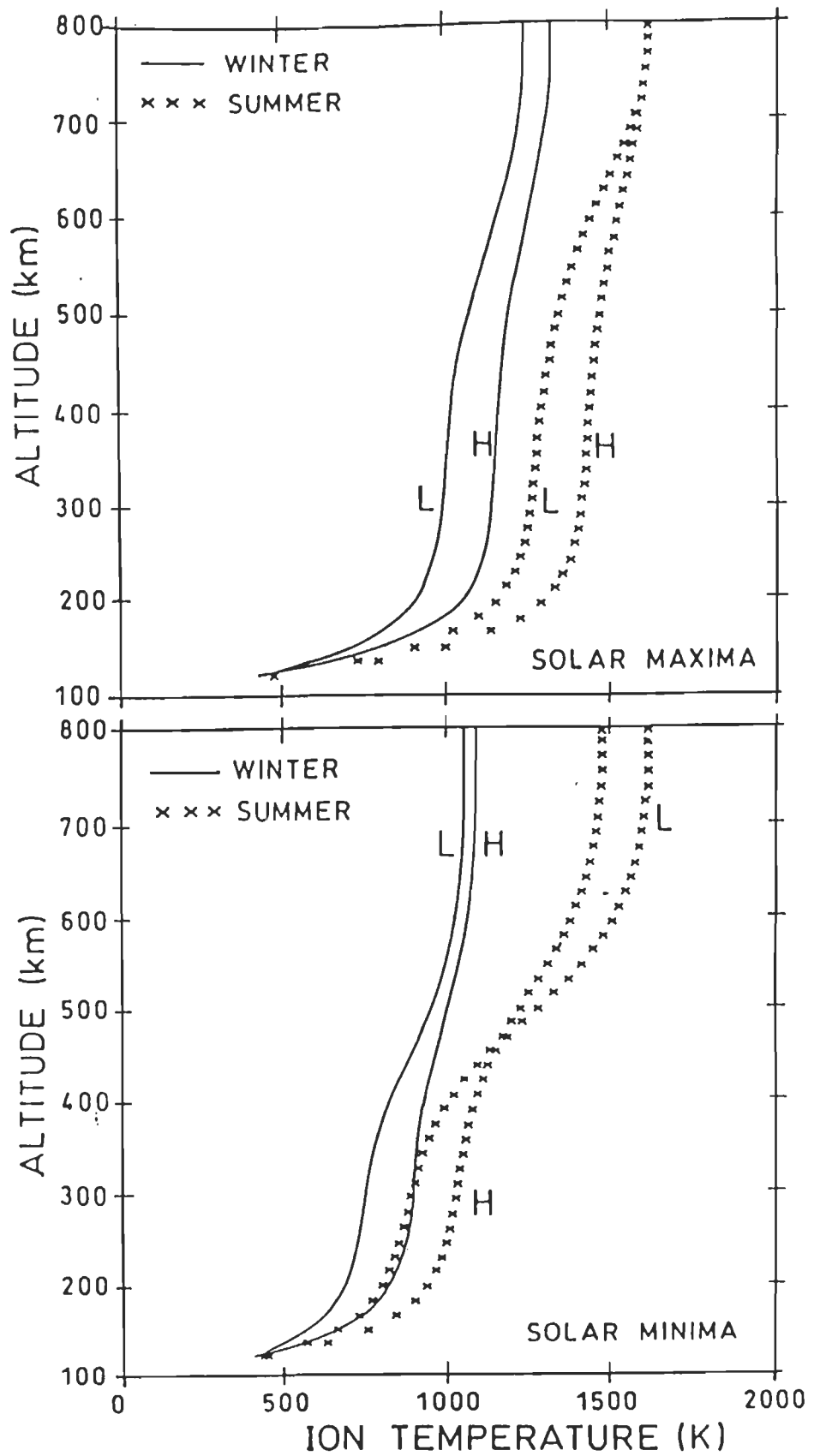
Figure 1.6 Ion (O^+) temperature profiles for solar maximum and solar minimum for summer and winter and for high (H) and low (L) geomagnetic activity (Schunk and Sojka, 1982).
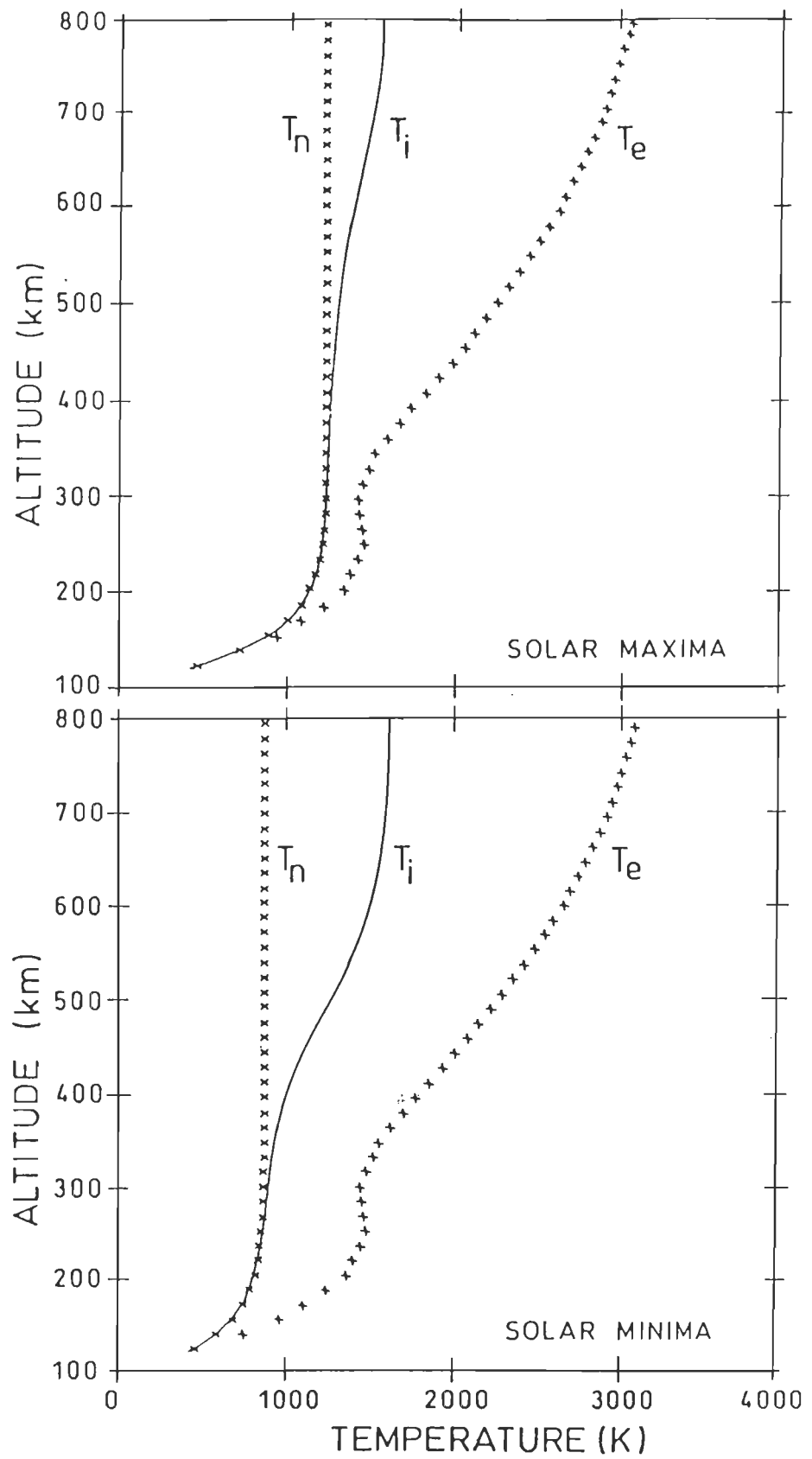
Figure 1.7 Ion (O$^+$), electron and neutral temperature profiles for solar maximum and solar minimum for summer and low geomagnetic activity (Schunk and Sojka, 1982).

Chapter 2

Data Source, Selection And Determination Of Ionospheric Parameters

During last four decades many researchers have studied the ionosphere extensively. These studies include experimental measurement of ionospheric parameters as well as development of theoretical models for estimating those parameters. The experiments can be performed with the help of balloons, rockets, satellites, coherent and incoherent scatter radar, magnetometers and a number of ground-based instruments (Farley et al., 1967; Evans, 1973; Hanson et al., 1973; Oyama and Hirao, 1975; Titheridge, 1976; Brace and Theis, 1978; Oyama et al., 1985; Kleusberg, 1992; Su et al., 1995; Watanabe et al., 1995; Bhuyan et al., 2000; Joshi, 2001 and others). Many globalize models were also developed to study the ionosphere (Dalgarno et al., 1963; Geisler and Bowhill, 1965; Banks and Nagy, 1970; Mayr, 1972; Bailey et al., 1975; Schunk and Raitt, 1980; Schunk and Sojka, 1982 and others). It has been well established that ionospheric properties change with altitude, latitude, longitude, universal time, season, solar cycle and geomagnetic activity. These changes occur due to solar UV radiation, energetic particle precipitation, diffusion, thermospheric winds, electrodynamic drifts, energy-dependent chemical reactions, solar flares, sunrise effect, seismic activity, thunderstorms, lightning and sprites etc. These processes affect the density, composition, and temperatures of ion, electron and neutral in the ionosphere. At mid-latitudes, the average electron density distribution tends to be uniform, with a gradual transition from dayside high densities to night side low densities.

The ionosphere may vary in composition and temperature appreciably from hour to hour, day to day and season to season. The ionospheric weather disturbances can affect over-the-horizon radars, transionospheric radio signals surveying and navigation systems that use global positioning system (GPS), satellite tracking, satellite lifetime, power grids and meganetetullric sources on the earth (Chamberlin and Hunten, 1987; Kleusberg, 1992; Shapka, 1992 and others).

There are several agencies with whom the infrastructure has been created to study the ionospheric system and their effects on other natural atmospheric processes and many man-made activities. National Aeronautics and Space Administration (NASA), National Oceanic and Atmospheric Administration (NOAA), Indian Space Research Organization (ISRO), European Space Agency (ESA) etc. are playing a leading role in the study of the ionosphere.

The description of the Retarding Potential Analyzer (RPA) payload of Stretched Rohini Series Satellite (SROSS-C2) launched by ISRO has been presented in this chapter. This chapter also deals with the details of data source, selection and analysis, which are used in the study of the ionospheric temperature anomalies.

2.1   SROSS-C2 Satellite and RPA Payload

The SROSS-C2 satellite was launched with the help of Augmented Satellite Launch Vehicle (ASLV-D4) rocket on May 4, 1994 in the orbit of about 930 km x 425 km. After two months of its operation the apogee of satellite was

brought down to about 625 km and operated continuously for seven years. The satellite returned to earth on July 12, 2001. SROSS-C2 was the fourth satellite of the Stretched Rohini Series Satellite Programme of ISRO and it was designed, developed, fabricated and tested in ISRO Satellite Center (ISAC), Bangalore. The weight of the satellite was 114 kg, which carried 6 kg hydrazine fuel and generated 50-watt onboard power (Garg and Das, 1995). Figure 2.1 shows the configuration of satellite with its main parts. Orbital inclination of the satellite was 46° with the equatorial plane. This was a spin-stabilized satellite with its spin axis perpendicular to its longitudinal axis and the rate of spin was 5 revolutions per minute (rpm). The orbital motion of the satellite is shown in Figure 2.2. The satellite moves in the orbit keeping the spin axis perpendicular to the orbital plane. In this kind of orbital motion RPA sensors face the velocity vector once in each spin cycle of satellite. The angle θ between the sensor normal and satellite velocity vector keeps on changing from 0 to 360° at the rate of 30°/sec. The RPA measurements are taken when the sensor normal faces the satellite velocity vector. But in a spin stabilized satellite this situation remains for a fraction of a second. The RPA sensors collect data within ±30° (for ions) and within ±90° (for electrons) of the satellite velocity vector once in each spin period.

The Retarding Potential Analyzer (RPA) payload was designed and developed at National Physical Laboratory (NPL), New Delhi for SROSS series of satellites. The RPA payload was switched on in orbit first time on May 21, 1992 using SROSS-C satellite through ground commands issued from ISRO Satellite Tracking Canter (ISTRAC), Bangalore. Again on May 4, 1994 the RPA

payload placed in orbit by SROSS-C2 mission. NPL was taken up to design and develop the RPA for SROSS series of satellites under SROSS aeronomy satellite project (SASP). The instrument was designed for minimum power consumption, size and weight to have maximum possible reliability and flexibility of its operation in space through ground commands.

The RPA payload consists of two sensors, viz. electron and ion sensors and associated electronics. The electron and ion RPAs are used for *in situ* measurements of ionospheric electron and ion parameters. In addition, a spherical Langmuir probe is included and is used as a potential probe for estimating the variation of spacecraft potential during spinning of the satellite. The electron and ion sensors both have planar geometry and consist of multi-grid Faraday cups with a collector electrode. The different grids in the sensor are designated as the entrance grid, the retarding grid, the suppressor grid and the screen grid. These grids are made of gold-plated tungsten wire mesh having 90-95% optical transparency. The two sensors are mechanically identical but have different grid voltages suitable for the collection of electrons and ions, respectively. The charged particles whose energies are greater than the applied voltage on the retarding grid pass through various grids and finally reach the collector electrode to cause the sensor current. This current is measured by a linear auto-gain ranging electrometer.

2.2   Objective of SROSS Mission

The scientific objectives of SROSS mission are (Garg et al., 1992):

(i)   To study the behavior of electron and ion density and temperature anomaly in the low latitude region.

(ii)   To study the special features of the energetics of equatorial and low latitude ionosphere.

(iii)   To establish the response of the thermal structure to the dynamical effects.

(iv)   To study the effects of magnetic storms and spread F on thermal structure.

For achieving these scientific objectives the RPA payload measured the following ionospheric parameters:

(a) Total ion density N_i

(b) Ion temperature T_i

(c) Ion composition O^+, O_2^+, NO^+, H^+, He^+

(d) Electron temperature T_e

(e) Suprathermal electron flux (STEF) (upto 30 eV)

(f) Irregularities in the electron and ion densities

(g) Satellite potential with respect to plasma

Accuracy of measurements:

Parameter	Accuracy
N_i and N_e	$\pm 5\%$
T_i and T_e	± 50 K
STEF	$\pm 10\%$

2.3 The Principle of RPA Operation

The RPA sensor is analogous to pentode vacuum tube where ionospheric plasma serves as the cathode. The ion and electron enter the sensor through its open aperture and pass through the region, which is electrically segmented by a series of very fine gold plated tungsten wire electrode and then reach the collector electrode. The current thus collected over the collector plate varies from tens of microamperes down to the fraction of pico-amperes. By changing the bias voltage on the retarding grid, different energy electrons/ions reach the collector plate to cause the collector current. This gives the measurement of flux in different energy ranges. Characteristic curves (Figure 2.3) of the collector current (I) versus retarding grid bias (V) are generated separately for electrons and ions. These characteristic curves are used for deriving different ionospheric parameters of interest.

2.4 Data Source, Selection and Analysis

The RPA data were obtained from National Physical Laboratory (NPL) under the Indian Space Research Organization (ISRO) programme "Scientific utilization of SROSS-C2 data". The raw data have been obtained in the form of LOTUS file. These files are divided into months and marked the data corresponding to satellite orbit number from separate dated file. The data have been marked for four years from January 1995 to December 1998. To study the behavior of ionospheric temperatures, their diurnal, seasonal and latitudinal variations during solar minimum year (1995-96) over Indian region and

temperature anomaly related to solar phenomena and thunderstorms during the period from 1995 to 1998 over different location in India.

2.4.1 Determination of ion density from ion RPA data

For determining the total ion density during a satellite pass, the selected file data sets satisfy the following conditions (Garg et al., 1996):

(i)   The angle θ should be less than 20° or more than 340°

(ii)   The ion RPA retarding grid bias is zero volt

The selected data is then subjected to $cos\theta$ correction i.e. ion current is divided by $cos\theta$. Then the total ion density is calculated by the following formula

$$N = \eta A e U_s I \tag{2.1}$$

where, N = Total ion density, η = efficiency of the sensor = 0.5

A = collector area = 20 cm^2, e = electron charge = 1.6×10^{-19} C

U_s = satellite velocity = 7.8 km/sec, I = $cos\theta$ corrected ion current

2.4.2 Determination of ion temperature and composition

Ionosphere is known as multi-constituent plasma populated by different ion species. The most common ion species of our interest in the altitude range from 425-625 km are O^+, O_2^+, NO^+, H^+ and He^+. These ions retarded at different voltages due to their masses, result in the decrease of ion current at different voltages corresponding to the ion masses giving rise to a composite I-V curve as shown in Figure 2.3 (a). The ion current reaching the sensor in response to the retarding voltages is governed by the equation (Garg et al., 1996).

$$I = AeU_s\eta\cos\theta\sum_{i=0}^{n}N_i\left\{\frac{1}{2}+\frac{1}{2}erf(x)+C_i\frac{\exp(-x^2)}{2\sqrt{\pi}U_s\cos\theta}\right\}$$ (2.2)

where, θ = angle between the velocity vector and probe normal

N_i = density of ith ion (m^{-3})

$x = U_s\cos\theta - [\{e(V+V_s)\}^{1/2}/kT_i]$,

V_s = the satellite potential w.r.t. plasma,

V = probe potential w.r.t. satellite,

k = Boltzmann constant = 1.38×10^{-23} JK^{-1}

$C_i = (2kT_i/m_i)^{1/2}$, most probable velocity of the ion constituent

T_i = ion temperature (K), m_i = mass of ion (kg)

Once the I-V curve is obtained, the main task is to recover the ion density and temperature using the above equation. Ion density gives the total ion concentration as well as information on the composition of the major ion constituents. Satellite potential is also one of the unknown parameters. The U_s and θ, are available from the measurements. Equation (2.2) is a non-linear equation and therefore unknown parameters are obtained by computerized curve fitting (Garg et al., 1996). The approach is that the computer programme first constructs a model I-V curve with the help of the above equation by using typical values of the unknown variables N_i, T_i, V_s, which are selected as reasonable approximations for the anticipated ambient ionospheric conditions. Estimation procedure involves adjusting these parameters in the computer generated curve applying least square method of minimizing standard errors. By iteration we update the model curve step by step using the variables. Every time the standard error is calculated and iterations are continued until the best

least square fit to the measured curve is obtained. When the two curves match, the fitted variables will yield the needed plasma parameters corresponding to the experimental curve.

The saturation current around zero volt retarding voltage gives the total ion density as all the ions reach the sensor and collected by probe without any retardation. Equation (2.2) reduces to

$$I_{i,o} = N_i e\eta A U_s \cos\theta \qquad\qquad (2.3)$$

where, $I_{i,o}$ = Saturation current for the ith ion at zero retarding voltage

Therefore total ion density can be calculated first by knowing U_s and θ without having any information of T_i and V_s.

To find the temperature from I-V curve from RPA data, the limit of theta ±40° is considered for ion temperature analysis. For generating I-V curve 64 sets of data are taken in one complete sweep. Each set of data is collected after every 22 msec; duration of each sweep becomes 1.408 sec. During this period retarding grid voltage is swept from 0 to 22 V in up and down sweeps and theta changes by 45° at 5 rpm spin rate (Garg and Das, 1995). For each sweep of ion RPA one set file is created. The T_i values and different ion compositions so derived are put in a file in a specified format. The file is finally processed in MS Excel program.

2.4.3 Determination of electron temperature

The I-V curve obtained from the electron RPA curve is shown in Figure 2.3 (b). Here the log of electron current measured by the probe is plotted against the retarding grid voltage. Three distinct regions are identified in this

curve. When the probe voltage is positive relative to plasma, electrons are accelerated towards the probe and a fairly flat saturation portion of the probe characteristics obtained. When the probe voltage is made negative with respect to plasma, the incoming electrons experience a retarding field and the probe current decreases exponentially resulting in retarding region of characteristic. The region is linear on a semi log scale. As the probe is made more negative, the low energy thermal electrons repelled away. But probe still collects a small current, which is due to higher energy suprathermal electrons. The lower flat portion of the curve denotes the suprathermal region. In the daytime this flux is more and also get contaminated by the plate electrons if its probe is sunlit. The retarding region of I-V curve is related to the distribution of electron energies and hence can be used to obtain electron temperature (T_e).

The relationship between the collector current (I) and retarding grid voltage (V) can be given by

$$I_e = I_o \exp\left[\frac{-e(V + V_s)}{kT_e}\right] \qquad (2.4)$$

where, $I_o = \frac{1}{4}\eta e A N_e U_e =$ the random current when probe is at plasma potential i.e. for $V+V_s = 0$

η = Efficiency of the probe, A = area of the probe = 20 cm^2

N_e = electron density (m^{-3}), e = electron charge = 1.6×10^{-19} C

U_e = mean thermal velocity of the electron = $\sqrt{\frac{8kT_e}{\pi m_e}}$

m_e = mass of electron = 9.1×10^{-31} kg

T_e = electron temperature (K), V = retarding grid voltage w.r.t satellite

V_s= satellite potential w.r.t. plasma

Equation (2.4) may be written as

$$\ln I_e = \ln I_o - \frac{e(V + V_s)}{kT_e}$$ (2.5)

During a single I-V curve the satellite potential can be assumed to remain constant. Therefore I_o and V_s may be taken as constant. The above equation represents a linear relationship in $\ln I_e$ and V with slope (e/kT_e), the temperature can be determined from the slope of the semi logarithmic plot of the I-V curve. Therefore above equation now becomes

$$\frac{d}{dV}(\ln I_e) = -\frac{e}{kT_e}$$ (2.6)

By using the values of e and k the electron temperature can be obtained easily from equation (2.6). The slope of the linear region of the I-V curve gives the electron temperature. The approach that has been adopted for evaluating the slope is the linear curve fitting in which least square technique is employed to fit a straight line to the measured data in the retarding region. The data within $\pm 60°$ of the angle of θ limits has been considered for electron temperature analysis and the file is finally processed in MS Excel program.

2.5   Thunderstorms Data

The data on thunderstorms have been obtained from India Meteorological Department (IMD), Pune for the same period. Thunderstorm is the main source of lightning/ sprites, which influence the ionospheric temperatures. To study the influence of lightning/ sprites and it's effects on the ionospheric temperatures in *F2* region, the thunderstorm data for ten different

35

low latitude locations: Aurangabad (19.53° N, 75.23° E), Bhopal (23.16° N, 77.36° E), Chennai (13.04° N, 80.17° E), Cochin (09.58° N, 76.17° E), Indore (22.44° N, 75.50° E), Nagpur (21.09° N, 79.09° E), Panji (15.30° N, 73.55° E), Pune (18.31° N, 73.55° E), Trivandrum (08.29° N, 76.59° E) and Varanasi (25.20° N, 83.00° E) in India have been obtained from IMD. These IMD locations are shown in Figure 2.4 in a map of India. These locations were chosen for the maximum number of passes of satellite SROSS-C2 over India in the altitude range 425-625 km.

2.6   Solar Flares Data

Many agencies may play important role in changing the ionospheric temperature in $F2$ region. One of them is the solar flare, which directly affects the ionosphere and radio communication on earth and also releases energetic particles into the space. These energetic particles accelerated in space are dangerous to astronauts and interfere with the electronic systems in satellite and spacecrafts. The effect of solar flare on the earth's ionosphere has become an important study of the day. For this purpose, the data on solar flare has been obtained from National Geophysical Data Center (NGDC), Boulder, Colorado (USA) from the period 1995 to 1998 in the present study.

2.7   The International Reference Ionosphere

The International Reference Ionosphere (IRI) is an international project sponsored by the Committee on Space Research (COSPAR) and the International Union on Radio Science (URSI). The IRI model data for the same

period were downloaded from the Internet and used for the purpose of comparison. The IRI describes the median or average value of electron density, ionospheric temperatures (electron, ion and neutrals temperatures) and ion composition as a function of height, location, local time and sunspot number for magnetically quite conditions. It is an empirical model based on the data from the worldwide network of ionosonde stations, incoherent scatter radar, the ISIS and Alouette topside sounders and *in situ* measurements by several satellites and rockets. We have used the IRI-1995 model to find out the enhancement in ionospheric parameters during disturbed conditions taking it as a reference level.

The next chapter presents our studies on the diurnal, seasonal and latitudinal variations of ionospheric temperatures during the solar minimum year 1995-96.

BELT ARRAY

VHF ANTENNA

POTENTIAL SENSOR

GAMMA RAY ELECTRONICS

GAMMA RAY DETECTOR

BELT ARRAY

ELECTRON SENSOR

ION SENSOR

POWER ELCTRONICS
RPA ELCTRONICS
VHF TRANSMITTER
MAGNETOMETER
VHF RECEIVER
SENSOR ELECTRONICS
THERMOCOUPLE JUNCTION
PAY LOAD DATA HANDLING
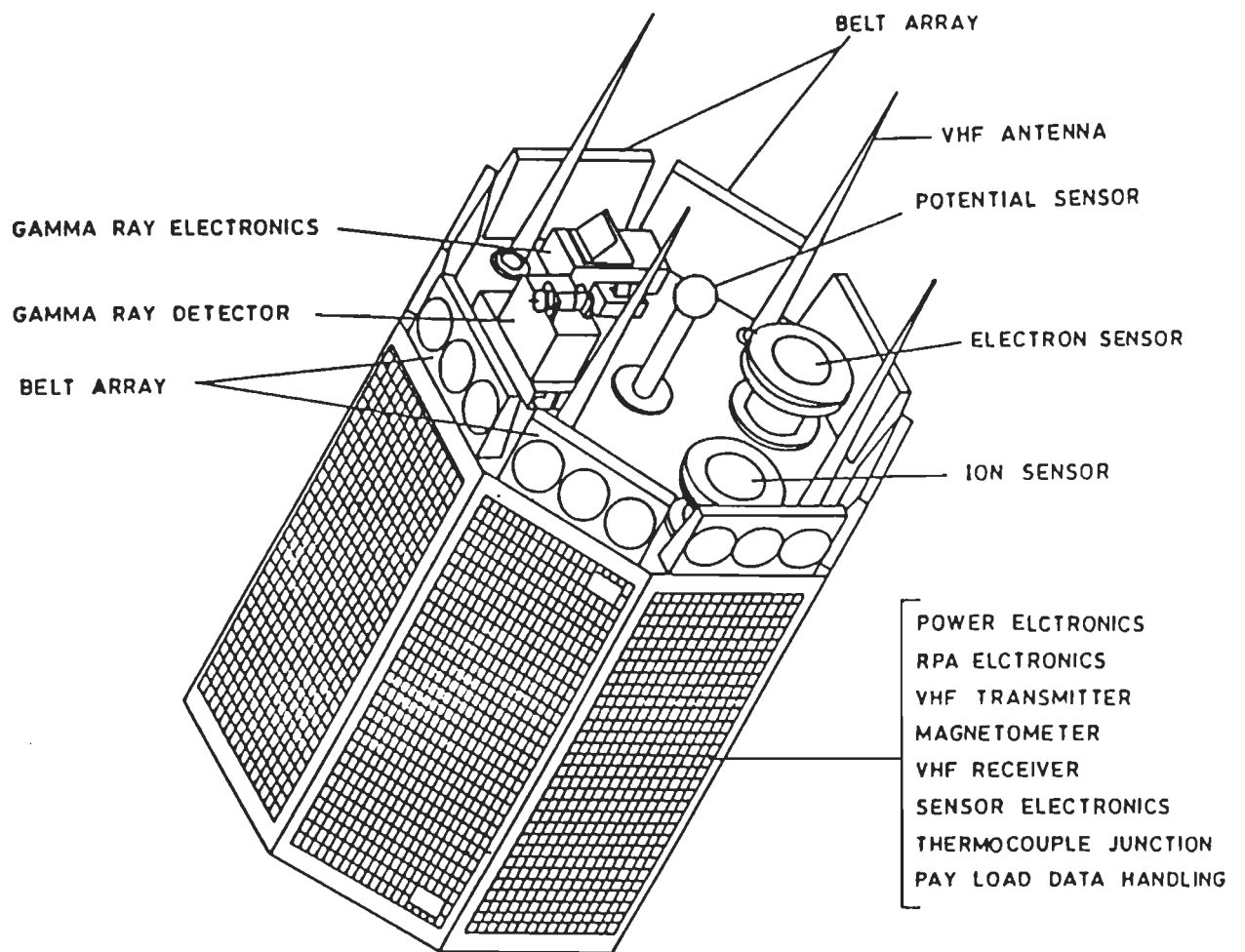
Figure 2.1 Orbital configuration of SROSS-C2 satellite (Garg et al., 1996).
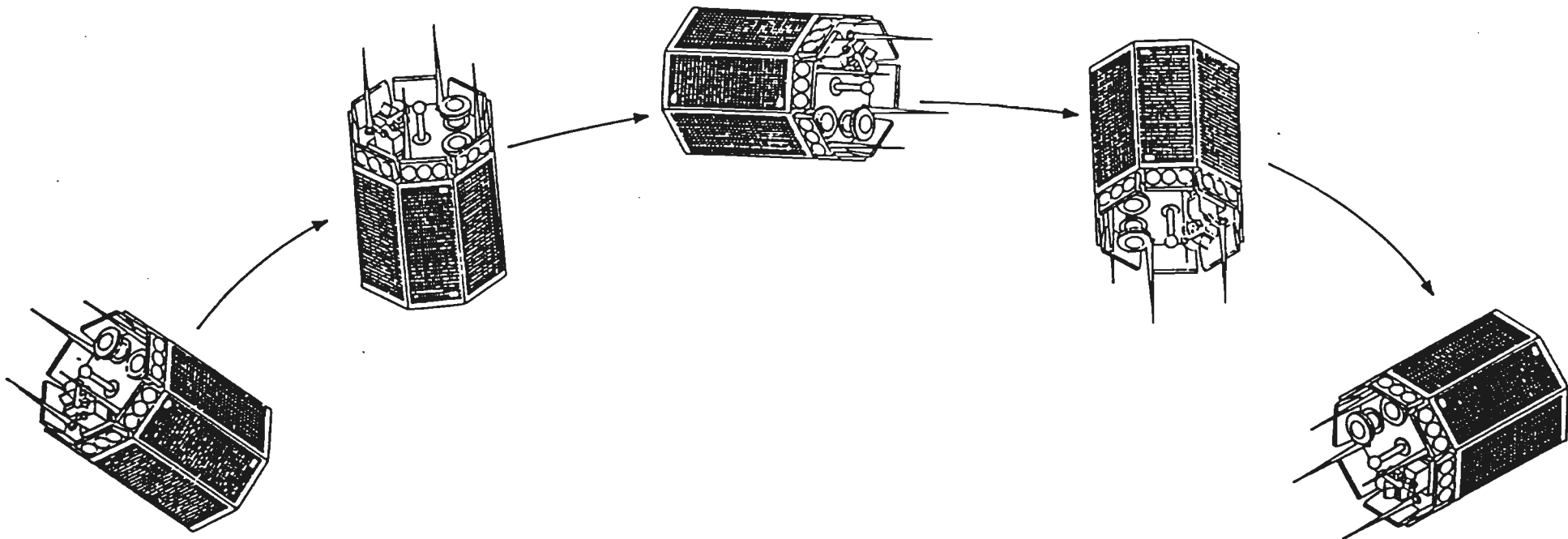
Figure 2.2   Motion of SROSS-C2 satellite in orbit (Garg et al., 1996).

ION-RPA CURVE

(a)

H⁺, He⁺

O⁺ → Vs

→ ION TEMPERATURE

O₂⁺, NO⁺

CURRENT (Amp)

RETARDING POTENTIAL (Volt)

ELECTRON-RPA CURVE

(b)

SATURATION

ELECTRON TEMPERATURE → RETARDING

SUPRATHERMAL FLUX

CURRENT (Amp)

RETARDING POTENTIAL (Volt)
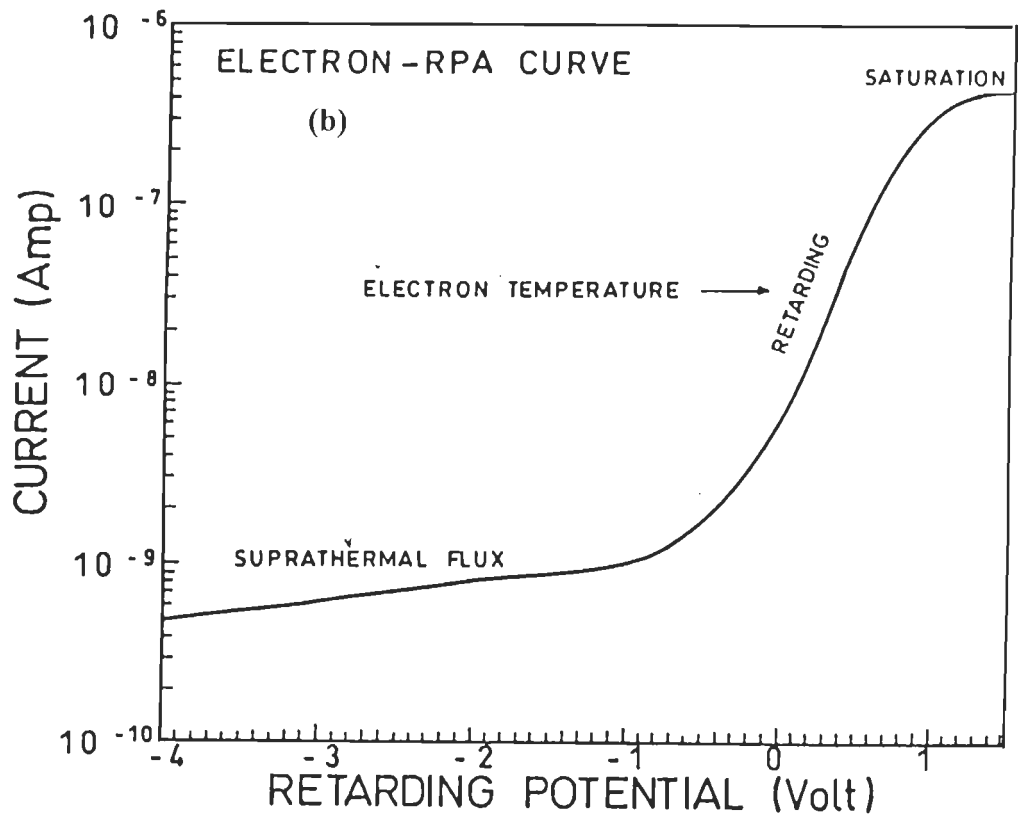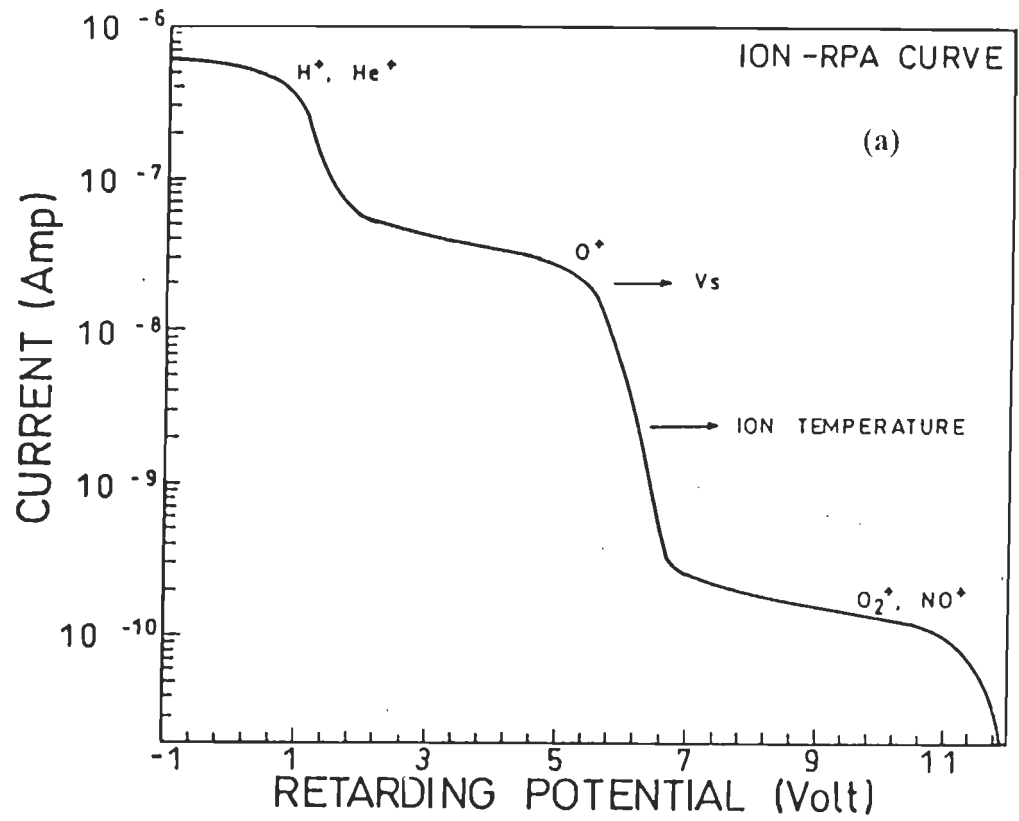
Figure 2.3   Characteristic curves of ion and electron RPA (Garg and Das, 1995).
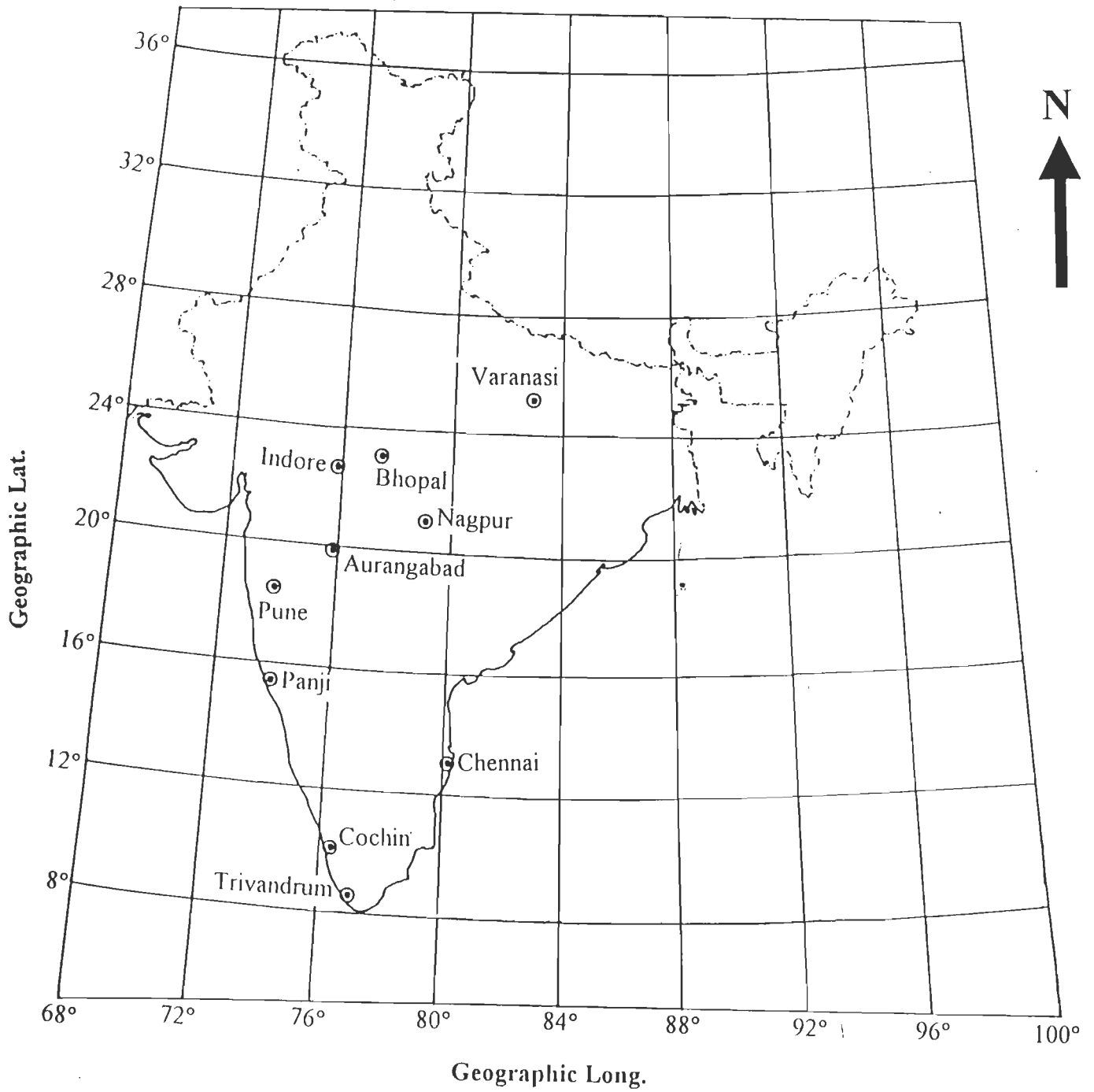
Figure 2.4   Selected ten meteorological data stations in India.

Chapter 3

Diurnal, Seasonal And Latitudinal Variation Of Ionospheric Temperatures During Solar Minimum Year 1995-96

The diurnal, seasonal and latitudinal variation of ionospheric electron and ion temperatures measured by RPA payload aboard SROSS-C2 satellite during the low solar activity (mean sunspot number, 13.9) period. The satellite coverage is 31° S to 34° N latitude and 40° E to 100° E longitude at an average altitude of ~500 km. The measured electron and ion RPAs data have been analysed for three different seasons; summer, winter and equinoxes. The aim of this study is to investigate the diurnal, seasonal and latitudinal variation of the ionospheric electron and ion temperatures during the solar minimum year 1995-96 using the data recorded by SROSS-C2 satellite. The observations are also used to assess the predictability of the IRI-95 model in estimating electron and ion temperatures over Indian region covered by the SROSS-C2 satellite.

3.1   Introduction

In the low and mid latitude ionosphere solar radiation is the main source of energy and it influences both the gas temperature and wind, and hence related with ionospheric temperature (Sushasini et al., 2001). The motion of charge particles in the *F* region ionosphere is governed by the geomagnetic field. The Japanese Hinotori satellite which had a near circular orbit at an altitude of ~600 km provided an ideal database for study of the temporal and spatial variation of

the electron density and temperature in the topside ionosphere (Watanabe and Oyama, 1996; Oyama et al., 1985, 1996a, 1996b; Balan et al., 1997). However, the Hinotori data are limited to a period of medium and high solar activity. The Indian satellite SROSS-C2 was launched an orbit of apogee about 625 km with 425 km perigee and resulting in an average height of ~500 km. It carried Retarding Potential Analyzer (RPA) payload for measuring the ionospheric temperatures. The details of satellite and RPA payload have already been discussed in chapter-II.

Watanabe and Oyama (1996) studied the electron temperature observed by the Hinotori satellite with the low inclination at the height of ~600 km in terms of local time, season, latitude, magnetic inclination and the solar flux intensity for 16 month period during 1981 to 1982. They found that the electron temperature shows a steep rise in the early morning and decreases after that and again increases at ~18:00 hrs LT. Hanson et al., (1973) observed the electron and ion temperatures with the Ogo 6 satellite near the magnetic equator above about 500 km altitude. They also showed that the equatorial troughs of electron and ion temperatures occur in the topside ionosphere during nighttime. The plasma cooling was also measured by ISS-b satellite at ~1100 km altitude (Sagawa et al., 1981). In the present study SROSS-C2 satellite data have been used for solar minimum year (1995-96) over Indian region.

3.2   Data Selection

The satellite data have been selected over Indian region from 5° N to 35° N latitude and 65° E to 95° E longitudes, which cover the maximum passes of the SROSS-C2 satellite over India. The measured electron and ion RPA data have been analysed for three different seasons; summer (May, June, July and August), winter (November, December, January and February) and equinoxes (March, April, September and October) during the solar minimum year 1995-96 to study the diurnal, seasonal and latitudinal behaviour of electron and ion temperatures.

3.3   Diurnal and Seasonal Variation of Ionospheric Temperatures

The diurnal variations of electron temperature are shown in Figure 3.1(a-c) and for ion temperature in Figure 3.2(a-c) for summer, winter and equinoxes seasons respectively. Figure 3.1 and 3.2 indicate the diurnal behaviour of electron and ion temperatures during solar minimum year 1995-96. Figure 3.1 shows the clear peak during sunrise hours and also a diffused peak corresponding to the secondary enhancement in electron temperature during evening hours. However, for ion temperature the sunrise peak and evening temperature enhancement (Figure 3.2) are smaller in comparison of electron temperature. Smoothing of measured temperature variations have been done by computing hourly average and the same are presented in Figure 3.3 and 3.4 for electron and ion temperature respectively. In the above figures measured temperature data have also been compared with the estimated values by IRI-95 model for the same time and location. It has been observed that the electron temperature sharply rises during

the sunrise hours (5:00-7:00 LT) and a secondary enhancement has also been observed during the sunset hours (16:00-18:00 LT) for all seasons during the solar minimum year 1995-96. In the summer season the electron temperature at the sunrise time rises to 3742 K from the nighttime average temperature of 844 K whereas evening temperature goes upto 2508 K during the secondary enhancement at the time of sunset (Figure 3.3a) from mid-day average temperature of 2023 K. The similar enhancements have also been observed during the winter and equinox seasons at the time of sunrise and sunset. In the winter season the electron temperature at the sunrise time rises to 3553 K from the nighttime average temperature of 738 K whereas evening temperature enhanced to 1922 K during the secondary enhancement at the time of sunset (Figure 3.3b) from mid-day average temperature 1728 K. During the equinox season the electron temperature at the sunrise time rises to 4131 K from the nighttime average temperature of 832 K whereas evening temperature enhanced to 2081 K during the secondary enhancement at the time of sunset (Figure 3.3c) from mid-day average temperature 1730 K. The IRI-95 model estimated values show a good agreement with the measured values of electron temperature during the night hours. The sunrise enhancements have also been obtained by the IRI-95 model. However, the computed values are under estimated in comparison to the measured values. The IRI-95 model predicted values are unable to show the secondary enhancements in electron temperature.

The ion temperature enhancements during sunrise and sunset hours have also been studied. Its magnitude is smaller in comparison with the corresponding enhancements in electron temperature. The IRI-95 model predicated values show a general increase in daytime ion temperature. There are no specific peaks in ion temperature during sunrise and sunset hours in the values predicated by the IRI-95 model. Similar pre-sunrise ion temperature enhancement in the low and mid latitude ionosphere at altitude 600 km has also been reported recently by Chao et al. (2003). These observations indicate that IRI-95 model is non-responsive to the detailed ion temperature behaviour. The spatial and temporal variations of the electron temperature at equatorial anomaly latitudes has also been studied by Su et al. (1996) using the Hinotori satellite at altitude about 600 km. They have observed similar morning rise in electron temperature. Thus the results obtained from SROSS-C2 satellite data are consistent with the Japanese satellite Hinotori.

3.4 Latitudinal Variation of Ionospheric Temperatures

The data from electron and ion RPAs have been analysed for electron and ion temperatures for different orbits. These orbits having orbital time falling nearer to 12:00 noon and 12:00 mid-night local time are considered for the study of latitudinal variation of electron and ion temperatures. The recorded electron and ion temperature data for above-mentioned time have been plotted for different seasons viz. summer, winter and equinox at the altitude ~500 km. The latitudinal variations of the electron temperature are shown in Figure 3.5(a-c) for 12:00 noon and for 12:00 mid-night in Figure 3.6(a-c) during different seasons of solar

minimum year. The ion temperature variation is shown in Figure 3.7 (a-c) for 12:00 noon and for 12:00 mid-night in Figure 3.8 (a-c) for all above-mentioned seasons. A straight line fit to these data is also shown in Figures 3.5-3.8 for electron and ion temperatures. The electron and ion temperature variation with latitude during nighttime is negligible and falling within the error limit (±50 K) of the measurements. However, daytime temperature shows the latitudinal variation in both electron and ion temperatures. The maximum variation in electron temperature is observed during summer and minimum during equinox seasons. The straight line fit indicates that the latitudinal variations in electron temperature over Indian region studied are 1218 K, 670 K and 541 K in summer, winter and equinox seasons respectively. However, the latitudinal variations of ion temperature over above studied region are 385 K, 395 K and 160 K in summer, winter and equinox seasons respectively.

3.5   Conclusions

The diurnal, seasonal and latitudinal variation of electron and ion temperatures have been studied using the SROSS-C2 satellite data during the solar minimum year 1995-96. This study reveals that the electron and ion temperatures have lowest values during nighttime and show variations during daytime in all seasons. The daytime electron temperature shows at least two clear peak values with different magnitudes. The peak during sunrise hours has been observed to be relatively sharp and high in magnitude and the other peak during sunset hours is diffused and also lower in magnitude. A similar variation in the ion

temperature has also been observed. However, their amplitude and sharpness is smaller in comparison to the electron temperatures. The predicated values by IRI-95 model show a good agreement with electron and ion temperature during night hours. The daytime electron temperature variations and sunrise peak values are under estimated by IRI-95 model. The IRI-95 model is unable to produce secondary peak during the sunset hours. The electron and ion temperatures show a positive correlation with latitude during daytime. Whereas no latitude effect has been observed during night hours over the Indian region at an altitude of ~500 km.

The next chapter deals with the sunrise effect on the ionospheric electron and ion temperatures.
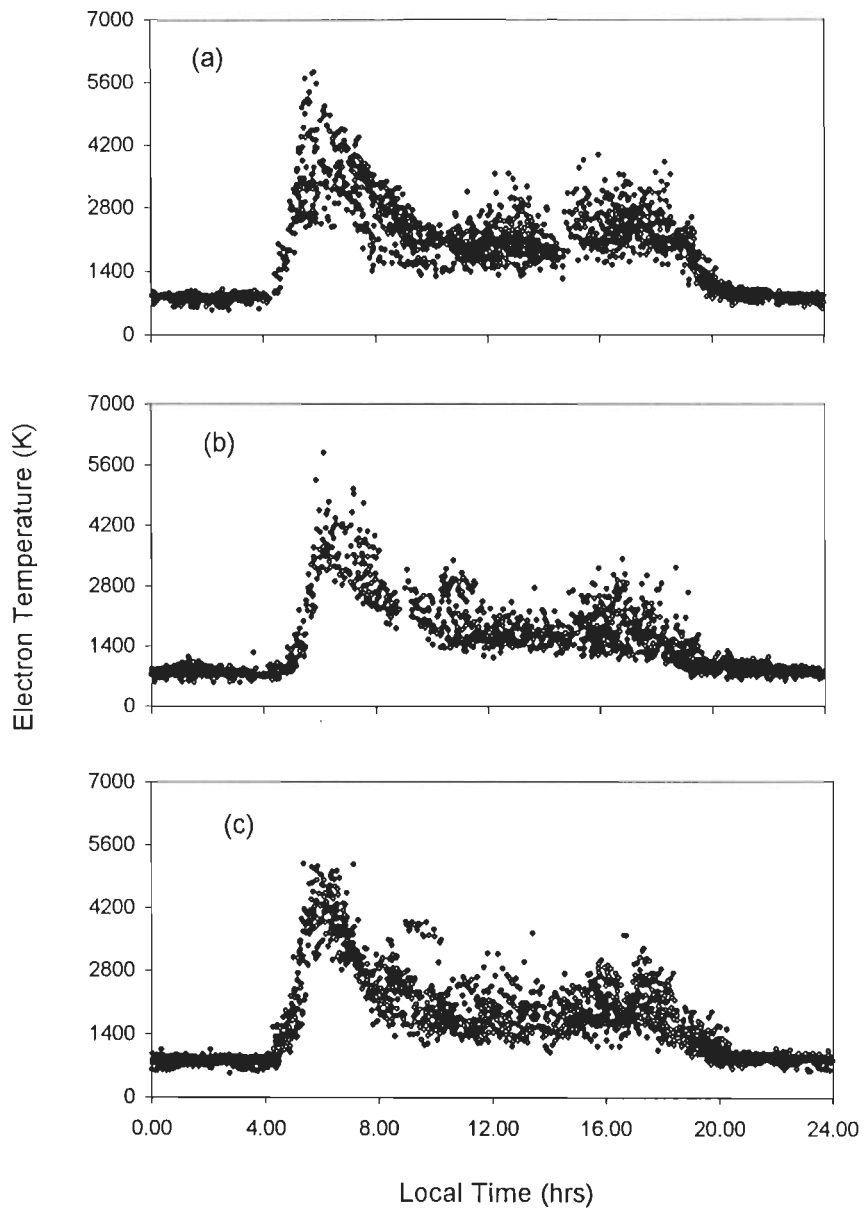
Figure 3.1 Diurnal variation of Electron Temperature for different seasons:(a) summer, (b) winter and (c) equinoxes recorded by SROSS-C2 satellite during solar minimum year 1995-96.
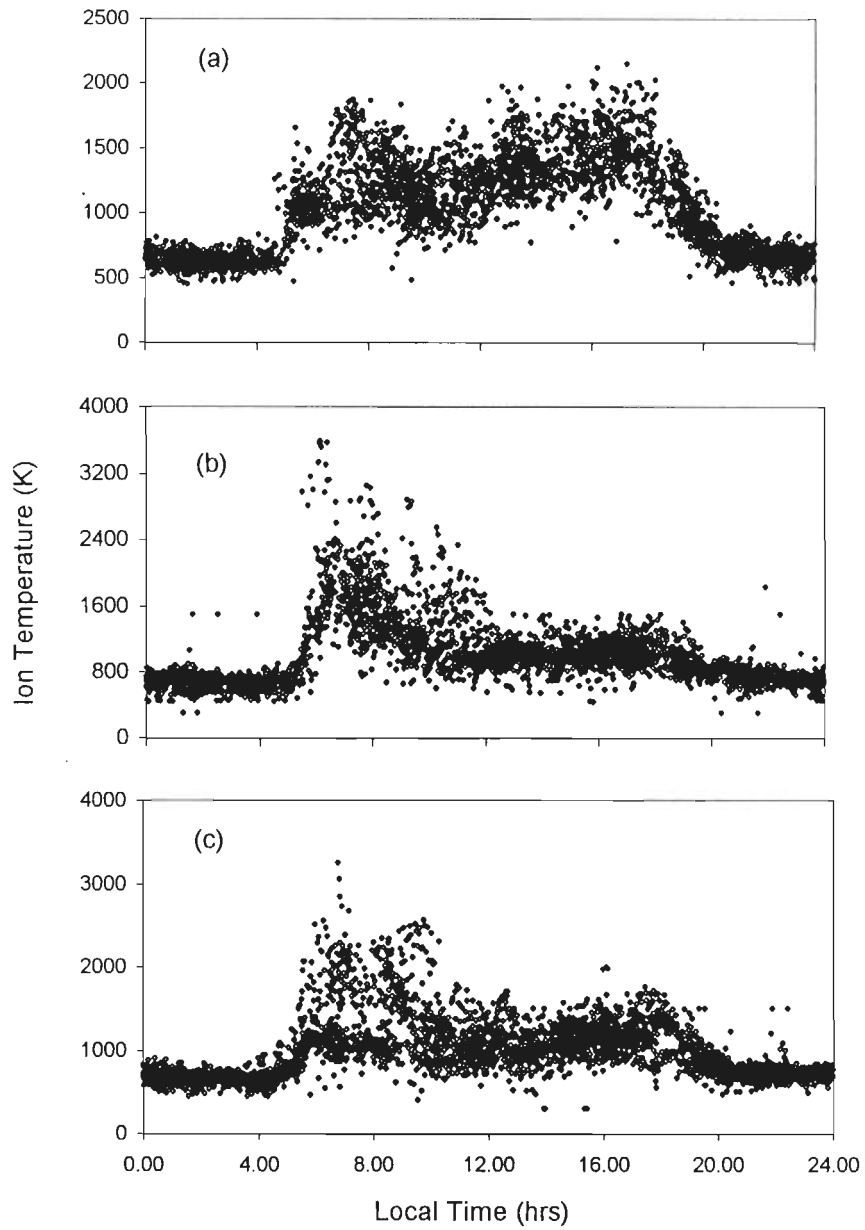
Figure 3.2 Diurnal variation of Ion Temperature for different seasons:(a) summer, (b) winter and (c) equinoxes recorded by SROSS-C2 satellite duing solar minimum year 1995-96.
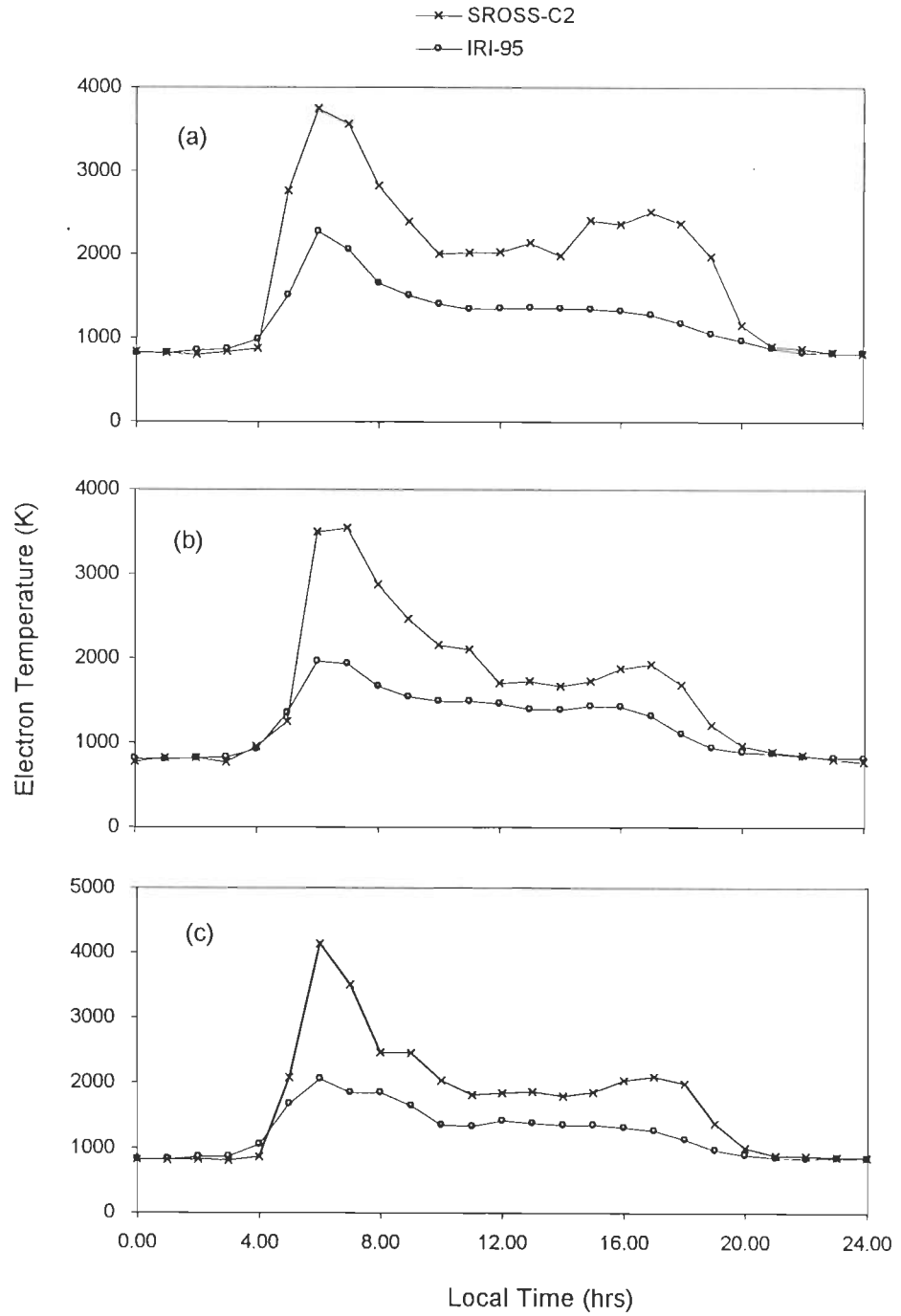
Figure 3.3 Smoothed diurnal variation of electron temperature for different seasons: (a) summer, (b) winter and (c) equinoxes recorded by SROSS-C2 satellite along with the IRI predicated values at ~500 km duing solar minimum year 1995-96.
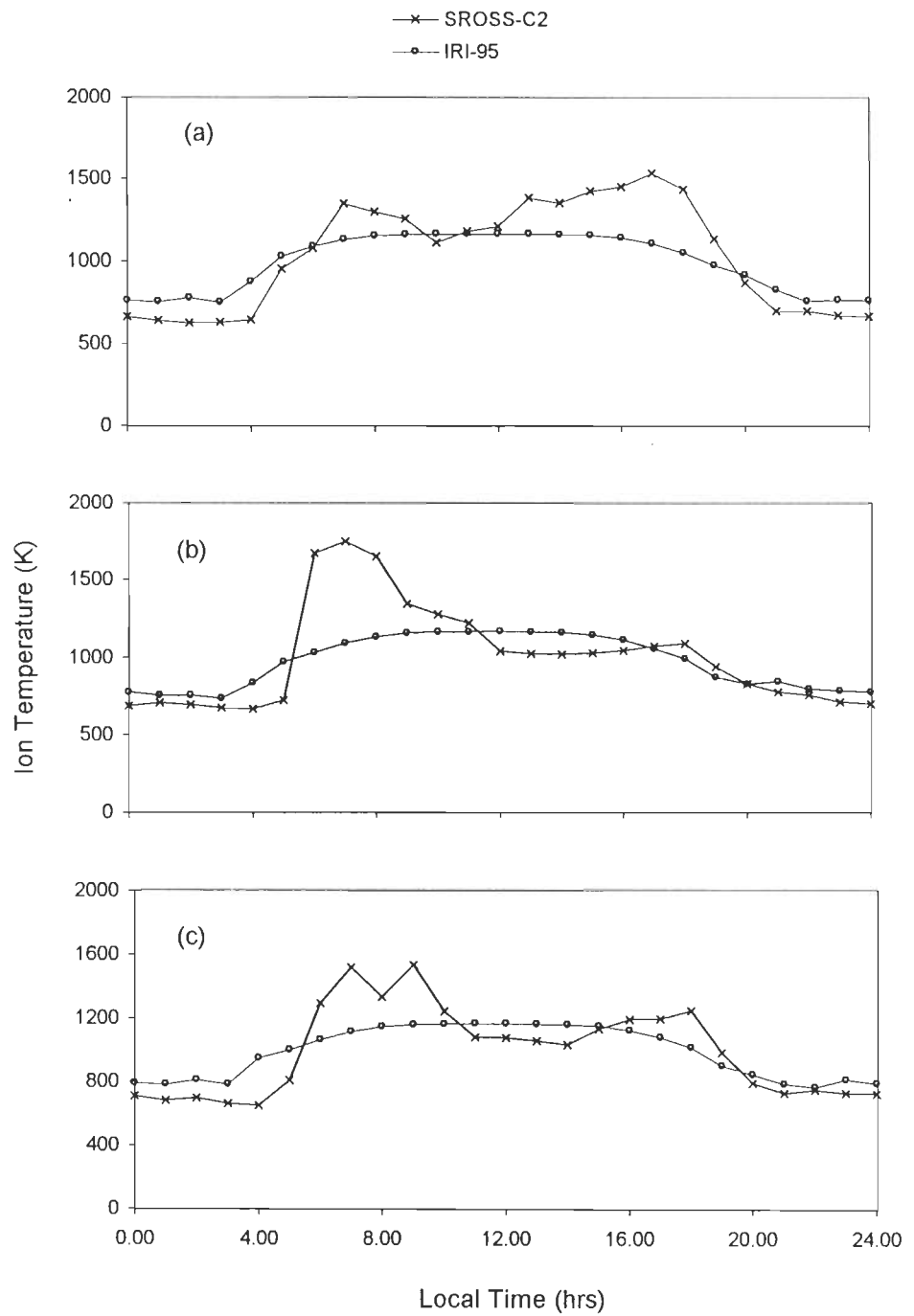
Figure 3.4 Smoothed diurnal variation of ion temperature for different seasons: (a) summer, (b) winter and (c) equinoxes recorded by SROSS-C2 satellite along with the IRI predicated values at ~500 km duing solar minimum year 1995-96.
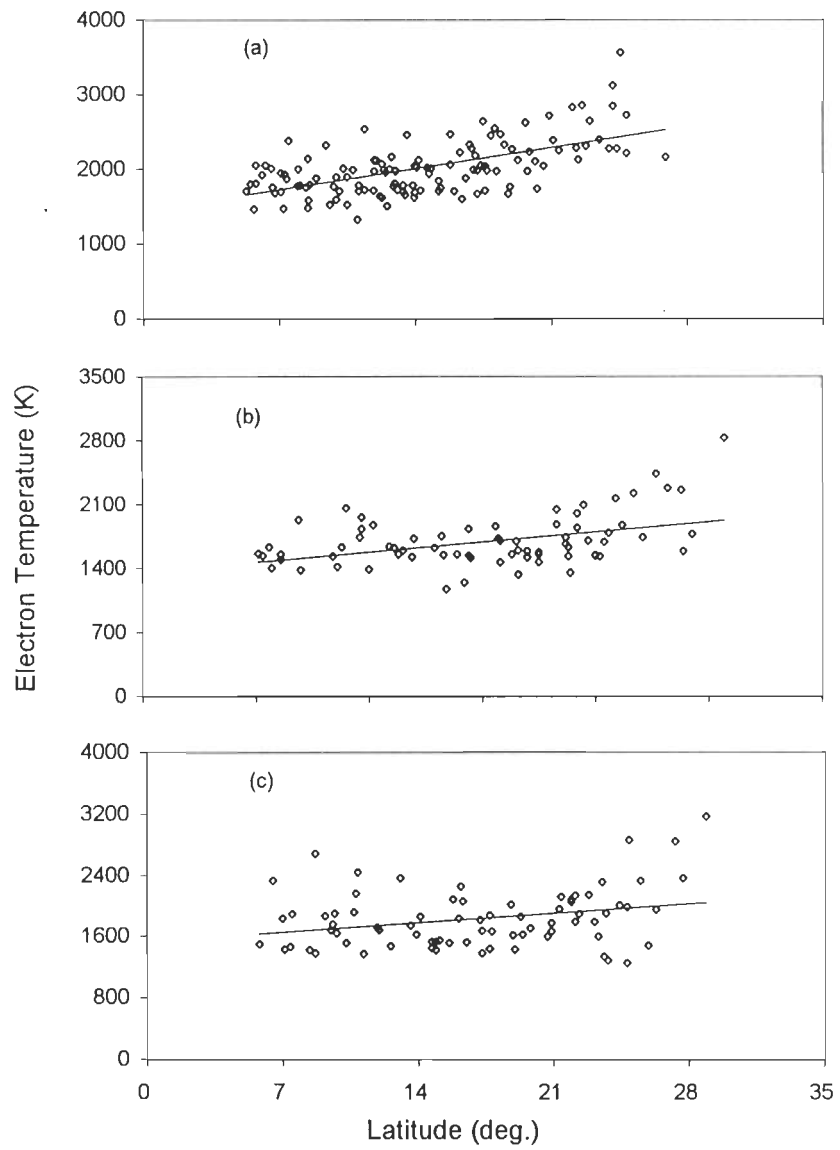
Figure 3.5 Latitudinal variation of electron temperature during noon local time (LT) for different seasons: (a) summer, (b) winter and (c) equinoxes recorded by SROSS-C2 satellite over Indian region.
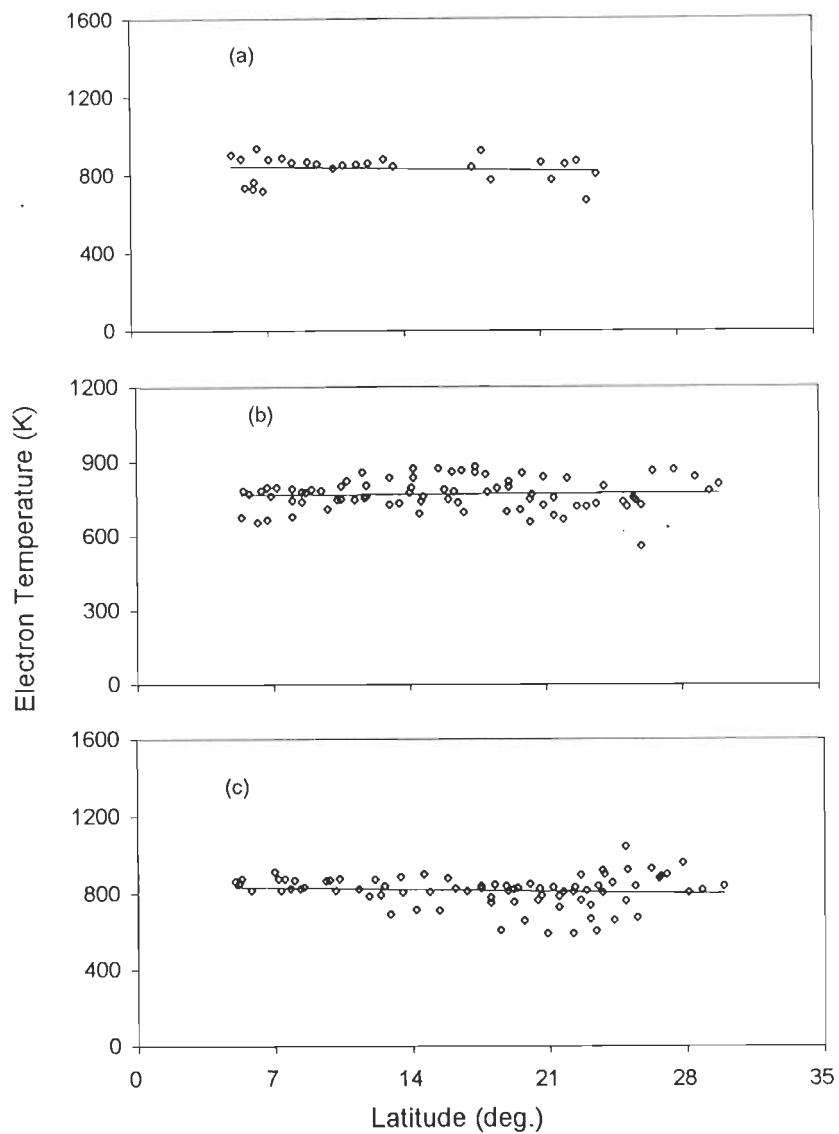
Figure 3.6 Latitudinal variation of electron temperature during mid-night local time (LT) for different seasons: (a) summer, (b) winter and (c) equinoxes recorded by SROSS-C2 satellite over Indian region.
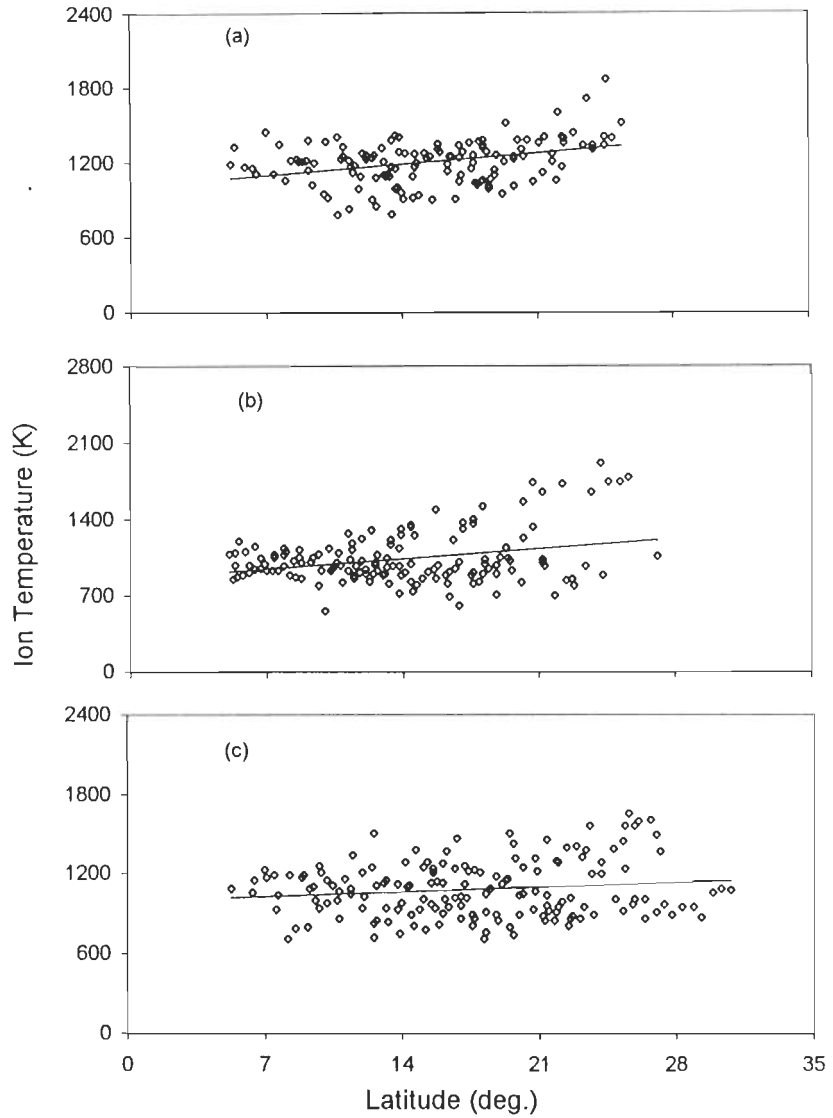
Figure 3.7 Latitudinal variation of ion temperature during noon local time (LT) for different seasons: (a) summer, (b) winter and (c) equinoxes recorded by SROSS-C2 satellite over Indian region.
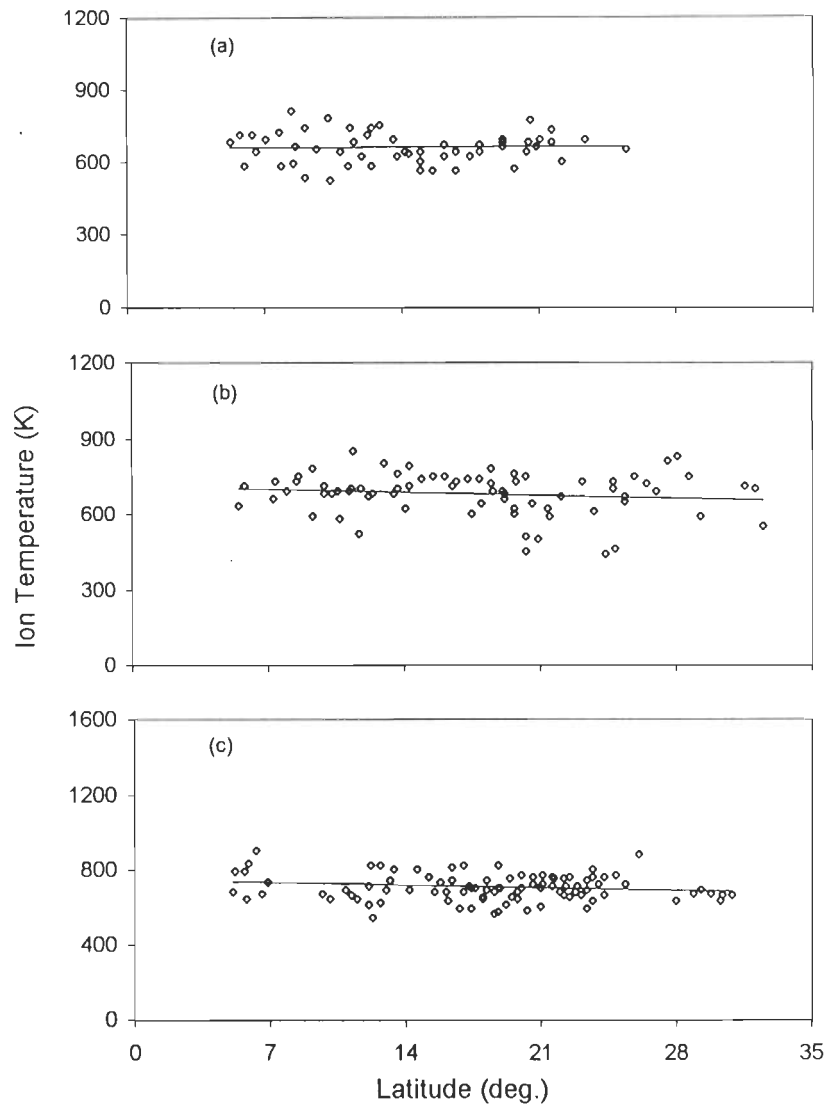
Figure 3.8 Latitudinal variation of ion temperature during mid-night local time (LT) for different seasons: (a) summer, (b) winter and (c) equinoxes recorded by SROSS-C2 satellite over Indian region.

Chapter 4

# Sunrise Effect On Ionospheric Temperatures

The ionospheric electron and ion temperatures are directly related to the position of sun with respect to earth. The Retarding Potential Analyzer (RPA) experiment flown aboard Indian SROSS-C2 satellite has yielded valuable data on ionospheric temperatures and composition. The data collected during the period from 1995 to 1998 for two different locations (Bhopal and Chennai) over India have been analyzed to study the electron and ion temperature variations in the ionosphere at low latitude $F2$ region.

4.1   Introduction

At sunrise, photoelectron production begins in the ionosphere through the ionization of neutral particles. As the photoelectrons share their high energy with the ambient electrons, the electron temperature (T_e) increases. This increase is rapid in the early morning hours due to the low electron density. As more and more electrons are produced as sunrise progress, the share of energy for each electron decreases. Thus, the T_e after reaching a maximum decreases and attains a steady state value as the day progress. The sunrise effect on electron and ion temperatures in the earth's ionosphere have been studied extensively by many workers (Chao et al., 2003; Oyama et al., 1996a, 1996b; Watanabe et al., 1995; Bhuyan et al., 2000; Sharma et al., 2002; and others). For the present study, we have used the data obtained by SROSS-C2 satellite as described earlier.

4.2   Data Selection for Specific Locations

The satellite data has been analyzed to study the behavior of ionospheric electron and ion temperatures (T_e and T_i). The data has been analysed for two different locations: Bhopal (23.16° N, 77.36° E) and Chennai (13.04° N, 80.17° E). These locations were chosen for the maximum number of passes of satellite SROSS-C2 over India in the altitude range 425-625 km. The electron and ion temperatures have been selected at these locations with ±1° variation in longitude and latitude.

4.3   Sunrise Effect on Electron Temperature

The yearly data for Te recorded at Bhopal and Chennai from 1995 to 1998 are shown in Figure 4.1(a-d) and Figure 4.3(a-d) respectively. The sunrise time varies between 5:00 to 7:00 Indian Standard Time (IST) in Indian region throughout the year. During this time we have observed a sharp increases in T_e at both stations. The maximum T_e at Bhopal reached upto 3334K in 1995, 4231K in 1996, 3403K in 1997 and 3438K in 1998 during sunrise hours. At Chennai in 1995 the maximum T_e goes upto 5763K, 3495K in 1996, 4667K in 1997 and 4784K in 1998. At Chennai double peak was observed in 1997 (Figure 4.3c). The second peak may be due to some other solar activities, which could not be characterized. The nighttime average T_e varies from 745 to 915K at Bhopal and from 754 to 883K at Chennai during 1995 to 1998. Table-4.1 shows the details of T_e variations over these stations from 1995 to 1998.

46

The spatial and temporal variations of the electron temperature at equatorial anomaly latitudes have been studied by Su et al., (1996) using the Hinotori satellite at an altitude of about 600 km. They observed similar morning rise in T_e. Thus the results obtained from SROSS-C2 satellite data are consistent to the Japanese satellite Hinotori (Su et al., 1996).

Oyama et al. (1996a) studied the morning overshoot of T_e by the downward plasma drift in the equatorial topside ionosphere and found that the rapid increase in electron temperature in the early morning period is the well known T_e phenomenon called 'morning overshoot'. Oyama et al. (1996b) have also studied the diurnal, seasonal, and longitudinal variations of the electron temperature at the height of about 600km in the low latitude region. They found that an electron temperature enhancement occurs in the morning period (between 5:00 to 8:00 LT). The peak value is highest at the magnetic equator and reaches about 5000K for the high solar activity. Our study also pertains to low latitude and observed that the highest peak of T_e is about 5763K at Chennai in 1995 (Figure 4.3a).

4.4　Sunrise Effect on Ion Temperature

The yearly data for T_i recorded at Bhopal and Chennai from 1995 to 1998 are shown in Figure 4.2(a-d) and Figure 4.4(a-d) respectively. The T_i also shows the similar behavior at these stations. However, the change in T_i is relatively less than Te. During the time of sunrise we have observed a sharp increases in T_i at both stations. The maximum T_i at Bhopal reaches upto 2860K in 1995, 1270K in 1996, 1870K in 1997 and 2230K in 1998 during sunrise hours. At Chennai in 1995 the maximum T_i was 1890K, 1760K in 1996, 2930K

in 1997 and 2400K in 1998. The nighttime average T_i varied from 618 to 832K at Bhopal and from 626 to 776K at Chennai during 1995 to 1998. Table-4.2 shows the details of T_i variations over these stations from 1995 to 1998.

4.5   Conclusions

The sunrise effect on the ionospheric electron and ion temperatures as measured by the SROSS-C2 satellite during the period from 1995 to 1998 (which cover the solar minimum year of 1995-96) for specific location of Bhopal (23.16° N, 77.36° E) and Chennai (13.04° N, 80.19° E) in India have been studied. It has been found that the electron and ion temperatures are minimum during the local night hours and maximum at the local sunrise time. The nighttime electron temperature varies from 745 to 915 K and rises sharply at sunrise to 3334 K or more. The nighttime ion temperature varies from 618 to 832 K and also rises at sunrise to 1270 K or more.

A part from the sunrise the ionospheric plasma is also affected by the tropospheric disturbances. In next chapter we have explained the effect of thunderstorms on ionospheric electron and ion temperatures.

Table 4.1

The electron temperature (T_e) at Bhopal and Chennai from 1995 to 1998

Year	*Bhopal*			*Chennai*		
	Maximum Temp. at Sunrise (K)	Average Temp. at Daytime (K)	Average Temp. at Nighttime (K)	Maximum Temp. at Sunrise (K)	Average Temp. at Daytime (K)	Average Temp. at Nighttime (K)
1995	3334	2089	879	5763	2121	807
1996	4231	2121	745	3495	1618	754
1997	3403	2059	789	4667	1995	777
1998	3438	2114	915	4784	3132	883

Table 4.2

The ion temperature (T_i) at Bhopal and Chennai from 1995 to 1998

Year	Bhopal			Chennai		
	Maximum Temp. at Sunrise (K)	Average Temp. at Daytime (K)	Average Temp. at Nighttime (K)	Maximum Temp. at Sunrise (K)	Average Temp. at Daytime (K)	Average Temp. at Nighttime (K)
1995	2860	1312	702	1890	1099	646
1996	1270	1254	658	1760	1153	626
1997	1870	1278	618	2930	1140	675
1998	2230	1163	832	2400	1247	776

Figure 4.1 Variation of Electron Temperature at Bhopal from 1995 to 1998.
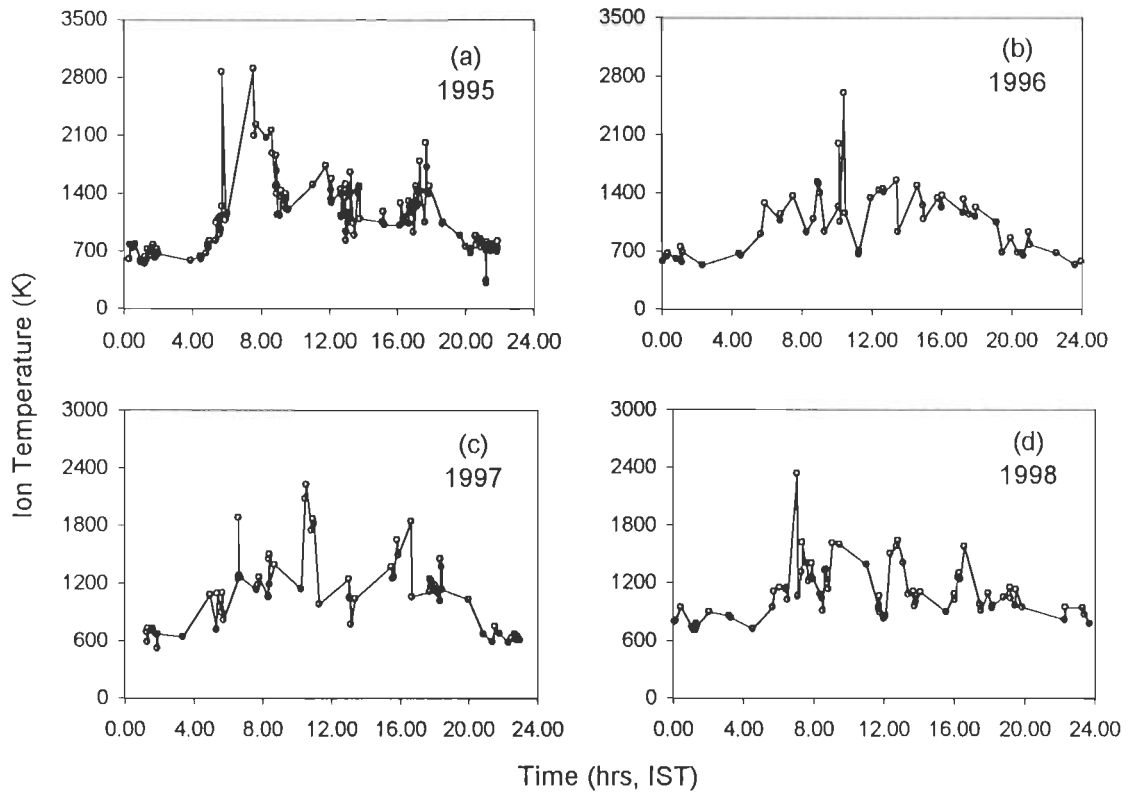
Figure 4.2 Variation of Ion Temperature at Bhopal from 1995 to 1998.
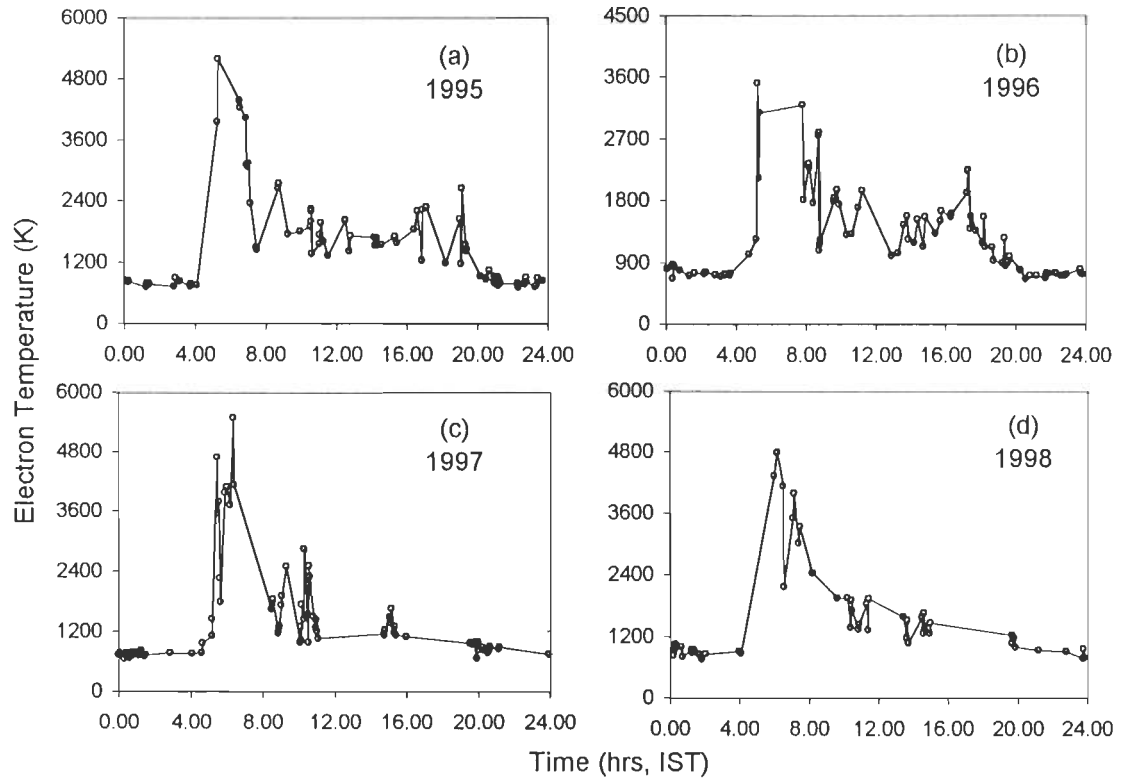
Figure 4.3 Variation of Electron Temperature at Chennai from 1995 to 1998.
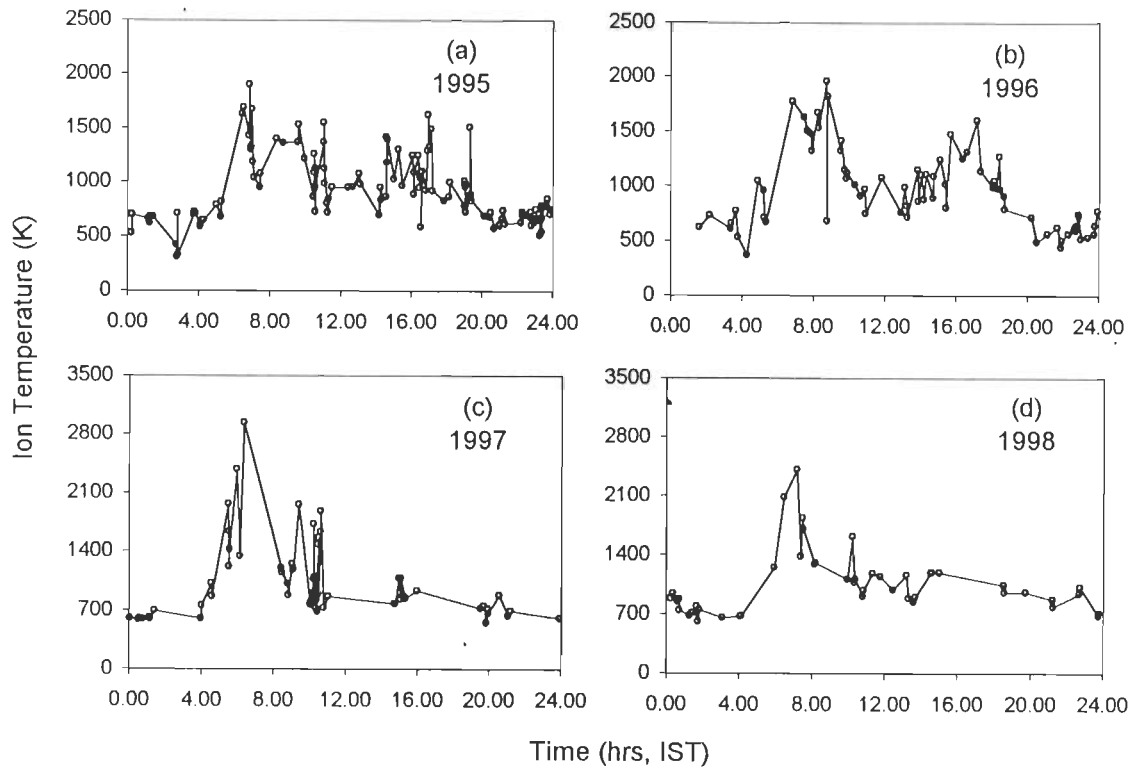
Figure 4.4 Variation of Ion Temperature at Chennai from 1995 to 1998.

Chapter 5

Ionospheric Response To The Thunderstorms

Many modern technological systems are affected by ionospheric phenomena. The understanding, monitoring and forecasting changes of ionospheric weather play an important role in communication, navigation, exploration of near earth space and even exploration of deeper part of earth interior. Natural electromagnetic fields generated by the interaction of solar wind with magnetosphere and ionosphere as well as generated by thunderstorms and lightning/sprites affect the ionosphere weather (Rai, 1973; Chauzy and Raizonville, 1982; Chauzy and Soula, 1987; Taranenko et al., 1993a, 1993b; Rycroft, 1994; Rycroft and Cho, 1998; Lehtinen et al., 1997, 1999; Yukhimuk et al., 1998, 1999; Singh et al., 2001, etc.). The ionospheric temperatures (electron and ion temperatures) were measured by the RPA payload aboard the Indian SROSS-C2 satellite. Further, the data at low latitudes falling in the Indian subcontinent in the height range 425-625 km for the period 1995-98 were used to study the effect of thunderstorm activity on ionospheric temperatures. The thunderstorm data for the same period were obtained from India Meteorological Department (IMD), Pune. To see the effect of active thunderstorms, the ionospheric electron and ion temperatures have been compared to the values on normal days (free from other activities). The results on the above studies have been presented in this chapter.

5.1 Troposphere - Ionosphere Interaction

Lightning, sprites, internal atmospheric waves (planetary waves, tides, gravity waves) generated in the troposphere and stratosphere due to thunderstorm activity are the sources of coupling between the troposphere and the ionosphere (Kazimirovsky et al., 2003). A thundercloud is charged positively in its upper and negatively in its lower part (Mitra, 1992). Such a cloud has an intense electric field in its interior directed downward. This field drives any electron present either due to radioactive origin or produced by local discharges, upward within the cloud. Since the gain in energy during its travel in the electric field exceeds the loss of energy due to collision along its path, the energy of the electron will rapidly increase and may approach a limiting value of 5×10^9 eV. After the spark discharge, the spray of such 'run-away' electrons moves upward with high velocity. Secondly, the electric field due to the cloud doublet may be intense in the neighborhood of the lower boundary of E region that an electron accelerated by the field is able to produce electric discharge in this region. The third possible process, the electric discharge of a thundercloud causes radiation of electromagnetic waves (e. g. atmospherics). The intensity of such radiation field may be sufficiently strong to increase the ionization in the upper atmospheric region (ionosphere) where collision frequency is less than 10^6 collisions per seconds. Rai et al. (1973) have presented evidence that the acoustic gravity waves produced by the thunderstorm may propagate upward and may affect the ionospheric parameters.

50

5.2   Selection of Satellite Data for Thunderstorm Events

The data collected by SROSS-C2 satellite using RPA payload during the period from 1995-1998 has been analyzed for anomalous variations due to thunderstorms activity at the altitude range from 425 to 625 km. The data on thunderstorm activity for the same period was obtained from India Meteorological Department (IMD).

It is a difficult task to study the ionospheric temperature using the satellite data in respect of thunderstorm activity because very rarely passes of satellite match the thunderstorm activity at a meteorological data station. The first task is to match the satellite data corresponding to the thunderstorm activity. During the period from 1995 to 1998, it has been found that seven events of thunderstorms correspond to the satellite data.   The recorded average electron and ion temperature during active thunderstorms have been compared with the average normal days electron and ion temperatures for the same time interval. Care has been taken to select the satellite data, which is free form diurnal, seasonal, latitudinal, longitudinal and altitudinal effects. The average of normal time electron and ion temperatures have been computed for a month, starting almost 15 days before the thunderstorm day and continuing to 15 days more after that. Thus the possibility of seasonal effect has completely been ruled out because all data points correspond to the same season. A window of 5° in latitude and longitude for the satellite observation at the meteorological data center has enabled the latitudinal and longitudinal effect to be ineffective. The averaging of electron and ion temperatures at nearly the same hours of the day as that of the active thunderstorm has made it free from

the diurnal effect. All analysis has been done for the altitude ranges from 425 to 625 km only thus making it independent of the altitude.

To remove the effects of solar flare activity, the data on solar flares have been obtained from National Geophysical Data Center (NGDC), Boulder, Colorado (USA). Only those thunderstorm days have been considered in this study, which are free from the solar flares. Similarly, in another study (reported in next chapter), only those solar flare events were considered which were free form the thunderstorm activities.

This study has a limitation in the sense that only seven thunderstorm days have been found which correspond to the satellite passes. However, in each satellite pass many data points were recorded at the regular intervals with the window of $5°$ in latitude and longitude. In all the seven events 110 data points were obtained and in each case the electron and ion temperatures were above the normal day observations. On many occasions during the satellite passes, the PRA sensors could not record the electron and ion temperatures. All temperature data recorded by SROSS-C2 satellite are within the error limit of ± 50 K. Thus the seven events have been found to correspond to the satellite data over three different IMD locations at Bhopal ($23.16°$ N, $77.36°$ E), Trivandrum ($08.29°$ N, $76.59°$ E) and Panji ($15.30°$ N, $73.55°$ E) in India during the study period.

5.3   Thunderstorm Effects on the Ionospheric Temperatures

In 1995 the two events have been recorded which correspond to Bhopal and two to Trivandrum. Figure 5.1 shows the comparison of electron

temperature during thunderstorms and normal days for the events recorded in 1995. At Bhopal, there were active thunderstorms on January 11 and August 29, 1995. During the thunderstorms the average electron temperature was enhanced by 1.2 to 1.3 times [Figure 5.1(a, d)] over the normal day average electron temperature. However, at Trivandrum it was enhanced by 1.2 to 1.4 times [Figure 5.1(c, b)] during the active thunderstorms on April 13 and April 28, 1995 over the normal days. Figure 5.2 shows the comparison of ion temperature during active thunderstorms and normal days for these four events. In 1995, the average ion temperature at Bhopal was enhanced by 1.2 times [Figure 5.2 (a, d)] for both events and at Trivandrum it was enhanced by 1.1 to 1.5 times over the normal days [Figure 5.2 (b, c)] during the active thunderstorms.

Two events were found in 1997, one corresponds to Trivandrum on June 27 and another at Bhopal on December 10. At Trivandrum, the average electron temperature was enhanced by 1.7 times (Figure 5.3a) and at Bhopal it was enhanced by 1.4 times (Figure 5.3b) during the active thunderstorms as compared to the normal days. However, the average ion temperature was enhanced by 1.3 times [Figure 5.4(a, b)] to that of normal days temperature at both locations.

In 1998, one event has been found at Panji. There was an active thunderstorm recorded during two consecutive days (August 15 and 16) at the same time. The average electron temperature was enhanced by 1.5 times (Figure 5.5) and the average ion temperature by 1.3 times (Figure 5.6) during the active thunderstorms to that of normal days temperature. The average

electron and ion temperature during thunderstorms and normal days for all seven events have been shown in Table 5.1 and 5.2. The table also shows the time, duration and location of thunderstorm activities.

The above analysis shows that there is a consistent enhancement of ionospheric electron and ion temperatures recorded during active thunderstorm periods. This enhancement was for the average electron temperature ranging from 1.2 to 1.7 times compared to the average normal days temperature. However, for ion temperature it ranged from 1.1 to 1.5 times during the active thunderstorms compared to average normal days ion temperature. It may be mentioned that in the present analysis the data window are selected in such a way that the effect of diurnal, seasonal, latitudinal, longitudinal and altitude effects are minimized. Thus the temperature anomalies are directly related to the thunderstorm events.

The enhancements in ionospheric electron and ion temperatures have been attributed to different kind of lightning activity, which are associated with active thunderstorms. Recent observations of optical phenomena such as sprites, blue jets, blue starters, elves and associated phenomena (Pasko et al., 1996, 1997; Sentman et al., 1995; Taranenko et al., 1992; Lehtimen et al., 1996, 2000; Bell et al., 1995; Cummer and Inan, 1997; Gupta, 1997) propagating from top of the active thunderstorm may generate radiations from ULF to VLF (Inan et al., 1991, 1996; Otsuyama et al., 1999), which in turn, may propagate still upward and heat the local plasma in the ionosphere (Sharma et al., 2004).

5.4   Conclusions

The SROSS-C2 data have been analysed to study the electron and ion temperature anomalies during the thunderstorms day over the normal day temperature. The study reveals that the electron and ion temperatures show a consistent enhancement during the thunderstorm events. The enhancement in case of electron temperature is slightly higher than the enhancement of ion temperature during the active thunderstorm events over the normal days.

A part from the tropospheric disturbances the ionosphere may get influenced by the solar disturbances. Keeping this in view we have examined the effect of solar flares on the ionospheric temperatures.

Table 5.1

Comparison of average electron temperature during thunderstorm and during normal days

S. No.	Date of Event	Time and Duration of Thunderstorm	Location of Thunderstorms	Electron Temperature (K)	
				Average during Normal days	Average during Thunderstorms day
1.	Jan 11, 1995	1201-1500 IST (0259 hrs)	23.16° N, 77.36° E	1457	1940
2.	Apr 13, 1995	0601-0900 IST (0259 hrs)	08.29° N, 76.59° E	1769	2451
3.	Apr 28, 1995	1501-1800 IST (0259 hrs)	08.29° N, 76.59° E	1449	1684
4.	Aug 29, 1995	1201-1500 IST (0259 hrs)	23.16° N, 77.36° E	1762	2160
5.	June 27, 1997	0601-0900 IST (0259 hrs)	08.29° N, 76.59° E	1316	2184
6.	Dec 10, 1997	0901-1200 IST (0259 hrs)	23.16° N, 77.36° E	2280	3202
7.	Aug 15-16, 1998	1501-1800 IST (0259 hrs)	15.30° N, 73.55° E	1502	2224

Table 5.2

Comparison of average ion temperature during thunderstorms and during normal days

S. No.	Date of Event	Time and Duration of Thunderstorm	Location of Thunderstorms	Ion Temperature (K)	
				Average during Normal days	Average during Thunderstorms day
1.	Jan 11, 1995	1201-1500 IST (0259 hrs)	23.16° N, 77.36° E	960	1151
2.	Apr 13, 1995	0601-0900 IST (0259 hrs)	08.29° N, 76.59° E	925	1045
3.	Apr 28, 1995	1501-1800 IST (0259 hrs)	08.29° N, 76.59° E	900	1343
4.	Aug 29, 1995	1201-1500 IST (0259 hrs)	23.16° N, 77.36° E	1167	1441
5.	June 27, 1997	0601-0900 IST (0259 hrs)	08.29° N, 76.59° E	876	1166
6.	Dec 10, 1997	0901-1200 IST (0259 hrs)	23.16° N, 77.36° E	1715	2147
7.	Aug 15-16, 1998	1501-1800 IST (0259 hrs)	15.30° N, 73.55° E	1033	1348
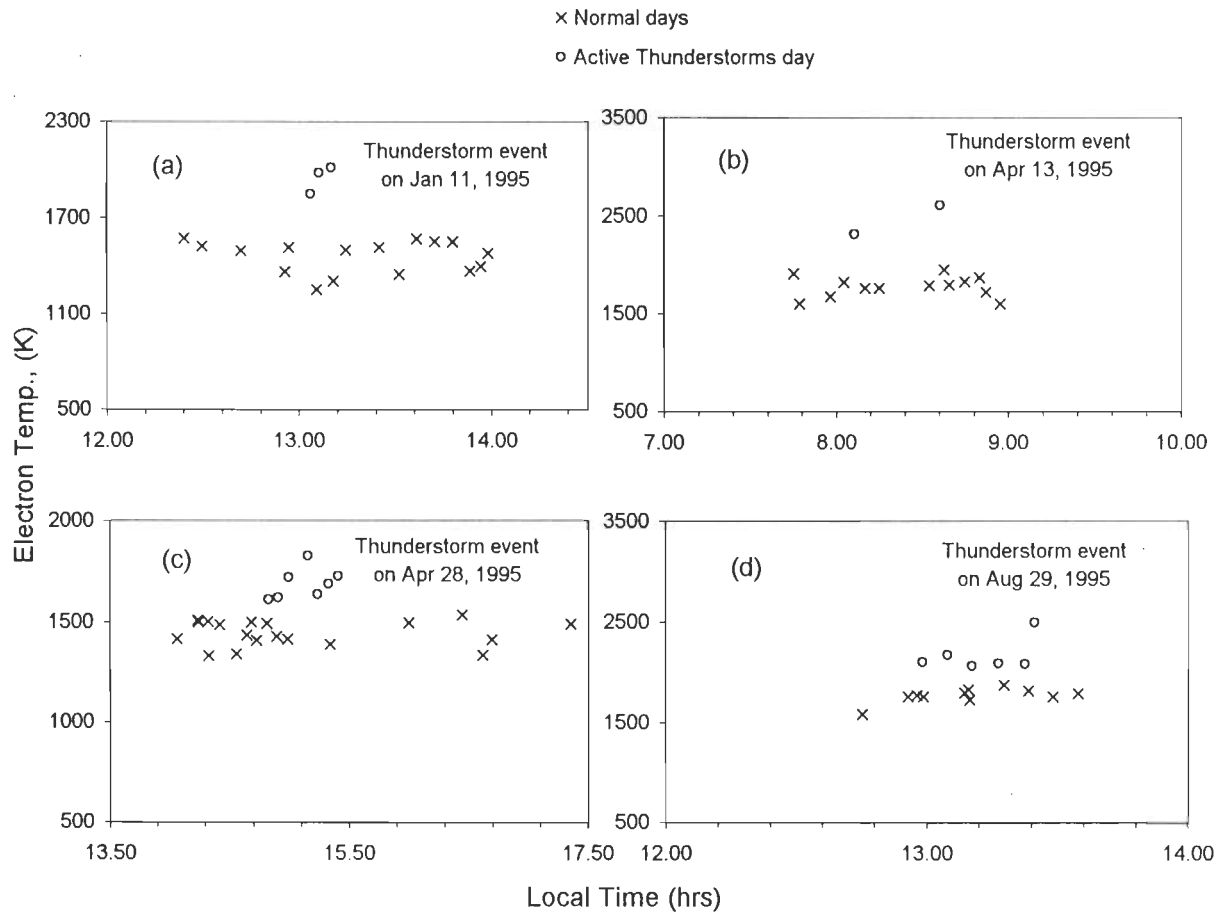
Figure 5.1 Variation of Electron Temperature during thunderstorm and normal days for the events recorded at Bhopal (a, d) and at Trivandrum (b, c) in 1995.
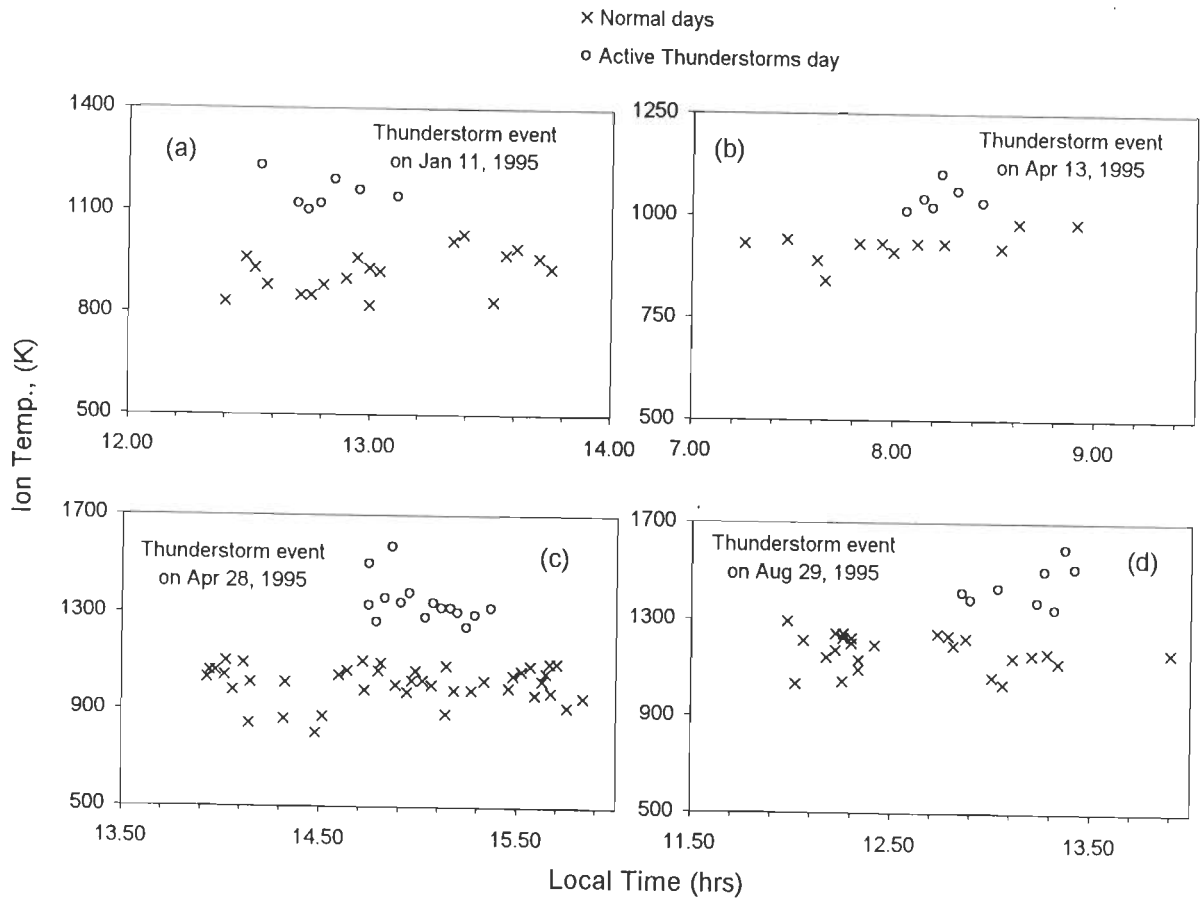
Figure 5.2 Variation of Ion Temperature during thunderstorm and normal days for the events recorded at Bhopal (a, d) and at Trivandrum (b, c) in 1995.
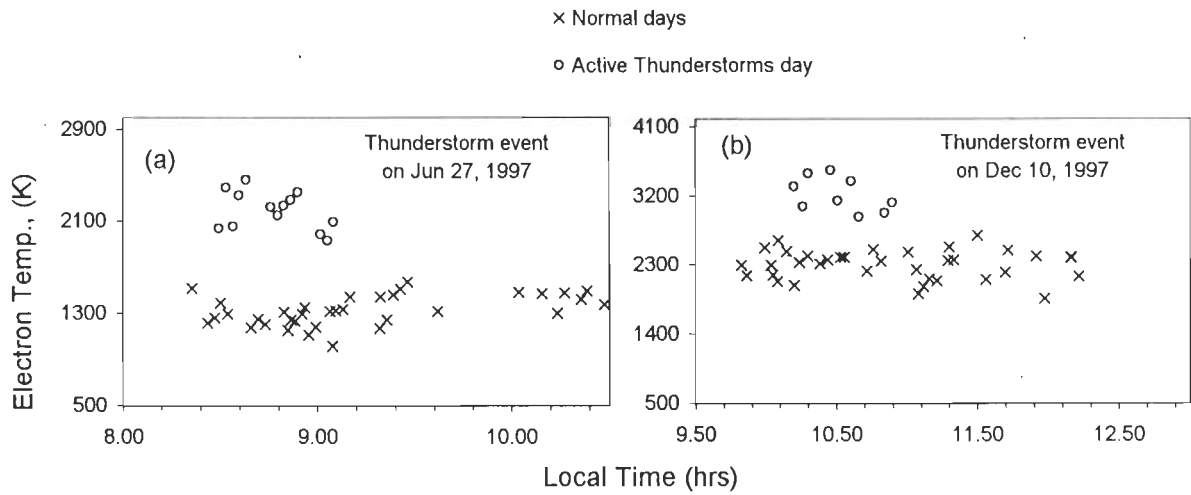
Figure 5.3 Variation of Electron Temperature during thunderstorm and normal days for the events recorded at Trivandrum (a) and at Bhopal (b) in 1997.
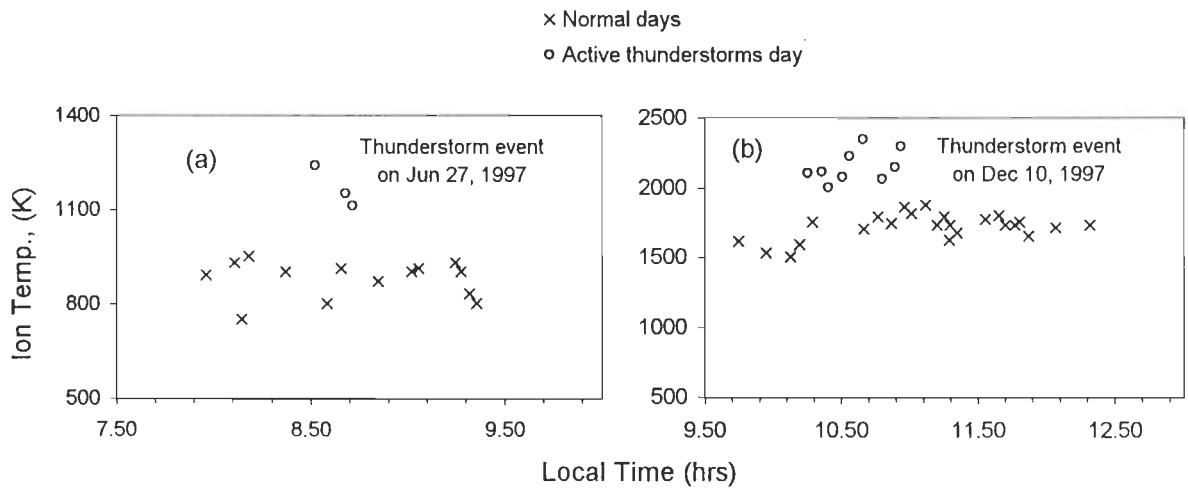
Figure 5.4 Variation of Ion Temperature during thunderstorm and normal days for the events recorded at Trivandrum (a) and at Bhopal (b) in 1997.
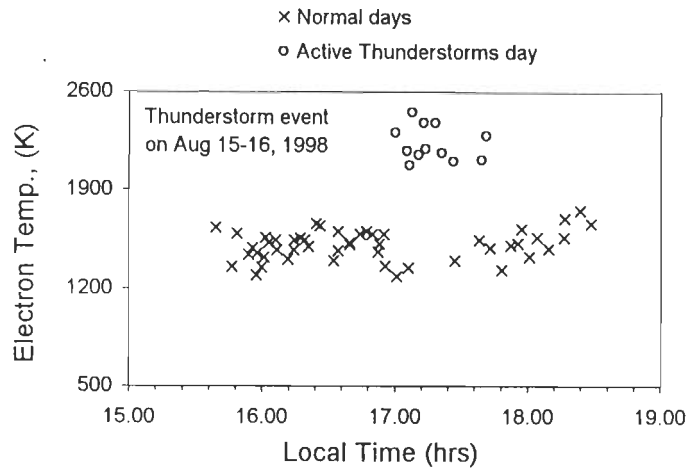
Figure 5.5 Variation of Electron Temperature during thunderstorm and normal days for the events recorded at Panji in 1998.
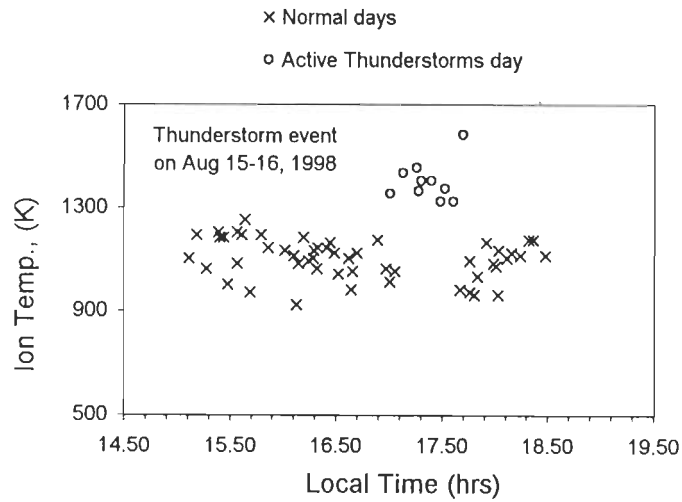
Figure 5.6 Variation of Ion Temperature during thunderstorm and normal days for the events recorded at Panji in 1998.

Chapter 6

Effect Of Solar Flares On The Ionospheric Temperatures

Various phenomena related to the sun play a significant role in changing the plasma temperature in $F2$ region of the ionosphere (Ma et al., 1995; Mahajan et al., 1983; Shapka, 1992; Schunk and Sojka, 1996; Sharma et al., 2003 and others). One of them is the solar flare, which directly affects the ionosphere and radio communication on earth and also releases energetic particles into the space. These energetic particles accelerated in space are dangerous to astronauts and interfere with the electronic systems in satellite and spacecrafts. So, the effect of solar flare on the earth's ionosphere has become the most important study of the day. This chapter is devoted to study the effect of solar flares on the ionospheric electron and ion temperatures.

6.1   Introduction

Many researchers (Afraimovich et al., 2001; Anastasiadis, 1999; Avakyan, 2001; Carrington, 1860 and Charikov, 2000) have studied the effect of solar flares using GPS and other satellite data. Afraimovich et al., (2001) have studied the effects of the solar flares of September 23, 1998 and July 29, 1999 on ionosphere with the help of GPS network. They found that the fluctuation of total electron content (TEC) and its time derivative by removing the linear trend of TEC with a time window, are coherent for all stations on the dayside earth and no such effect of solar flares was detected on the night side of the earth. The effect of solar flares on the ionospheric F region has also been studied

(Mendillo et al., 1974) by VHF radio beacons experiment on geo-stationary satellite and noticed enhancement of TEC. Global observation of the outstanding flares of August 7, 1972 using 17 stations in North America, Europe and Africa (Mendillo et al., 1974) revealed that the TEC was increased by 15-30% during the solar flares. The low latitudes showed a larger increase of TEC compared with the high latitude. Some events of solar flares have also been studied (Donnelly, 1976; Kanellakos et al., 1962) to see the effect on E and F regions of ionosphere and it has been found that the electron density was enhanced at these heights. Thome and Wagner (1971) theoretically studied the effect of soar flares on electron density and found that the electron density is enhanced in E and F regions of the ionosphere. However, to the author knowledge no major work has been done on the effect of solar flares on the ionospheric temperatures.

6.2 SROSS-C2 Data Selection Related to Solar Flares

The data collected during the period from 1995-1998 have been analyzed for anomalous variation in the electron and ion temperatures related to the solar flares. The data on solar flare has been obtained from National Geophysical Data Center (NGDC), Boulder, Colorado, USA.

It is a difficult task to study the ionospheric temperatures variation due to solar flare using the satellite. One of the reasons is limited availability of the satellite passes during the solar flare period. For the present study, we have analyzed the SROSS-C2 satellite data over ten IMD locations in India during the period 1995-1998. However, only five flare events were found matching

with the satellite data. One event corresponds to solar flare activity over Bhopal (23.16° N, 77.36° E), two at Panji (15.30° N, 73.55° E) and two at Pune (18.31° N, 73.55° E). The satellite data for electron and ion temperatures were selected for these flare events and analyzed at an altitude range from 425-625 km. Care has been taken to select the satellite data, which is free form diurnal, seasonal, latitudinal, longitudinal and altitude effects during the data selection by using the appropriate data window at fixed locations. A window of 5° in latitude and longitude for the satellite observations at the meteorological data center has been used to minimize the effect of latitude and longitude. The electron and ion temperatures data for normal days were selected as nearly the same time for a month, starting almost 15 days before the solar flares and continuing to 15 days more after that. Thus the possibility of diurnal and seasonal effects has been ruled out.

Care has also been taken to select the flare events, which are free form active thunderstorms and its associated phenomena. The active thunderstorm and its associated phenomena may also change the ionospheric temperatures (Sharma et al, 2004). The selected satellite data were ascertained to be free from thunderstorm activities, by using the data of thunderstorms obtained from India Meteorological Department (IMD), Pune. Recently it was observed that the ionospheric temperatures and density are also influence by earthquakes (Hayakawa et al., 1996; Molchanov and Hayakawa, 1998; Srivastava, 2000). Care has been taken to make sure that the chosen events are also free from earthquake events.

The area covered by a great flare may be as large as 10^9 km^2. A flare

area smaller than about 3×10^8 km^2 is known as subflare (Hanssen and Emslie, 1988). In the present analysis all solar flare events fall in the category of subflare. They had nearly same area and brightness but the time duration were different. The brilliancy is faint on a three level scale. The intensity of a subflare is approximately 5sfu (solar flux unit)

6.3   Enhancement in Ionospheric Temperatures during Solar Flares

During 1995-1998, total five events of solar flare on the dayside of earth to correspond at Bhopal, Panji and Pune in India have been analyzed. These stations were chosen on the basis of maximum passes of SROSS-C2 satellite to correspond to the solar flare events and also on the basis of IMD data, which provided the information on thunderstorm activity at above locations. It was ascertained that the events chosen are free from the thunderstorm and seismic activities.

One event has been found corresponding to Bhopal. There was a solar flare from 5.60-6.17 LT (local time) on November 9, 1998. During the solar flare the average electron temperature enhancement was by 1.9 times (Figure 6.1) over the normal days average electron temperature. However, the average ion temperature was also enhanced. This enhancement has been found to be 1.2 times (Figure 6.2) over the normal days average ion temperature.

Two events have been analysed corresponding to Panji. There were solar flare events from 16.67-17.03 LT on May 19, 1995 and from 10.67-11.27 LT on July 10, 1996. During the solar flare (May 19, 1995) the enhancement in average electron temperature was by 1.3 times (Figure 6.3a) and for average

ion temperature was by 1.2 times (Figure 6.4a) over the normal days average temperature. During the solar flare events of July 10, 1996 the average electron temperature was enhanced by 1.5 times (Figure 6.3b) and the average ion temperature was enhanced by 1.4 times (Figure 6.4b) over the normal day's average temperatures.

At Pune there were two events of solar flares form 8.90-10.03 LT on June 5, 1995 and from 9.04-9.83 LT on December 28, 1998. The enhancement in average electron temperature during the solar flare on June 5, 1995 was by 1.5 times (Figure 6.5a) and for average ion temperature it was enhanced by 1.4 times (Figure 6.6a) over the normal days average temperatures. During the solar flare on December 28, 1998 the enhancement in average electron temperature was by 1.8 times (Figure 6.5b) and for average ion temperature was by 1.3 times (Figure 6.6b) over the normal days average temperatures.

The average electron and ion temperatures during solar flares and normal days for all five events have been shown in Table 6.1and 6.2. The tables also show the time and duration of solar flares.

These enhancements have been found in the dayside of the earth's ionosphere due to solar flares. To see the effect of solar flares on night side on the ionosphere we have found two events above Chennai (13.04° N, 80.17° E) and Panji. At Chennai the SROSS-C2 data was available for the solar flare event of February 2, 1997 (19.07-21.30 LT) and for Panji on May 4, 1998 (22.20-23.00 LT). Both the solar flares occurred after sunset over India. We did not find any significant change in electron and ion temperature over aforesaid locations during the solar flares. Thus it may be concluded that the solar flares

do not affect the nightside ionosphere. A similar result have been reported for flare events on September 23, 1998 and July 29, 1999 by Afraimovich et al. (2001) with the help of GPS network data. Some events of solar flares have also been studied (Kanellakos et al., 1962) to see the effect on E and F region ionosphere and it has been found that the electron density was enhanced in the F2 region. Our studies also pertain to the F2 region and reveal the enhancement in electron and ion temperatures.

The enhancement in ion density and ionospheric temperature is mainly due to X-rays production (Charikov, 2000) during a solar flare. These X-rays reach the earth's ionosphere about 8 minutes after the occurrence of the solar flare (Kocharov et al., 2000). Therefore, the time difference between the occurrence of solar flare and the ionospheric heating is not very large.

The above analysis shows that there is a consistent enhancement of the ionospheric electron and ion temperatures recorded during the solar flares. This enhancement was for the average electron temperature ranging from 1.3 to 1.9 times compared to the normal days average temperature. However, for ion temperature it was ranging from 1.2 to 1.4 times to the normal days average temperature. It may be mentioned that for the present analysis the data window was selected in such way that the effect of diurnal, seasonal, latitudinal, longitudinal and altitude effects are minimized. Thus the temperature anomalies reported here directly relate to the solar flares.

The solar flare events selected for the present study had the intensity of about 5 sfu. However, one expects the enhancements of electron and ion temperature to be dependent on the intensity of solar flares. In absence of the

ionospheric data corresponding to more intense solar flares, such a study could not be undertaken.

6.4   Conclusions

The SROSS-C2 data have been analysed to study the electron and ion temperature anomalies during the solar flares. The study reveals that the electron and ion temperatures show a consistent enhancement during the solar flares. The enhancement in case of electron temperature is slightly higher than the enhancement in ion temperature.

The studies performed in this thesis have been summarized in the next chapter.

Table 6.1

Comparison of average electron temperature during solar flare and during normal days

S. No.	Date of Event	Time and Duration of Solar Flares	Study location	Electron Temperature (K)	
				Average during Normal days	Average during Solar Flares day
1.	May 19, 1995	16.67-17.03 LT	15.30° N, 73.55° E	1897	2419
2.	June 5, 1995	8.90-10.03 LT	18.31° N, 73.55° E	1613	2367
3.	July 10, 1996	10.67-11.27 LT	15.30° N, 73.55° E	1382	2005
4.	Nov 9, 1998	5.60-6.17 LT	23.16° N, 77.36° E	1795	3446
5.	Dec 28, 1998	9.04-9.83 LT	18.31° N, 73.55° E	1485	2637

Table 6.2

Comparison of average ion temperature during solar flare and during normal days

S. No.	Date of Event	Time and Duration of Solar Flares	Study location	Ion Temperature (K)	
				Average during Normal days	Average during Solar Flares day
1.	May 19, 1995	16.67-17.03 LT	15.30° N, 73.55° E	1050	1262
2.	June 5, 1995	8.90-10.03 LT	18.31° N, 73.55° E	950	1311
3.	July 10, 1996	10.67-11.27 LT	15.30° N, 73.55° E	1175	1630
4.	Nov 9, 1998	5.60-6.17 LT	23.16° N, 77.36° E	1005	1188
5.	Dec 28, 1998	9.04-9.83 LT	18.31° N, 73.55° E	1233	1630

Figure 6.1 Variation of Electron Temperature during solar flares and normal days at Bhopal.

Figure 6.2 Variation of Ion Temperature during solar flares and normal days at Bhopal.
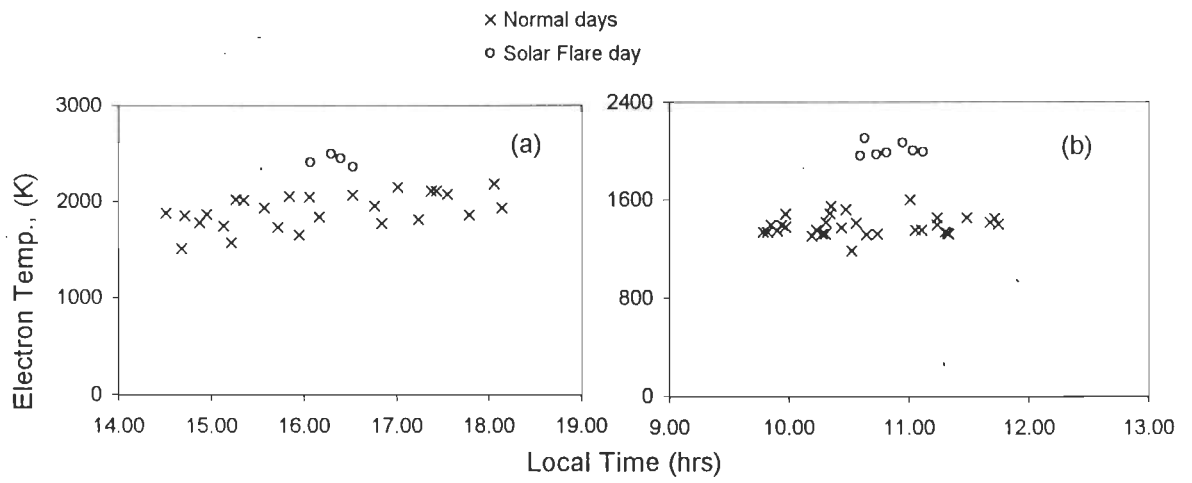
Figure 6.3 Variation of Electron Temperature during solar flares and normal days at Panji.

× Normal days
o Solar Flare day
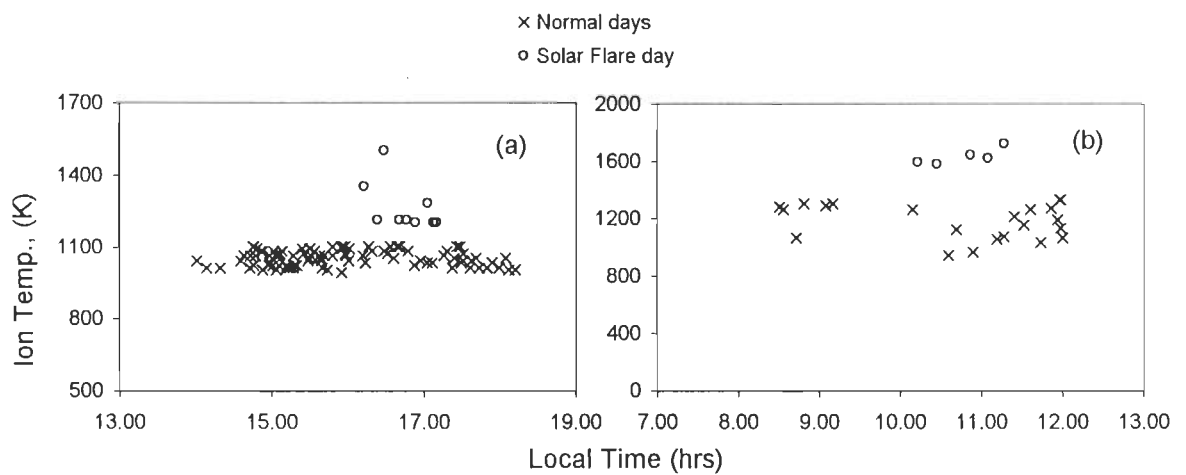
Figure 6.4 Variation of Ion Temperature during solar flares and normal days at Panji.
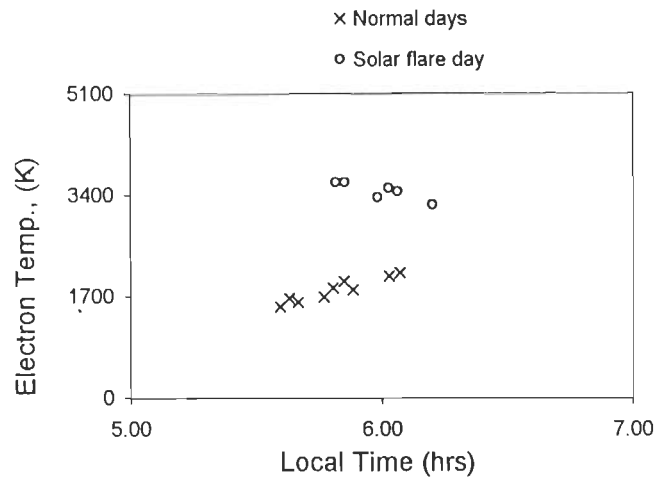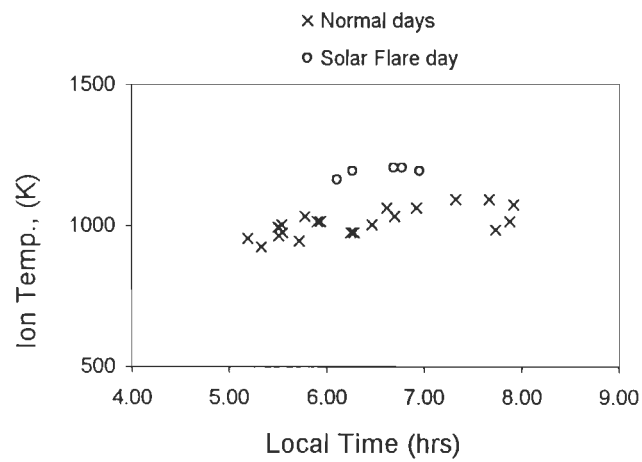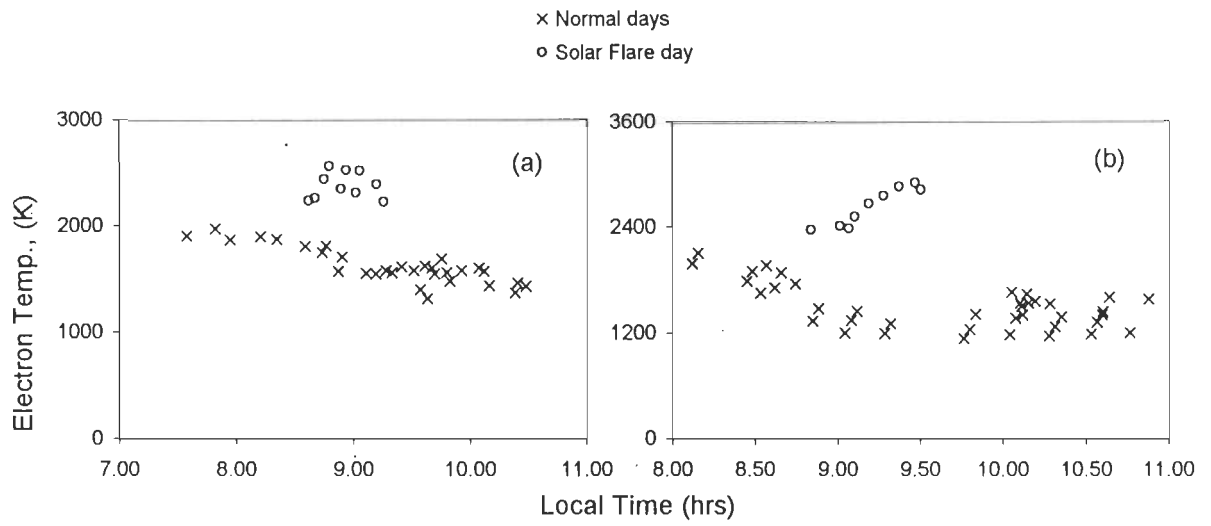
Figure 6.5 Variation of Electron Temperature during solar flares and normal days at Pune.
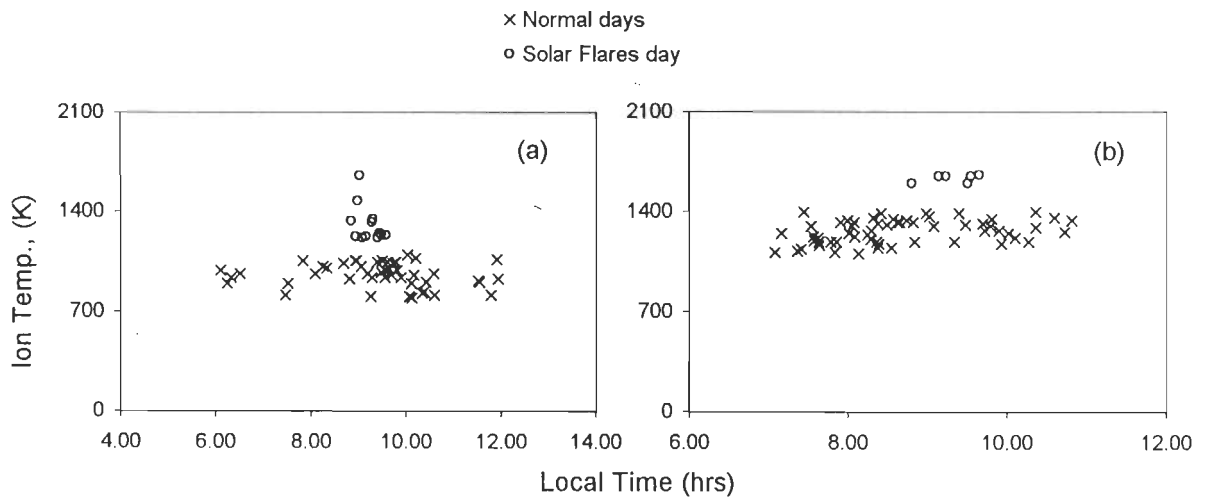
Figure 6.6 Variation of Ion Temperature during solar flares and normal days at Pune.

Chapter 7

Conclusions And Recommendations

7.1 Summery and Conclusions

The purpose of the present thesis is to study the behavior of ionospheric electron and ion temperatures, the diurnal, seasonal and latitudinal variations and their response to thunderstorms and solar phenomena. Some studies on tropospheric aerosols in relation to meteorological parameters have also been carried out in the present thesis.

The ionospheric weather plays an important role in communication, navigation, exploration of near earth space and even exploration of deeper part of earth's interior. Natural electromagnetic fields generated by the interaction of solar wind and magnetosphere in the frequency range of less than 1 Hz generated by thunderstorms and lightning/sprites in the frequency range grater than 1 Hz are directly affected by the ionospheric weather. Understanding the role of ionosphere in generating, propagating and attenuating these fields are crucial for an effective exploration program using magnetotelluric method. The natural electromagnetic fields in the frequency range from 10^4 Hz to 10^{-4} Hz are used as a source in magnetotelluric method of exploration of the earth interior. These electromagnetic field radiations propagate throughout the globe in the electrically charged earth ionosphere waveguide and penetrate in the earth crust. Rapid attenuation of electromagnetic field at the onset of sunrise as observed recently (Garcia and Jones, 2002) may be related to the increase in ionospheric temperature during

63

sunrise. Thus understanding the temperature anomalies in ionosphere will be useful to improve the data quality in magnetotelluric investigation.

The data have been recorded by RPA payload aboard SROSS-C2 satellite during the period from 1995 to 1998. Thunderstorm data were obtained from India Meteorological Department (IMD), Pune, India and that on Solar flares from National Geophysical Data Center (NGDC), Boulder, Colorado, U. S. A. The International Reference Ionosphere (IRI) model values for the same period were used for comparison. Description of RPA payload aboard SROSS-C2 satellite used in the measurement of ionospheric temperatures and methodology for data selection and analysis has been discussed in detail.

Diurnal, seasonal and latitudinal variation of ionospheric temperatures of the topside F region ionosphere over India during the solar minimum year (1995-96) at an average altitude of ~500 km have been studied. The measured electron and ion temperature data have been analysed for three different seasons; summer (May, June, July and August), winter (November, December, January and February) and equinoxes (March, April, September and October) during the solar minimum year. This study reveals that the electron and ion temperatures have minimum values during night hours and show variations during daytime in all seasons. The daytime electron temperature shows atleast two peak values with different magnitudes. The peak during sunrise hours is relatively sharp and high in magnitude and the peak during sunset hours is diffused and lower in magnitude. Similar variations in the ion temperature have also been observed. However, the

amplitude and sharpness of the peaks are smaller in comparison with that behaviour of electron temperature. The predicted values by IRI-95 model show a good agreement with electron and ion temperatures during night hours. The daytime electron temperature variation and sunrise peak values are under estimated by IRI-95 model. However, the secondary peaks during sunset are not seen in the data predicated by IRI-95. The electron and ion temperatures show a positive correlation with latitude during daytime over the geographical region studied. No latitudinal dependence has been observed during nighttime at an average altitude of ~500 km.

The sunrise effect on the ionospheric electron and ion temperatures as measured by the SROSS-C2 satellite during the period from 1995 to 1998 (which cover the solar minimum year of 1995-96) for specific location of Bhopal (23.16° N, 77.36° E) and Chennai (13.04° N, 80.19° E) in India have been done. It has been found that the electron and ion temperatures are minimum during the local night hours and maximum at the local sunrise time. The nighttime electron temperature varies from 745 to 915 K and rises sharply at sunrise to 3334 K or more. The nighttime ion temperature varies from 618 to 832 K and also rises at sunrise to 1270 K or more.

The effect of thunderstorms on ionospheric temperatures shows that there is a consistent enhancement of electron and ion temperatures recorded during active thunderstorms over the normal day temperatures. This enhancement for the average electron temperature is from 1.2 to 1.7 times compared to the average

normal days temperature, whereas, for ion temperature it was ranging from 1.1 to 1.5 times during the active thunderstorms compared to average normal days ion temperature. The data were selected in such a way that the effect of diurnal, seasonal, latitudinal, longitudinal and altitude variations are minimized. Hence the ionospheric temperature anomalies are related to the thunderstorm events. The enhancements in ionospheric electron and ion temperatures have been attributed to the lightning/sprites activity and the associated phenomena.

A consistent enhancement of the ionospheric electron and ion temperatures recorded during solar flares has also been observed. The enhancement in case of electron temperature is slightly higher than the enhancement in ion temperature. This enhancement for the average electron temperature is from 1.3 to 1.9 times compared to the normal days average temperature. However, for ion temperature it was ranging from 1.2 to 1.4 times to the normal days average temperature.

7.2   Recommendations for Future Studies

1. In the present study the data of SROSS-C2 satellite have been used for four years to examine the effect of thunderstorms and solar phenomena. Out of a large number of observations only a few satellite passes which correspond to thunderstorm activity at the ground surface have been selected for present study to draw any definite conclusion a large number of observations for many years is necessary. Data from other satellite may also be used for this kind of study.

2. For a concrete study on the effect of lightning on ionospheric temperatures, the knowledge of the kind of lightning and the enhancement caused by them is necessary. Instruments must be developed to differentiate between the clod to ground and intracloud discharges and sprites.

3. Rapid attenuation of electromagnetic fields at the onset of sunrise as observed recently (Garcia and Jones, 2002) may be due to the increase in ionospheric temperature during sunrise. Such studies must be performed on detail.

4. The seismic activity is also known to influence the ionospheric parameters. A correlative study of the earthquakes and change in the ionospheric temperatures and ion density will help in better understanding of the ionosphere.

Apart from the studies on electron and ion temperature changes in the ionosphere, some studies on the nature of tropospheric aerosols were done by the author. This kind of work is presented in an appendix next to this chapter.

Appendix

Summer Variation Of The Atmospheric Aerosol Number Concentration

A.1. Introduction

The atmospheric aerosol number concentration has been measured at Roorkee (29°52'N, 77°53'E, 275 m above mean sea level) in northern India during November 1998 to August 1999 at a height of 9m above ground level. The aerosol number concentration in summer season (April to July 1999) for morning, noon and evening periods has been analyzed, and the daily variation of aerosol number concentration has been related to some meteorological parameters like: relative humidity, temperature, rainfall and wind speed. The aerosols number concentration was measured by an optical particle counter.

A.1.1 Aerosols

Atmospheric aerosols are suspended solid or liquid particles or mixture of both floating in air. They play an important role in the atmosphere to control the atmospheric radiation budget and hence are important in the variation of weather and climate and numerous effects on human health (Manson, 1965). These are most complex and least understood atmospheric constituents. Due to incomplete knowledge of many inherent unknown properties of aerosols such as physico-chemical, spatio-temporal, source-sink, cycle transformation patterns etc., their realistic assessment is difficult to make.

There is an increasing realization in recent years throughout the globe that the aerosol characteristics are changing significantly due to man made

activities and it has created substantial interest in the estimation of their optical parameters and their influence on climate. In the troposphere and stratosphere the aerosols play a major role in climate change process, particularly as a counter-balance to the effects of warming due to the greenhouse gases (Harshvardhan, 1993). These aerosols also affect air and water quality in the troposphere. Their properties depend regionally and as a function of meteorological parameters viz. temperature, relative humidity, wind speed and direction, atmospheric pressure, rainfall, altitude etc.

A.1.2 Shape and Size of Aerosols

The aerosols are generally considered as a spherical particle. The size range of aerosols varies from $0.001\mu m$ to about 100 μm in radius. This size range can be divided into three groups based on atmospheric effects. The smallest particles size with radii less than 0.1 μm are called Aitken particles and are important in atmospheric electricity (Meyerott et. al., 1984). Particles in the size range 0.1 μm to 1.0 μm are referred to as large particles and are effective in atmospheric optics and in radiation budget (Krishna Murthy, 1988). These are also effective as condensation nuclei (Alofs and Liu, 1981). Particles of size greater than 1.0 μm play an important role in cloud formation and precipitation and are effective as condensation nuclei (Singh, 1985), which are called giant particles (Junge, 1960, Flochini, et al., 1976; McCartney, 1976; Davies; 1974).

A.1.3 Aerosol Sources

The aerosol sources are divided into two parts, one is natural source and the other is anthropogenic. The various natural sources contribute a large

amount of aerosols in the earth's atmosphere. Among of them a few are discussed below:

(a) Interplanetary dust: A large amount of interplanetary dust, approximately 10^7 tons per year, is collected (Petterssen, 1960) by the earth's atmosphere, which increases the earth's mass by a factor of 4×10^{-6} in a billion year. The interplanetary dust becomes important in the stratosphere and above.

(b) Volcanic eruptions: Every year hundreds of volcanoes erupt throughout the globe and they inject a huge amount of ash into the atmosphere. Some of the well-known volcanic eruptions were at Krakatau in 1883, Gunnung Agug in 1963, Mount St. Helens in 1980 and El-Chichon in 1982, which were extremely violent in nature and some of them re-erupted in a decade's time. The violent eruptions inject particulate matter directly into the stratosphere for a year and produce lightning effects and influence the climate.

(c) Bursting of bubbles at sea surface: Due to cresting waves over the ocean surface large number of water bubbles are formed, which burst continuously. The bursting bubbles inject small droplets of seawater (Blanchard, 1967; Mason, 1975) into the atmosphere, which have an effective diameter of 2.0 to 3.0 μm. Most of the droplets are caught up by the wind and transfer over great distances. They also carry with them the solid NaCl particles.

(d) Soil dust blown by surface winds: The surface winds exceeding a few km per hour are effective in lifting up and transporting the soil and contribute to the huge amount of aerosols in the atmosphere. The wind speed and the structure

70

of the soil, both are important for this mechanism. The surface winds blow more dust in desert areas during dry seasons.

(e) Anthropogenic sources: Besides above discussed natural sources, the human activities are also responsible for large amount of aerosols. Many industrial operations, agricultural activities, construction activities, household activities, running automobiles etc. are prolific sources of anthropogenic aerosols. These particles are mostly non-hygroscopic and exist over a wide range of sizes. The larger ones settle down within minutes of their origin and cover the ground surface for miles around, while particles below about 1.0 μm in size move with wind and remain suspended in air for days.

Natural and industrial combustion products usually contain low boiling point vapours, which condense to droplets or directly form the solid particles. Aerosol particles formed by gas-to-particle conversion mechanism cover a wide range of sizes with a majority in the Aitken particles size range. This conversion also results from the reaction between various atmospheric gases in the presence of ultraviolet light. Coal burning and photochemical smog are two examples in which particles are produced by gas-to-particle conversion.

A.1.4 Aerosol Removal Processes

Aerosols are ultimately removed from the atmosphere by the two removal processes. One is dry deposition and another is the precipitation scavenging due to gravity. Dry deposition is the process of direct fallout or deposition of particles onto different surfaces. Larger particles (diameter >20 μm) have large settling velocity and very small particles (diameter <0.1 μm)

behave like gases and undergo random brownian motion resulting in collision with the gas molecules. Particles in the size range 0.1to 1.0 μm diameter have appreciable Brownian motion and hence deposit least rapidly. This size range particles undergo collisions and coagulate resulting in increasing sizes till they become sufficiently large.

Precipitation scavenging or wet deposition is also divided into two parts namely rainout and washout processes. In the rainout process, the aerosol particles may act as condensation or ice forming nuclei in the process of cloud formation or may get attached to cloud droplets and removed from the atmosphere. Washout involves incorporation of a material into precipitation as a consequence of processes occurring below the cloud. Some physical processes responsible for the attachment of particles to cloud elements is the same in case of both rainout and washout processes.

A.1.5 Implications of Aerosols

(a) Direct effects of aerosols on climate: Aerosols may influence the earth's climate directly or indirectly. It's directly influence on climate by scattering and absorbing and indirectly by altering the cloud properties. Scattering of the solar radiation back to space decreases the amount of the solar radiation energy reaching on the earth surface. The magnitude of the direct radiative forcing by aerosols at any location and time depends on the amount of aerosols present, their optical properties, underlying surface albedo and the solar zenith angle. The major difference between the radiative forcing by green house gases (CO_2, CH_4 etc.) and aerosols is that the direct greenhouse gases forcing is both

during day and nighttime and applicable for both cloudy and cloud free conditions, while the aerosol direct forcing is restricted to only day time conditions and highest in cloud free condition. Most of the greenhouse gases have very long life compared to aerosols and hence they are well mixed and forcing is more or less uniform throughout the globe. Various number of numerical modeling studies have been undertaken to assess the effect of increasing greenhouse gases on the earth climate (Cubasch et. al., 1992; Manabe et. al., 1992; Meehl and Washington, 1993; Mikasa, 1992; Murphy and Mitchell, 1995; Tiwari and Goyal, 1997). On the other hand the aerosol lifetime is very short compared to greenhouse gases and hence the aerosol forcing is limited near to the aerosol sources.

(b) Indirect effects of aerosols on climate: the aerosol number concentration increases with the cloud condensation nuclei (CCN), which leads to cloud with higher number of smaller size cloud droplets. An increase in the number of cloud droplets enhances multiple scattering of light within the cloud, which increases the optical depth and albedo of the cloud. This effect of the aerosols on cloud is in general termed as the indirect effect. The formation of precipitation in cloud depends on the cloud droplet size distribution. One possible effect of reduced cloud droplet size is an increase in the cloud lifetime in the atmosphere because of the reduced precipitation. The quantitative estimate of the indirect effect of aerosols on climate is more difficult compared to the direct radiative effect of the aerosol on the climate because the CCN concentration and cloud drop number concentration is determined by various

microphysical processes. A schematic formation of CCN and cloud droplet in the marine atmosphere is shown below:

```
Sea salt                        Activation
                                            Cloud
Dimethyl sulfate        H₂O                 droplet
  H₂SO₄            CCN
Organics

Anthropogenic aerosol
brought from continents      Evaporation
```
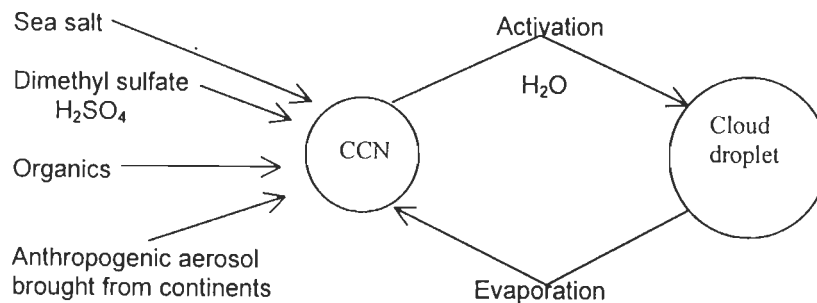
(c) Effect of aerosols on hydrological cycle: Aerosols play a crucial role in the hydrological cycle of the atmosphere. Cloud cycling is the major mechanism, which modifies aerosols in lower atmosphere (Turco, et al., 1981). Khemani et al. (1982) studied aerosols concentration, size distribution and chemical composition of precipitation from different type of cloud forming over the Deccan plateau during south-west monsoon season. Their results indicated that all the chemical components, sulphate and nitrate aerosols play an important role in cloud formation and hence they have an impact on weather and climate.

A.2   Brief history on the earlier aerosol studies

Aerosols play an important role in the atmosphere. They control the atmospheric radiation budget and hence are important in the variation of weather and climate. The atmospheric aerosols either independently or in combination with atmospheric ions act as cloud condensation nuclei (CCN) and affect precipitation (Singh, 1985). Devara and Raj (1998) measured the aerosols during two successive monsoon seasons. Hanel (1976) and Shaw

(1988) have tried to study the size distribution of atmospheric aerosol in different meteorological conditions. Singh et al., (1997) measured the concentration of aerosols during monsoon period and found that the concentration decreases with increasing precipitation. This phenomenon has been attributed to the scavenging of large aerosol particles due to rain.

The aerosol distribution can be measured by using various techniques available such as Cascade impactor (Pahwa et. al., 1994; Zhang et. al., 2001), Lidar (Devara and Raj, 1998; McCormick, 1978), Low-pressure impactor (Parameswarn and Vijaykumar, 1994) Laser scatterometer (Singh et. al., 1997), Optical counter (Bansal and Verma, 1998) etc.

In the present study, we have measured the aerosol number concentration with an optical counter. The summer variation of atmospheric aerosol number concentration in different size bins for morning, noon and evening periods and their behavior with some selected meteorological parameters: relative humidity, temperature, rainfall and wind speed have been studied.

A.3   Experimental Technique used in the present study

The optical counter model KC-01A (Rion Co. Ltd. Tokyo, Japan) has been used in the present study, which is based on the principle of Mie scattering of light. The internal layout of the particle counter has been shown in Figure A.1. The instrument has been well calibrated and has a provision for inbuilt calibration. A light beam intersects a flow of ambient air containing aerosols, which is chopped by a light chopper. The light incident on aerosol particles is scattered and received by a Photo Multiplier Tube (PMT) at an

angle of 90°. The output of the PMT is amplified and then fed to a Pulse Height Analyzer (PHA), which divides the aerosol response into different size ranges. The pulse height is directly proportional to the particle size. The instrument sucks the ambient air at the rate of 1 liter in two minutes. The sucked air is monitored for two minutes only and the number concentration of particles is measured in the unit of particles per liter. The whole equipment is the microprocessor controlled and gives direct print out of aerosol particle number concentration for different size ranges of 0.3-0.5 μm, 0.5-1.0 μm, 1.0-2.0 μm and 2.0-5.0 μm. The error in all size ranges measurement is less than 5%. The detailed description of the instrument can be found in the work of Bansal and Verma, 1998. The observations were made at a height of 9m above the ground surface on second floor of the physics department building inside the IIT campus. The IIT campus is located in Roorkee (29°52' N, 77°53' E) at a height of 275 m from the sea level. The surrounding is free from polluting industries; the man made aerosols are mainly due to household activities and automobiles.

The observation time for the present study was chosen for the period from April to July 1999 and data were recorded continuously from 9:00AM to 6:00PM. The number concentration of aerosols in the above size ranges was recorded at every half an hour interval and the data of meteorological parameters were recorded at the National Institute of Hydrology (NIH), Roorkee, which is located at a distance about 300m from the aerosol observation site.

A.4 Results and Discussion

The measurements have been grouped for morning, noon and evening periods. Analysis has been done in all the size ranges and observation period from April to July has been chosen for the present study because in this period the premonsoon and monsoon activities both occur. The aerosol number concentration has a diurnal variation. In the evening the aerosol number concentration decreases as reported by Vakeva et al., (2000). At noon it is increased due to prevailing sun and wind. The morning aerosols have different characteristics due to continued condensation because of high humidity and low temperature (Parameswarn and Vijaykumar, 1994). Therefore in present study we have also divided the period of measurement in three groups *i. e.* morning, noon and evening periods.

Aerosols data have been recorded for four size ranges (0.3-0.5 μm, 0.5-1.0 μm, 1.0-2.0 μm and 2.0-5.0 μm). The average concentration of aerosols for the evening period (1600 to 1800 o'clock) for summer months is shown in Figure A.2. In the size range 0.3 to 0.5 μm [Figure A.2 (a, b)] the evening aerosol concentration varies from about 4×10^4 to above 2×10^5 particles/liter in the month of April, most of the particles remaining under the upper size range of 10^5 particles/liter. The concentration of the particles remains nearly the same in the month of May 1999. However in the month of June the concentration of these particles was decreased. Most of the particles remain in the range 1.5×10^4 to 9×10^4 particles/liter. In the month of July the concentration had further decreased and most of the particles fall in the range 1×10^4 to 8×10^4 particles/liter.

77

This trend continues in the size range 0.5 to 1.0 μm. Most of the particles remain around 4×10^4 particles/liter both in the months of April and May. The concentration in this range had decreased in the months of June and July. The lowest concentration goes up to about 10^3 particles/liter in July.

In the size range 1.0 to 2.0 μm the concentration is lower than the previous size ranges. In April, though the concentration ranges from above 1×10^3 to 4.75×10^3 particles/liter, most of the particles remain within the upper limit of 2.5×10^3 particles/liter. The concentration remains at the same level in the month of May. In the month of June the average concentration of particles (1×10^3 to 5.6×10^3 particles/liter) has slightly increased compared to the month of April and May, though there are high fluctuations in this month. In July the concentration of particles had decreased drastically, most of the particles (leaving first few days) remaining in the range about 200 to 1400 particles/liter. In this size range the increase of particles in the month of June can be attributed to the larger particles being airborne due to heat, that causes desiccation and wind. However, in the month of July the lowering of aerosol number concentration can be attributed to the scavenging of aerosols by monsoon rain.

A similar situation prevails in the size range 2.0 to 5.0 μm [Figure A.2 (c, d)]. In the month of April and May the level of concentration remains the same (300 to 1200 particles/liter). In June the concentration increases drastically ranging from about 400 to 5600 particles/liter. However, in July the concentration had decreased drastically with most of the particles lying in the concentration range 50 to 300 particles/liter.

During the noon period (from 10:30 AM to 3:00 PM) the daily average concentration [Figure A.3 (a, b)] in the size range 0.3 to 0.5 μm is at the same level as for evening for the whole summer from April to July. In the size range 0.5 to 1.0 μm the noon time average concentration is higher than the evening concentration during the month of April (1×10^4 to 8×10^4 particles/liter) but most of the particles remaining within the upper limit of 4×10^4 particles/liter and in the month of May it is slightly higher than the evening concentration (1.5×10^4 to 5×10^4 particles/liter). This higher trend for noon concentration remains in the months of June and July. In the size range 1.0 to 2.0 μm the noon concentration is higher than the evening concentration in the months of April, May and July. However, in June they are almost similar. The noon concentration in the size range 2.0 to 5.0 μm is [Figure A.3 (c, d)] maximum in June and minimum in July. During all the four months the time variation of noon aerosols have similar pattern as for the evening aerosols. The nature of time variation for evening and noon aerosols in the above size ranges are also similar.

The concentration of aerosols during morning period (9:00 AM to 10:00 AM) in the size range 0.3 to 0.5 μm is nearly in the same range as for noon and evening period for the whole summer of 1999 [Figure A.4 (a, b)]. The same is the case for the size range 0.5 to 1.0 μm. In the size range 1.0 to 2.0 μm also the level of concentration and time variation are the same as for noon and evening periods. In the size range 2.0 to 5.0 μm [Figure A.4 (c, d)] the level of concentration and time variation in all other months are the same as in the

above size ranges except in the month of May, where the level of concentration is higher and it varies from about 800 to 5500 particles/liter.

The time variation of aerosols in three size ranges shows that for 0.3-0.5 μm, 0.5-1.0 μm and 1.0-2.0 μm the morning concentrations are larger than the evening concentration and show a steady decrease from 0900 to 1400 o'clock and then become steady. Figure A.5 shows the daily behaviour of 0.3-0.5 μm and 2.0-5.0 μm size ranges. Because of the low temperature and high humidity the contribution to aerosol number concentration in the lower size ranges during morning period is due to water vapour condensation. With the rise of the Sun the temperature increases and the droplets get evaporated. However, the large size range of 2.0 to 5.0 μm dominates. With the rise of temperature and occurrence of high velocity winds the aerosol number concentration increases. The atmospheric temperature becomes high around 1400 o'clock and after that both the temperature and wind velocity decrease. This causes a maximum around 1400 o'clock in large size range in the aerosol concentration. This trend is clearly visible in the months of April and July. In July the concentration is lowest in all size ranges due to scavenging. But the high velocity wind around 1400 o'clock might have caused a peak at that time in the size range 2.0 to 5.0 μm in the months of May and June. After about 1000 o'clock the concentration (2.0 to 5.0 μm size) becomes almost constant till evening. The absence of peaks in May and June and their lower concentration compared to April has been attributed to the low intensity rain in these months.

Devara and Raj (1998) studied the columnar content of aerosols over Pune using lidar. Their results revealed contrasting nature of variation in the year

1987 and 1988. In 1987 the concentration was minimum in the month of May while in 1988 it was maximum in this month, both in the height range 50-1100m and 50-200m from the ground surface. Their result showed that the aerosol concentration was minimum during rainy season. This is in good agreement with our observation that the aerosol number concentration had gone minimum in the month of July when the monsoon over Roorkee was in full swing.

Pahwa et al., (1994) studied the aerosols of different composition and the total suspended particles (TSP) at Delhi. Their study revealed that during May 1986 the TSP concentration was 543.13 μg/m^3. It had increased to 777.17 μg/m^3 in the month of June. In July and August the concentration had gone to 231.88 μg/m^3 and 173.36 μg/m^3 respectively. As the onset of monsoon over Roorkee and Delhi are nearly at the same time, their results can be compared with our observation that in July the aerosol number concentration in all size ranges is decreased drastically. In their studies the minimum concentration was in August. The maximum rain occurs in August, which decreases the aerosol number concentration due to scavenging.

Figure A.6 shows the day-to-day variation of aerosol number concentration occurs, it is seen that the variation of average concentration of aerosols for different size ranges differs. For large size particles (2.0-5.0 μm), the concentration is lowest and the concentration is maximum for small size particles (0.3 – 0.5 μm) during the whole period of observation. The small size 0.3-0.5 μm, aerosol number concentration is about 3x10^5 particles/liter in the month of April. Most of the particles remain in the upper range of 10^5 particles/liter [Figure A.6 (a, b)]. The concentration of particles is nearly the

same in the month of May but is less in comparison to the month of April. In the month of June, the concentration of aerosol decreases and most of the particles remain in the concentration range 2.3×10^5 to 9×10^4 particles/liter. A further decrease in concentration is observed in July.

This trend continues in the size range 0.5-1.0 μm [Figure A.6 (c, d)]. Most of the particles remain in the range 7×10^4 to 8×10^3 particles/liter in the months of April and May. The concentration in this range decreases in the month of June and July. The lowest concentration goes to 10^3 particles/liter.

In the size range 1.0-2.0 μm [Figure A.6 (e, f)] the concentration is lower than that in the pervious range. In the month of April the concentration range from 2.5×10^2 to 6.4×10^3 particles/liter. It is nearly the same in the month of May and is lower in June than in July. In the month of July the aerosol number concentration varies from 6.4×10^3 to 1×10^2 particles/liter.

A similar situation prevails in the size range 2.0-5.0 μm [Figure A.6 (g, h)]. During the months of April and May the concentration of aerosol was nearly the same (50 to 100 particles/liter), while in June, the concentration increases, ranging from 50 to 200 particles/liter. There is a significant decrease in the concentration in July and most of the particles lie in the concentration range 15 to 50 particles/liter.

The fluctuation of aerosol number concentration depends upon meteorological parameters. The relative humidity (RH) was minimum in the month of April and increases in May and became maximum in July [Figure A.7 (a, b)]. In the month of June the RH was less than the month of July. Present study reveals that the aerosol number concentration was more affected by RH

during South-East (SE) premonsoon season of the year 1999 over Roorkee. Parameswaran and Vijaykumar (1994) found that the RH significantly affects the aerosol concentration and size distribution above about 90%. Here at Roorkee in the months of June and July 1999 average RH was almost close to this limit. Devara and Raj (1998) observed a higher humidity and lower temperature during South-West premonsoon in the year 1988 at Pune. The effect of premonsoon scenario (Aher and Agashe, 1997) on aerosols at Pune caused by the growth of cloud droplets results in higher rainfall. The same physical process appears to have taken place in 1999 at Roorkee during SE premonsoon. The maximum temperature was lower in April than the month of May (Figure A.7c) and is maximum in June and also decreases in month of July (Figure A.7d). The minimum temperature was higher in July and nearly the same in June and is lower in the month of April and increases slightly in May [Figure A.7 (e, f)]. The wind speed is nearly same in the months of April and May (Figure A.7i) and is higher in June and again decreases in the month of July (Figure A.7j). The rain plays an important role to modulate the aerosol size as larger particles take part in the scavenging process (Devara and Raj, 1998; Byrne et. al., 1993 and Sparmacher et. al., 1993). In the month of April and May the rainfall is nearly zero (Figure A.7g) so there is no significant effect on aerosol number concentration. The SE monsoon is effective (Figure A.7h) after mid of June, so the concentration of aerosol decreases and it is in phase with the increasing monsoon activity. This is attributed to the rainfall, which is a powerful factor to lower the aerosol number concentration involving rainout

process. The monthly means of aerosol number concentration along with standard deviations (σ) have been shown in Table-A.1.

The average number concentration of aerosols is shown in Figure A.8(a, b) and the average of meteorological parameters (relative humidity, temperature, rainfall, and wind speed) in Figure A.9(a, b, c) for summer season 1999 over Roorkee. In the small size ranges (0.3-0.5 μm and 0.5-1.0 μm) particle average concentration is maximum in the month of April and May and decreases continuously in June and July while the RH forms minimum in April and May and goes to maximum in June and July. The wind speed (Figure A.9c) remains almost constant throughout the period of observation. In the large size ranges (1.0-2.0 μm and 2.0-5.0 μm) the average particle concentration increases, going to maximum in the middle of June, after which its starts decreasing.

The aerosol number concentration is expected to be dependent on meteorological parameters. The comparisons with meteorological parameters like relative humidity, wind speed, temperature and rainfall with aerosol number concentration have been shown in Figures A.10-A.14 along with the equation of linear regression fits and the correlation coefficient.

Figure A.10 shows the correlation of average aerosol number concentration to the relative humidity. The number concentration in all size ranges decreases with humidity. The increasing humidity removes the aerosol particles in all size ranges due to condensation on aerosol particles and subsequent falling down of the drops or droplets takes to the ground. Pranesha and Kamra (1996) in their laboratory studies have found that the particles are

actually removed from the air due to condensation. The correlation coefficient (R) is large for the lower size range particles (0.3 to 0.5 μm and 0.5 to 1.0 μm) and small for upper size range particles (1.0 to 2.0 μm and 2.0 to 5.0 μm). This shows that the smaller particles acts as condensation nuclei and the contribution of larger particles to this process are very small. Figure A.11 shows the slight increase in number concentration with increasing wind speed. This can be attributed to the dust particles from the soil becoming air-borne due to wind and an increase in the number concentration is expected. However the correlation coefficient in all the size ranges is very small and a definite relation can't be established.

The concentration decreases slightly with increasing minimum temperature (Figure A.12). The correlation coefficient (R) is about -0.50 for lower size ranges and it becomes very small for the upper size range particles (-0.22). This has further been attributed to the process on condensation at small size particles. The increasing minimum temperature decreases the condensation and hence a negative trend in the regression line of fit has been obtained. On the other hand the average concentration slightly increases with increasing maximum temperature (Figure A.13). With the rise of maximum temperature more and more drops/droplets are vaporized leaving behind the aerosols.

Figure A.14 shows the decrease of aerosol number concentration with rainfall is as expected which is attributed to the scavenging of aerosol particles (Devara and Raj, 1998; Byrne et al., 1993; Sparmacher et al., 1993 and others).

One may doubt the conclusion drawn regarding the influence of meteorological parameters on aerosol number concentration. Pranesha and Kamra (1996) have performed laboratory studies and have found that the suspended particles are removed from air due to condensation.

Hanel (1976) found that the particle size decreases with decrease in RH. Parameswran and Vijaykumar (1994) studied the aerosol size distribution using a low-pressure impactor (LPI) and concluded that the aerosol size decreases with decreasing RH. Vakeva et al., (2000) studied the nucleation phenomena in the humid urban atmosphere and found that the ultra fine particles (diameter 10 nm or less) are produced due to nucleation. However, our interest lies in large particles (0.3 μm and larger) and their results are not much relevance to our studies.

Vakeva et al., (2000) also studied the effect of wind on aerosol concentration. They found that during moderate wind the sub-micron size particles increase in concentration in the urban environment. They also found that the aerosol concentration is a function of wind direction. In our studies we have not considered the wind direction but have found that the aerosol number concentration increases with increasing wind speed.

Shaw (1988) has found that the aerosol concentration in the size range 0.36 to 0.40 μm increases with increasing temperature. In his studies a very high level of aerosol concentration was found in summer (about 4 times as a rough estimate) than the winter months. Further, the sun increased the aerosol concentration in the above size range. The aerosol number concentration dependence on both minimum and maximum temperatures are shown in

Figure A.12 and A.13. In all size ranges the aerosol number concentration decreases with increasing the minimum temperature. The correlation coefficient ranges from −0.22 (for largest size range) to −0.52 (for smallest size range). However, the variation with maximum temperature is quite contrary. In all size ranges it increases with increasing maximum temperature. The correlation coefficients are 0.39 (0.3-0.5 μm), 0.50 (0.5-1.0 μm), 0.36 (1.0-2.0 μm) and 0.43 (2.0-5.0 μm).

In all the above discussions the correlation coefficient (R) between aerosol number concentration and meteorological parameters is not very high and the data points are scattered. The linear regression model here does not work well. The aerosol particles depend upon many parameters including natural and man made sources and almost all the meteorological condition act the same time. Therefore a linear relationship between the aerosol number concentration (in different size ranges) and meteorological parameters individually are not very responsible.

A.5 Conclusions

In the present study the behavior of aerosols number concentration during morning, noon and evening periods in summer season (April to July, 1999) for different size ranges of the aerosols (0.3-0.5 μm, 0.5-1.0 μm, 1.0-2.0 μm and 2.0-5.0 μm) have been investigated. Aerosol number concentration for small size ranges (0.3-0.5 μm and 0.5-1.0 μm) was higher than that for large size ranges (1.0-2.0 μm and 2.0-5.0 μm). The variation of aerosol number concentration in morning was found to be less than noon and it was observed

maximum during evening. The time variation of aerosols was highly dependent on size. For small size ranges the number concentration decreased monotonically till the end of July. For large size ranges it increased becoming maximum in June and minimum in July. The study reveals the fact that the aerosol size and number concentration are affected by the meteorological parameters. The larger particles are especially sensitive to variations in meteorological parameters. The relative humidity, temperature, rainfall and wind speed play important role to modulate the aerosol behavior but large amount of precipitation (heavy rainfall) can alter the number density and size distribution of atmospheric aerosols more efficiently than RH and wind speed.

Table-A.1

Monthly mean of aerosol number concentration and standard deviation (σ)

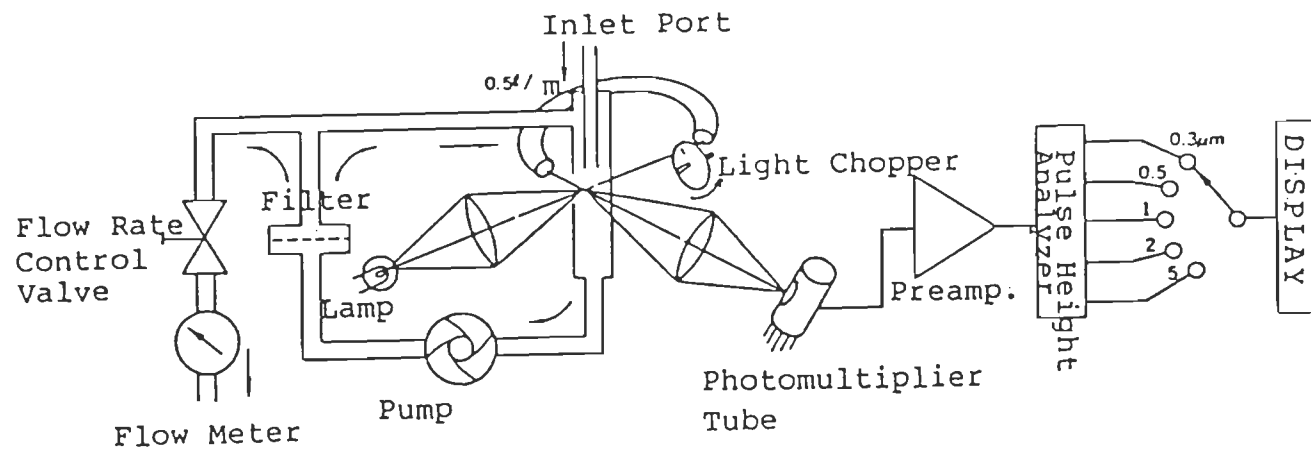| Months	Size range 0.3-0.5 μm		Size range 0.5-1.0 μm		Size range 1.0-2.0 μm		Size range 2.0-5.0 μm	
	Conc. mean (liter^{-1})	Standard deviation	Conc. mean (liter^{-1})	Standard deviation	Conc. mean (liter^{-1})	Standard deviation	Conc. mean (liter^{-1})	Standard deviation
April	16.46×10^4	8.80×10^4	35.03×10^3	10.46×10^3	29.57×10^2	18.69×10^2	7.78×10^1	2.46×10^1
May	11.51×10^4	5.19×10^4	25.95×10^3	7.34×10^3	16.32×10^2	10.13×10^2	9.87×10^1	6.86×10^1
June	8.73×10^4	4.98×10^4	28.07×10^3	12.68×10^3	16.86×10^2	14.46×10^2	8.92×10^1	5.62×10^1
July	5.61×10^4	5.03×10^4	13.96×10^3	17.18×10^3	8.50×10^2	8.54×10^2	2.56×10^1	1.60×10^1

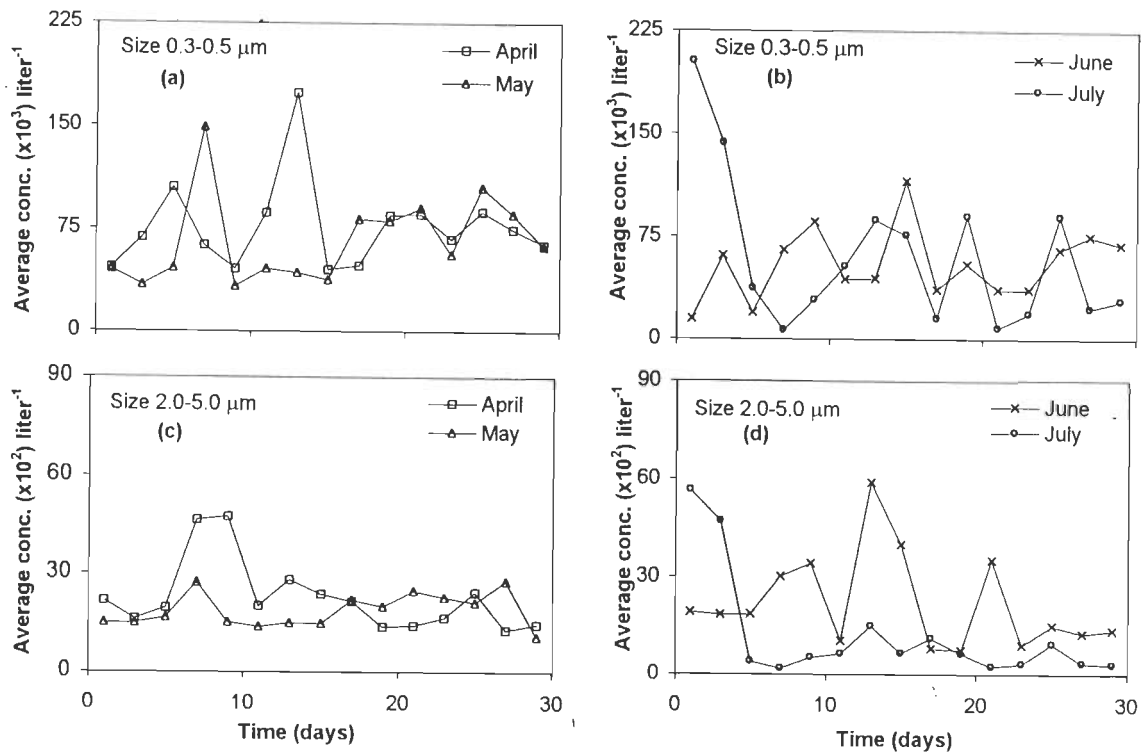Figure A.1   Internal layout of the particle counter.

Figure A.2 Variation of average number concentration of aerosol in evening period for summer season (April-July 1999) for lower and upper size range.
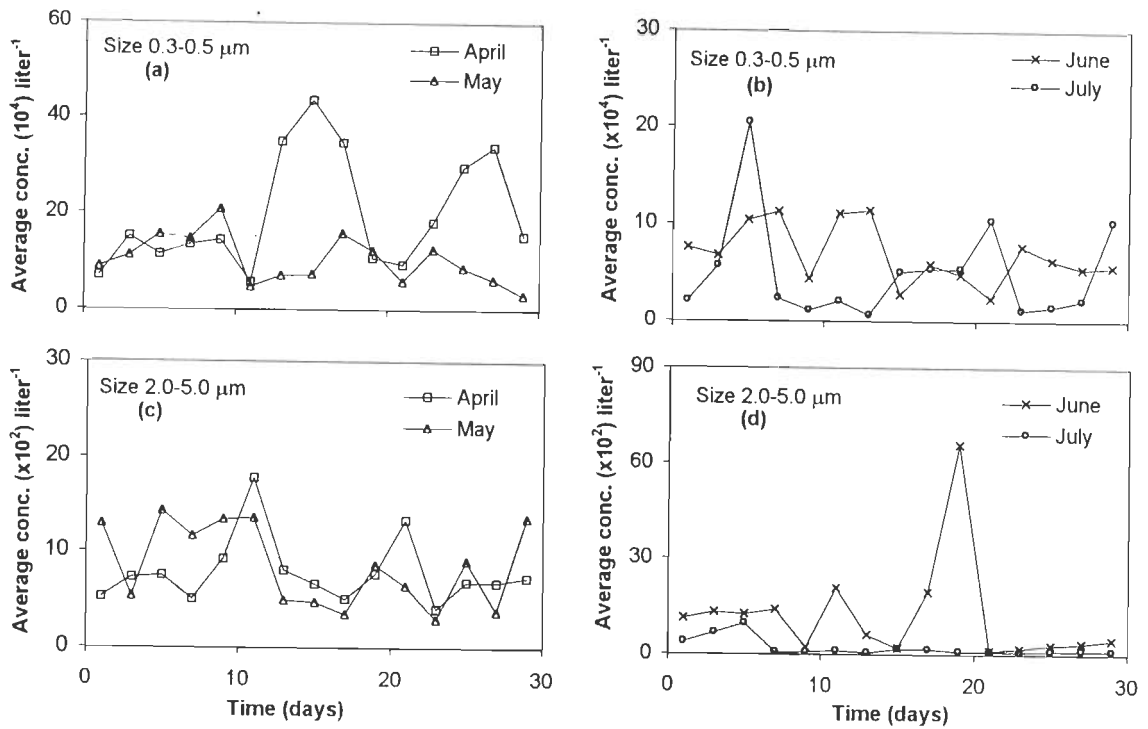
Figure A.3 Variation of average number concentration of aerosol in noon period for summer season (April-July 1999) for lower and upper size range.
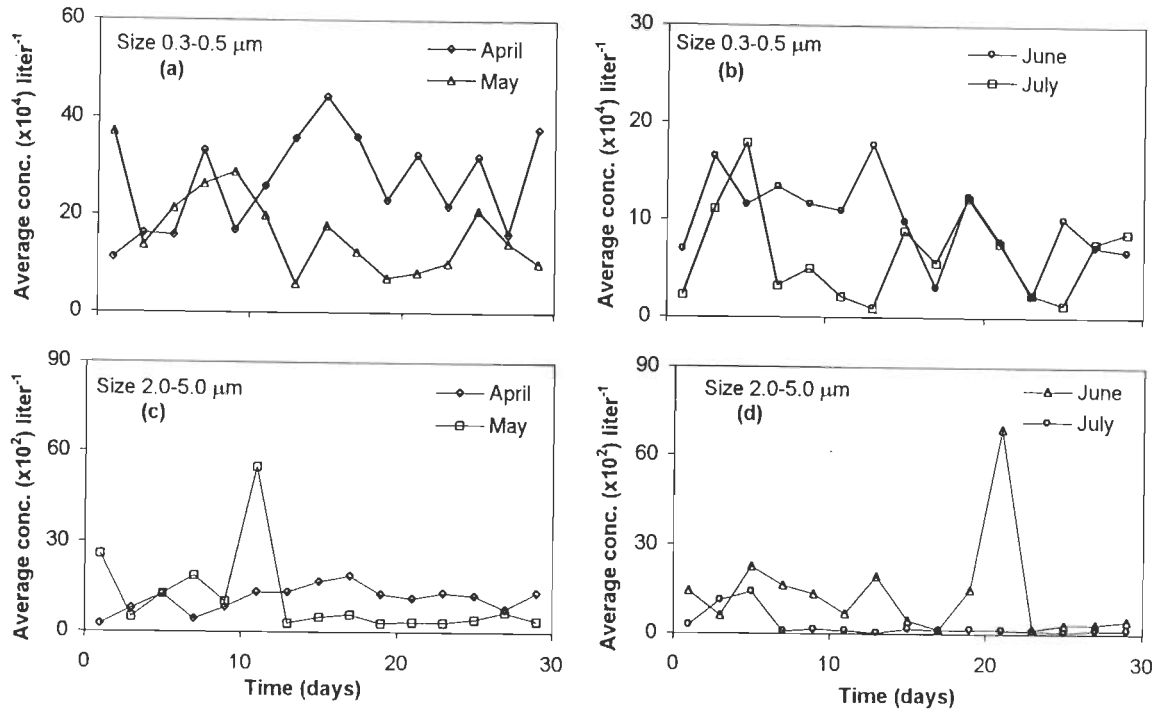
Figure A.4 Variation of average number concentration of aerosol in morning period for summer season (April-July 1999) for lower and upper size range.
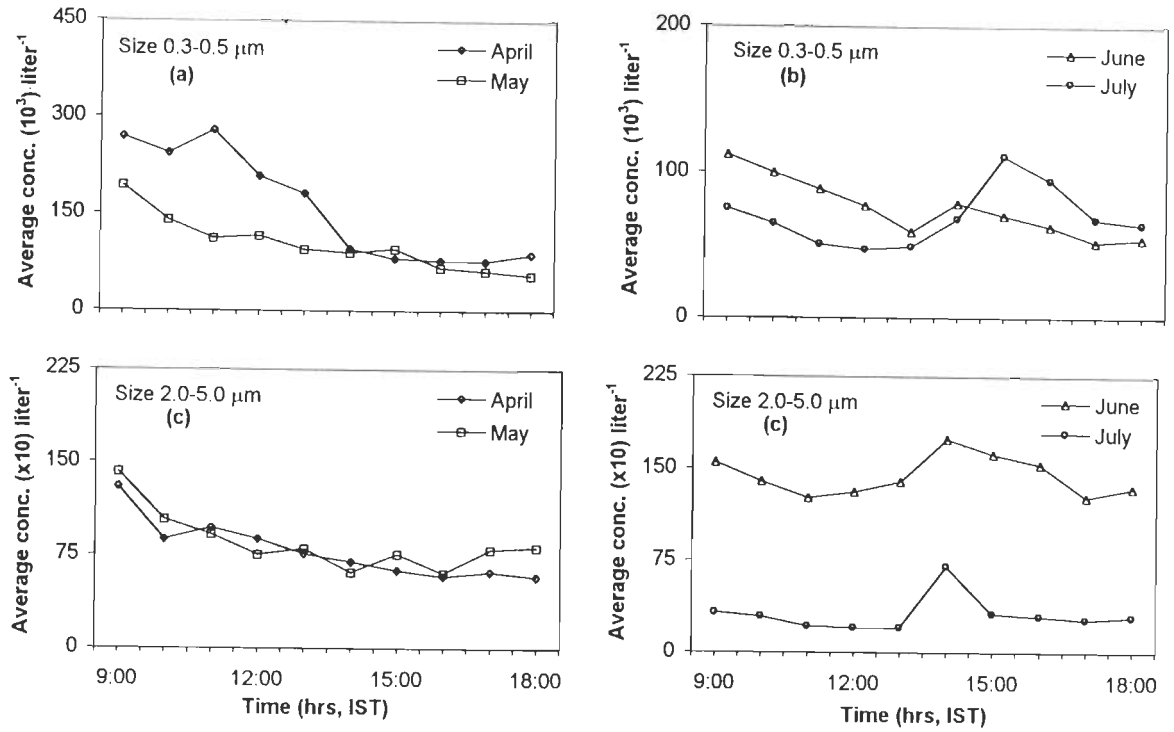
Figure A.5 The time variation of average number concentration of aerosol in summer season (April-July 1999) for lower and upper size range.
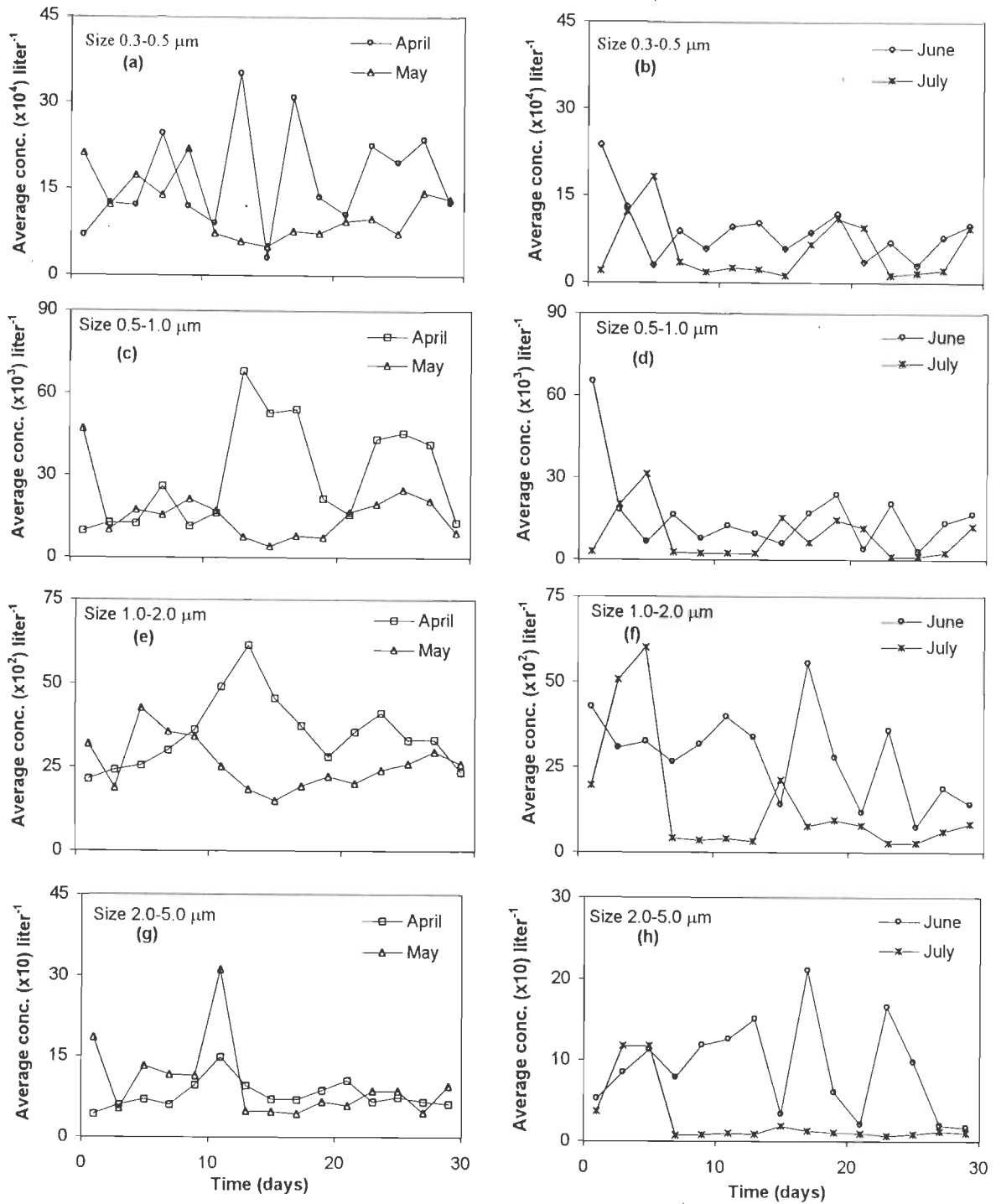
Figure A.6 Variation of average number concentration of aerosol in summer season (April-July 1999) for different size ranges.

Figure A.7 Variation of average meteorological parameters (relative humidity, temperature, rainfall and wind speed) in summer season (April-July 1999).
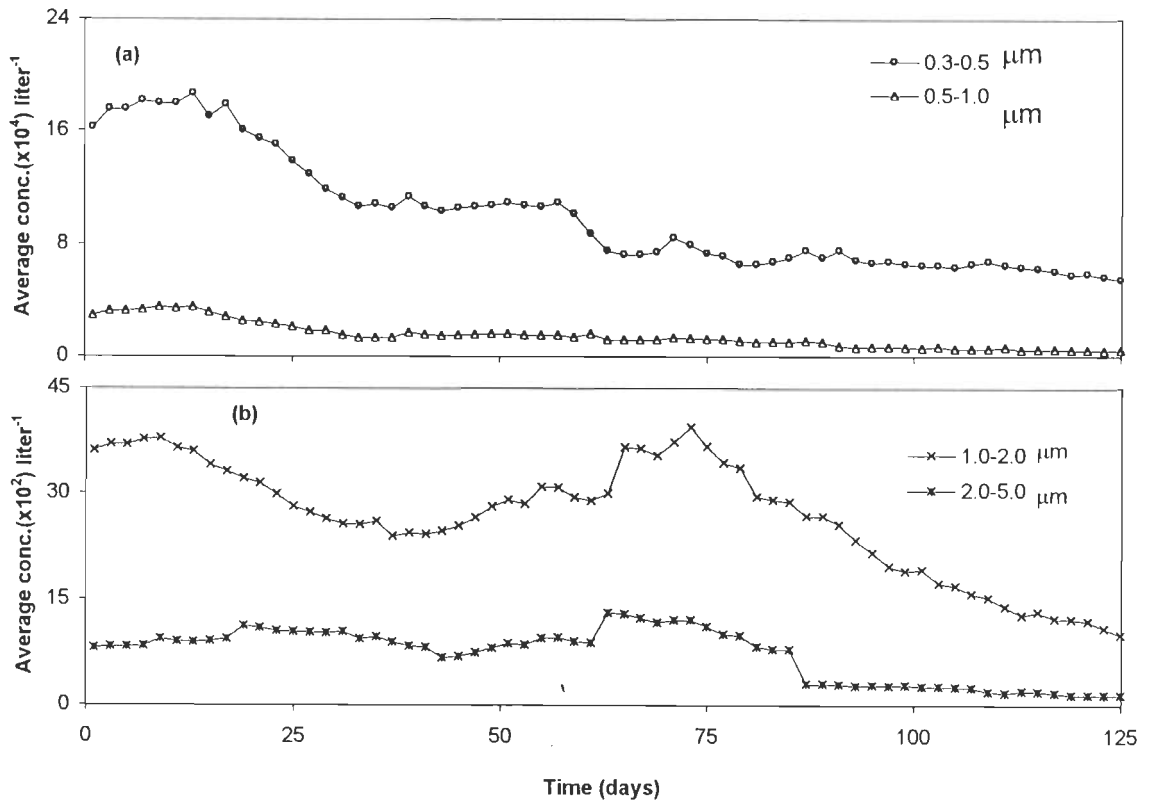
Figure A.8 The running mean average number concentration of aerosols in summer season (April-July 1999).
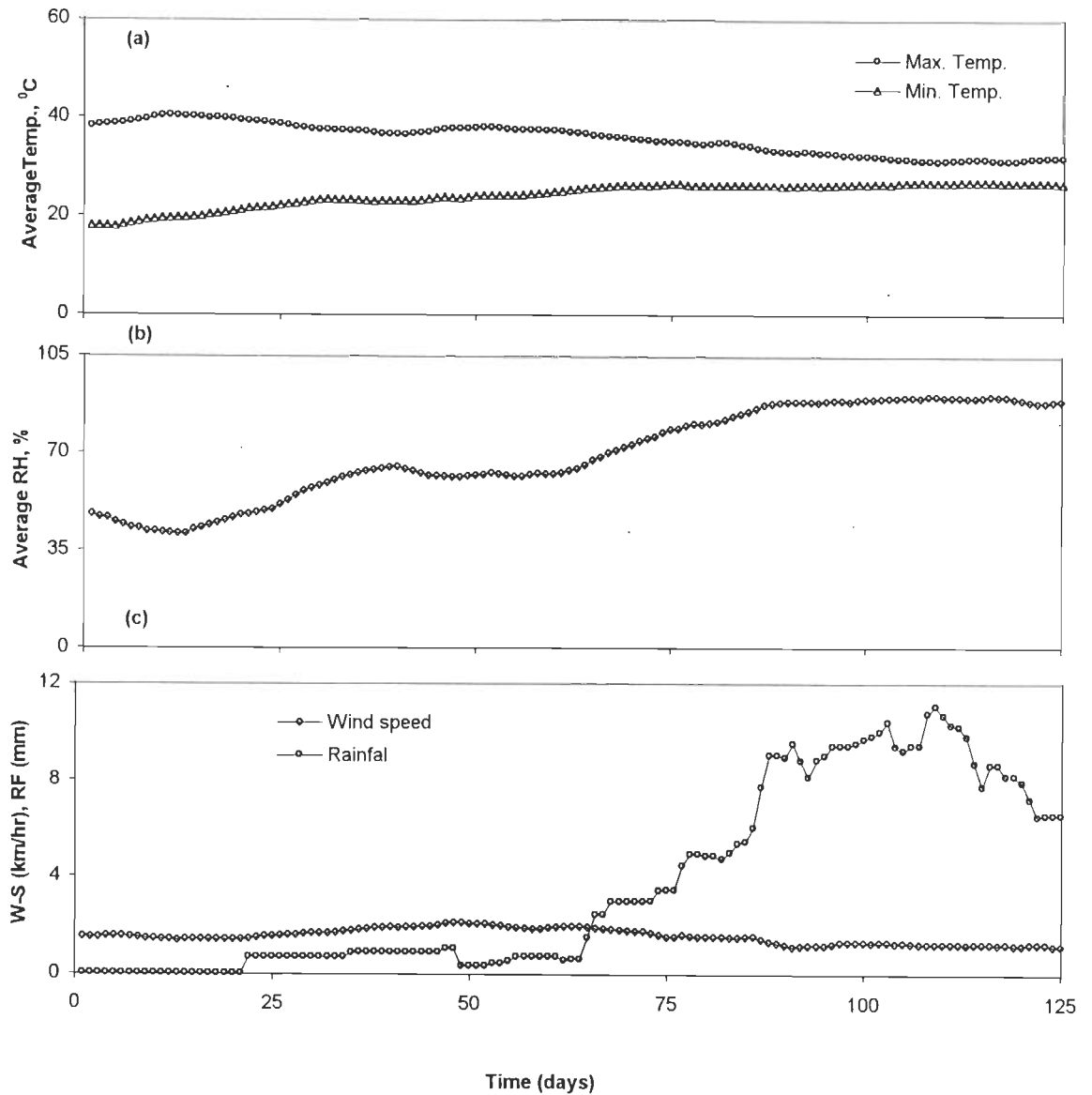
Figure A.9 The running mean average of meteorological parameters (relative humidity, temperature, rainfall and wind speed in summer season (April-July 1999).
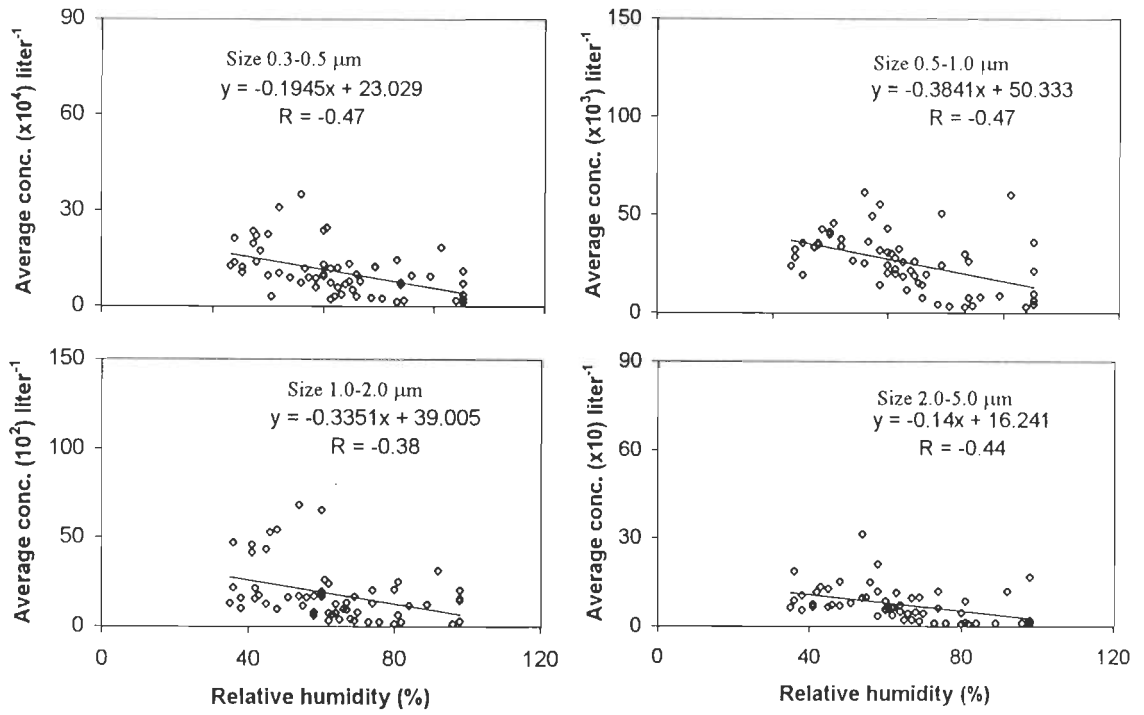
Figure A.10 Variation of average aerosol number concentration versus relative humidity during April-July 1999 for different size ranges.
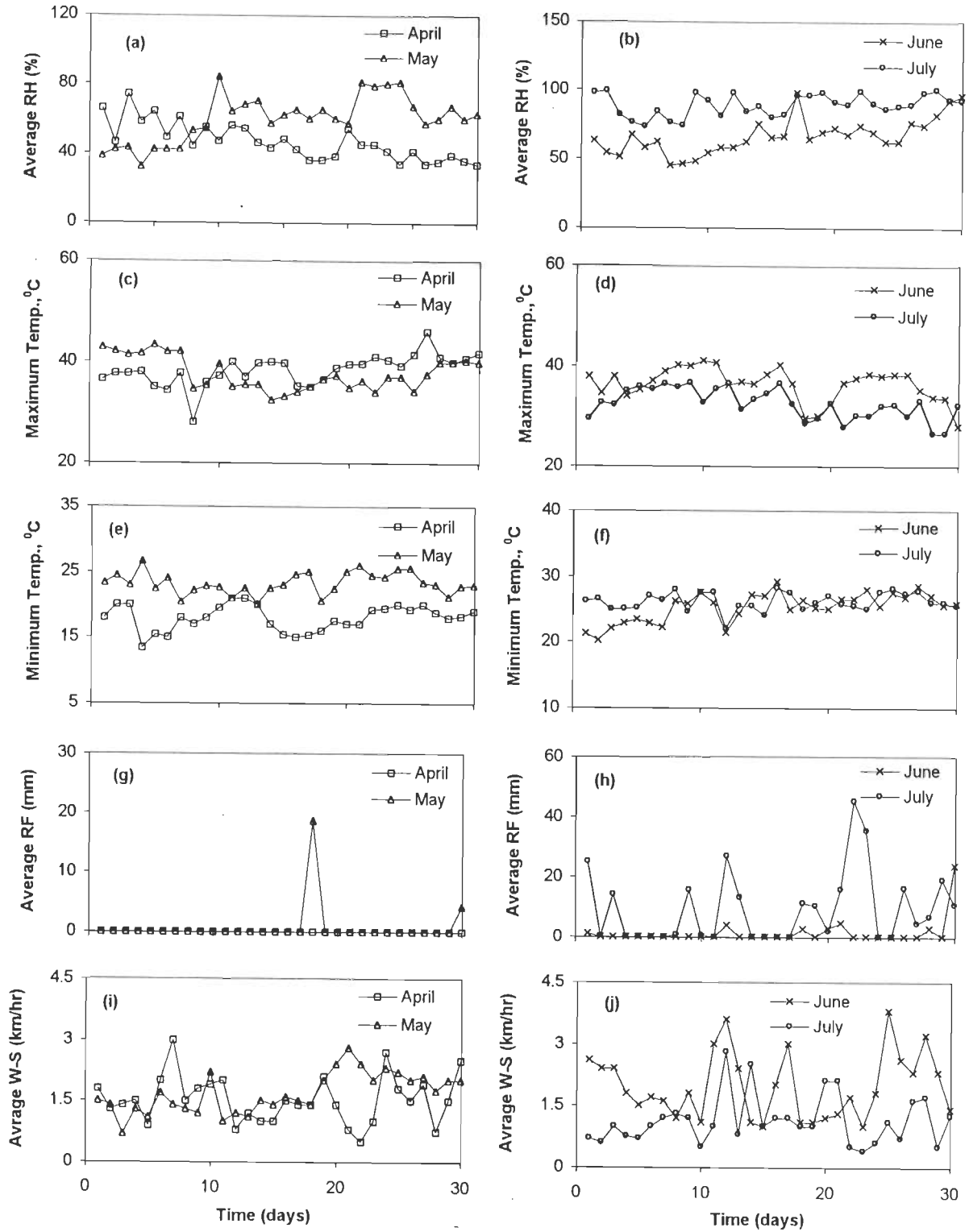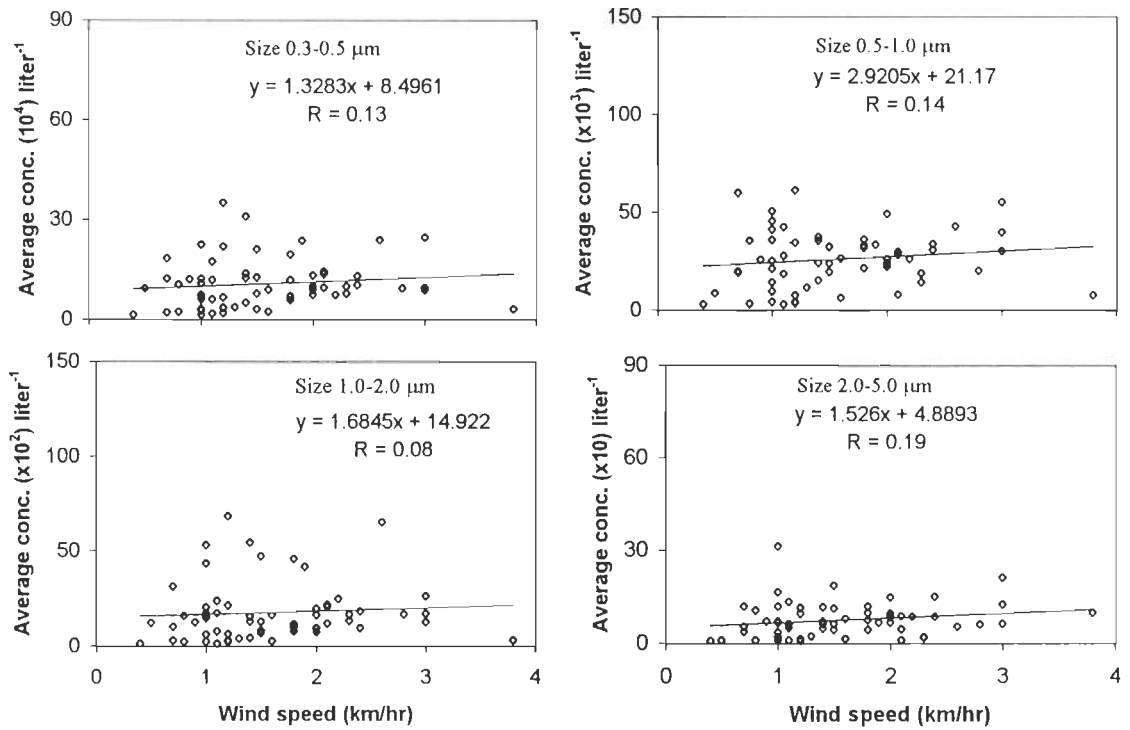
Figure A.11 Variation of average aerosol number concentration versus wind speed during April-July 1999 for different size ranges.
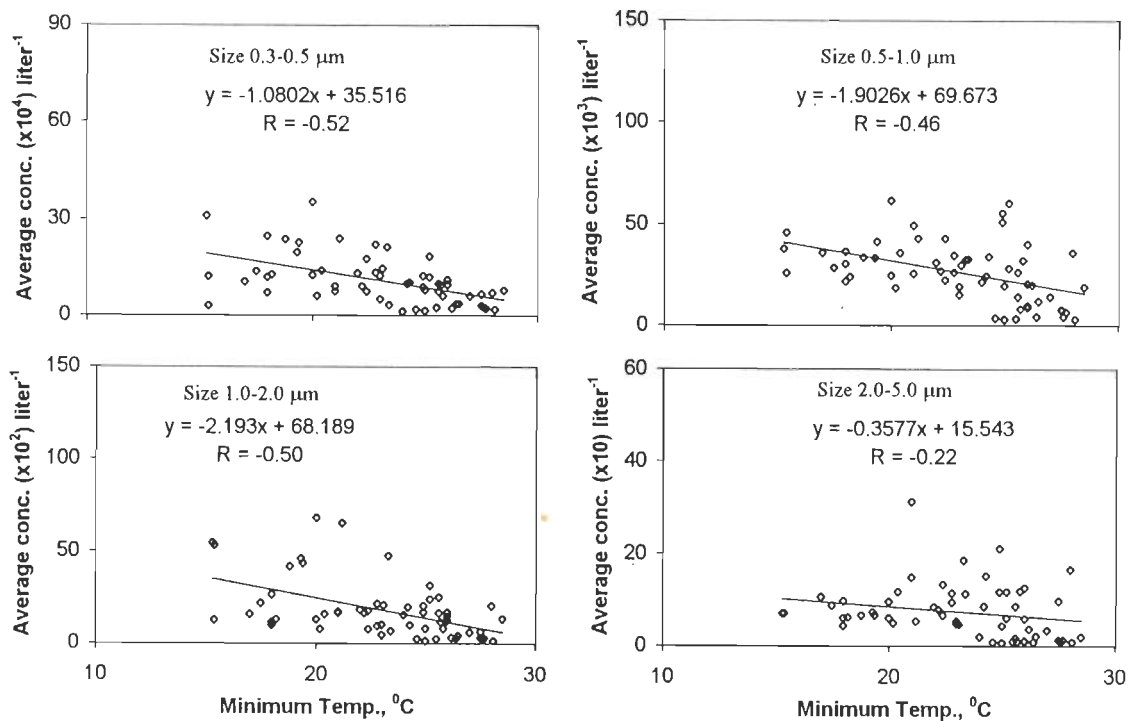
Figure A.12 Variation of average aerosol number concentration versus minimum temperature during April-July 1999 for different size ranges.
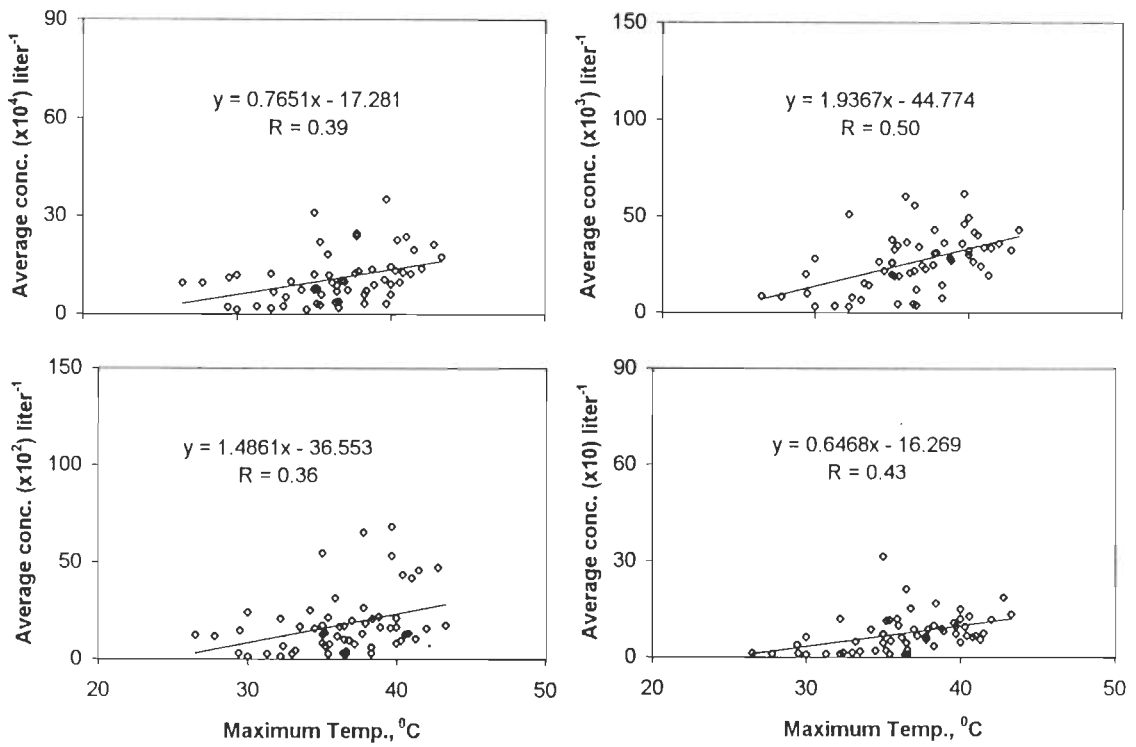
Figure A.13 Variation of average aerosol number concentration versus maximum temperature during April-July 1999 for different size ranges.
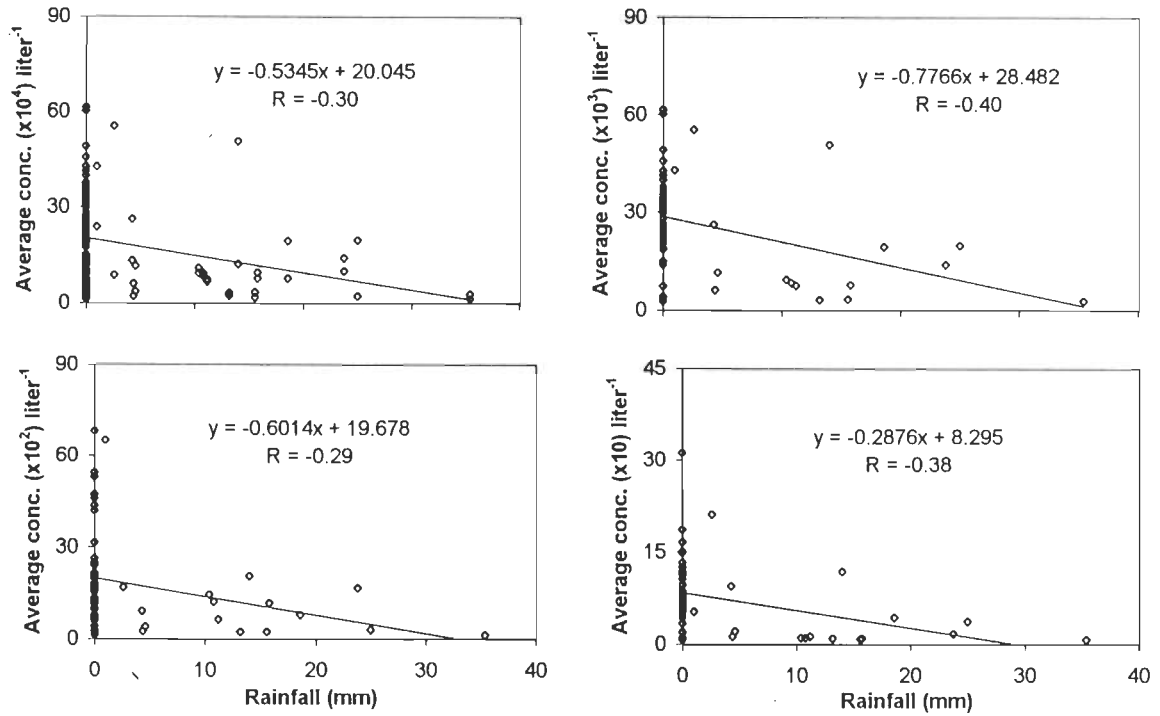
Figure A.14 Variation of average aerosol number concentration versus rainfall temperature during April-July 1999 for different size ranges.

References

1. Afraimovich, E. L., Altyntsev, A. T., Kosogorov, E. A., Larina, N. S., and Leonovich, L. A., "Ionospheric effects of the solar flares of September 23, 1998 and July 29, 1999 as deduced from GPS network data", *J. Atmos. & Solar Terr. Phys.*, 63, 1841-1849, 2001.

2. Agarwal, R. R., "Some theoretical studies on atmospheric electricity with solar terrestrial relationship over Indian Subcontinent", *Ph. D. Thesis*, University of Roorkee, India, 1995.

3. Aher, G. R., and Agashe, V. V., "Effect of premonsoon scenario on aerosols at Pune", *Abstract book* of TROPMET 97, IISc. Bangalore, India, 31-32, 1997.

4. Alofs, D. J. and Liu, T., "Atmospheric measurements of CCN in the super-saturation range 0.013-0.681%", *J. Atmos. Sci.*, 38, 2772-2778, 1981.

5. Anastasiadis, A., "Electron acceleration in solar flares by spatially random DC electric fields", *Phys. Chem. Earth (C)*, 24, 269-274, 1999.

6. Avakyan, S. V., "Some purposes and methods of the satellite measurements of the ignorospheric response on the solar flares", *Phys. Chem. Earth (C)*, 26, 259-263, 2001.

7. Bailey, G. J., Moffett, R. J., and Swartz, W. E., "Effect of photoelectron heating and interhemisphere transport on daytime plasma temperature at low latitudes", *Planet. Space Sci.*, 23, 599-607, 1975.

8. Balan, N., Oyama, K. I., Bailey, G. J., Fukao, S., Watanabe, S., and Abdu, M. A., "A plasma temperature anomaly in the equatorial topside ionosphere", *J. Geophys. Res.,* 102, 7485-7492, 1997.

9. Banks, P. M., and Nagy, A. F., "Concerning the influence of elastic scattering upon photoelectron transport and escape", *J. Geophys. Res.,* 75, 1902-1911, 1970.

10. Banks, P. M., and Kockarts, G., "Vertical temperature distribution in the earth's atmosphere with emphasis on thermosphere", Academic Press, New York, USA, Part-A, pp 3, 1973.

11. Banks, P. M., Schunk, R. W., and Raitt, W. J., "NO^+ and O^+ in the high latitude F region", *Geophys. Res. Lett.,* 1, 239-242, 1974.

12. Bansal, M. K., and Verma, T. S., "Aerosol measurements at Roorkee relating to the total solar eclipse of 24 Oct. 1995", *Indian J. Radio & Space Phys.,* 27, 260-265, 1998.

13. Bell, T. F., Pasko, V. P., and Inan, U. S., "Runaway electron as a source of Red Sprites in the mesosphere", *Geophys. Res. Lett.,* 22, 2127-2130, 1995.

14. Bhuyan, P. K., and Kakoty, P. K., "Comparison of electron and ion temperature measurements at ± 10° magnetic latitudes from SROSS-C2 with the IRI", *Abstract book* on NSSS-2K, Puri, India, pp 99, 2000.

15. Blanchard, D. C., "From raindrops to volcanoes", *Doubleday,* Garden City, New York, USA, 1967.

16. Brace, L. H., and Theis, R. F., "An empirical model of daytime electron temperature in the thermosphere at solar minimum", *Geophys. Res. Lett.*, 5, 275-278,1978.

17. Brinton, H. C., Grebowsky, J. M., and Brace, L. H., "The high-latitude winter *F* region at 300 km: Thermal plasma observations from AE-C", *J. Geophys. Res.*, 83, 4767-4776, 1978.

18. Bristow, W. A., Greenwald, R. A., and Samson, J. C., "Identification of high latitude acoustic gravity wave source using the Goose Bay HF radar", *J. Geophys. Res.*, 99, 319-331, 1994.

19. Byrne, M. A., and Jennings, S. G., "Scavenging of sub-micrometer aerosol particles by water drops", *Atmos. Environ., Part A*, 27, 2099-2105, 1993.

20. Carrington, R. C., "Description of a singular appearance seen in the sun on September 1, 1859", *Monthly Notice of the Royal Astronomical Society*, 20, 13-15, 1860.

21. Chamberlin, J. W., and Hunten, D. M., "Theory of planetary atmospheres", *International Geophysical Series*, 36, Academic Press, New York, USA, 1987.

22. Chao, C. K., Su, S. Y., and Yeh, H. C., "Presunrise ion temperature enhancement observed at 600 km low and mid-latitude ionosphere", *Geophys. Res. Lett.*, 30, 1187-1190, 2003.

23. Charikov, Y. E., "X-ray precursors in solar flares", *Phys. Chem. Earth (C)*, 25, 407, 2000.

24. Chauzy, S., and Raizonville, P., "Space charge layers created by corona at ground level below thundercloud: measurements and modeling", *J. Geophys. Res.*, 87, 3143-3148, 1982.

25. Chauzy, S., and Soula, S., "General interpretation of space electric field variations between lightning flashes", *J. Geophys. Res.*, 92, 5676-5684, 1987.

26. Chestnov, F. I., "The ionosphere and its riddles", Foreign languages publishing house, Moscow, Russia, 1956.

27. Christian, H.J., Blakeslee, R.J., Boccippio, D.J., Boeck, W.L., Buechler, D.E., Driscoll, K.T., Goodman, S.J., Hall, J.M., Koshak, W.J., Mach, D.M., and Stewart, M.F., "Global frequency and distribution of lightning as observed by the Optical Transient Detector", in Proc. *11th International Conference on Atmospheric Electricity*, Alabama, USA, 1999.

28. Cooray, V., and Lundquist, S., "On the characteristics of some radiation fields from lightning and their possible origin in positive ground flashes", *J. Geophys. Res.*, 87, 11203-11214, 1982.

29. Cooray, V., "Horizontal fields generated by return strokes", *Radio Sci.*, 27, 529-537, 1992.

30. Cubasch, U., Hasselmann, K., Hock, H., Mauer-Reimer, E., Mikolajewicz, U., Santer, B. D., and Sausen, R., "Time-dependent green house warming computations with a coupled ocean atmosphere model", *Clim. Dyn.*, 8, 55-69, 1992.

31. Cummer, S. A., and Inan, U. S., "Measurements of charge transfer in sprite-producing lightning using ELF radio atmospherics", *Geophys. Res. Lett.*, 24, 1731-1734, 1997.

32. Dalgarno, A., McElory, M. B., and Moffett, R. J., "Electron temperatures in the ionosphere", *Planet. Space Sci.*, 11, 463-472, 1963.

33. Davies, C. N., "Size distribution of atmospheric particles", *J. Aerosol Sci.*, 5, 293-300, 1974.

34. Devara, P. C. S., and Raj, P. E., "A lidar study of atmospheric aerosols during two contrasting monsoon season", *Atmosfera*, 11, 199-204, 1998.

35. Divya, and Rai, J., "Parallel and perpendicular electric field components of a lightning discharge", *Geoexploration*, 23, 227-237, 1985.

36. Donnelly, R. F., "Empirical models of solar flare X-rays and EUV emission for use in studying their E and F region effects", *J. Geophys. Res.*, 81, 4745-4753, 1976.

37. Eack, K. B., Suszcynsky, D. M., William, H. B., Roussel-Dupre, R. A., and Symbalisity, E. M. D., "Gamma-ray emissions observed in a thunderstorm anvil", *Geophys. Res. Lett.*, 2, 185-188, 2000.

38. Evans, J. V., "Seasonal and sunspot cycle variations of F region electron temperatures and protonospheric heat fluxes", *J. Geophys. Res.*, 78, 2344-2349, 1973.

39. Farley, D. T., McClure, J. P., Sterling, D. L., and Green, J. L., "Temperature and composition of the equatorial ionosphere", *J. Geophys. Res.*, 72, 5837-5846, 1967.

40. Fesen, C.G., Roble, R.G., and Duboin, M.L., "Simulations of seasonal and geomagnetic activity effects at Saint Santin", *J. Geophys. Res.*, 100, 21377-21407, 1995.

41. Fishman, G. J., Bhat, P. N., Malozzi, R., Horack, J. M., Koshut, T., Kouveliotou, C., Pendleton, G. N., Meegan, C. A., Wilson, R. B., Paciesas, W. S., Goodman, S. J., and Christian, H. J., "Discovery of intense gamma ray flashes of atmospheric origin", *Science*, 264, 1313, 1994.

42. Flochini, R. G., Cabill, T. A., Shadon, D. J., Lange, S., Eldred, R. A., Feeney, P. J., Walfe, G. W., Simmeroth, D. C., and Sundar, J. K., "Monitoring California's aerosols by size and elemental composition", *Envir. Sci. Technol.*, 10, 76-82, 1976.

43. Forbes, J.M., and Vial, F., "Monthly simulations of the solar semidiurnal tide in the mesosphere and lower thermosphere", *J. Atmos. & Terr. Phys.*, 51, 649-661, 1989.

44. Forbes, J.N., Roble, R. G., and Fesen, C. G., "Acceleration, heating and compositional mixing of the thermosphere due to upwards propagating tides", *J. Geophys. Res.*, 98, 311-321, 1993.

45. Fritts, D. C., and Vincent, R. A., "Mesospheric momentum flux studies at Adelaide, Australia: observations and gravity waves tidal interaction model", *J. Atmos. Sci.*, 44, 605, 1987.

46. Garcia, X., and Jones, A. G., "Atmospheric sources for audio-magnetotelluric (AMT) sounding", *Geophysics*, 67, 448-458, 2002.

47. Garg, S. C., Bahl, M., Maini, H. K., Chopra, P., Jhon, T., Singh, V., and Singh, D., "NPL's aeronomy experiment in space", *NPL Technical Bulletin*, New Delhi, India, 1992.

48. Garg, S. C., and Das, U. N., "Aeronomy experiment on SROSS-C2", *J. Spacecraft Technology*, 5, 11-15, 1995.

49. Garg, S. C., Bahl, M., Maini, H. K., Chopra, P., Jhon, T., Singh, V., and Singh, D., "RPA payload data processing and analysis", Document prepared for RPA data analysis and utilization training program, ISRO, Bangalore, India, 1996.

50. Geisler, J. E., and Bowhill, S. A., "Exchange of energy between the ionosphere and the photonosphere", *J. Atmos. & Terr. Phys.*, 27, 751-763, 1965.

51. Goldberg, R. A., "Electrodynamics in the high latitude mesosphere", *J. Geophys. Res.*, 94, 14661-14672, 1989.

52. Gupta, S. P., "Role of the sprites in stratosphere and mesosphere", *Abstract book* on NSSS-1997, Ahmedabad, India, pp 84, 1997.

53. Hanson, W. B., Nagy, A. F., and Moffett, R. J., "Ogo 6 measurements of super cooled plasma in the equatorial exosphere", *J. Geophys. Res.*, 78, 751-756, 1973.

54. Hanssen, E. T., and Emslie, A. G., "The physics of solar flares", Cambridge University Press, UK, 1988.

55. Hanel, G., "The properties of atmospheric aerosol particles as a function of relative humidity at thermodynamic equilibrium with the surrounding of moist air", *Advance in Geophysics*, edited by H. E. Landsberg and J. Van Meighen (Academic Press Inc., New York, USA) 19, 73-188, 1976.

56. Harshvardhan, "Aerosol-climate interactions", edited by P. V. Hobbs, *International Geophysical Series*, 54, 75-95, 1993.

57. Hayakawa, M., Kawate, R., Molchanov, O. A., and Yumoto, K., "Results of ultra-low-frequency magnetic field measurements during the Guam earthquake of August 8, 1993", *Geophys. Res. Lett.*, 23, 241-244, 1996.

58. Hays, P. B., and Roble, R.G., "A quasi-static model of global atmospheric electricity, 1. The lower atmosphere", *J. Geophys. Res.,* 84, 3291-3305, 1979.

59. Herman, J. R., and Goldberg, R. A., "Sun, Weather and Climate", NASA-SP 426, Washington D. C., USA, 1978.

60. Hill, R. D., "Lightning induced by nuclear bursts", *J. Geophys. Res.*, 78, 6355-6358, 1973.

61. Hill, R. D., "A survey of lightning estimates", *Rev. Geophys. Space Phys.*, 17, 155-164, 1979.

62. Horner, F., and Bradley, P. A., "The spectra of atmospherics from near lightning discharges", *J. Atmos. & Terr. Phys.*, 26, 1155-1166, 1964.

63. Inan, U. S., Bell, T. F., and Ridriguez, J. V., "Heating and ionization of the lower ionosphere by lightning", *Geophys. Res. Lett.*, 18, 705-708, 1991.

64. Inan, U. S., Reising, S. C., Fishman, G. J., and Horack, J. M., "On the observation of the terrestrial gamma ray bursts with lightning and implication for sprites", *Geophys. Res. Lett.*, 23, 1017-1020, 1996.

65. Jacobson, A. R., Cummins, K. L., Carter, M., Klingner, P., Roussel-Dupre, D., and Knox, S. O., "FORTE radio-frequency observations of lightning strokes detected by the National Lightning Detection Network", *J. Geophys. Res.*, 105, 15653-15662, 2000.

66. Joshi, P. C., "Satellite data for cloud observation", Lecture notes, *second SERC school on Cloud Physics and Atmospheric Electricity- Frontiers*, IITM, Pune, India, 2001.

67. Junge, C. E., "Aerosols", Handbook of Geophysics, edited by Campen et al., McMillan, New York, USA, 1960.

68. Kamra, A. K., "Electrification in an Indian dust storm", *Weather*, 24, 145-146, 1969.

69. Kamra, A. K., "Measurements of electrical parameters of dust storms", *J. Geophys. Res.*, 77, 5183-5200, 1972.

70. Kanellakos, D. P., Chan, K. L., and Villard O. G., "On the altitude at which some solar flare induced ionization is released", *J. Geophys. Res.*, 67, 5-12, 1962.

71. Kazimirovsky, E., Herraiz, M., and Delamoena, B. A., "Effect on the ionosphere due to phenomena occurring below it", *Survey in Geophysics*, 24, 139-184, 2003.

72. Khemani, L. T., Momin, G. A., Niak, M. S., Vijaykumar, R., and Ramana Murty, B. V., "Chemical composition and size distribution of atmospheric aerosol over Deccan Plateau, India", *Tellus*, 34, 151-158, 1982.

73. Kleusberg, A., "The global positioning system and ionospheric conditions", *Solar Terrestrial Predictions IV*, 142-146, 1992.

74. Knudsen, W. C., "Magnetospheric convection and the high-latitude $F2$ ionosphere", *J. Geophys Res.*, 79, 1046-1065, 1974.

75. Knudsen, W. C., Banks, P. M., Winningham, J. D., and Klumpar, D. M., "Numerical model of the convicting $F2$ ionosphere at high latitudes", *J. Geophys. Res.*, 82, 4784-4782, 1977.

76. Kocharov, G. E., Charikov, Y. E., Lazutkov, V. P., Matveev, G. A., Nitsora, Y. N., Savchenko, M. I., and Skorodumov, D. V., "Soft X-rays in the 00:18 UT solar flare on April 22, 1994", *Phys. Chem. Earth (C)*, 25, 405-406, 2000.

77. Kudryashev, G. S., and Avakyan, S. V., "Ionization and excitation of the upper atmosphere during solar flares", *Phys. Chem. Earth (C)*, 25, 511-514, 2000.

78. Krehbiel, P. R., Brook, M., and Roy, A., McCrory, "An Analysis of the charge structure of lightning discharges to ground", *J. Geophys. Res.*, 84, 2432-2456, 1979.

79. Krishna Murthy, B. V., "Aerosol and radiation budget in the middle atmosphere", *Indian J. Radio Space Phys.*, 17, 203-219, 1988.

80. Krishna Murthy, B. V., and Reddi, C. R., "Ionospheric structure and its variation, space environment and its interactions with spacecraft", edited by Ubreoi, C., and Chakravarty, S. C., 23-41, 2000.

81. Lanzerotti, L. J., "Measures of energetic particles from sum, in the solar output and its variation", edited by White, O. R., Colorado Associated University Press, Boulder, USA, 383-703, 1977.

82. Lehtinen, N. G., Walt, M., Inan, U. S., Bell, T. F., and Pasko, V. P., "γ-ray emission produced by a relativistic beam of runaway electrons accelerated by quasi-electrostatic thundercloud fields", *Geophys. Res. Lett.*, 23, 2645-2648, 1996.

83. Lehtinen, N. G., Bell, T. F., Pasko, V.P., and Inan, U. S., "A two-dimensional model of runaway electron beams driven by quasi-electrostatic thundercloud fields", *Geophys. Res. Lett.*, 24, 2639-2641, 1997.

84. Lehtinen, N. G., Bell, T. F., and Inan, U. S., "Monte Carlo simulation of runaway MeV electron breakdown with application to red sprites and terrestrial gamma ray flashes", *J. Geophys. Res.*, 104, 24699-24712, 1999.

85. Lehtinen, N. G., Inan, U. S., and Bell, T. F., "Trapped energetic electron curtains produced by thunderstorm driven relativistic runaway electron", *Geophys Res Lett*, 27, 1095-1098, 2000.

86. Lyons, W. A., "Characteristics of luminous in the stratospheres above thunderstorms as imaged by low light video", *Geophys. Res. Lett.*, 21, 875-878, 1994.

87. Ma, S. Y., Xu, L., and Yeh, K. C., "A study of Ionospheric electron density and deviations during two great storms", *J. Atmos. & Terr. Phys.*, 57, 1037-1043, 1995.

88. Mahajan, K. K., Panday, V. K., and Jain, V. C., "Relationship between electron density and electron temperature as a function of solar activity", *Adv. Space Res.*, 2, 247-249, 1983.

89. Mahajan, K. K., and Shastri, S., "Has the ionospheric $F2$ region changed permanently during the last thirty years", *Adv. Space Res.*, 20(11), 2157-2160, 1997.

90. Manabe, S., Spelman, M. J., and Stouffer, F. J., "Transient response of a coupled ocean-atmosphere model to gradual changes of atmospheric CO_2: Part-2 Seasonal Response", *J. Climate*, 5, 105-126, 1992.

91. Manson, J. E., "Aerosols, Hand-book of Geophysics and Space Environment", edited by Valley, S. L., McGraw-Hill, New York, 1965.

92. Markerras, D., "A Comparison of discharge process in cloud and ground lightning flashes", *J. Geophys. Res.,* 73, 1175-1183, 1968.

93. Mason, B. J., "Clouds, rain and rainmaking", Cambridge University Press, Cambridge, UK, 1975.

94. Mayr, H. G., "A theoretical model of the ionospheric dynamics within the thermosphere coupling", *J. Atmos. & Terr. Phys.,* 34, 1659-1680, 1972.

95. McCarthy, M. and Parks, G. K., "Further observations of X-rays inside thunderstorms", *Geophys. Res. Lett.,* 12, 393-396, 1985.

96. McCartney, E. J., "Optics of the atmosphere", John Willy & Sons, New York, USA., 1976.

97. McCormick, M. P., Swissler, T. J., Chu, W. P., and Fuller, W. H., "Post-volcanic stratospheric aerosol decay as measured by Lidar", *J. Atmos. Sci.,* 35, 1296-1303, 1978.

98. Meehl, G. A., and Washington, W. M., "South Asian summer monsoon variability in a model with doubled atmospheric carbon dioxide concentration", *Science,* 260, 1101-1104, 1993.

99. Mendillo, M., Klobuchar, J. A., Fritz, R. B., Darosa, A. V., Kersley, L., Yeh, K. C., Flaherty, B. J., Rangaswamy, S., Schmid, J. R., Evans, J. V., Schodel, J. P., Matsoukas, D. A., Koster, J. R., Webster, A. R., and Chin,

P., "Behavior of the ionospheric *F-* region during the great solar flare of August 7, 1972", *J. Geophys. Res.*, 79, 665-672, 1974.

100. Meyerott, R. E., Reagan, J. B., and Evans, J. E., "Volcanism and global atmospheric electricity in the lower atmosphere", in Proc. *7th Int. Conf. Atmos. Elect., Am. Meteorol. Soc.*, New York, USA, 1984.

101. Mikasa, H., "Latest technologies aid in measuring air pollution", *J. Electr. Engg.*, 29(310), 26-32, 1992.

102. Mitra, S. K., "The Upper Atmosphere", The Asiatic Society, Monograph Series, V, Calcutta, India, 1992.

103. Molchanov, O. A., and Haykawa, M., "Subionospheric VLF signal perturbations possibly related to earthquakes", *J. Geophys. Res.*, 103, 17489-17504, 1998.

104. Murgatroyad, R., "The structure and dynamics of the stratosphere, in the global circulation of the atmosphere", edited by Gorby, G., *Royal Meteorol. Soc.*, London, UK, 159-195, 1970.

105. Murphy, J. M., and Mitchell, J. F. B., "Transient response of Hadley centre coupled model to increasing carbon dioxide: Part 2-Temporal and Spatial Evolution of Patterns", *J. Climate*, 8, 57-80, 1995.

106. Neher, H. V., "Cosmic rays at high latitudes and altitudes covering four solar maxima", *J. Geophys. Res.*, 76, 1637-1651, 1971.

107. Ogawa, T., Oike, K., and Miura, T., "Electromagnetic radiation from rocks", *J. Geophys. Res.*, 90, 6245-6259, 1964.

108. Ochabova, P., "Geomagnetic latitude aspects of the effect of the interplanetary parameters on geomagnetic storms", *Studia Geophysicaet Geodaetica*, 33(4), 362-378, 1989.

109. Otsuyama, T., Hobara, Y., and Hayakawa, M., "EM radiation associated with sprites", in Proc. *11th International conference on Atmospheric Electricity*, Alabama, USA, 96-98, 1999.

110. Oyama, K. I., and Hirao, K., "Electron temperature probe experiments on the satellite TAIYO", *J. Geomagn. Geoelectr.*, 27, 321-330, 1975.

111. Oyama, K. I., Hirao, K., and Yasuhara, F., "Electron temperature probe on board Japan's 9th scientific satellite OHZORA", *J. Geomagn. Geoelectr.*, 37, 413-430, 1985.

112. Oyama, K. I., Balan, N., Watanabe, S., Takahashi, T., Isoda, F., Bailey, G. J., and Oya, H., "Morning overshoot of *Te* enhanced by downward plasma drift in the equatorial topside ionosphere", *J. Geomagn. Geoelectr.*, 48, 959-966, 1996a.

113. Oyama, K. I., Watanabe, S., Su, Y., Takahashi, T., and Hirao, K., "Season, local time and longitudinal variations of electron temperature at the height of ~600 km in the low latitude region", *Adv. Space Res.*, 18, 269-278, 1996b.

114. Pahwa, D. R., Singhal, S. P., and Khemani, L. T., "Study of aerosol at Delhi", *Mausam*, 45, 1, 49-56, 1994.

115. Parks, G. K., Mauk B., Spiger, B., and Chin, J., "X-ray enhancements detected during thunderstorm and lightning activity", *Geophys. Res. Lett.*, 8, 1176-1179, 1981.

116. Pasko, V. P., Inan, U.S., Bell, T. F., and Taranenko, Y. N., "Heating, ionization and upward discharges in the mesosphere due to intense quasi-electrostatic thundercloud fields", *Geophys. Res. Lett.*, 22, 365-368, 1995.

117. Pasko, V. P., Inan, U. S., Bell, T. F., and Taranenko, Y. N., "Sustained heating of the ionosphere above thunderstorms as evidenced in 'early/fast' VLF events", *Geophys. Res. Lett.*, 23, 1067-1070, 1996.

118. Pasko, V. P., Inan, U. S., Bell, T. F., and Taranenko, Y. N., "Sprites produced by quasi-electrostatic heating and ionization in the lower ionosphere", *J. Geophys. Res.*, 102, 4529-4561, 1997.

119. Pathak, P. P., Rai, J., and Varshneya, N. C., "Electrochemical charge separation in clouds", *Ann. Geophys.*, 36, 613-621, 1980.

120. Petterssen, H., "Cosmic spherules and meteoritic dust", *Sci. Am.*, 123-132, 1960.

121. Parameswarn, K., and Vijaykumar, G., "Effect of atmospheric relative humidity on aerosol size distribution", *Indian J. Radio & Space Phys.*, 23, 175-188, 1994.

122. Pranesha, T. S., and Kamra, A. K., "Scavenging of aerosol particles by large water drops, 1- Natural case", *J. Geophys. Res.*, 101, 23373-23381, 1996.

123. Priest, E. R., "Basic magnetic configuration and energy supply processes for an interacting flux model of eruptive solar flares", edited by Svestka, Z., *Lecture Notes in Physics*, 399, 15, 1992.

124. Rai, J., Rao, M., and Tantry, B. A. P., "Bremsstrahlung as a source of UHF emission from lightning", *Nature (Physical Science)*, 238, 59-60, 1972.

125. Rai, J., Bhattacharya, P. K., and Sapru, M. L., "Ionospheric disturbances due to thunderstorms", *Int. J. Electronics*, 34(6), 757-760, 1973.

126. Rai, J., "Some studies of lightning discharge and radio atmospherics", *Ph.D. Thesis*, Banaras Hindu University, Varanasi, India, 1974.

127. Rai, J., "On the origin of UHF atmospherics", *J. Atmos. & Terr. Phys.*, 40, 475-478, 1978.

128. Rakov, V. A., "Lightning and Tall Structures", in Proc. *International Lightning Detection Conference*, Tucson, Arizona, USA, 2002.

129. Rao, M., "Corona currents after the return stroke and the emission of ELF waves in a lightning flash to earth", *Radio Sci.*, 2, 241-244, 1967.

130. Rosenberg, T. J., and Ianzerotti, L. J., "Direct energy inputs to the middle atmosphere, Middle Atmosphere Electrodynamics", edited by N. C. Maynard, NASA CP-2090, USA, 43-70, 1979.

131. Rycroft, M.J., "Some effects in the middle atmosphere due to lightning", *J. Atmos. & Solar Terr. Phys.*, 56, 343-348, 1994.

132. Rycroft, M.J., and Cho, M., "Modeling electric and magnetic fields due to thunderclouds and lightning from cloud-tops to the ionosphere", *J. Atmos. & Solar Terr. Phys.*, 60, 889-893, 1998.

133. Sagawa, E., Miyazaki, S., and Mori, H., "Nighttime electron temperature troughs in the equatorial topside ionosphere revealed from PRA experiments on the ISS-b satellite", *J. Atmos. & Terr. Phys.*, 43, 1165-1173, 1981.

134. Schunk, R. W., and Banks, P. M., "Auroral N_2 excitation and the electron density trough", *Geophys. Res. Lett.*, 2, 239-242, 1975.

135. Schunk, R. W., Banks, P. M., and Raitt, W. J., "Effect of electric fields and other processes upon the nighttime and high-latitude *F* layer", *J. Geophys. Res.*, 81, 3271-3282, 1976.

136. Schunk, R. W., and Raitt, W. J., "Atomic nitrogen and oxygen ions in the daytime high-latitude *F* region", *J. Geophys. Res.*, 85(A3), 1255-1272, 1980.

137. Schunk, R. W., and Sojka, J. J., "Ion-temperature variations in the daytime high-latitude *F* region", *J. Geophys. Res.*, 87(A7), 5169-5183, 1982.

138. Schunk, R. W., and Sojka, J. J., "Ionosphere-thermosphere space weather issue", *J. Atmos. & Terr. Phys.*, 58(14), 1527-1574, 1996.

139. Sentman, D. D., and Wescott, E. M., "Observations of upper atmospheric optical flashes recorded from an aircraft", *Geophys. Res. Lett.*, 20, 2857-2859, 1993.

140. Sentman, D. D., Wiscoott, E. M., Osborne, D. L., Hampton, D. L., and Heavner, M J., "Preliminary results from the Sprites 94 aircraft campaign: Red Sprites", *Geophys. Res. Lett.*, 22, 1205-1208, 1995.

141. Shalimov, S., "Lithosphere ionosphere coupling before earthquakes", *Episodes*, 15, 252-260, 1992.

142. Shapka, R., "Geomagnetic effects on modern pipeline system", *Solar-Terristrial Predictions IV*, 163-170, 1992.

143. Sharma, D. K., Rai, J., Israil, M., and Garg, S. C., "Temperature and Density variation in ionospheric plasma over different locations in India", in Proc. *National Conference on Advances in Contemporary Physics & Energy*, IIT Delhi, India, 265-278, 2002.

144. Sharma, D. K., Rai, J., Israil, M., Shalni, P., Subrahmanyam, P., Chopra, P., and Garg, S. C., "Sunrise effect on ionospheric temperature as measured by SROSS-C2 satellite", *J. Ind. Geophys. Uni.*, 7, 117-123, 2003.

145. Sharma, D. K., Rai, J., Israil, M., Subrahmanyam, P., Chopra, P., and Garg, S. C., "Enhancement in ionospheric temperatures during thunderstorms", *J. Atmos. & Solar Terr. Phys.*, 66, 51-56, 2004.

146. Shaw, G. E., "Aerosol-size temperature relationship", *Geophys. Res. Lett.*, 15, 133-135, 1988.

147. Singh, N., "Role of atmospheric ions on condensation and cloud formation process", *Ph. D. Thesis*, University of Roorkee, Roorkee, India, 1985.

148. Singh, R. P., Singh, A. K., Singh, U. P., and Singh, R. N., "Wave ducting and scattering properties of ionospheric irregularities", *Adv. Space Res.*, 14(9), 225-228, 1994.

149. Singh, A. K., Rai, J., Niwas, S., Kumar, A. and Rai, A., "Measurements of aerosols during monsoon, Roorkee". *Abstract book* of TROPMET'97, IISc. Bangalore, India, pp 77, 1997.

150. Singh, R. P., and Patel, R. P., "Lightning generated ELF, VLF, Optical waves and their diagnostic features", in Proc. *National Workshop on Recent Developments in Atmospheric and Space Sciences*, IIT Roorkee, India, 9-32, 2001.

151. Sparmacher, H., Fullberg, K., and Bonko, H., "Scavenging of aerosol particles: Particle-bound radionuclides- experimental", *Atmos. Environ., Part A*, 27, 605-618, 1993.

152. Spiro, R. W., Heelis, R. A., and Hanson, W. B., "Ion convection and the formation of the mid-latitude *F* region ionization trough", *J. Geophys. Res.*, 83, 4255-4264, 1978.

153. Srivastava, S. K., "Monitoring of Earthquakes in India", *Abstract book* on International Workshop on Seismo-Electromagnetics and Space Sciences, Agra, India, 2-3, 2000.

154. Su, Y. Z., Oyama, K. I., Bailey, G. J., Takahashi, T., and Watanabe, S., "Comparison of satellite electron density and temperature measurements at

low latitudes with a plasmasphere-ionosphere model", *J. Geophys. Res.*, 100, 14591-14604, 1995.

155. Su, Y. Z., Oyama, K. I., Bailey, G. J., Fukao, S., Takahashi, T., and Oya, H., "Longitudinal variations of the topside ionosphere at low latitudes: satellite measurements and mathematical modeling", *J. Geophys. Res.*, 101, 17191-17205, 1996.

156. Suhasini, R., Raghavarov, R., Mayr, H. G., Hoegy, W. R., and Wharton, L. E., "Equatorial temperature anomaly during solar minimum", *J. Geophys. Res.*, 106, 24777-24783, 2001.

157. Takagi, M., and Takeuti, T., "Atmospherics radiations from lightning discharges", in Proc. *Res. Inst. Atmos.*, Nagoya University, 10, 1-11, 1963.

158. Taranenko, Y. N., Inan, U. S., and Bell, T. F., "Optical signature of lightning induced heating of *D* region", *Geophys. Res. Lett.*, 19, 1815-1818, 1992.

159. Taranenko, Y. N., Inan, U. S., and Bell, T. F., "Interaction with the lower ionosphere of electromagnetic pulses from lightning: heating, attachment and ionization", *Geophys. Res. Lett.*, 20, 1539-1542, 1993a.

160. Taranenko, Y. N., Inan, U. S., and Bell, T. F., "Interaction with the lower ionosphere of electromagnetic pulses from lightning: excitation of optical emissions", *Geophys. Res. Lett.*, 20, 2675-2678, 1993b.

161. Tarantsev, A., and Birfild, Y., "Discovery: Influence of the seismic activity on ionosphere by acoustic waves", *Short description of discoveries*, Russia, 128-157, 1973.

162. Taylor, W. L., "Radiation field characteristics of lightning discharge in the band 1kc/s to 100 kc/s", *J. Res. NBS*, 67 D, 539-550, 1963.

163. Taylor, W. L., and Jean, A. G., "Very low frequency spectrum of lightning discharges", *J. Res. NBS* 63 D, 199-204, 1959.

164. Thome, G. D., and Wagner, L. S., "Electron density enhancements in the *E* and *F* regions of the ionosphere during solar flares", *J. Geophys. Res.*, 76, 6883-6895, 1971.

165. Titheridge, J. E., "Plasma temperatures from Alouette 1 electron density profiles", *Planet. Space Sci.*, 24, 247-258, 1976.

166. Tiwari, G. N., and Goyal, R. K., "Thermal modeling of a greenhouse: A pollution free controlled environment for crop productions", in *Proc. Int. Symp. of Asian Monsoon and Pollution over the Monsoon Environment*, IIT Delhi, India, pp 179, 1997.

167. Turco, R. P., Toon, O. B., Hamill, P., and Whitten, R. C., "Effect of meteoric debris on stratospheric aerosols and gases", *J. Geophys. Res.*, 86, 1113-1128, 1981.

168. Uman, M. A., Seacord, D. F., Price, G. H., and Pierce, E. T., "Lightning induced by thermonuclear detonations", *J. Geophys. Res.*, 77, 1591-1596, 1972.

169. Uman, M. A., "Lightning", McGraw-Hill, New York, USA, 1969.

170. Vakeva, M., Hameri, K., Puhakka, T., Nilsson, E. D., Hohti, H., and Makela, J. M., "Effect of meteorological process on aerosol particle size distribution in an urban background area", *J. Geophys. Res.,* 105, 9807-9821, 2000.

171. Velinov, P. I., and Mateyev, L. N., "The action of the cosmic rays and highly energetic particles on the parameters of the global atmospheric electric circuit", *Geomagnetism and Aeronomy,* 30(4), 468-670, 1990.

172. Vyas, B. M., Pandey, R., and Rai, R. K., "Planetary scale predictions in ionospheric absorption", in Proc. Int. Workshop on Long Term Changes and Trends in Atmosphere, IITM Pune, India, pp 46, 1999.

173. Wang, C. P., "Lightning discharges in the tropics 2. Component ground-strokes and cloud dart streamers", *J. Geophys. Res.,* 68, 1951-1958, 1963.

174. Watanabe, S., Oyama, K. I., and Abdu, M. A., "A computer simulation of electron and ion densities and temperature in the equatorial F region and comparison with Hinotori results", *J. Geophys. Res.,* 100, 14581-14590, 1995.

175. Watanabe, S., and Oyama K. I., "Effect of neutral wind on the electron temperature at a height of 600 km in the low latitude region", *Annales Geophysicae,* 14, 290-296, 1996.

176. Watkins, B. J., "A numerical computer investigation of the polar F-region ionosphere", *Planet. Space Sci.,* 26, 559-569, 1978.

177. Wescott, E. M., Sentman, D. D., Osborne, D. L, Hampton, D. L., and Heavner, M. J., "Preliminary results from the Sprites94 aircraft campaign: 2. Blue jets", *Geophys. Res. Lett.*, 22, 1209-1212, 1995.

178. Wescott, E. M., Sentman, D. D., Heavner, M. J., Hampton, D. L., Osborne, D. L., and Vaughan(Jr), O. H., "Blue Starters: Brief upward discharges from an intense Arkansas thunderstorm", *Geophys. Res. Lett.*, 23, 2153-2156, 1996.

179. Yamada, I., Matsuda, K., and Mizutani, H., "Electromagnetic and acoustic emission associated with rock fracture", *Phys. Earth Planet. Int.*, 57, 157-168, 1989.

180. Yukhimuk, V., Roussel-Dupre, R. A., and Symbalisty, E. M. D., "Optical characteristics of Blue Jets produced by runaway air breakdown simulation results", *Geophys. Res. Lett.*, 25, 3289-3292, 1998.

181. Yukhimuk, V., Roussel-Dupre, R. A., and Symbalisty, E. M. D., "On the temporal evolution of red sprites: Runaway theory versus data", *Geophys. Res. Lett.*, 26, 679-682, 1999.

182. Zhang, X. Y., Arimoto, R., Cao, J. J., Zhi S. A., and Wang D., "Atmospheric dust aerosol over Tibetan Plateau", *J. Geophys. Res.*, 106, 18471-18476, 2001.

Reprints

Enhancement in ionospheric temperatures during thunderstorms

D.K. Sharma[a], Jagdish Rai[a,*], M. Israil[b], P. Subrahmanyam[c], P. Chopra[c], S.C. Garg[c]

[a]*Department of Physics, Indian Institute of Technology, Roorkee 247 667, India*
[b]*Department of Earth Sciences, Indian Institute of Technology, Roorkee 247 667, India*
[c]*Radio and Atmospheric Science Division, National Physical Laboratory, New Delhi, India*

Abstract

It has been realized in recent years that the ionospheric temperatures and ion densities are influenced by the lightning activity. The ionospheric temperature (electron and ion temperature) were measured by the retarded potential analyzer payload aboard the Indian SROSS-C2 satellite. The data at low latitudes falling in the Indian subcontinent in the height range of 425–625 km for the period 1995–1998 were used for this study. The data on thunderstorm activity for the same period were obtained from India Meteorological Department. To see the effect of active thunderstorm the ionospheric electron and ion temperatures have been compared to the values on normal days.

It has been found that the average electron temperature is enhanced during thunderstorm activity by 1.2–1.7 times over the normal days. A similar enhancement has been found in ion temperature by 1.1–1.5 times. It is suspected that the ULF to VLF radiations generated during lightning and sprites from thunderstorm (Geophys. Res. Lett. 18 (1991) 705; 23 (1996) 1067) may cause of the enhancement in electron and ion temperatures.
© 2003 Elsevier Ltd. All rights reserved.

Keywords: Ionospheric temperatures; Thunderstorm; Sprites; VLF radiation; RPA payload

1. Introduction

It is believed that the space weather changes influence some of the tropospheric parameters and create disturbances in communication and navigation (Schunk and Sojka, 1996). On the other hand, the tropospheric disturbances are known to influence the ionospheric (Rai et al., 1973; Taranenko et al., 1993a,b; Lehtinen et al., 1996; Yukhimuk et al., 1999; Singh and Patel, 2001 and others) phenomena. The purpose of this paper, therefore, is to see the influence of thunderstorms on ionospheric electron and ion temperatures.

In the last four decades many researchers (Mahajan et al., 1983; Taranenko et al., 1992; Pasko et al., 1995; Wescott et al., 1996; Rai et al., 1972; Yukhimuk et al., 1998; Eack et al., 2000; Singh and Patel, 2001 and others) have extensively

studied the ionosphere for various aspects. These studies include experimental as well as theoretical methods for the determination of ionospheric composition, temperature anomalies and density etc. The experimental study can be carried out using aircraft-based, balloon-based, satellite-based (Oyama et al., 1996; Sharma et al., 2002 and others), coherent and incoherent scatter radar, magnetometers and a number of ground-based instruments. For the present study, the data were obtained by retarded potential analyzer (RPA) payload aboard Indian SROSS-C2 satellite.

1.1. The experimental technique

The RPA payload aboard SROSS-C2 satellite consists of two sensors viz., electron and ion sensors and associated electronics (Garg and Das, 1995). The electron and ion RPAs are used for in situ measurements of ionospheric electron and ion temperature. In addition, a spherical Langmuir probe is included and used as potential probe for estimating

* Corresponding author. Fax: +91-1332-27360.
E-mail addresses: dksphdes@iitr.ernet.in, dksphdes@rediffmail. com (D.K. Sharma).

the variation of spacecraft potential during spinning of the satellite. The electron and ion sensors, both, have planar geometry and consist of multigrided Faraday cups with a collector electrode. The different grids in the sensor are designated as entrance grid, retarding grid, suppressor grid and screen grid. These grids are made of gold-plated tungsten wire mesh having 90–95% optical transparency. The two sensors are mechanically identical but have different grid voltages suitable for collection of electrons and ions respectively. The charged particles whose energies are greater than the applied voltage on retarding grid pass through various grids and finally reach collector electrode to cause sensor current. This current is measured by a linear autogain ranging electrometer, which gives the value of electron and ion temperatures.

The electron and ion temperatures measured by the above-described RPA payload aboard the Indian SROSS-C2 satellite. The SROSS-C2 satellite was launched by Indian Space Research Organization (ISRO) on May 4, 1994 to study the ionospheric composition and temperature anomalies. It has yielded valuable data on electron and ion temperatures over low latitude locations in the altitude in range 425–625 km.

2. Data analysis

The data collected by SROSS-C2 satellite using RPA payload during the period 1995–1998 has been analyzed for anomalous variations due to thunderstorm activity in the altitude range from 425–625 km. The data on thunderstorm activity for the same period was obtained from India Meteorological Department (IMD). The measurements corresponding to three different locations, viz. Bhopal (23.16°N, 77.36°E), Panji (15.30°N, 73.55°E) and Trivandrum (08.29°N, 76.59°E) have been analyzed.

It is a difficult task to study the ionospheric temperature using the satellite data in respect of thunderstorm activity, because, passes of satellite very rarely match the thunderstorm activity at a meteorological data station. The first task is to match the satellite data corresponding to the thunderstorm activities. During the period 1995–1998, it has been found that seven events of thunderstorms correspond to the satellite data. The recorded average electron and ion temperature during active thunderstorms have been compared with the average normal days electron and ion temperature for the same time interval. Care has been taken to select the satellite data, which is free from diurnal, seasonal, latitudinal, longitudinal and altitude effects. The averages of normal time electron and ion temperatures have been calculated over a month, starting almost 15 days before the day of thunderstorm and ending 15 days after. Thus the possibility of seasonal effect has completely been ruled out because all data points correspond to the same season. A window of 5° in latitude and longitude for the satellite observation at the meteorological data center has enabled the latitudinal and longitudinal effect to be ineffective. The averaging of elec-

tron and ion temperatures at nearly the same hours of the day as that of the active thunderstorm has made it free from the diurnal effect. The analysis has been made for the altitude range 425–625 km only, thus making it independent of the altitude.

To see the effect of solar flare activity, the data on solar flares were obtained from National Geophysical Data Center (NGDC), Boulder, Colorado (USA). Only those thunderstorm days have been considered in this study, which are free from the solar flares. Similarly in another study (to be reported later) only those solar flare events were considered, which were free from the thunderstorm activity. Care has also been taken to choose the data only from those days, which are free from earthquakes.

The present study has a limitation in the sense that only seven thunderstorm days have been found which correspond to the satellite passes. However, in each satellite pass many data points were recorded at regular intervals. In all the seven events, 110 data points were obtained and in each case the electron and ion temperatures were above the normal day observations. On many occasions during its passes above the thunderstorm, the sensors could not record the electron and ion temperatures. All temperature data recorded by SROSS-C2 satellite are within the error limit of ±50 K.

3. Results and discussion

In 1995 two events corresponding to Bhopal (23.16°N, 77.36°E) and two to Trivandrum (08.29°N, 76.59°E) were recorded. Fig. 1 shows the comparison of electron temperature during thunderstorms and normal days for the events recorded above. At Bhopal, there were thunderstorms on January 11 and August 29, 1995. During these events the average electron temperature was enhanced by 1.2–1.3 times (Fig. 1a,d) over the normal day average electron temperature. However, at Trivandrum it was enhanced by 1.2–1.4 times (Fig. 1c,b) during the active thunderstorms on April 13 and 28, 1995 compared to the normal days. Fig. 2 shows the comparison of ion temperatures obtained during active thunderstorms and normal days for the above four events. In 1995, the average ion temperature at Bhopal was enhanced by 1.2 times (Fig. 2a,d) for both events and at Trivandrum it was enhanced by 1.1–1.5 times (Fig. 2b,c) during the thunderstorm activities.

Two events were recorded in 1997; one corresponding to Trivandrum on June 27 and another to Bhopal (23.16°N, 77.36°E) on December 10. At Trivandrum, the average electron temperature was enhanced by 1.7 times (Fig. 3a) and at Bhopal it was enhanced by 1.4 times (Fig. 3b) during the active thunderstorms as compared to the normal days. However, the average ion temperature was enhanced by 1.3 times (Fig. 4a,b) to that of normal days temperature at both locations.

In 1998, one event has been recorded at Panji (15.30°N, 73.55°E). There were two active thunderstorms recorded over two consecutive days (August 15 and 16) at the same
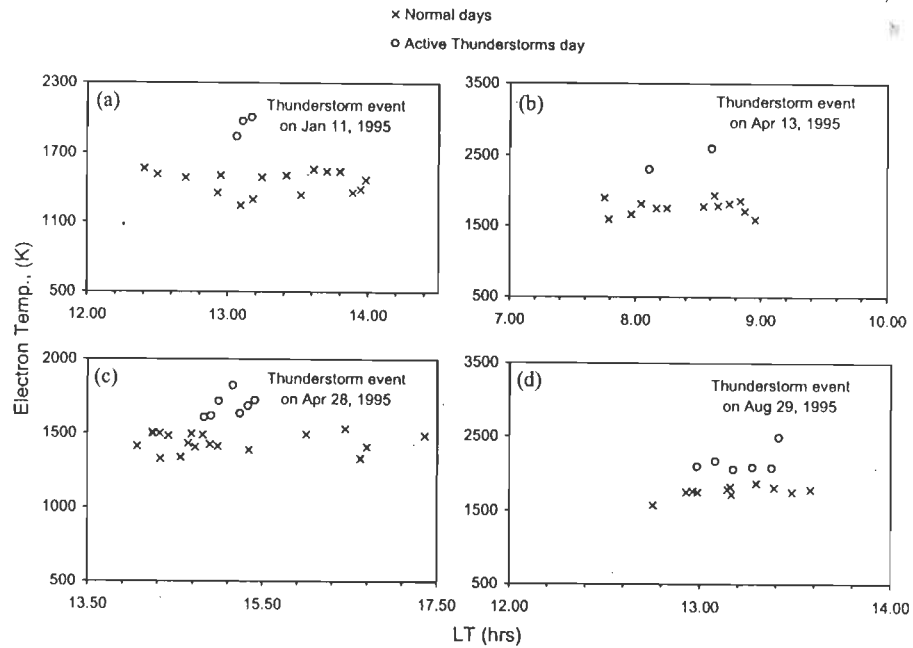
Fig. 1. Variation of electron temperature during thunderstorms and normal days for the events recorded at (a,d) Bhopal and (b,c) Trivandrum in 1995.
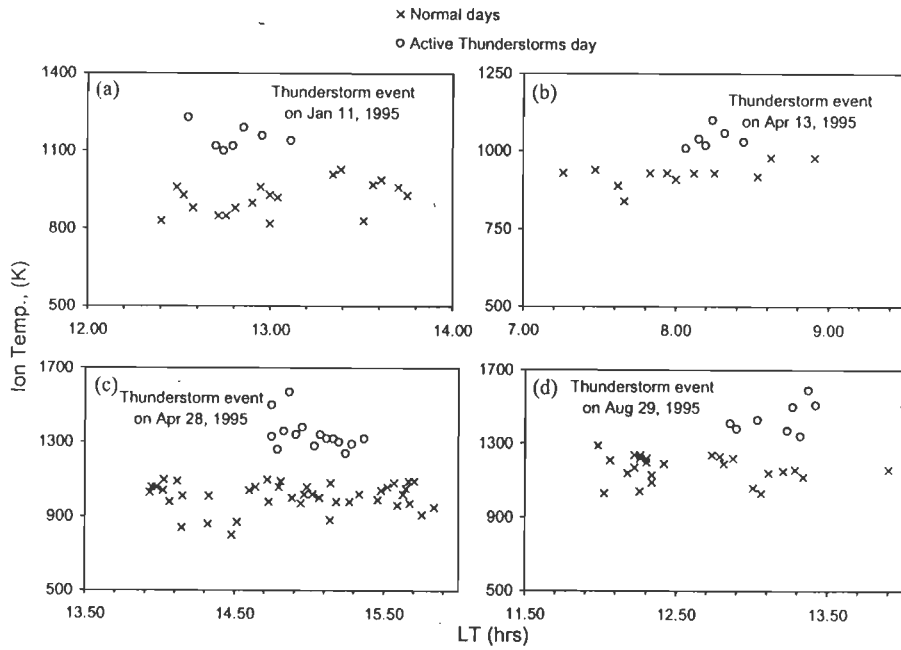

Fig. 2. Variation of ion temperature during thunderstorms and normal days for the events recorded at (a,d) Bhopal and (b,c) Trivandrum in 1995.

time. The average electron temperature was enhanced by 1.5 times (Fig. 5) and the average ion temperature by 1.3 times (Fig. 6) to that of normal day's temperature.

The average electron and ion temperatures during thunderstorm and normal days for all seven events have been shown in Table 1. The table also shows the time, duration and location of thunderstorm activities.

The above analysis shows that there is a consistent enhancement of ionospheric electron and ion temperatures recorded during active thunderstorms period. This
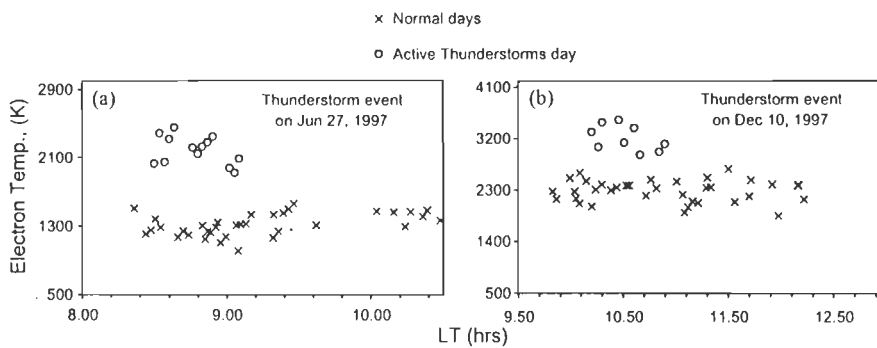
Fig. 3. Variation of electron temperature during thunderstorms and normal days for the events recorded at (a) Trivandrum and (b) Bhopal in 1997.
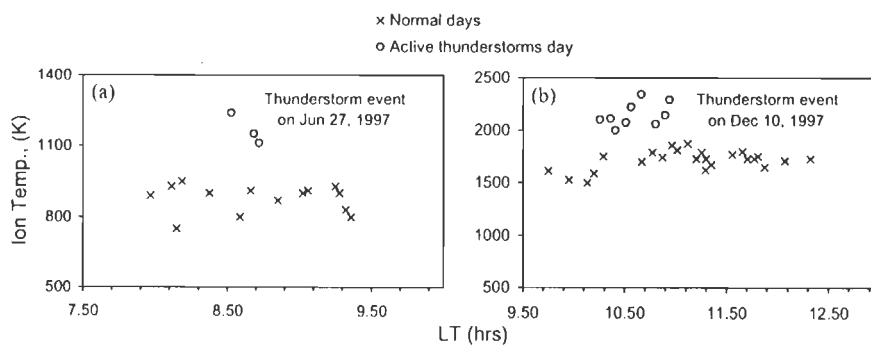

Fig. 4. Variation of ion temperature during thunderstorms and normal days for the events recorded at (a) Trivandrum (a) and (b) Bhopal in 1997.
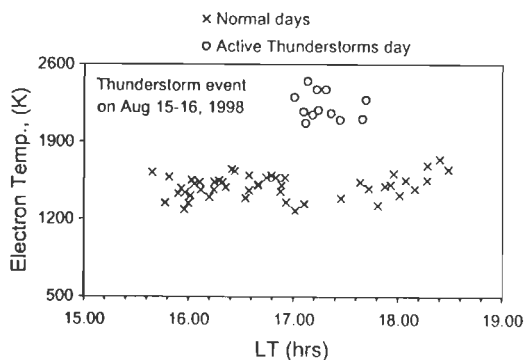

Fig. 5. Variation of electron temperature during thunderstorms and normal days for the events recorded at Panji in 1998.
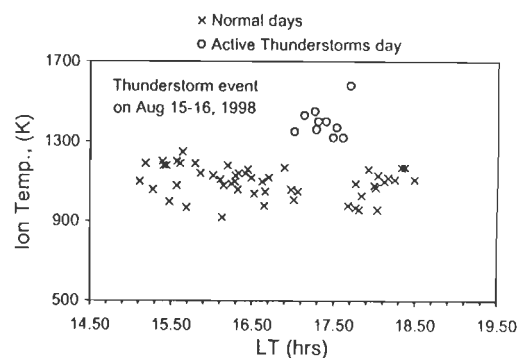

Fig. 6. Ion temperature during thunderstorms and normal days for the events recorded at Panji in 1998.

enhancement was for the average electron temperature ranging from 1.2 to 1.7 times compared to the average normal day's temperature. However, for ion temperature this enhancement was from 1.1 to 1.5 times. It is worth mentioning here that in the present analysis the data were selected in such a way that the effect of diurnal, seasonal, latitudinal, longitudinal and altitude effects are minimized. Thus the tem-

perature anomalies are directly related to the thunderstorm events.

The enhancement in ionospheric electron and ion temperatures has been attributed to different kinds of lightning activity, which are associated with active thunderstorms. Recent observation of optical phenomena such as sprites, blue jets, blue starters, elves and associated phenomena

Table 1
Comparison of average electron and ion temperatures during thunderstorms and during normal days

S. no.	Date of event	Time and duration of thunderstorm	Location of thunderstorms	Electron temperature (K)		Ion temperature (K)	
				Average during normal days	Average during thunderstorms day	Average during normal days	Average during thunderstorms day
1.	Jan 11, 1995	1201–1500 IST (0259 h)	23.16°N, 77.36°E	1457	1940	960	1151
2.	Apr 13, 1995	0601–0900 IST (0259 h)	08.29°N, 76.59°E	1769	2451	925	1045
3.	Apr 28, 1995	1501–1800 IST (0259 h)	08.29°N, 76.59°E	1449	1684	900	1343
4.	Aug 29, 1995	1201–1500 IST (0259 h)	23.16°N, 77.36°E	1762	2160	1167	1441
5.	June 27, 1997	0601–0900 IST (0259 h)	08.29°N, 76.59°E	1316	2184	876	1166
6.	Dec 10, 1997	0901–1200 IST (0259 h)	23.16°N, 77.36°E	2280	3202	1715	2147
7.	Aug 15–16, 1998	1501–1800 IST (0259 h)	15.30°N, 73.55°E	1502	2224	1033	1348

(Pasko et al., 1996,1997; Sentman et al., 1995; Taranenko et al., 1992; Lehtinen et al., 1996, 2000; Bell et al., 1995; Gupta, 1997) propagating from top of the active thunderstorm may generate radiations from ULF to VLF (Inan et al., 1991, 1996; Otsuyama et al., 1999), which in turn, may propagate still upward and heat the local plasma in the ionosphere. This is only the possibility proposed by the authors. Any authentic work in this area must include the detailed theoretical calculations or experimental observations, which is beyond the scope of this communication.

4. Conclusions

The SROSS-C2 data have been analyzed to study the electron and ion temperatures anomalies during the thunderstorm days over the normal day's temperature. The study reveals that the electron and ion temperatures show a consistent enhancement during the thunderstorm events. The enhancement in case of electron temperature is slightly higher than the enhancement of ion temperature during the active thunderstorms over the normal days.

Acknowledgements

References

Bell, T.F., Pasko, V.P., Inan, U.S., 1995. Runaway electron as a source of Red Sprites in the mesosphere. Geophysical Research Letters 22, 2127–2130.

Eack, K.B., Suszcynsky, D.M., William, H.B., Roussel-Dupre, R.A., Symbalisity, E.M.D., 2000. Gamma-ray emissions observed in a thunderstorm anvil. Geophysical Research Letters 2, 185–188.

Garg, S.C., Das, U.N., 1995. Aeronomy experiment on SROSS-C2. Journal of Spacecraft Technology 5, 11–15.

Gupta, S.P., 1997. Role of the sprites in stratosphere and mesosphere. PRL, Ahmedabad, India, Abstract Book on NSSS-1997, 84pp.

Inan, U.S., Bell, T.F., Ridriguez, J.V., 1991. Heating and ionization of the lower ionosphere by lightning. Geophysical Research Letters 18, 705–708.

Inan, U.S., Pasko, V.P., Bell, T.F., 1996. Sustained heating of the ionosphere above thunderstorms as evidenced in "early/fast" VLF events. Geophysical Research Letters 23, 1067–1070.

Lehtinen, N.G., Walt, M., Inan, U.S., Bell, T.F., Pasko, V.P., 1996. γ-Ray emission produced by a relativistic beam of runaway electrons accelerated by quasi-electrostatic thundercloud fields. Geophysical Research Letters 23, 2645–2648.

Lehtinen, N.G., Inan, U.S., Bell, T.F., 2000. Trapped energetic electron curtains produced by thunderstorm driven relativistic runaway electron. Geophysical Research Letters 27, 1095–1098.

Mahajan, K.K., Panday, V.K., Jain, V.C., 1983. Relationship between electron density and electron temperature as a function of solar activity. Advances in Space Research (UK) 2, 247–249.

Otsuyama, T., Hobara, Y., Hayakawa, M., 1999. EM radiation associated with sprites. Proceedings of the 11th International Conference on Atmospheric Electricity, Alabama USA, pp. 96–98.

Oyama, K.I., Watanabe, S., Su, Y., Takahashi, T., Hirao, K., 1996. Season, local time and longitudinal variations of electron

temperature at the height of ~ 600 km in the low latitude region. Advances in Space Research 18, 269–278.

Pasko, V.P., Inan, U.S., Bell, T.F., Taranenko, Y.N., 1995. Heating, ionization and upward discharges in the mesosphere due to intense quasi-electrostatic thundercloud fields. Geophysical Research Letters 22, 365–368.

Pasko, V.P., Inan, U.S., Bell, T.F., Taranenko, Y.N., 1996. Sustained heating of the ionosphere above thunderstorms as evidenced in "early/fast" VLF events. Geophysical Research Letters 23, 1067–1070.

Pasko, V.P., Inan, U.S., Bell, T.F., Taranenko, Y.N., 1997. Sprites produced by quasi-electrostatic heating and ionization in the lower ionosphere. Journal of Geophysical Research 102, 4529–4561.

Rai, J., Rao, M., Tantry, B.A.P., 1972. Bremsstrahlung as a possible source of UHF emission from lightning. Nature (Physical Science) 238, 50–60.

Rai, J., Bhattacharya, P.K., Sapru, M.L., 1973. Ionospheric disturbances due to thunderstorms. International Journal of Electronics 34 (6), 757–760.

Schunk, R.W., Sojka, J.J., 1996. Ionosphere–thermosphere space weather issue. Journal of Atmospheric & Solar Terrestrial Physics 58 (14), 1527–1574.

Sentman, D.D., Wescott, E.M., Osborne, D.L., Hampton, D.L., Heavner, M.J., 1995. Preliminary results from the Sprites 94 aircraft campaign: 1. Red sprites. Geophysical Research Letters 22, 1205–1208.

Sharma, D.K., Rai, J., Israil, M., Garg, S.C., 2002. Temperature and density variation in ionospheric plasma over different locations in India. Proceedings of the National Conference on Advances in Contemporary Physics & Energy, IIT Delhi, pp. 265–278.

Singh, R.P., Patel, R.P., 2001. Lightning generated ELF, VLF, Optical waves and their diagnostic features. Proceedings of the National Workshop on Recent Developments in Atmospheric and Space Sciences, IIT Roorkee, pp. 9–32.

Taranenko, Y.N., Inan, U.S., Bell, T.F., 1992. Optical signature of lightning induced heating of the D region. Geophysical Research Letters 19, 1815–1818.

Taranenko, Y.N., Inan, U.S., Bell, T.F., 1993a. Interaction with the lower ionosphere of electromagnetic pulses from lightning: heating, attachment and ionization. Geophysical Research Letters 20, 1539–1542.

Taranenko, Y.N., Inan, U.S., Bell, T.F., 1993b. Interaction with the lower ionosphere of electromagnetic pulses from lightning: excitation of optical emissions. Geophysical Research Letters 20, 2675–2678.

Wescott, E.M., Sentman, D.D., Heavner, M.J., Hampton, D.L., Osborne, D.L., Vaughan Jr, O.H., 1996. Blue Starters: brief upward discharges from an intense Arkansas thunderstorm. Geophysical Research Letters 23, 2153–2156.

Yukhimuk, V., Roussel-Dupre, R.A., Symbalisty, E.M.D., 1998. Optical characteristics of Blue Jets produced by runaway air breakdown simulation results. Geophysical Research Letters 25, 3289–3292.

Yukhimuk, V., Roussel-Dupre, R.A., Symbalisty, E.M.D., 1999. On the temporal evolution of red sprites: runaway theory versus data. Geophysical Research Letters 26, 679–682.

Sunrise effect on ionospheric temperature as measured by SROSS-C2 satellite

D.K.Sharma, Jagdish Rai, M.Israil[1], Shalini Priti[2], P.Subrahmanyam[3], P.Chopra[3] and S.C.Garg[3]

Department of Physics, Indian Institute of Technology, Roorkee – 247 667
[1]Department of Earth Sciences, Indian Institute of Technology, Roorkee – 247 667
[2]College of Engineering Roorkee, Roorkee – 247 667
[3]Radio & Atmospheric Science Division, National Physical Laboratory, New Delhi - 110 012

Abstract

The ionospheric electron and ion temperatures are known to be dependent on the position of Sun with respect to Earth. The Retarding Potential Analyzer (RPA) experiment flown aboard Indian SROSS-C2 satellite has yielded valuable data on ionospheric temperatures and composition. The data collected during the period from 1995 to 1998 for two different locations (Bhopal and Chennai) over India have been analyzed.

The night time electron temperature (Te) varies from 745 to 915°K and rises sharply at sunrise 3334 to 4231°K and then falls off slowly becoming minimum after the sunset at Bhopal. Whereas at Chennai the nighttime Te varies from 754 to 883°K and rise sharply at sunrise from 3495 to 5763°K. The nighttime ion temperature (Ti) varies from 618 to 832°K at Bhopal and it also increases at sunrise from 1270 to 2860°K. At Chennai the nighttime Ti varies from 626 to 776°K and increases at sunrise from 1760 to 2930°K. These enhancements of electron and ion temperatures have been found for both stations. However, due to latitude effect the minor difference is observed in Te and Ti behavior at above two stations.

INTRODUCTION

At sunrise, photoelectron production begins in the ionosphere through the ionization of neutral particles. As the photoelectrons share their high energy with the ambient electrons, the electron temperature (Te) increases. This increase is rapid in the early morning hours due to the low electron density. As more and more electrons are produced as sunrise progress, the share of energy for each electron decreases. Thus, the Te after reaching a maximum decreases and attains a steady state value as the day progress. The electron and ion temperature variations in the Earth's ionosphere have been studied extensively through ground-based and in situ observations (Farley et al. 1967; Evans 1973; Hanson, Nagy & Moffett 1973; Oyama & Hirao 1975; Tithe ridge 1976; Brace & Theis 1978; Oyama, Hirao & Yasuhara 1985; Su et al. 1995; Watanabe, Oyama & Abdu 1995; Bhuyan et al. 2000; Sharma et al. 2002 and others) and through theoretical calculations (Dalgarno et al. 1963; Geisler & Bowhill 1965; Banks & Nagy 1970, Mayr et al. 1972; Bailey et al. 1975 and others). The purpose of the present paper is to study the electron and ion temperature variations in the ionosphere at low latitude F$_2$ region (425-625km) over India for the period from 1995 to 1998. For this purpose, we have used the Stretched Rohini Series Satellite (SROSS-C2) data. The SROSS-C2 was launched by ISRO on May 4, 1994 to study the ionospheric composition and temperature anomalies. The SROSS-C2 is a spin-stabilized satellite with its spin axis perpendicular to its longitudinal axis. Orbital inclination of the satellite is 46° with the equatorial plane. The spin rate of the satellite is about 5 revolutions per minute (rpm).

Data Analysis

The data obtained using RPA payload aboard SROSS-C2 satellite for the period from January 1995 to December 1998 have been analyzed to study the behavior of ionospheric temperatures (Te and Ti). The data were obtained for ten different locations: Aurangabad (19.53° N, 75.23° E), Bhopal (23.16° N, 77.36° E), Chennai (13.04°N, 80.17° E), Cochin (09.58° N, 76.17° E), Indore (22.44°N, 75.50° E), Nagpur (21.09° N, 79.09° E), Panji (15.30° N, 73.55° E), Pune (18.31°N, 73.55° E), Trivandrum (08.29° N, 76.59° E) and Varanasi (25.20° N, 83.00° E). These stations were chosen for the maximum number of passes of satellite SROSS-C2 over India in the altitude range 425-625 km. The electron and ion temperatures have been obtained at fixed locations with ± 1° variation in longitude and latitude. In the present paper we have analyzed the temperature variation data for two stations data: Bhopal (23.16° N, 77.36° E) and Chennai (13.04° N, 80.17° E) in details.

The Retarding Potential Analyzer (RPA) payload consists of two sensors viz., electron and ion sensors and associated electronics (Garg & Das 1995). The electron and ion RPAs are used for insitu measurements of ionospheric electron and ion parameters. In addition a spherical Langmuir probe is included and is used as potential probe for estimating the variation of spacecraft potential during spinning of the satellite. The electron and ion sensors both have planar geometry and consist of multigrid Faraday cups with a collector electrode. The different grids in the sensor are designated as the Entrance grid, the Retarding grid, the Suppressor grid and the Screen grid. These grids are made of gold plated tungsten wire mesh having 90 to
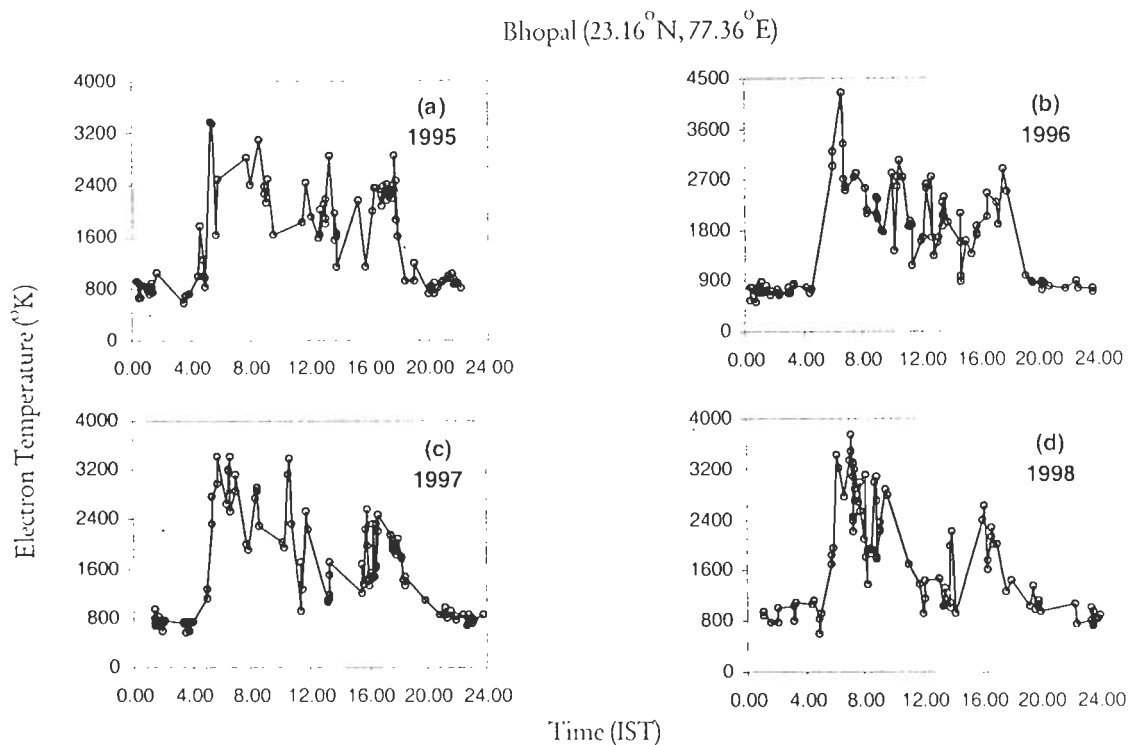
Bhopal (23.16°N, 77.36°E)

Figure 1. Variation of *Te* at Bhopal form 1995 to 1998.
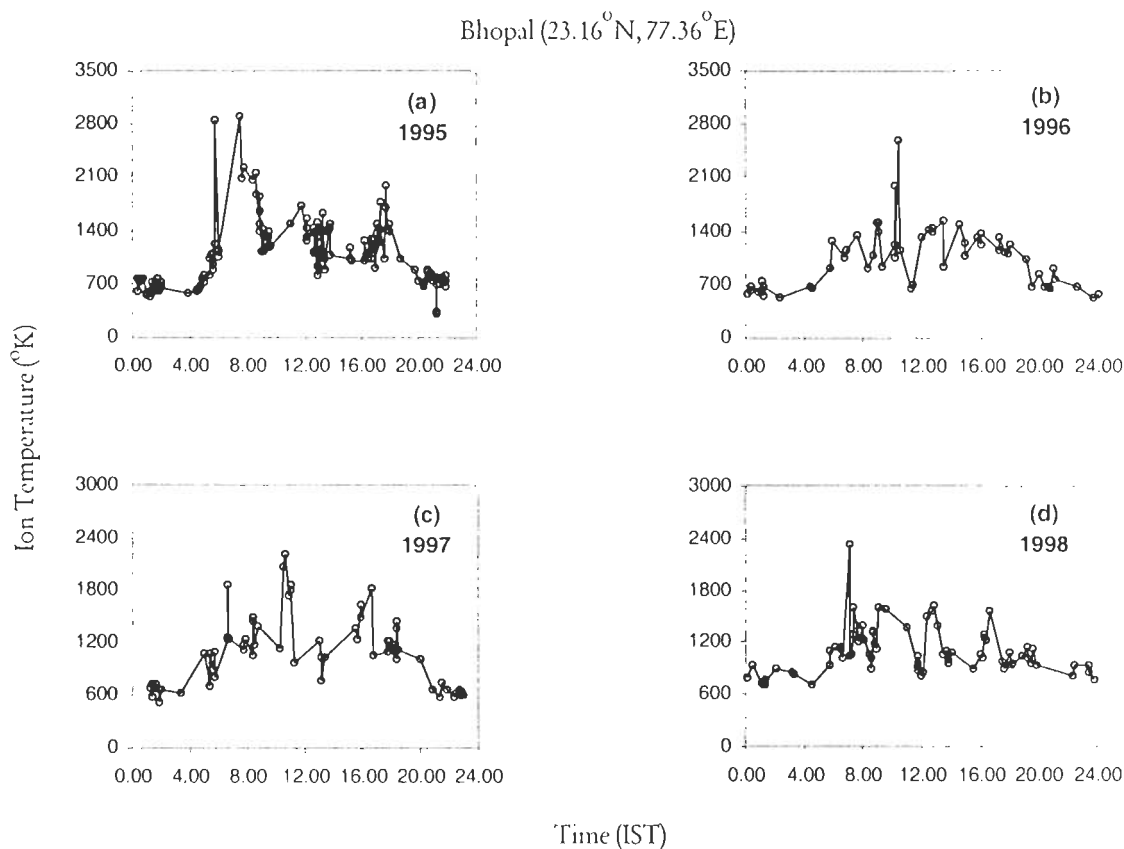
Bhopal (23.16°N, 77.36°E)

Figure 2. Variation of *Ti* at Bhopal form 1995 to 1998.

Table-1a: Comparison of *Te* at Bhopal and Chennai from 1995 to 1998.

Year	Bhopal			Chennai		
	Maximum Temp. at Sunrise (°K)	Average Temp. at Daytime (°K)	Average Temp. at Nighttime (°K)	Maximum Temp. at Sunrise (°K)	Average Temp. at Daytime (°K)	Average Temp. at Nighttime (°K)
1995	3334	2089	879	5763	2121	807
1996	4231	2121	745	3495	1618	754
1997	3403	2059	789	4667	1995	777
1998	3438	2114	915	4784	3132	883

Table-1b: Comparison of *Ti* at Bhopal and Chennai from 1995 to 1998.

Year	Bhopal			Chennai		
	Maximum Temp. at Sunrise (°K)	Average Temp. at Daytime (°K)	Average Temp. at Nighttime (°K)	Maximum Temp. at Sunrise (°K)	Average Temp. at Daytime (°K)	Average Temp. at Nighttime (°K)
1995	2860	1312	702	1890	1099	646
1996	1270	1254	658	1760	1153	626
1997	1870	1278	618	2930	1140	675
1998	2230	1163	832	2400	1247	776

Table-2: After sunrise the decay equation of *Te* and *Ti* at Bhopal and Chennai.

Year	Electron Temperature		Ion Temperature	
	Bhopal	Chennai	Bhopal	Chennai
	Decay Equation	Decay Equation	Decay Equation	Decay Equation
1995	$Y = 5232.8e^{-0.0759X}$	$Y = 5812.9e^{-0.0884X}$	$Y = 1945.5e^{-0.0459X}$	$Y = 3848.3e^{-0.0740X}$
1996	$Y = 4853.3e^{-0.0775X}$	$Y = 4964.8e^{-0.0848X}$	$Y = 2346.4e^{-0.0576X}$	$Y = 1636.3e^{-0.0275X}$
1997	$Y = 4865.1e^{-0.0734X}$	$Y = 6387.6e^{-0.1018X}$	$Y = 2492.8e^{-0.0644X}$	$Y = 2149.3e^{-0.0442X}$
1998	$Y = 4408.0e^{-0.0704X}$	$Y = 5576.9e^{-0.0851X}$	$Y = 2024.8e^{-0.0422X}$	$Y = 1735.0e^{-0.0293X}$

Chennai (13.04°N, 80.17°E)

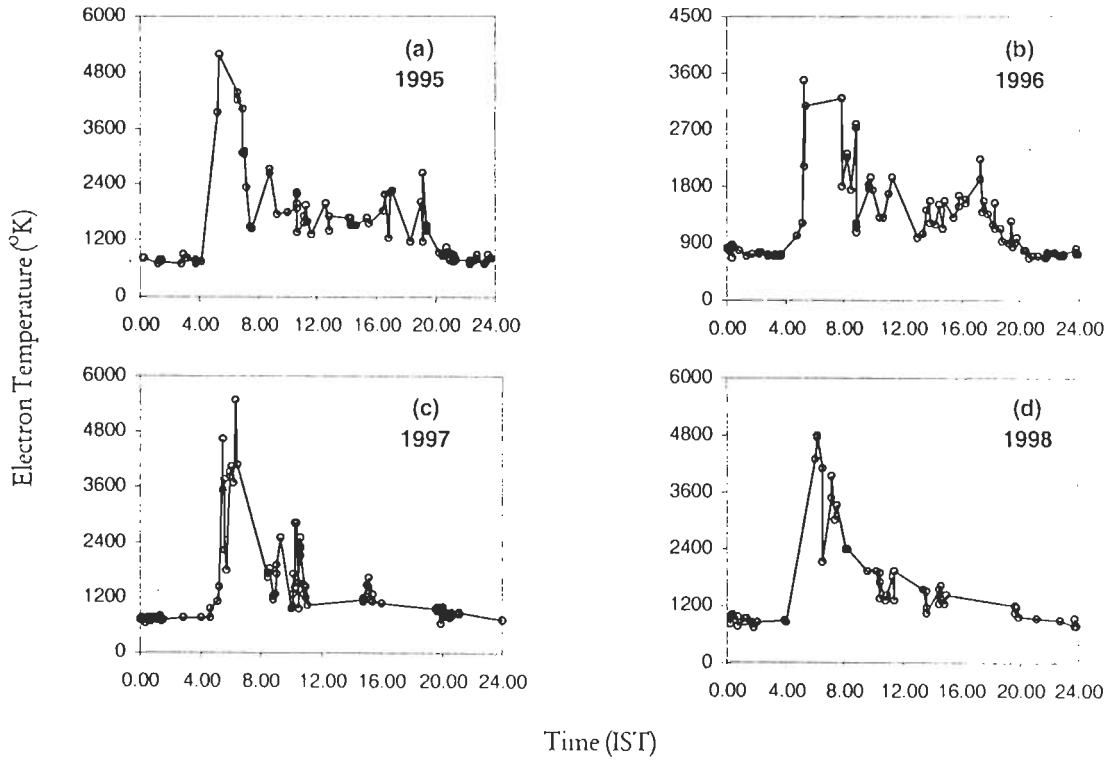
Figure 3. Variation of Te at Chennai form 1995 to 1998.
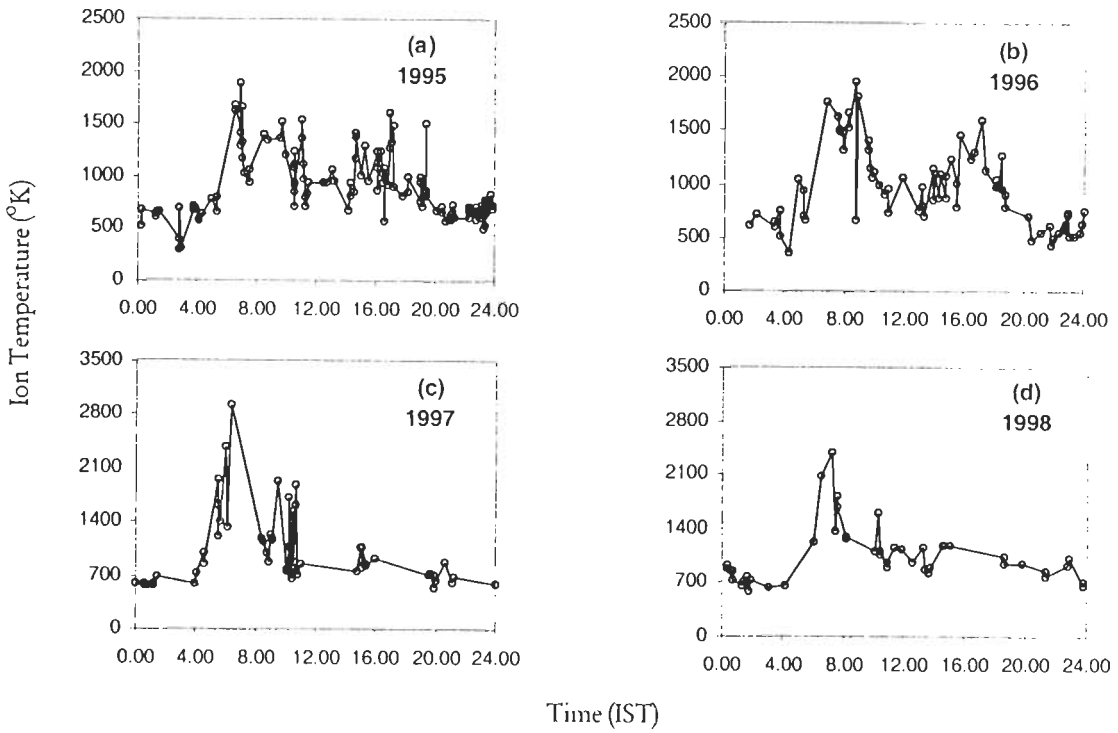
Chennai (13.04°N, 80.17°E)
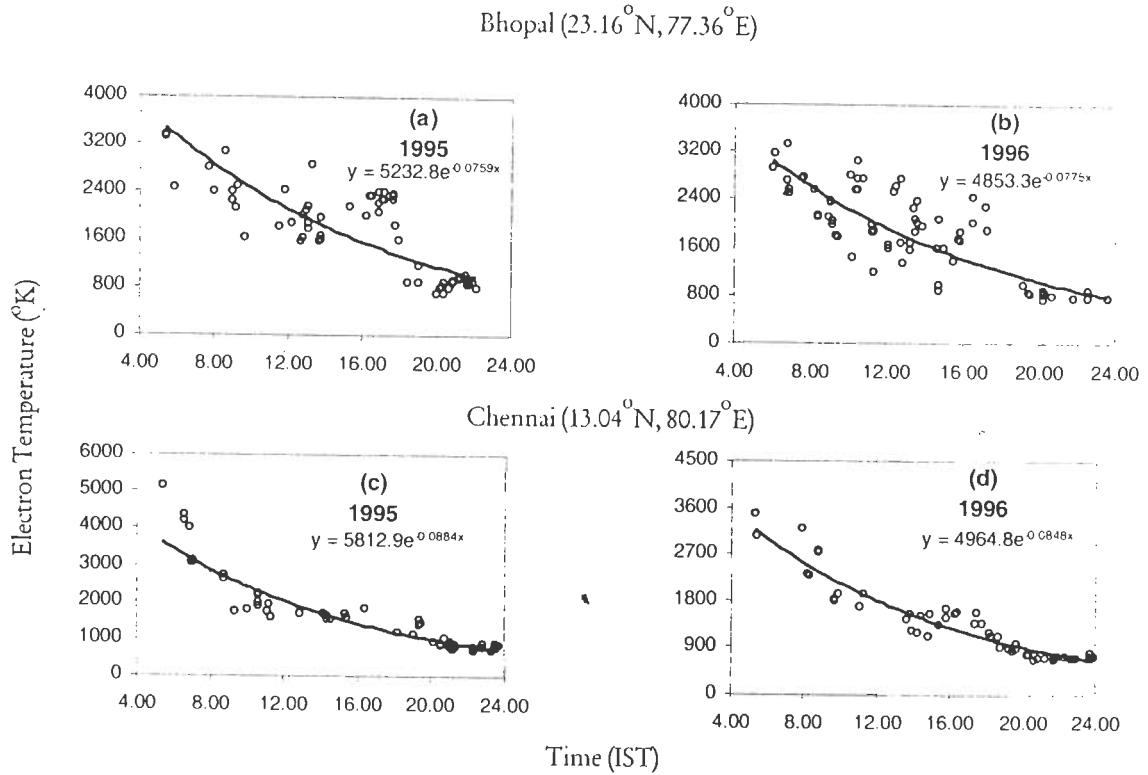

Figure 4. Variation of Ti at Chennai form 1995 to 1998.

Bhopal (23.16°N, 77.36°E)

Chennai (13.04°N, 80.17°E)

Figure 5. After sunrise the exponential decay of *Te* at Bhopal and Chennai.

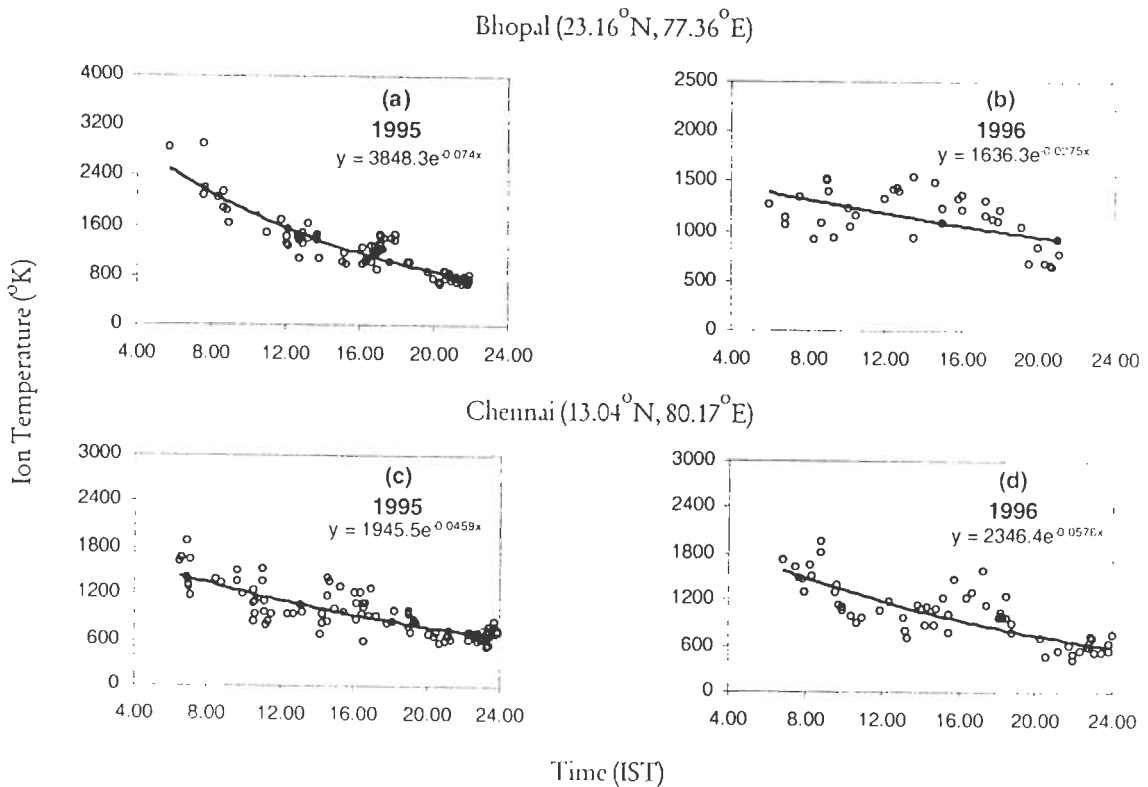Bhopal (23.16°N, 77.36°E)

Chennai (13.04°N, 80.17°E)

Figure 6. After sunrise the exponential decay of *Ti* at Bhopal and Chennai.

95% optical transparency. The two sensors are mechanically identical but have different grid voltages suitable for collection of electrons and ions respectively. The charged particles whose energies are greater than the applied voltage (Garg & Das 1995) on the retarding grid pass through various grids and finally reach collector electrode to cause the sensor current. This current is measured by a linear auto-gain ranging electrometer. The raw data in the form of LOTUS file are obtained from Indian Space Research Organization (ISRO).

Results and Discussion

The yearly data for Te recorded at Bhopal and Chennai from 1995 to 1998 are shown in Fig.1 (a, b, c and d) and Fig.3 (a, b, c and d) respectively. The sunrise time varies between 5:00 to 7:00 IST depending upon the season. During this time we have observed a sharp increases in Te at both stations. The maximum Te at Bhopal reaches up to 3334°K in 1995, 4231°K in 1996, 3403°K in 1997 and 3438°K in 1998 during sunrise hours. Whereas at Chennai in 1995 maximum Te goes up to 5763°K, 3495°K in 1996, 4667°K in 1997 and 4784°K in 1998. At Chennai double peak is observed in 1997 (Fig. 3c). The cause for the appearance of the second peak is not understood. The nighttime average Te varies from 745 to 915°K at Bhopal and from 754 to 883°K at Chennai during 1995 to 1998. Table 1a shows the details of Te variations over these stations from 1995 to 1998.

The spatial and temporal variations of the electron temperature at equatorial anomaly latitudes has been studied by Su et al. (1996) using the Hinotori satellite at about 600km. They have observed similar morning rise in Te. Thus the results obtained from SROSS-C2 satellite data are consistent with the Japanese satellite Hinotori (Su et al. 1996) data.

Oyama et al. (1996a) have studied the morning overshoot of Te by the downward plasma drift in the equatorial topside ionosphere and found that the rapid increase in electron temperature in the early morning period is the well known Te phenomenon called 'morning overshoot'. Oyama et al. (1996b) have also studied the season, local time and longitude variations of the electron temperature at the height of about 600km in the low latitude region. They found that an electron temperature enhancement occurs in the morning period (between 5:00 to 8:00 LT). The peak value is highest at the magnetic equator and reaches about 5000°K for the high solar activity. Our study also pertains to low latitude and observed that the highest peak of Te is about 5763°K at Chennai in 1995 (Fig.3a). It is similar to the value reported for equatorial region by Oyama et al. (1996b).

The yearly data for Ti recorded at Bhopal and Chennai from 1995 to 1998 are shown in Fig. 2 (a, b, c and d) and Fig.4 (a, b, c and d) respectively. The Ti also shows the similar behavior at these stations. However, the change in Ti is relatively less than Te. During the time of sunrise we have observed a sharp increases in Ti at both stations. The maximum Ti at Bhopal reaches up to 2860°K in 1995, 1270°K in 1996, 1870°K in 1997 and 2230°K in 1998 during sunrise hours. Whereas at Chennai in 1995 maximum Ti is 1890°K, 1760°K in 1996, 2930°K in 1997 and 2400°K in 1998. The nighttime average Ti varies from 618 to 832°K at Bhopal and from 626 to 776°K at Chennai during 1995 to 1998. Table.1b shows the details of Ti variations over these stations from 1995 to 1998.

The Te and Ti decrease almost exponentially after reaching the maximum value at both stations. The exponential decay in Te at Bhopal is shown in Fig.5 (a and b) and at Chennai in Fig. 5 (c and d) respectively for the year 1995 to 1996. The Ti decay at Bhopal is shown in Fig.6 (a and b) and at Chennai in Fig.6 (c and d) during the year of 1995 and 1996 after the sunrise hours. Similar exponential decay has also been observed for the year 1997 and 1998. The generalized decay equation can be written as:

$$Y = Ae^{B X}$$

Where A and B are two arbitrary constant, the value of A and B are shown in Table.2 for both stations Bhopal and Chennai during 1995 to 1998. The valve of A varies from 4000 to 6500 for Te and from 1500 to 4000 for Ti. The value of B for Te varies from 0.07 to 0.10 and from 0.02 to 0.07 for Ti for both the stations.

CONCLUSIONS

The variation of Te and Ti over two Indian stations (Bhopal and Chennai) during the solar minimum (1994) to solar maximum (2000) has been studied using SROSS-C2 satellite data. Due to latitude effect the maximum Te at Chennai is higher than Bhopal. Generally the behavior of ionospheric temperatures and morning overshoot are in consistent with other similar observation using the data from different satellites.

ACKNOWLEDGEMENT

REFERENCES

Bailey, G.J., Moffett, R.J. & Swartz, W.E., 1975. Effect of photoelectron heating and interhemisphere transport on daytime plasma temperature at low latitudes, Planet. Space Sci., 23, 599-607.

Banks, P.M. & Nagy, A.F., 1970. Concerning the influence of elastic scattering upon photoelectron transport and escape, J. Geophys. Res., 75, 1902-1911.

Bhuyan, P.K. & Kakoty, P. K..,2000. Comparison of electron and ion temperature measurements at ± 10° magnetic latitudes from SROSS-C2 with the IRI, Abstract book on NSSS-2K, Puri, India, pp 99.

Brace, L. H. & Theis, R. F., 1978. An empirical model of day time electron temperature in the thermosphere at solar minimum, Geophys. Res. Lett. 5, 275-278.

Dalgarno, A., McElory, M. B. & Moffett, R..J., 1963. Electron temperatures in the ionosphere, Planet. Space Sci., 11, 463-472.

Evans, J. V., 1973. Seasonal and sunspot cycle variations of F region electron temperatures and protonospheric heat fluxes, J. Geophys. Res., 78, 2344-2349.

Farley, D.T., McClure, J.P., Sterling, D.L. & Green, J. L., 1967. Temperature and composition of the equatorial ionosphere, J. Geophys. Res., 72, 5837-5846.

Garg, S.C. & Das, U.N., 1995. Aeronomy experiment on SROSS-C2, J. Spacecraft Technology, 5, 11-15.

Geisler, J.E. & Bowhill, S.A., 1965. Exchange of energy between the ionosphere and the photonosphere, J. Atmos. Terr. Phys., 27, 751-763.

Hanson, W. B., Nagy, A. F. & Moffett, R. J., 1973. Ogo 6 measurement of super cooled plasma in the equatorial exosphere, J. Geophys. Res., 78, 751-756.

Mayr, H.G., 1972. A theoretical model of the ionospheric dynamics with interhemisphere coupling, J. Atmos. Terr. Phys., 34, 1659-1680.

Oyama, K. I. & Hirao, K., 1975. Electron temperature probe experiments on the satellite TAIYO, J. Geomagn. Geoelectr., 27, 321-330.

Oyama, K. I., Hirao, K. & Yasuhara, F., 1985. Electron temperature probe on board Japan's 9th scientific satellite OHZORA, J. Geomagn. Geoelectr., 37, 413-430.

Oyama, K. I., Balan, N., Watanabe, S., Takahashi, T., Isoda, F., Bailey, G. J. & Oya, H., 1996a. Morning overshoot of Te enhanced by downward plasma drift in the equatorial topside ionosphere, J. Geomagn. Geoelectr., 48, 959-966.

Oyama, K. I., Watanabe, S., Su, Y., Takahashi, T., & Hirao, K., 1996b. Season, local time and longitudinal variations of electron temperature at the height of ~600 km in the low latitude region, Adv. Space Res., 18, 269-278.

Sharma, D. K., Rai, J., Israil, M. & Garg, S. C., 2002. Temperature and Density variation in ionospheric plasma over different locations in India, Proc. National Conference on Advances in Contemporary Physics & Energy, IIT Delhi, 265-278

Su, Y. Z., Oyama, K. I., Bailey, G. J., Takahashi, T. & Watanabe, S., 1995. Comparison of satellite electron density and temperature measurements at low latitudes with a plasmasphere-ionosphere model, J. Geophys. Res., 100, 14591-14604.

Titheridge, J. E., 1976. Plasma temperatures from Alouette 1 electron density profiles, Planet. Space Sci., 24, 247-258.

Watanabe, S., Oyama, K.I. & Abdu, M.A., 1995. A computer simulation of electron and ion densities and temperature in the equatorial F region and comparison with Hinotori results, J. Geophys. Res., 100, 14581-14590.

123

Summer variations of the atmospheric aerosol number concentration over Roorkee, India

D.K. Sharma[a],*, J. Rai[a], M. Israil[b], Pratap Singh[c]

[a]*Department of Physics, Indian Institute of Technology, Roorkee 247 667, India*
[b]*Department of Earth Sciences, Indian Institute of Technology, Roorkee 247 667, India*
[c]*National Institute of Hydrology (NIH), Roorkee 247 667, India*

Abstract

The atmospheric aerosol number concentration has been measured at Roorkee (29°52′N, 77°53′E, 275 m above mean sea level) in northern India during November 1998–August 1999 at a height of 9 m above ground level. The aerosol number concentration in summer season (April–July 1999) for morning, noon and evening periods has been analyzed, and the daily variation of aerosol number concentration has been related to selected meteorological parameters like: relative humidity, temperature, rainfall and wind speed. The measurements were carried out with an optical particle counter. The counter monitors the number concentration of aerosols in the diameter size range from 0.3–5.0 μm. The aerosol number concentration for upper size ranges (1.0–2.0 and 2.0–5.0 μm) is maximum in June and minimum in July. The aerosol number concentration in small size ranges (0.3–0.5 and 0.5–1.0 μm) decreases monotonically till the end of July.
© 2003 Elsevier Ltd. All rights reserved.

1. Introduction

Aerosols play an important role in the atmosphere. They control the atmospheric radiation budget and hence are important in the variation of weather and climate. The atmospheric aerosols either independently or in combination with atmospheric ions act as cloud condensation nuclei and affect precipitation (Singh, 1985). Devara and Raj in 1998 measured the aerosols during two successive monsoon seasons. Hanel (1976) and Shaw (1988) have tried to study the size distribution of atmospheric aerosol in different meteorological conditions. Singh et al. (1997) measured the concentration of aerosols during monsoon period and found that the concentration decreases with increasing precipitation. This phenomenon has been attributed to the scavenging of large aerosol particles due to rain.

The study on aerosol distribution can be done by using various techniques available such as Cascade impactor

(Pahwa et al., 1994; Zhang et al., 2001), Lidar (Devara and Raj, 1998; McCormick et al., 1978), Low-pressure impactor (Parameswarn and Vijaykumar, 1994), Laser scatterometer (Singh et al., 1997, 1999), Optical counter (Bansal and Verma, 1998; Sharma et al., 2002), etc.

In the present study, we have measured the aerosol number concentration with an optical counter. The summer variation of atmospheric aerosol number concentration in different size bins for morning, noon and evening periods and their behavior with some selected meteorological parameters: relative humidity, temperature, rainfall and wind speed have been studied.

2. Experimental technique

The optical counter model KC-01A (Rion Co. Ltd. Tokyo, Japan) has been used in the present study, which is based on the principle of Mie scattering of light. The instrument has been well calibrated and has a provision for inbuilt calibration. A light beam intersects a flow of ambient air

---

* Corresponding author.
E-mail address: dksphdes@rediffmail.com (D.K. Sharma).

containing aerosols, which is chopped by a light chopper. The light incident on aerosol particles is scattered and received by a photo-multiplier tube (PMT) at an angle of 90°. The output of the PMT is amplified and then fed to a pulse height analyzer, which divides the aerosol response into different size ranges. The pulse height is directly proportional to the particle size. The instrument sucks the ambient air at the rate of 1 l for 2 min. The sucked air is monitored for 2 min only and the number concentration of particles is measured in the unit of particles/l. The whole equipment is microprocessor-based and gives direct printout of aerosol particle number concentration for different size ranges of 0.3–0.5, 0.5–1.0, 1.0–2.0 and 2.0–5.0 μm. The error in all size ranges measurement is less than 5%. The detailed description of the instrument can be found in the work of Bansal and Verma (1998). The observations were made at a height of 9 m above the ground surface on second floor of the physics department building inside the IIT campus. The IIT campus is located in the city of Roorkee (29°52′N, 77°53′E) at a height of 275 m from the sea level. The surrounding is free from industries; the man-made aerosols are mainly due to household activities and automobiles.

The observation times for the present study were chosen for the period from April to July 1999 and data were recorded continuously from 9:00 AM to 6:00 PM. The number concentration of aerosols in the above size ranges was recorded at every half an hour interval and the data of meteorological parameters were recorded at the National Institute of Hydrology, Roorkee, which is located at a distance about 300 m from the aerosol observation site.

3. Results and discussion

The measurements have been grouped for morning, noon and evening variations. Analysis has been done in all the size ranges and observation period from April to July has been chosen for the present study because in this period both the premonsoon and monsoon activities occur. The aerosol number concentration has a diurnal variation. In the evening the aerosol number concentration decreases as reported by Vakeva et al. (2000). At noon it is increased due to prevailing sun and wind. The morning aerosols have different characteristics due to continued condensation because of high humidity and low temperature (Parameswarn and Vijaykumar, 1994). Therefore, in the present study we have divided the period of measurement in three groups, i.e. morning, noon and evening periods.

Aerosols data have been recorded for four size ranges (0.3–0.5, 0.5–1.0, 1.0–2.0 and 2.0–5.0 μm). However, we have chosen to present two sizes (0.3–0.5 and 2.0–5.0 μm) only to reduce the number of figures and improve the presentation quality. The average concentration of aerosols for the evening period (16:00–18:00 h) for summer months is shown in Fig. 1. In the size range 0.3–0.5 μm [Fig. 1(a,b)],

the evening aerosol concentration varies from about 4×10^4 to above 2×10^5 particles/l in the month of April, most of the particles remaining under the upper size range of 10^5 particles/l. The concentration of the particles remains nearly the same in the month of May 1999. However, in the month of June the concentration of these particles was decreased. Most of the particles remain in the range 1.5×10^4–9×10^4 particles/l. In the month of July, the concentration had further decreased and most of the particles fall in the range 1×10^4–8×10^4 particles/l.

This trend continues in the size range 0.5–1.0 μm. Most of the particles remain around 4×10^4 particles/l both in the months of April and May. The concentration in this range had decreased in the months of June and July. The lowest concentration goes up to about 10^3 particles/l in July.

In the size range 1.0–2.0 μm, the concentration is lower than the previous size ranges. In April, though the concentration ranges from above 1×10^3–4.75×10^3 particles/l, most of the particles remain within the upper limit of 2.5×10^3 particles/l. The concentration remains at the same level in the month of May. In the month of June the average concentration of particles (1×10^3–5.6×10^3 particles/l) has slightly increased compared to the month of April and May, though there are high fluctuations in this month. In July the concentration of particles had decreased drastically, most of the particles (leaving first few days) remaining in the range about 200–1400 particles/l. In this size range the increase of particles in the month of June can be attributed to the larger particles being airborne due to heat, that causes desiccation and wind. However, in the month of July the lowering of aerosol number concentration can be attributed to the scavenging of aerosols by monsoon rain.

A similar situation prevails in the size range 2.0–5.0 μm [Fig. 1(c,d)]. In the month of April and May, the level of concentration remains the same (300–1200 particles/l). In June the concentration increases drastically ranging from about 400–5600 particles/l. However, in July the concentration had decreased drastically with most of the particles lying in the concentration range 50–300 particles/l.

During the noon period (from 10:30 AM to 3:00 PM), the daily average concentration [Fig. 2(a,b)] in the size range 0.3–0.5 μm is at the same level as for evening for the whole summer from April to July. In the size range 0.5–1.0 μm, the noon time average concentration is higher than the evening concentration during the month of April (1×10^4–8×10^4 particles/l) but most of the particles remaining within the upper limit of 4×10^4 particles/l and in the month of May it is slightly higher than the evening concentration (1.5×10^4–5×10^4 particles/l). This higher trend for noon concentration remains in the months of June and July. In the size range 1.0–2.0 μm, the noon concentration is higher than the evening concentration in the months of April, May and July. However, in June they are almost similar. The noon concentration in the size range 2.0–5.0 μm is [Fig. 2(c,d)] maximum in June and minimum in July. During all the 4 months the time variation of noon aerosols have
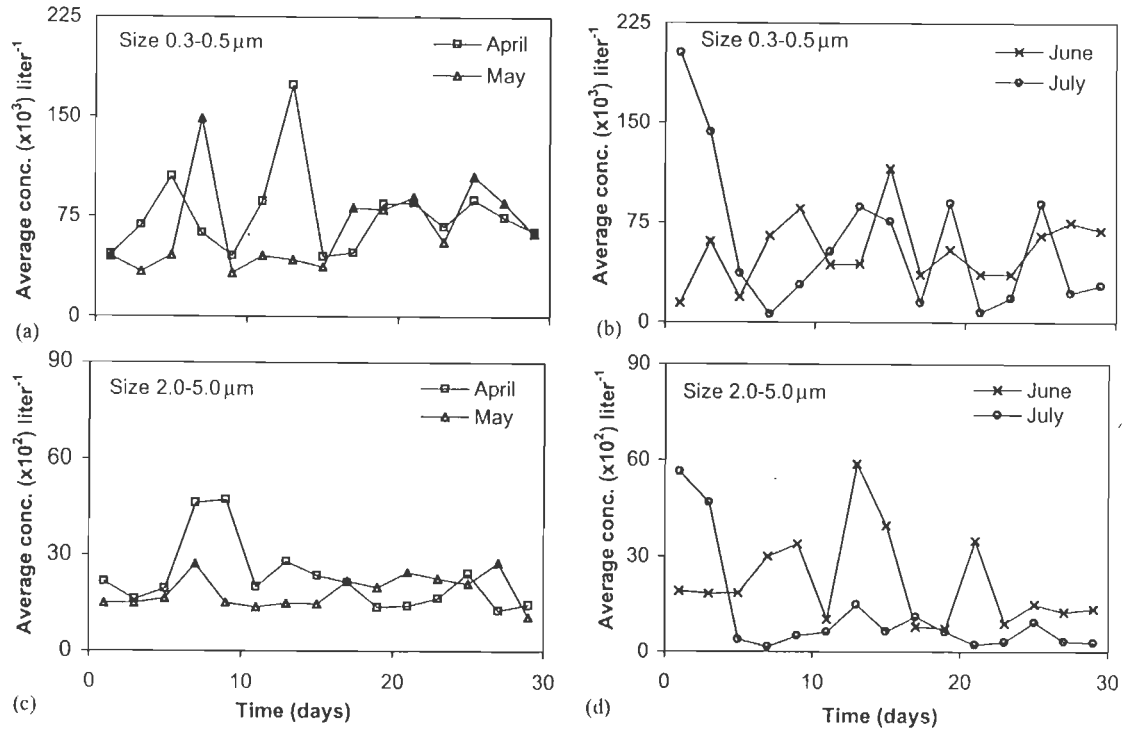
Fig. 1. Variation of average number concentration of aerosol in evening period for summer season (April–July 1999) for lower and upper size range.

similar pattern as for the evening aerosols. The nature of time variation for evening and noon aerosols in the above size ranges are also similar.

The concentration of aerosols during morning period (9:00–10:00 AM) in the size range 0.3–0.5 μm is nearly in the same range as for noon and evening period for the whole summer of 1999 [Fig. 3(a,b)]. Same is the case for the size range 0.5–1.0 μm. In the size range 1.0–2.0 μm also the level of concentration and time variation are the same as for noon and evening periods. In the size range 2.0–5.0 μm [Fig. 3(c,d)], the level of concentration and time variation in all other months are the same as in the above size ranges except in the month of May, where the level of concentration is higher and it varies from about 800–5500 particles/l.

The time variation of aerosols in three size ranges shows that for 0.3–0.5, 0.5–1.0 and 1.0–2.0 μm the morning concentrations are larger than the evening concentration and shows a steady decrease from 09:00 to 14:00 h and then became steady. Fig. 4 shows the daily behavior of 0.3–0.5 and 2.0–5.0 μm size ranges. Because of the low temperature and high humidity, the contribution to aerosol number concentration in the lower size ranges during morning period is due to water vapor condensation. With the rise of the Sun the temperature increases and the droplets get evaporated. However, the large size range of 2.0–5.0 μm dominates. With the rise of temperature and occurrence

of high-velocity winds the aerosol number concentration increases. The atmospheric temperature becomes high around 14:00 h and after that both the temperature and wind velocity decrease. This causes a maximum around 14:00 h in large size range in the aerosol concentration. This trend is clearly visible in the months of April and July. In July the concentration is lowest in all size ranges due to scavenging. But the high velocity wind around 14:00 h might have caused a peak at that time in the size range 2.0–5.0 μm in the months of May and June. After about 10:00 h the concentration (2.0–5.0 μm size) becomes almost constant till evening. The absence of peaks in May and June and their lower concentration compared to April has been attributed to the low-intensity rain in these months.

Devara and Raj (1998) studied the columnar content of aerosols over Pune using lidar. Their results revealed contrasting nature of variation in the years 1987 and 1988. In 1987, the concentration was minimum in the month of May while in 1988 it was maximum in this month, both in the height range 50–1100 and 50–200 m from the ground surface. Their result showed that the aerosol concentration was minimum during rainy season. This is in good agreement with our observation that the aerosol number concentration had gone minimum in the month of July when the monsoon over Roorkee was in full swing.

Pahwa et al. (1994), studied the aerosols of different composition and the total suspended particles (TSP) at
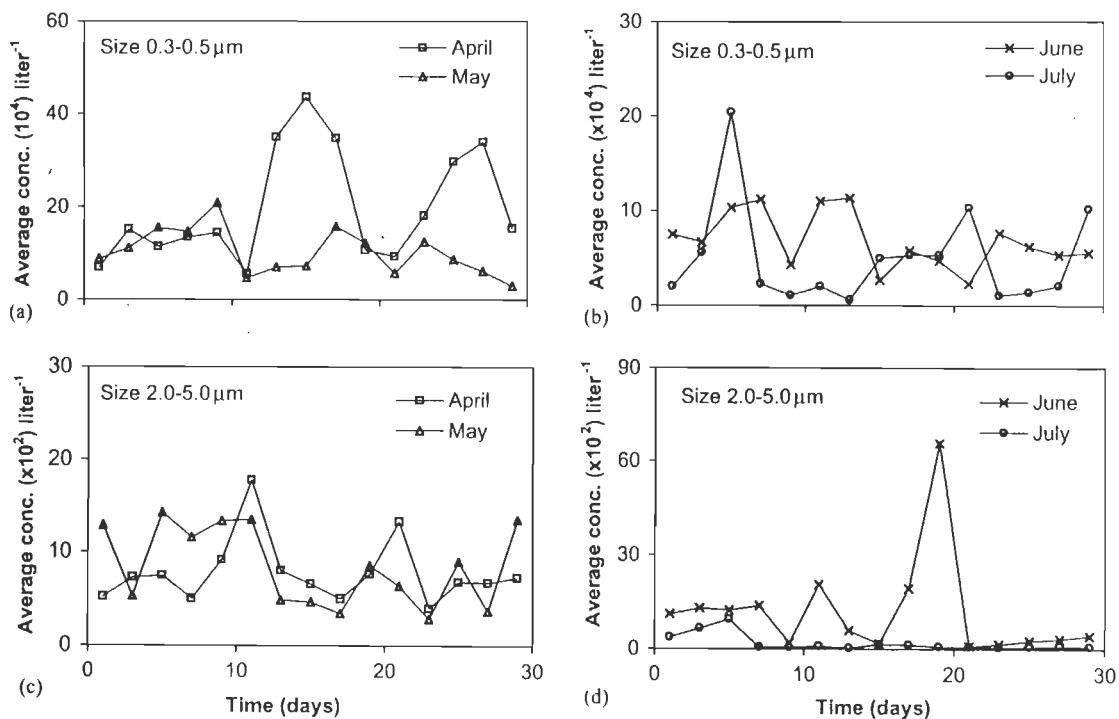
Fig. 2. Variation of average number concentration of aerosol in noon period for summer season (April–July 1999) for lower and upper size range.
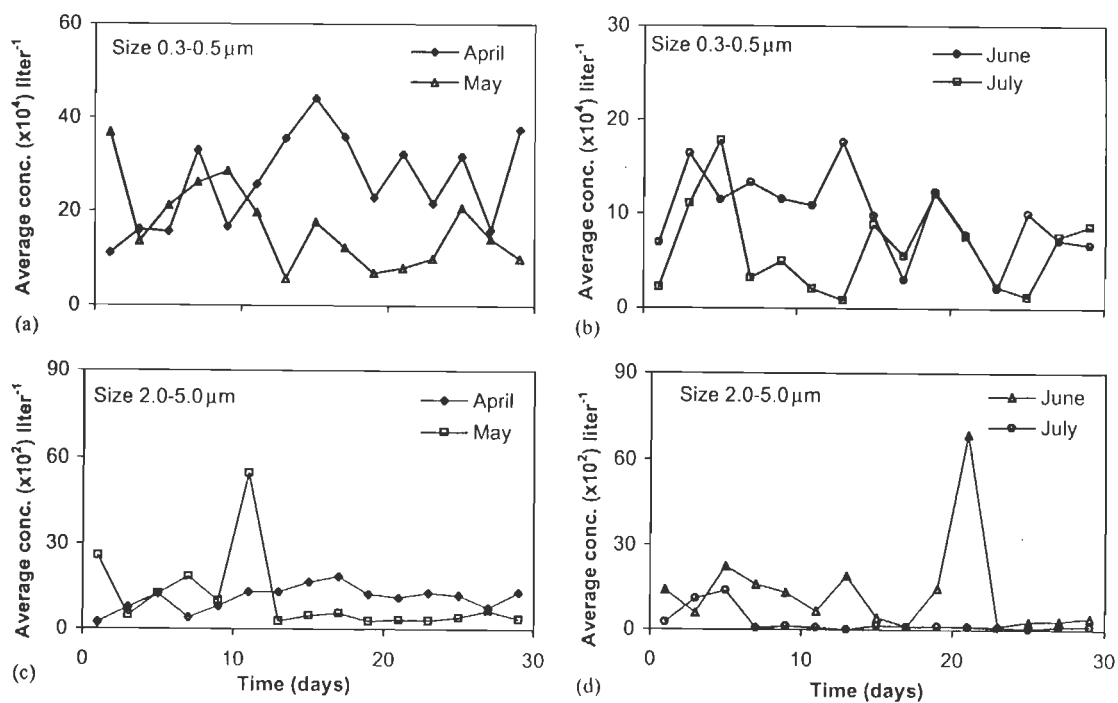

Fig. 3. Variation of average number concentration of aerosol in morning period for summer season (April–July 1999) for lower and upper size range.
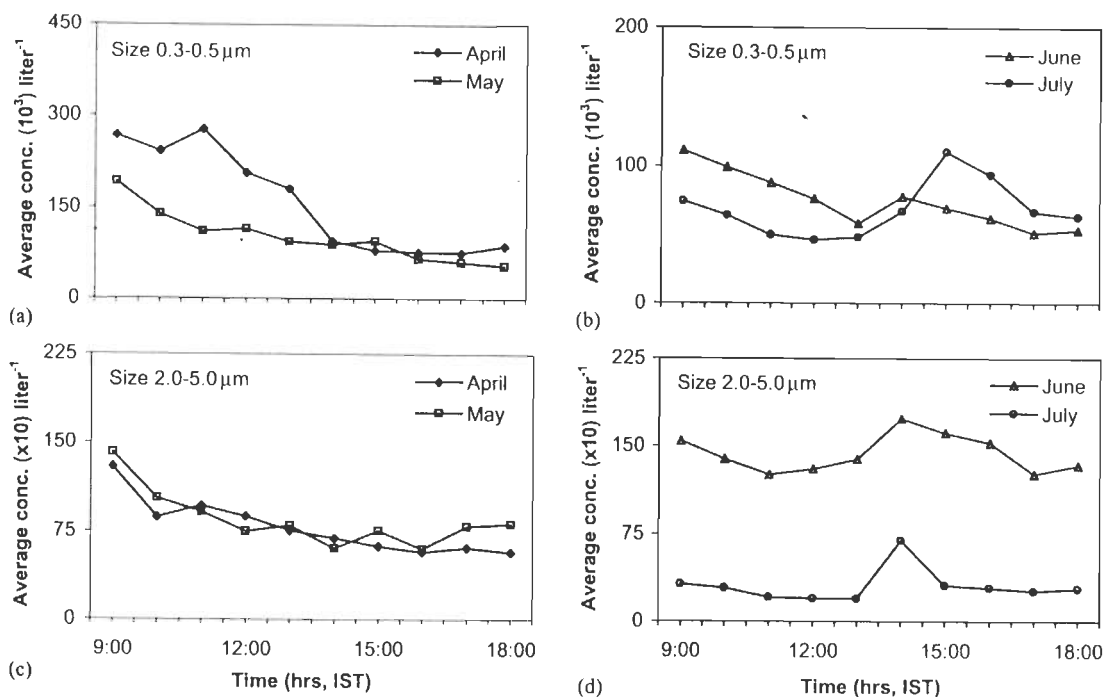
Fig. 4. The time variation of average number concentration of aerosols in summer season (April–July 1999) for lower and upper size range.

Delhi. Their study revealed that during May 1986, the TSP concentration was 543.13 µg/m³. It had increased to 777.17 µg/m³ in the month of June. In July and August, the concentration had gone to 231.88 and 173.36 µg/m³, respectively. As the onset of monsoon over Roorkee and Delhi are nearly at the same time, their results can be compared with our observation that in July the aerosol number concentration in all size ranges is decreased drastically. In their studies the minimum concentration was in August. The maximum rain occurs in August, which decreases the aerosol number concentration due to scavenging.

In Fig. 5, though day-to-day variation of aerosol number concentration occurs, it is seen that the variation of average concentration of aerosols for different size ranges differs. For large size particles (2.0–5.0 µm), the concentration is lowest and the concentration is maximum for small size particles (0.3–0.5 µm) during the whole period of observation. The small size 0.3–0.5 µm, aerosol number concentration is about 3×10^5 particles/l in the month of April. Most of the particles remain in the upper range of 10^5 particles/l [Fig. 5(a,b)]. The concentration of particles is nearly the same in the month of May but is less in comparison to the month of April. In the month of June, the concentration of aerosol decreases and most of the particles remain in the concentration range $2.3 \times 10^5 – 9 \times 10^4$ particles/l. A further decrease in concentration is observed in the month of July.

This trend continues in the size range 0.5–1.0 µm [Fig. 5(c,d)]. Most of the particles remain in the range $7 \times 10^4 – 8 \times 10^3$ particles/l in the months of April and May. The

concentration in this range decreases in the month of June and July. The lowest concentration goes to 10^3 particles/l.

In the size range 1.0–2.0 µm [Fig. 5(e,f)], the concentration is lower than that in the previous range. In the month of April the concentration ranges from 2.5×10^2 to 6.4×10^3 particles/l. It is nearly the same in the month of May and is lower in June than in July. In the month of July the aerosol number concentration varies from $6.4 \times 10^3 – 1 \times 10^2$ particles/l.

A similar situation prevails in the size range 2.0–5.0 µm [Fig. 5(g,h)]. During the months of April and May the concentration of aerosol was nearly the same (50–100 particles/l), while in June, the concentration increases, ranging from 50–200 particles/l. There is a significant decrease in the concentration in July and most of the particles lie in the concentration range 15–50 particles/l.

The fluctuation of aerosol number concentration depends upon meteorological parameters. The relative humidity (RH) was minimum in the month of April and increases in May and became maximum in July [Fig. 6(a,b)]. In the month of June the RH was less than the month of July. The present study reveals that the aerosol number concentration was more affected by RH during South-East (SE) premonsoon season of the year 1999 over Roorkee. Parameswarn and Vijaykumar (1994) found that the RH significantly affects the aerosol concentration and size distribution above about 90%. Here at Roorkee in the months of June and July 1999 average RH was almost close to this limit. Devara and Raj (1998) observed a higher humidity and lower temper-
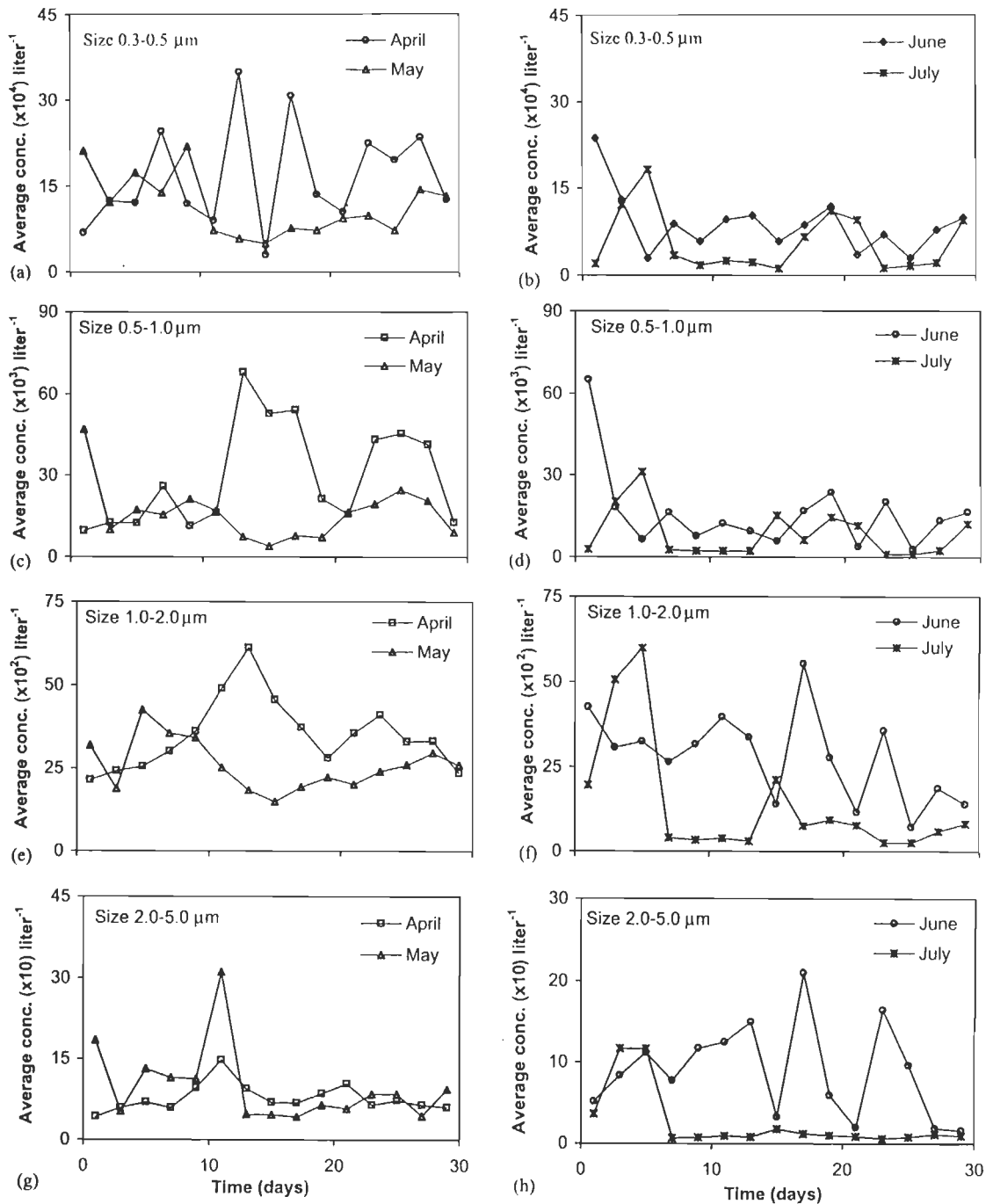
Fig. 5. Variation of average number concentration of aerosols in summer season (April–July 1999) for different size ranges.

ature during South-West premonsoon in the year 1988 at Pune. The effect of premonsoon scenario (Aher and Agashe, 1997) on aerosols at Pune caused by the growth of cloud droplets results in higher rainfall. The same physical process appears to have taken place in 1999 at Roorkee during SE premonsoon. The maximum temperature was lower in April than the month of May (Fig. 6c) and is maximum in June and also decreases in the month of July (Fig. 6d). The minimum temperature was higher in July and nearly the same in June and is lower in the month of April and increases slightly in May [Fig. 6(e,f)]. The wind speed is nearly same in the months of April and May (Fig. 6i) and
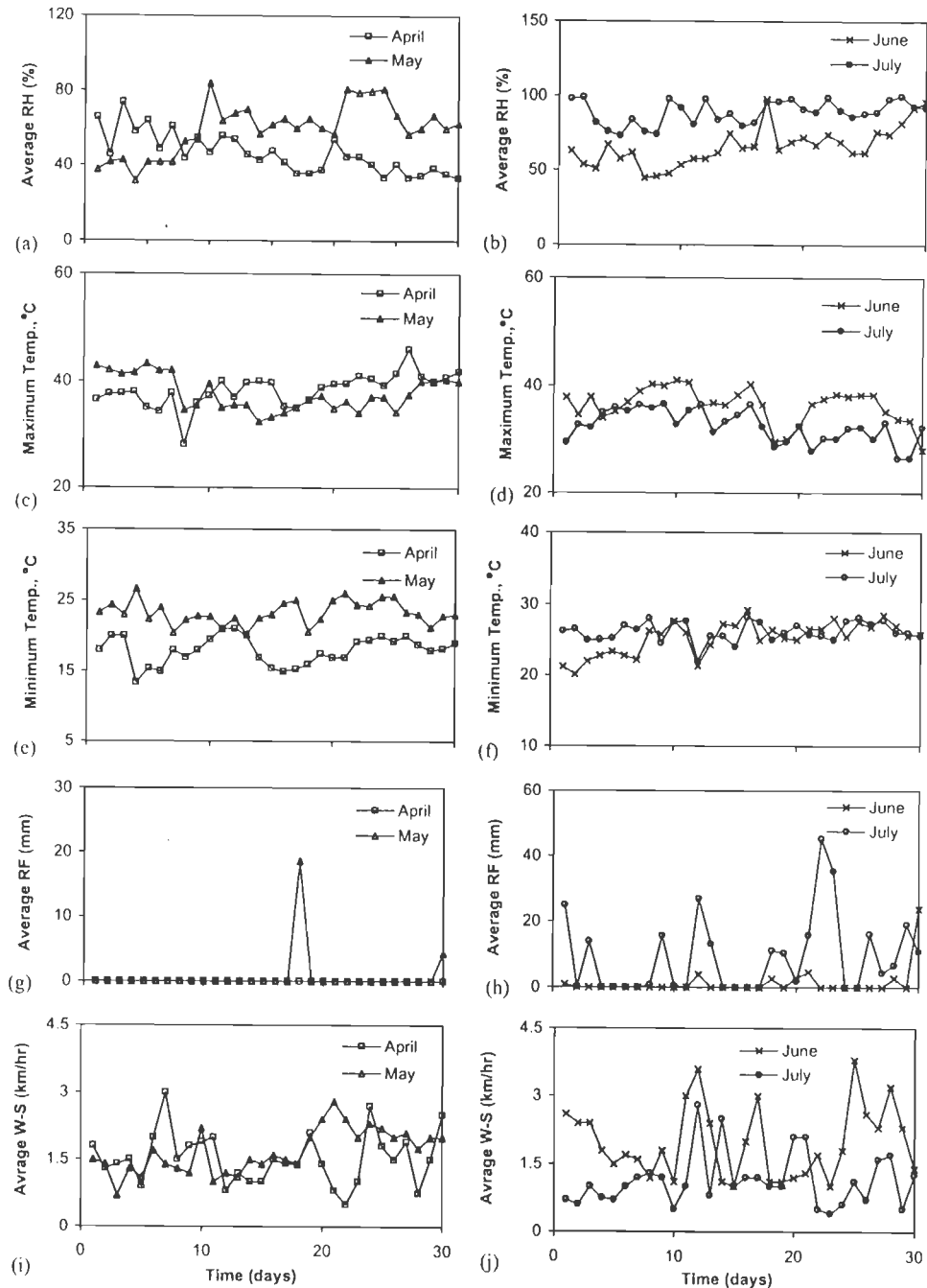
Fig. 6. Variation of average meteorological parameters (relativity humidity, temperature, rainfall and wind speed) in summer season (April–July 1999).

is higher in June and again decreases in the month of July (Fig. 6j). The rain plays an important role to modulate the aerosol size as larger particles take part in the scavenging process (Devara and Raj, 1998; Byrne and Jennings, 1993; Sparmacher et al., 1993). In the month of April and May the rainfall is nearly zero (Fig. 6g) so there is no significant

effect on aerosol number concentration. The SE monsoon is effective (Fig. 6h) after mid-June, so the concentration of aerosol decreases and it is in phase with the increasing monsoon activity. This is attributed to the rainfall, which is a powerful factor to lower the aerosol number concentration involving rain out process. The monthly means of aerosol

Table 1
Monthly mean of aerosol number concentration and standard deviation (σ)

Months	Size range 0.3–0.5 μm		Size range 0.5–1.0 μm		Size range 1.0–2.0 μm		Size range 2.0–5.0 μm	
	Conc. mean (l^{-1})	Standard deviation	Conc. mean (l^{-1})	Standard deviation	Conc. mean (l^{-1})	Standard deviation	Conc. mean (l^{-1})	Standard deviation
April	16.46×10^4	8.80×10^4	35.03×10^3	10.46×10^3	29.57×10^2	18.69×10^2	7.78×10^1	2.46×10^1
May	11.51×10^4	5.19×10^4	25.95×10^3	7.34×10^3	16.32×10^2	10.13×10^2	9.87×10^1	6.86×10^1
June	8.73×10^4	4.98×10^4	28.07×10^3	12.68×10^3	16.86×10^2	14.46×10^2	8.92×10^1	5.62×10^1
July	5.61×10^4	5.03×10^4	13.96×10^3	17.18×10^3	8.50×10^2	8.54×10^2	2.56×10^1	1.60×10^1

number concentration along with standard deviations (σ) have been shown in Table 1.

The average number concentration of aerosols is shown in Fig. 7(a,b) and the average of meteorological parameters (relative humidity, temperature, rainfall, and wind speed) in Fig. 8(a–c) for summer season 1999 over Roorkee. In the small size ranges (0.3–0.5 and 0.5–1.0 μm) particle average concentration is maximum in the month of April and May and decreases continuously in June and July while the RH forms minimum in April and May and goes to maximum in June and July. The wind speed (Fig. 8c) remains almost constant throughout the period of observation. In the large size ranges (1.0–2.0 and 2.0–5.0 μm) the average particle concentration increases, going to maximum in the middle of June, after which it starts decreasing.

The aerosol number concentration is expected to be dependent on meteorological parameters. Therefore, we have made comparisons with meteorological parameters like relative humidity, wind speed, temperatures and rainfall with aerosol number concentration. These have been shown in Figs. 9–13 along with the equation of linear regression fits and the correlation coefficient.

Fig. 9 shows the correlation of average aerosol number concentration to the relative humidity. The number concentration in all size ranges decreases with humidity. The increasing humidity removes the aerosol particles in all size ranges due to condensation on aerosol particles and subsequent falling down of the drops or droplets takes to the ground. Pranesha and Kamra (1996) in their laboratory studies have found that the particles are actually removed from the air due to condensation. The correlation coefficient (R) is large for the lower size range particles (0.3–0.5 and 0.5–1.0 μm) and small for upper size range particles (1.0–2.0 and 2.0–5.0 μm). This shows that the smaller particles act as condensation nuclei and the contribution of larger particles to this process is very small.

In Fig. 10, there is slight increase in number concentration with increasing wind speed. This can be attributed to the dust particles from the soil becoming air-borne due to wind and an increase in the number concentration is expected. However, the correlation coefficient in all the size ranges is very small and a definite relation cannot be established.

The concentration decreases slightly with increasing minimum temperature (Fig. 11). The correlation coefficient (R) is about -0.50 for lower size ranges and it becomes very small for the upper size range particles (-0.22). This has further been attributed to the process of condensation at small size particles. The increasing minimum temperature decreases the condensation and hence a negative trend in the regression line of fit has been obtained. On the other hand, the average concentration slightly increases with increasing maximum temperature (Fig. 12). With the rise of maximum temperature, more and more drops/droplets are vaporized leaving behind the aerosols.

In Fig. 13, the decrease of aerosol number concentration with rainfall is as expected which is attributed to the scavenging of aerosol particles (Devara and Raj, 1998; Byrne and Jennings, 1993; Sparmacher et al., 1993 and others).

One may doubt the conclusion drawn regarding the influence of meteorological parameters on aerosol number concentration. Pranesha and Kamra (1996) have performed laboratory studies and have found that the suspended particles are removed from air due to condensation.

Hanel (1976) found that the particle size decreases with decrease in RH. Parameswarn and Vijaykumar (1994) studied the aerosol size distribution using a low-pressure impactor and concluded that the aerosol size decreases with decreasing RH. Vakeva et al. (2000) studied the nucleation phenomena in the humid urban atmosphere and found that the ultrafine particles (diameter 10 nm or less) are produced due to nucleation. However, our interest lies in large particles (0.3 μm and larger) and their results are not much relevant to our studies.

Vakeva et al. (2000) also studied the effect of wind on aerosol concentration. They found that during moderate wind the sub-micron size particles increase in concentration in the urban environment. They also found that the aerosol concentration is a function of wind direction. In our studies we have not considered the wind direction but have found that the aerosol number concentration increases with increasing wind speed.

Shaw (1988) has found that the aerosol concentration in the size range 0.36–0.40 μm increases with increasing temperature. Summer months, in his studies were found to have very high level of aerosol concentration (about 4 times
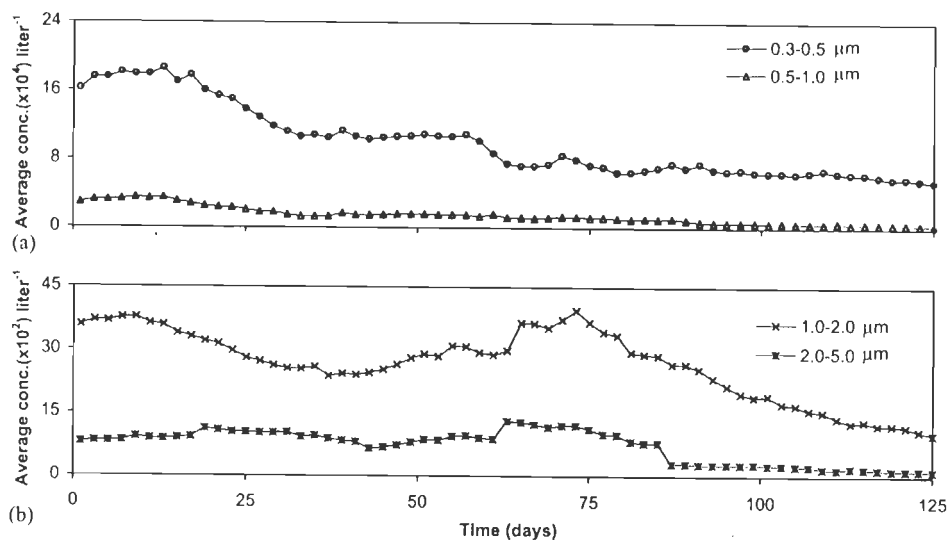
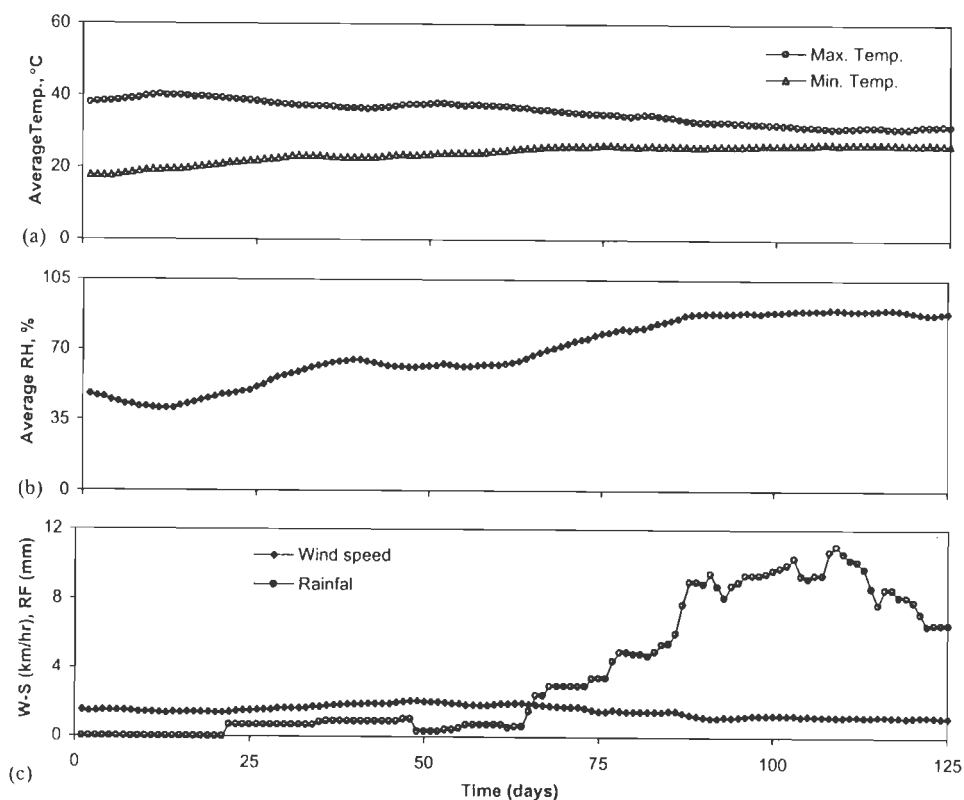Fig. 7. The running mean average number concentration of aerosols in summer season (April–July 1999).

Fig. 8. The running mean average of meteorological parameters (relative humidity, temperature, rainfall and wind speed) in summer season (April–July 1999).

as a rough estimate) than the winter months. Further, the sun increased the aerosol concentration in the above size range. The aerosol number concentration dependence on both minimum and maximum temperatures are shown in

Figs. 11 and 12. In all size ranges the aerosol number concentration decreases with increasing the minimum temperature. The correlation coefficient ranges from −0.22 (for largest size range) to −0.52 (for smallest size range). However, the
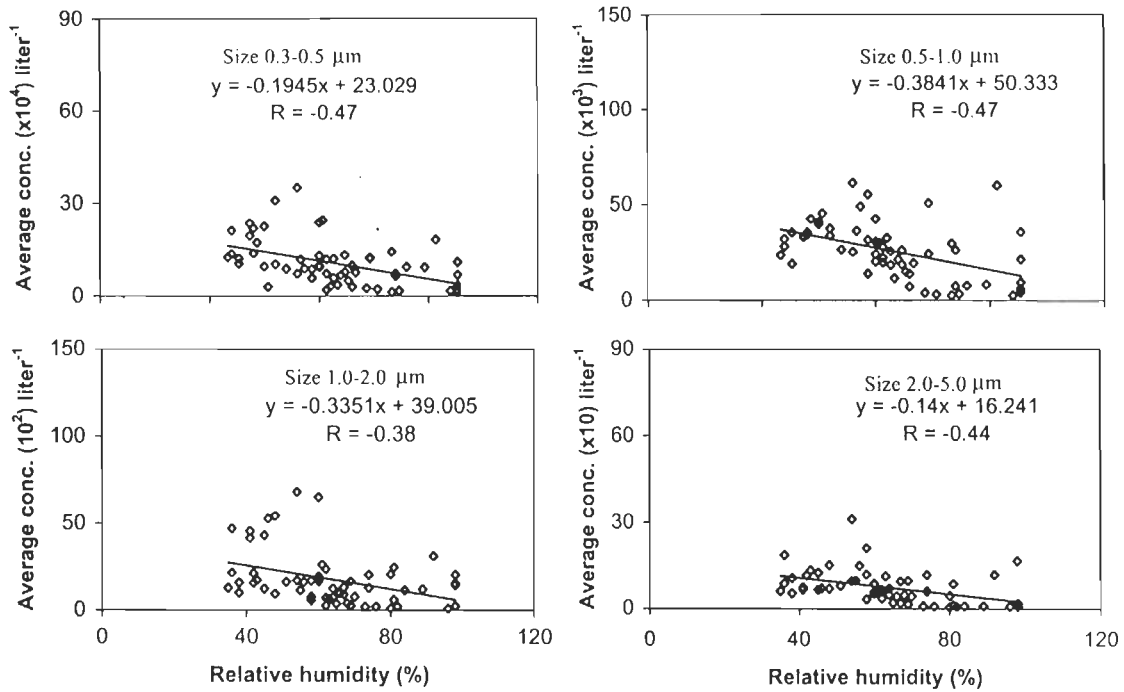
Fig. 9. Variation of average aerosol number concentration versus relativity humidity during April–July 1999 for different size ranges.
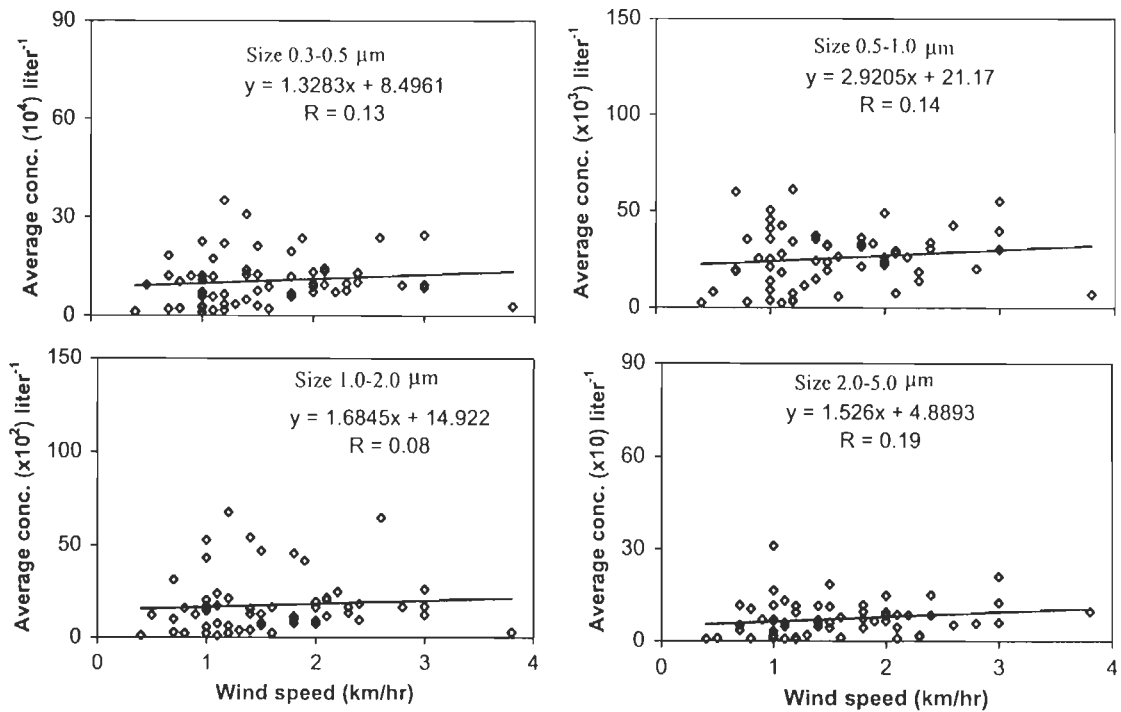

Fig. 10. Variation of average aerosol number concentration versus wind speed during April–July 1999 for different size ranges.
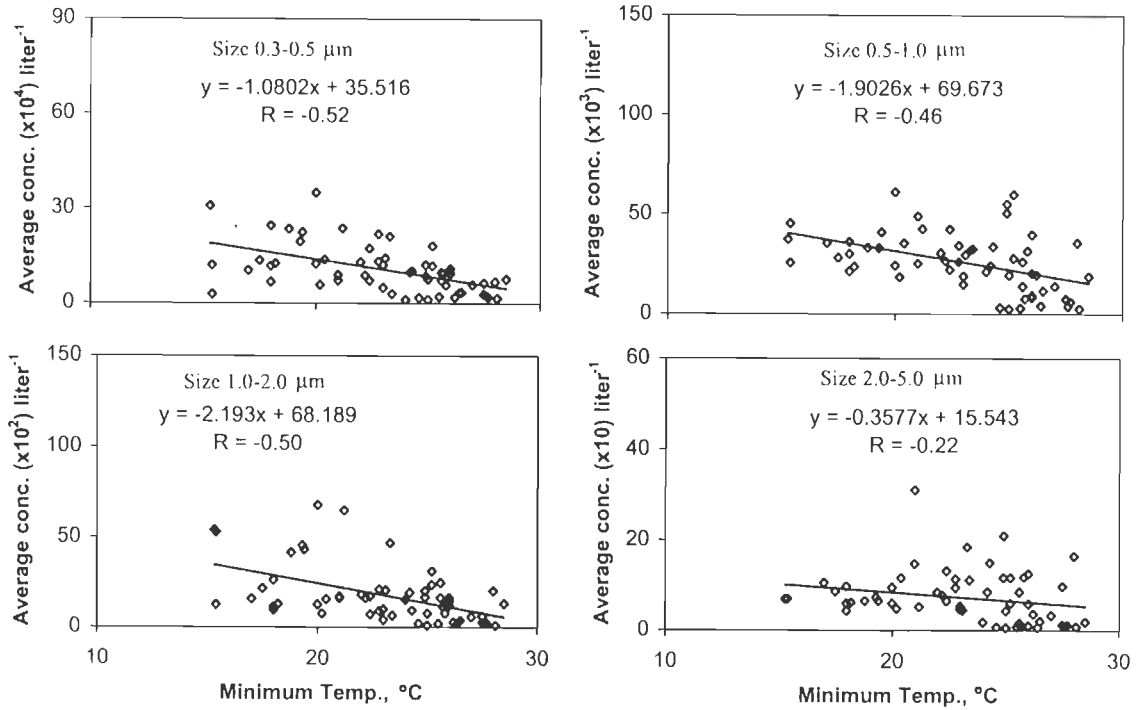
Fig. 11. Variation of average aerosol number concentration versus minimum temperature during April–July 1999 for different size ranges.
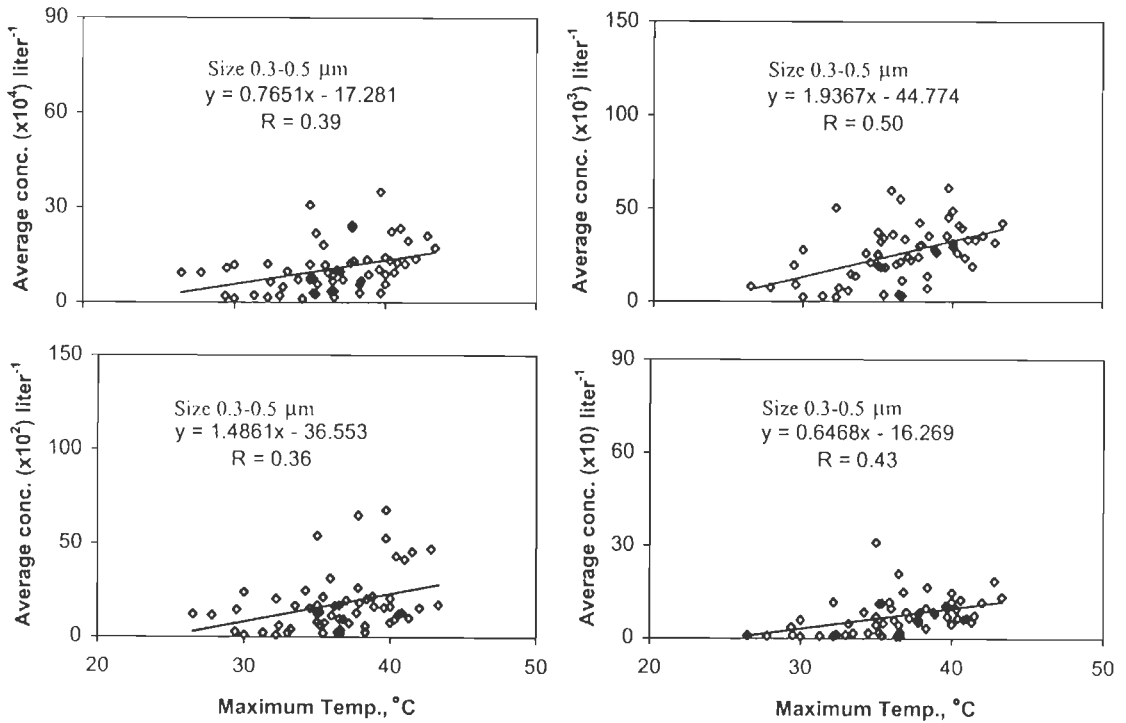

Fig. 12. Variation of average aerosol number concentration versus maximum temperature during April–July 1999 for different size ranges.
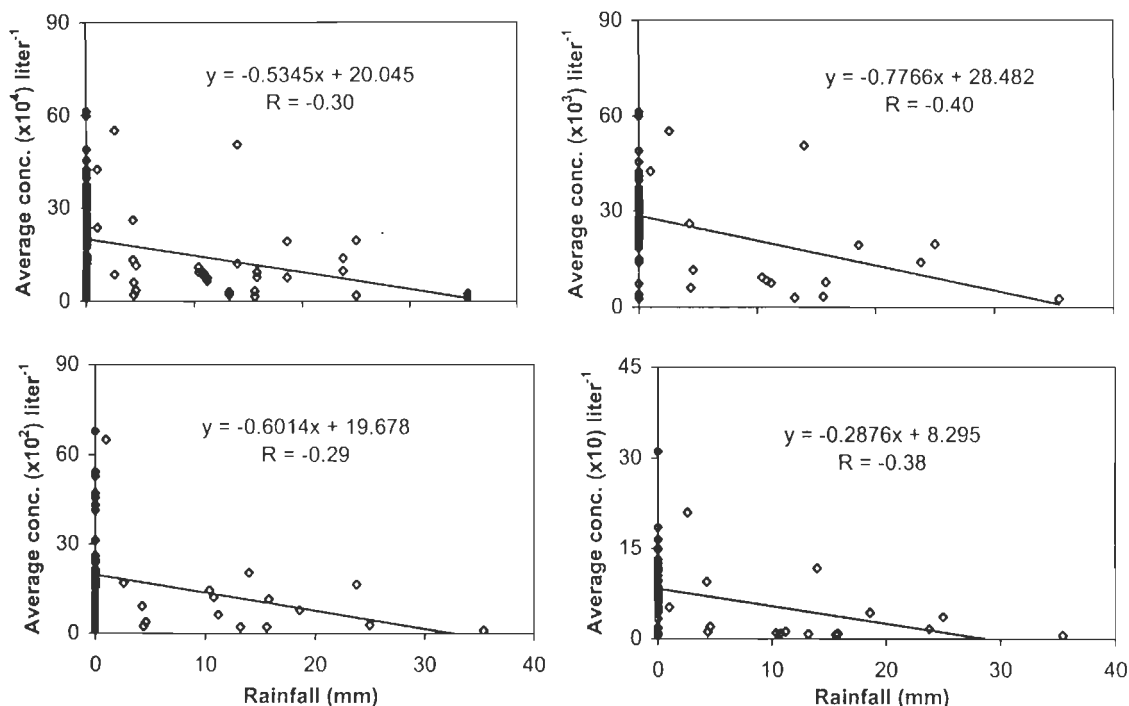
Fig. 13. Variation of average aerosol number concentration versus rainfall during April–July 1999 for different size ranges.

variation with maximum temperature is quite contrary. In all size ranges it increases with increasing maximum temperature. The correlation coefficients are 0.39 (0.3–0.5 μm), 0.50 (0.5–1.0 μm), 0.36 (1.0–2.0 μm) and 0.43 (2.0–5.0 μm).

In all the above discussions the correlation coefficient (R) between aerosol number concentration and meteorological parameters is not very high and the data points are scattered. The linear regression model here does not work well. The aerosol particles depend upon many parameters including natural and man-made sources and almost all the meteorological conditions act the same time. Therefore, a linear relationship between the aerosol number concentration (in different size ranges) and meteorological parameters individually cannot be established.

A comprehensive model of the aerosol number concentration in different size ranges as a function of meteorological parameters acting together becomes essential for proper understanding of the subject matter.

4. Conclusion

In the present study, the behavior of aerosols number concentration during morning, noon and evening periods in summer season (April–July) for different size ranges of the aerosols (0.3–0.5, 0.5–1.0, 1.0–2.0 and 2.0–5.0 μm) have been investigated. Aerosol number concentration for small size ranges (0.3–0.5 and 0.5–1.0 μm) was higher than that

for large size ranges (1.0–2.0 and 2.0–5.0 μm). The variation of aerosol number concentration in morning was found to be less than noon and it was observed maximum during evening. The time variation of aerosols was highly dependent on size. For small size ranges the number concentration decreased monotonically till the end of July. For large size ranges it increased becoming maximum in June and minimum in July. The study reveals the fact that the aerosol size and number concentration are greatly affected by the meteorological parameters. The larger particles are especially sensitive to variations in meteorological parameters. The relative humidity, temperature, rainfall and wind speed play important roles to modulate the aerosol behavior but large amount of precipitation (heavy rainfall) can alter the number density and size distribution of atmospheric aerosols more efficiently than RH and wind speed.

References

Aher, G.R., Agashe, V.V., 1997. Effect of premonsoon scenario on aerosols at Pune. Abstract book of TROPMET'97, IISc, Bangalore, pp. 31–32.

Bansal, M.K., Verma, T.S., 1998. Aerosol measurements at Roorkee relating to the total solar eclipse of 24 October 1995. Indian Journal of Radio & Space Physics 27, 260–265.

Byrne, M.A., Jennings, S.G., 1993. Scavenging of sub-micrometer aerosol particles by water drops. Atmospheric Environment, Part A 27, 2099–2105.

Devara, P.C.S., Raj, P.E., 1998. A lidar study of atmospheric aerosols during two contrasting monsoon season. Atmosfera 11, 199–204.

Hanel, G., 1976. The properties of atmospheric aerosol particles as a function of relative humidity at thermodynamic equilibrium with the surrounding of moist air. In: Landsberg, H.E., Van Meighen, J. (Eds.), Advance in Geophysics, Vol. 19. Academic Press, New York, USA, pp. 73–188.

McCormick, M.P., Swissler, T.J., Chu, W.P., Fuller, W.H., 1978. Post-volcanic stratospheric aerosol decay as measured by Lidar. Journal of Atmospheric Science 35, 1296–1303.

Pahwa, D.R., Singhal, S.P., Khemani, L.T., 1994. Study of aerosol at Delhi. Mausam 45 (1), 49–56.

Parameswarn, K., Vijaykumar, G., 1994. Effect of atmospheric relative humidity on aerosol size distribution. Indian Journal of Radio & Space Physics 23, 175–188.

Pranesha, T.S., Kamra, A.K., 1996. Scavenging of aerosol particles by large water drops, 1—Natural case. Journal of Geophysical Research 101, 23373–23381.

Sharma, D.K., Tyagi, D.K., Darmora, S., Rai, J., Israil, M., 2002. Study of aerosols during two alternative seasons: influence of meteorological parameters. Abstract book XII National Space Science Symposium, Bhopal, India, p. 49.

Shaw, G.E., 1988. Aerosol-size temperature relationship. Geophysical Research Letters 15, 133–135.

Singh, N., 1985. Role of atmospheric ions on condensation and cloud formation processes. Ph. D. Thesis, University of Roorkee, India.

Singh, A.K., Rai, J., Niwas, S., Kumar, A., Rai, A., 1997. Measurements of aerosols during monsoon, Roorkee. Abstract book of TROPMET'97, IISc, Bangalore, p. 77.

Singh, A.K., Niwas, S., Kumar, A., Rai, J., Nigam, M.J., 1999. Variation of atmospheric aerosols and electrical conductivity at Roorkee during the total solar eclipse of October 1995. Indian Journal of Radio & Space Physics 28, 1–10.

Sparmacher, H., Fullberg, K., Bonko, H., 1993. Scavenging of aerosol particles: particle-bound radionuclides—experimental. Atmospheric Environment, Part A 27, 605–618.

Vakeva, M., Hameri, K., Puhakka, T., Nilsson, E.D., Hohti, H., Makela, J.M., 2000. Effect of meteorological process on aerosol particle size distribution in an urban background area. Journal of Geophysical Research 105, 9807–9821.

Zhang, X.Y., Arimoto, R., Cao, J.J., Zhi, S.A., Wang, D., 2001. Atmospheric dust aerosol over Tibetan Plateau. Journal of Geophysical Research 106, 18471–18476.